Protein Sorption to Contact Lenses and Intraocular Lenses

by

Doerte Luensmann

A thesis
presented to the University of Waterloo
in fulfillment of the
thesis requirement for the degree of
Doctor of Philosophy
in
Vision Science

Waterloo, Ontario, Canada, 2009

Authors Declaration

I hereby declare that I am the sole author of this thesis. This is a true copy of the thesis, including any required final revisions, as accepted by my examiners.

I understand that my thesis may be made electronically available to the public.

Abstract

Purpose

To locate protein sorption on the surface and inside the matrix of soft contact lens materials and intraocular lenses (IOL).

Methods

The proteins albumin and lysozyme were investigated as they are highly abundant in blood serum and tears, respectively. Proteins were conjugated with organic fluorescent probes and using confocal laser scanning microscopy (CLSM) the sorption profile to contact lenses and IOL could be determined. Radiolabeled protein was used for quantification purposes.

- Albumin sorption to etafilcon A and lotrafilcon B was determined (Chapter 3)
- Different fluorescent probes were used for conjugation and the impact on albumin sorption behaviour was investigated (Chapter 4)
- Lysozyme sorption to nine different pHEMA-based and silicone hydrogel contact lenses was determined using two fluorescent probes (Chapter 5)
- The efficiency of protein removal from contact lenses using contact lens care regimens was investigated (Chapter 6)
- Albumin sorption to IOL materials was quantified and imaged using a modified CLSM technique (Chapter 7)

Results

Albumin and lysozyme sorption profiles differed between materials, and were influenced by the fluorescent probes used for conjugation. After one day of incubation, both proteins could be located within all contact lens materials, except for lotrafilcon A and lotrafilcon B, which primarily allowed deposition on the lens surface. An increase in protein accumulation was found for most materials over the maximum investigated period of 14 days, using CLSM and radiolabel techniques. The efficiency of contact lens care regimens to remove lysozyme and albumin depended on the lens material, care regimen and protein type investigated.

PMMA and silicone IOLs showed protein exclusively on the surface, while a hydrophilic acrylic IOL allowed penetration into the lens matrix over time. Despite the albumin penetration depth into hydrophilic acrylic, the highest albumin levels were determined for the silicone IOL.

Conclusions

CLSM provides detailed information that can describe the protein distribution in transparent biomaterials, with scanning depths up to a few hundred microns. However, the CLSM data are primarily of qualitative value, which necessitates a quantitative technique (e.g. radiolabeling) to determine the total protein content.

Acknowledgements

I sincerely thank my supervisor Dr. Lyndon Jones for his guidance, support and friendly encouragement throughout this research work. He has been a great source of inspiration, and gave me the motivation to make this contribution.

I would like to thank my committee member Dr. Trefford Simpson for his support and particularly for his ideas for interpreting and analyzing my data. I would also like to thank my other committee members, Dr. Craig Woods, and Dr. Elizabeth Meiering, for their willingness to provide guidance and suggestions on my experiments. I would like to acknowledge my external examiners Dr. Eric Papas and Dr. Brian Dixon for reviewing my thesis and giving me valuable comments.

Special thanks go to the research associates, Miriam Heynen and Elizabeth Martell for their intuitive ideas, patience and encouragement throughout this project.

I am thankful to get the opportunity to come to Waterloo and be part of the Centre for Contact Lens Research; my special thanks go to Dr. Desmond Fonn.

Finally, I would like to thank my parents who always believed in me.

This research was funded by grants from Natural Sciences and Engineering Research Council of Canada, a Vistakon Research Grant from the American Optometric Foundation (AOF), and the Canadian Optometric Education Trust Fund (COETF).

Dedication

For Marc, I could have never done it without you!

Table of Contents

List of Figures

List of Tables

List of Symbols and Abbreviations

Å	Angstrom
AA	Acuvue® Advance™
ACN/TFA	Acetonitrile/ 0.2% Trifluoroacetic acid
AC2	Acuvue®2
AH	Aqueous humour
ATM	Atomic force microscopy
ATR	Attenuated total reflectance
BAB	Blood-aqueous barrier
BP	Band pass filter
BSA	Bovine serum albumin
CCC	Correlation Coefficient of Concordance
CH	Conventional hydrogel
CLARE	Contact lens induced acute red eye
CLPU	Contact lens peripheral ulcers
CLPC	Contact lens-associated papillary conjunctivitis
CLSM	Confocal laser scanning microscopy
cm	Centimeter
CW	Continuous wear
Da	Dalton
DIC	Differential interference contrast
Dk	Oxygen permeability
Dk/t	Oxygen transmissibility

DPM	Disintegrations per minute
DMA	N,N-dimethylacrylamide
DOL	Degree of labeling
DTAF	5-(4,6-Dichloro-s-triazin-2-ylamino)fluorescein hydrochloride
DTT	Dithiothreitol
DW	Daily wear
EDTA	Ethylenediamine tetra acetic acid
EM	Emission
ESCA	Electron spectroscopy for chemical analysis
EW	Extended wear
EXC	Excitation
FDA	United States Food and Drug Administration
FITC	Fluorescein isothiocyanate
FLIP	Fluorescent loss in photobleaching
FND	Focus® Night & Day™
FRAP	Fluorescence recovery after photobleaching
FRET	Fluorescence resonance energy transfer
g	Gram
GPC	Giant papillary conjunctivitis
HFT	Main dichroic beam splitter (Hauptfarbteiler)
HSA	Human serum albumin
HEL	Hen egg lysozyme
HEMA	2-hydroxyethyl methacrylate
HPLC	High performance liquid chromatography
H_2O_2	Hydrogen peroxide

ICL	Iodine monochloride
IEP	Isoelectric point
IgE	Immunoglobulin E
IgG	Immunoglobulin G
IOL	Intraocular lens
Iop	Isoionic point
kDa	KiloDalton
kg	Kilogram
µg	Microgram
µl	Microlitre
LDS	Lithium dodecyl sulphate
LEC	Lens epithelial cell
LOA	Limits of agreement
LP	Long pass filter
LY	Lucifer yellow vinyl sulfone
LYS	Lysine
MAA	Methacrylic Acid
mg	Milligram
ml	Millilitre
mm	Millimetre
µm	Micrometre
MPS	Multipurpose care solution
MW	Molecular weight
NFT	Secondary dichroic beam splitter (Nebenfarbteiler)
ng	Nanogram

NVP	N-vinyl pyrrolidone
PBS	Phosphate buffered saline
PC	Phosphorylchlorine
PDMS	Polydimethylsiloxane
pHEMA	Poly-2-hydroxyethyl methacrylate
PHMB	Polyhexamethylene biguanide
PMMA	Poly-methyl methacrylate
ppm	Parts per million
pTTS	Poly-tris(trimethylsiloxy)silylstyrene
PV	PureVision™
PVDF	Polyvinylidene difluoride
PVP	Poly(vinylpyrrolidone)
RGP	Rigid gas permeable lenses
RITC	Rhodamine B isothiocyanate
S_1, S_2	Singlet excited states
SD	Standard deviation
SDS	Sodium dodecyl sulphate
SDS-PAGE	Sodium dodecyl sulphate-polyacrylamide gel electrophoresis
SEAL	Superior epithelial arcuate lesion
Sec	Second
SEM	Scanning electron microscopy
SH	Silicone hydrogel
T_1, T_2	Triplet excited states
TBS	Tris-buffered saline
TBS-Tw	Tris-buffered saline with 0.05% Tween® 20

TEM	Transmission electron microscopy
Tris	Trimethylsiloxy silane
TPVC	Tris-(trimethylsiloxysilyl) propylvinyl carbamate
USAN	United States Adopted Names
UV	Ultraviolet

1. INTRODUCTION

1.1 Contact Lenses

1.1.1 The development of soft contact lens materials

In 1960, Otto Wichterle described the essential requirements for plastic materials that could remain permanently in contact with living tissue, without causing unfavourable reactions to the organism in which it contacted.[1] He discussed the importance of the material's permeability to metabolites, polymer stability, the use of cross-linking agents to prevent deposition and further proposed the use of the copolymer of glycol-mono-methacrylate and glycol-dimethacrylate as a suitable hydrophilic material. Although Wichterle rapidly modified this copolymer into poly-2-hydroxyethyl methacrylate (pHEMA- see Figure 1-1),[1] it took another 10 years for a manufacturing method (spin-casting) to become proficient that soft lenses could become a commercial reality [2,3]

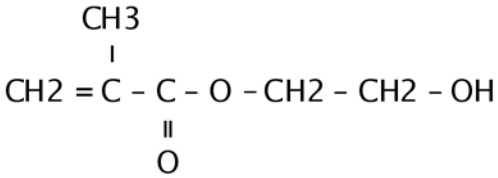

Figure 1-1: Chemical structure of HEMA (MW 130)

PHEMA, with a water content of 38%, appeared to be reasonably biocompatible and even today it is still used in a variety of biomedical fields such as blood-contacting implants, artificial organs, drug delivery devices and for intraocular lenses (IOL).[4,5] When used as a contact lens material, various cross-linking agents are typically incorporated into pHEMA to enable enhanced material strength, and specific polymerization and copolymerization further improve water-swelling properties.[2] Methacrylic acid (MAA) and N-vinyl pyrrolidone (NVP) are commonly used to increase the water content, which results in improved oxygen permeability of the material. Currently, more than 150 different types of soft contact lenses are available, most of which are still based on pHEMA compositions.[6]

In order to differentiate between lens material characteristics, the Food and Drug Administration (FDA) divided contact lens materials into 4 FDA groups. The groups are classified by ionicity and water content (FDA 1-4), as described in Table 1-1.

Table 1-1: FDA Soft Lens Classification

	Water content	Electrostatic charge
FDA - Group 1	< 50% water	Non-ionic (< 0.2% MAA)
FDA - Group 2	> 50% water	Non-ionic (< 0.2% MAA)
FDA - Group 3	< 50% water	Ionic (> 0.2% MAA)
FDA - Group 4	> 50% water	Ionic (> 0.2% MAA)

FDA (Food and Drug Administration); MAA (Methacrylic acid)

1.1.2 Corneal responses to contact lens wear

The healthy cornea is an avascular organ, which receives the required oxygen and nutrients for appropriate metabolic performance through the tears, with atmospheric oxygen being dissolved into the tear film and subsequently transferred to the cornea. However, during the wear of pHEMA-based contact lenses, the oxygen supply is immediately reduced by the presence of the lens, and the transfer of oxygen through the lens is limited by the water phase of the lens polymer. If the oxygen transport (or "oxygen permeability" – Dk - (cm^2 x ml O_2 / (sec x ml x mmHg))) is insufficient, the cornea may exhibit a variety of hypoxic complications, including limbal hyperemia, corneal neovascularization, epithelial microscysts, stromal striae, endothelial polymegethism and suppressed epithelial proliferation rates.[7-10] The only way to improve the oxygen permeability for pHEMA-based materials is to increase the percentage of water in the material, which is solely responsible for oxygen transport in this group of materials. The maximum possible water content for pHEMA-based contact lenses is approximately 79%, which (in lenses of appropriate thickness for this water content) corresponds to an oxygen transmissibility (Dk/t) of $40x10^{-9}$ (cm x ml O_2 / (sec x ml x mmHg)).[11] When contact lenses are worn overnight, this level of oxygen transmissibility is inadequate to limit corneal swelling to that seen with no lens wear and eye closure, of approximately 2.6-4% edema.[7,12,13] Oxygen transmissibilities (Dk/t) of $125x10^{-9}$ or higher have recently been proposed to avoid hypoxic-related complications,[7,13] which cannot be achieved with lenses that rely on the water phase for oxygen transport. This resulted in the development of new hydrogel materials, based on polymers that transport greater amounts of oxygen, such as silicone.

1.1.3 Silicone hydrogel lens materials

Pure silicone is highly gas permeable, but due to its hydrophobic character silicone-based contact lenses are poorly wettable[14] and show high lipid deposition rates.[15,16] To combine the benefit of the high oxygen permeability of siloxane-groups with the hydrophilic, ion-transporting property of pHEMA, silicone hydrogel (SH) materials were developed and became commercially available in 1999.[17,18] To-date, eight SH materials are commercially available, with oxygen transmissibilities ranging from 86 to 175×10^{-9} Dk/t (Table 1-2). SH lenses have more complex monomer compositions compared to pHEMA-based materials.[2,6] Typical components of silicone hydrogel contact lenses are DMA (N,N-dimethylacrylamide), PDMS (polydimethylsiloxane), TPVC (tris-(trimethylsiloxysilyl) propylvinyl carbamate), TRIS (trimethylsiloxy silane), PVP (polyvinyl pyrrolidone) and siloxane macromers.[6]

1.1.3.1 Surface modifications of silicone hydrogel lenses

Most silicone hydrogel lens materials require surface modification to overcome the hydrophobic nature of the silicone component. Balafilcon A, lotrafilcon A, lotrafilcon B and asmofilcon A are modified using different plasma treatments.[6,19] For balafilcon A, reactive gas plasma transforms the hydrophobic siloxane components on the surface of the lenses into hydrophilic silicate compounds ('glassy islands').[6,20] Lotrafilcon A and lotrafilcon B are permanently modified by a gas plasma treatment using a mixture of trimethylsilane, oxygen and methane to form a 25nm thin hydrophilic coating over the surface.[2,17,21] The lens surface of asmofilcon A is modified based on "Nanoglass" technology using a new plasma treatment, which combines plasma coating and surface oxidation.[22]

Galyfilcon A and senofilcon A utilise a different methodology to enhance wettability. Hydrophilic high molecular chains of poly(vinylpyrrolidone) (PVP) are incorporated during the polymerization process to shield the tear film from hydrophobic siloxane components.[23-27] The most recent SH materials, comfilcon A and enfilcon A, incorporate silicone which is based on siloxy-macromers instead of the commonly used TRIS-derivates. These lens materials have been described as highly wettable without the need for surface treatment.[28]

Table 1-2: List of currently available silicone hydrogel contact lenses

Trade Name	USAN	FDA Category	Manufacturer	Centre thickness (μm)	Water content (%)	Oxygen transmissibility (DK/t)	Principal monomers
ACUVUE® ADVANCE®	galyfilcon A	I	Johnson & Johnson	70	47	86	mPDMS, DMA, HEMA, EGDMA siloxane macromer, PVP
ACUVUE® OASYS™	senofilcon A	I	Johnson & Johnson	70	38	147	mPDMS, DMA, HEMA, TEGDMA siloxane macromer, PVP
Focus® NIGHT & DAY®	lotrafilcon A	I	CIBA Vision	80	24	175	DMA, TRIS, siloxane macromer
AIR OPTIX™ AQUA	lotrafilcon B	I	CIBA Vision	80	33	138	DMA, TRIS, siloxane macromer
PureVision®	balafilcon A	III	Bausch & Lomb	90	36	101	NVP, TPVC, NVA, PBVC
Biofinity®	comfilcon A	I	Cooper Vision	80	48	160	M3U, FM0411M, HOB, IBM, NVP, TAIC, VMA
AVAIRA®	enfilcon A	I	Cooper Vision	80	46	125	M3U, BHPEA, MMA, POE, TREGDMA, VMA
PremiO	asmofilcon A	I	Menicon	80	40	161	*

BHPEA (2-(4-benzoyl-3-hydroxyphenoxy)ethyl acrylate); DMA (N,N-dimethylacrylamide); EGDMA (ethyleneglycol dimethacrylate); FM0411M (2-ethyl [2-[(2-methylprop-2-enoyl)oxy]ethyl]carbamate); HEMA (poly-2-hydroxyethyl methacrylate); HOB ((2RS)-2-hydroxybutyl 2-methylprop-2-enoate); IBM (Isobornyl methacrylate); M3U (α-[[3-(2-[[2-(methacryloyloxy)ethyl] carbamoyloxy]ethoxy)propyl]dimethylsilyl]-ω-[3-(2-[[2-(methacryloyloxy)ethyl] carbamoyloxy]ethoxy)propyl]poly([oxy[(methyl) [3-[ω-methylpoly(oxyethylene)oxy]propyl]silylene]/[oxy[(methyl)(3,3,3-trifluoropropyl)]silylene]/oxy (dimethylsilylene)])); MA (methacrylic acid); MMA (methyl methacrylate); mPDMS (monofunctional polydimethylsiloxane); NCVE (N-carboxyvinyl ester); NVP (N-vinyl pyrrolidone); PBVC (poly[dimethysiloxy] di [silylbutanol] bis[vinyl carbamate]); PC (phosphorylcholine); POE 2-(2-propenyloxy)ethanol); PVP (poly(vinylpyrrolidone)); TAIC (1,3,5-triprop-2-enyl-1,3,5-triazine-2,4,6(1H,3H,5H)-trione); TEGDMA (tetraethyleneglycol dimethacrylate); TPVC (tris-(trimethylsiloxysilyl) propylvinyl carbamate); TREGDMA (triethylene glycol dimethacrylate); TRIS (trimethylsiloxy silane); VMA N-Vinyl-N-methylacetamide. *1: Principal monomers will be disclosed after USAN registration.

1.1.4 Trends in contact lens prescribing

Contact lens prescribing trends are very country specific and vary between the number of total fits as well as the choice of lens material and lens replacement frequency.[29-31] The first contact lenses were glass-blown scleral lenses, which were invented more than 100 years ago, followed by corneal lenses made of rigid polymethyl methacrylate (PMMA) and soft pHEMA-based lenses.[32] Current materials for rigid lenses are highly gas permeable due to silicone-methacrylate and fluorosilicone acrylate components, but this material group accounts for less than 10% of all new lens fits, because of the high success rate of soft lens materials.[3,29,33]

Prescribing trends for contact lenses are constantly changing with the development of new lens materials and lens designs. Until 1999, soft pHEMA-based lenses with intermediate water contents between 40-60% and high water content lenses of >60% water were fitted primarily.[29,34] However, the number of new fittings with pHEMA-based lenses decreased consistently after SH materials became available.[30,31,35,36] The high oxygen transmissibility of SH lenses allows longer wearing times when compared to pHEMA-based materials. Balafilcon A and lotrafilcon A are FDA certified to be worn for up to 30 days and nights continuously; lotrafilcon B, senofilcon A, comfilcon A and asmofilcon A are licensed to be worn on an extended schedule for up to six nights and seven days without cleaning. The remaining silicone hydrogel lenses enfilcon A and galyfilcon A are certified for daily wear only, with cleaning and disinfection required after each wear.

The majority of contact lenses that are prescribed today follow frequent replacement schedules and the lenses are replaced, either daily (27%), 1-2weekly (19%) or monthly (42%), with varying percentages being seen between countries.[37]

1.2 Contact lens care regimens

Contact lenses require frequent cleaning procedures in order to, primarily, disinfect the lens and to remove deposition of air-borne contaminants and tear film components.[38-43] Other tasks required from care regimens include their ability to rinse, store, rehydrate and lubricate the lenses without causing ocular irritation.[38] A number of care products are available, which are most simply divided into rigid and soft lens regimens.

1.2.1 Care regimens for gas permeable lenses

Rigid gas permeable (RGP) lenses are typically rubbed manually with an alcohol-based solution, which contains both emollient and foam stabilizers and, in some cases, microscopic polymeric beads that act to "polish" the lens surface.[44,45] Following this, lenses are soaked overnight in a storage solution that further disinfects the lens, rehydrates and rewets the surface. Two step systems and multipurpose care solutions (MPS) are available that contain antimicrobial agents, at higher concentrations than that contained in soft lens care regimens. This is possible because the RGP materials are typically non-ionic and have small pore sizes because of the negligible water content. The disinfectants do not penetrate into the lens material and adsorbed preservatives can be easily rinsed off the lens surface.[38] Enzymatic cleaners can periodically be used to remove tightly bound protein layers from the lens.[45]

1.2.2 Care regimens for soft lenses

The majority of cleaning solutions that are currently available have been developed to disinfect, clean and rehydrate pHEMA-based lens materials.[46,38] The two most common care regimens are MPS and hydrogen peroxide systems and the primary active ingredient of these regimens are the antimicrobial agents. The concentration of hydrogen peroxide (H_2O_2) is typically 3% (30,000ppm) and this is capable of destroying the most common bacteria and fungi; however it shows slightly reduced efficiency against acanthamoeba.[40,46-49] H_2O_2 requires neutralization before the lenses can be reinserted onto the ocular surface. The most popular technique is catalytic neutralization, using either a time release catalase tablet coated in hydroxypropyl methylcellulose or a platinum coated disc. In the past, chemical reactions with either sodium pyruvate or sodium thiosulphate were used to neutralise the H_2O_2, or the lenses were extensively rinsed with saline.[45,46] Despite the high tolerance to this preservative-free system,[50] it must be considered that as soon as the peroxide is decomposed to oxygen and water, the antimicrobial effect is eliminated and regrowth and contamination can occur over time.

Chlorhexidine and thimerosal were the first preservatives that were used as disinfectants in MPS systems. However, patients developed a variety of ocular complications against these biocides, exhibiting diffuse corneal staining, bulbar and palpebral hyperaemia, corneal infiltrates and palpebral conjunctivitis.[48,51-54] Today, two high molecular weight preservatives are typically found in MPS regimens: polyhexamethylene biguanide (PHMB) and polyquaternium-1 (Polyquad™). Both of these high molecular weight biocides attack pathogens by binding to the negatively charged phospholipids located in the cell membrane,

which results in cell lysis.[45,52] Other MPS components include surfactants, chelating agents, demulcents and a buffer system, all of which help to support the efficacy of the biocide or are involved in removing protein and lipids from the lens.[38,52] Additionally, single- and multi enzymatic cleaners based on papain and pancreatin are available to remove tightly bound protein from worn lenses,[55,56] although their use is now significantly reduced since the introduction of frequent replacement lenses.

1.3 Complications during contact lens wear

Contact lens wear impacts ocular physiology in a number of ways, including modifications in tear film composition,[57-59] changes in function and structure of the cornea and the production of various inflammatory conditions.[9,60,61] These changes can potentially result in new ocular disorders or exacerbate pre-existing conditions.[60-62,63]

1.3.1 Hypoxia-related complications

PHEMA-based lens materials reduce the oxygen supply to the cornea and increase the corneal carbon dioxide level.[64,65] Although oxygen transport through SH lens materials reduce these complications significantly,[7] some conditions can still be observed and will therefore be discussed in this section. Hypoxia related effects seen in the epithelium include suppression of cell proliferation rates, production of microcysts and epithelial thinning.[66] In the stroma, a decrease in pH,[67] increase in osmolality,[68] edema formation [69] and overall thinning [66] have been reported. In cases of clinically significant corneal edema, striae and folds can be observed within the

stroma when swelling rates exceed 5% or 10% respectively.[70] The innermost corneal layer, the endothelium, exhibits an increase in cell polymegethism [71] under hypoxic conditions and although this is typically asymptomatic, it may result in long-term contact lens intolerance.[62]

Limbal hyperemia is also closely related to the low oxygen transmissibility of contact lens materials. Limbal injection results from the local dilation of blood vessels and the development of new vessels (neovascularization) in normally avascular corneal regions.[72] Finally, hypoxia may be a predisposing factor for myopic shifts in refractive error.[73]

1.3.2 Inflammatory complications/infections

The development of inflammatory complications during contact lens wear typically start with redness, dryness, ocular discomfort and contact lens awareness.[9,74] Contact lens induced acute red eye (CLARE) is related to increased levels of (typically) gram negative bacteria on the ocular surface and the contact lens. This often causes marked conjunctival injection and multiple peripheral sterile corneal infiltrates.[60,75] Other inflammatory complications induced by contact lens wear (typically due to gram positive organisms) include contact lens peripheral ulcers (CLPUs) and symptomatic peripheral infiltrates.[60,75] If the cornea becomes infected with pathogenic organisms then it is termed microbial keratitis. Polymorphonuclear leucocytes have been identified in these infiltrates, which is an indicator that an inflammatory event has occurred.[76] It has been reported that certain combinations of contact lens materials and care regimens may be associated with infiltrates, particularly under hypoxic conditions.[60]

Microbial keratitis is the most severe potential complication during contact lens wear and is often caused by gram-negative bacteria, particularly Pseudomonas aeruginosa.[77] Various microorganisms are part of the normal tear film, and an increase in bacteria is typically measured after sleep.[78] This results in a higher risk of microbial keratitis, particularly when contact lenses are worn overnight.[79,80] Higher incidence rates of this potentially sight-threatening disease have been reported for SH lens wear, when worn for up to 30 days continuously when compared to pHEMA-based lenses that are worn for up to 6 nights and 7 days.[79]

1.3.3 Mechanical complications

Corneal deformation during lens wear has primarily been described with rigid lenses, and less often with pHEMA-based materials.[81,82] The 'first generation' of SH lenses however, showed signs of corneal reshaping due to the higher rigidity of these materials.[83] Mechanically induced lesions in the superior cornea, known as superior epithelial arcuate lesions (SEALs), were also observed with 'first generation' SH lenses, but are expected to occur less often with newer SH materials that exhibit a lower modulus.[63,75,84] Corneal erosions of the epithelium and outer stromal layer caused by a trauma or foreign body have been seen with all types of contact lenses.[61] Finally, the development of mucin balls between the cornea and the back surface of the contact lens may give rise to circular "imprints" in the epithelium.[85]

1.3.3.1 Giant papillary conjunctivitis

Giant papillary conjunctivitis (GPC) is an inflammatory condition of the upper tarsal conjunctiva and, if caused by contact lens wear, it is described as contact

lens-associated papillary conjunctivitis (CLPC).[75] A recent study by Forister has shown that neovascularization, papillae and CLPC account for the majority of contact lens induced complications.[86] CLPC is characterized by mucus discharge, increased hyperemia, and the development of polygonal or irregular papillae, which can either be localized or distributed across the tarsal plate.[61] CLPC has been reported with all kinds of lens materials, however, higher incidence rates have been observed with soft contact lenses, including silicone hydrogels, particularly if worn on an extended wear schedule.[87,88] [51] Typical symptoms of this condition are ocular discomfort, including itching, excessive lens movement, increased lens deposition and blurred vision, which finally leads to lens intolerance.[75]

The etiology of CLPC is multifactorial and is caused by a combination of mechanical lens rubbing on the tarsal conjunctiva and/or is an immune response caused by deposition on the lens surface.[89] In SH lens wear, papillae are typically isolated rather than distributed over the tarsal conjunctiva, which may be explained by mechanical lens-edge rubbing rather than an immunological response.[61,90,91] In addition, elevated levels of tear immunoglobulins (IgE, IgG), inflammatory mediators from the complement system and chemotactic factors have been detected in GPC, which provides evidence for an immunological basis in this inflammatory complication.[88,89]

Deposition of tear film proteins on contact lenses can be a factor that triggers this immune response, as they may act as antigenic stimuli.[91-95] This results in an increased production of tear immunoglobulins and activates the complement system. IgE antibodies are produced by B-lymphocytes and bind to stromal mast cells and circulating basophis. This interaction sensitizes the mast cells, which

respond with an immediate release of vasoactive amines (such as histamine), followed by eosinophilic chemotactic factors and tryptase.[88] Other immunological defense mechanisms are the release of arachidonic acid from plasma membranes and the production of prostaglandins and leukotrienes B4 and C4, which produce an inflammatory response. This immunological event is categorized as a Type I immediate hypersensitivity reaction (IgE mediated). CLPC is further accompanied by a cell mediated reaction, in which T-lymphocytes respond with a release of lymphokines and interleukins, within 24-48 hours of exposure. This delayed hypersensitivity reaction is categorized as a Type IV (T-cell mediated) response.[96]

SH contact lenses accumulate lower amounts of protein compared to conventional pHEMA-based materials.[97-99] However, the percentage of denatured protein is higher for SH materials, which increases the risk of an inflammatory response.[100-104] It is possible that surface-deposited proteins have a stronger impact on the development of CLPC, which raises the need for a better understanding of the protein location on the contact lens.

1.4 Proteins in the tear film

Proteins are a major component of the human tear film and perform a variety of important tasks to defend the ocular surface from microorganisms, have functions in transport, metabolism, immune response, cell structure, antioxidation, and act as protease inhibitors.[105] More than 100 different proteins have been identified in the human tear film [106,107] with a total concentration of 6.5-9.6 mg/ml.[108] But this concentration may change over the day,[109] during sleep [110] and under

specific conditions, including stimulated tearing,[111,112] age,[113] contact lens wear [114] and in various eye diseases such as Sjögren's syndrome.[115]

Lysozyme is of particular interest due to its high concentration and antimicrobial activity in the tear film.[111,112,116] It is overall positively charged with an IEP pH =11.1 and is constituted of 129 amino acids, which results in a molecular weight of 14.5 kDa.[117] Lysozyme is produced by the lacrimal glands and has a concentration in the tear film of 1.9 mg/ml.[110,112] It deposits in higher amounts to pHEMA-based contact lens materials that contain MAA as compared to pure pHEMA.[97,102,118,119] With the addition of MAA, the hydrogel material becomes negatively charged, which explains the attraction of the positively charged lysozyme.[120] The larger protein serum albumin (66kDa) is found in lower concentrations in the tear film and its overall negative charge (IEP pH= 4.7) shows a different sorption behaviour compared to lysozyme.[57,120-122] Albumin is highly abundant in blood serum and is therefore involved in the initial response to implanted biomaterials.[104]

Due to the relative lack of knowledge on albumin interactions with biomaterials, and its importance in the initial interaction with hydrogel biomaterials, albumin will be the major focus of this thesis and an extensive review describing albumin structure and sorption behaviour to contact lenses and other biomaterials can be found in Section 1.5.

1.5 Albumin adsorption to contact lens materials: A review

This section is published as follows:

Doerte Luensmann, Lyndon Jones

Centre for Contact Lens Research, School of Optometry, University of Waterloo, 200, University Avenue West, Waterloo, Ontario, N2L 3G1, Canada

Contact Lens & Anterior Eye 31 (2008) 179–187 - Reprinted with permission

1.5.1 Overview

During contact lens wear, tear film components such as lipids, mucins and proteins tend to deposit on and within the lens material and may cause discomfort, reduced vision and inflammatory reactions. The tear film protein that has attracted most interest when studying contact lens deposition is the small (14 kDa), positively charged protein lysozyme. Albumin, which is a much larger protein (66 kDa) with an overall net negative charge is also of interest, and shows very different adsorption patterns to lysozyme.

The concentration of albumin in the tear film is relatively low compared to the concentration in blood serum, but this value increases markedly under various conditions, including when the eye is closed, during contact lens wear and in various dry eye states.

Gaining an understanding of the manner in which albumin deposits on biomaterials is of importance for contact lens wear, as well as for other medical applications where HEMA-based materials are used for implants, artificial blood vessels or drug delivery devices.

This review paper summarizes the impact of individual material compositions, water content, hydrophobicity and electrostatic attraction on the adsorption behaviour of the protein albumin.

1.5.2 Introduction

Contact lens deposition with substances from the human tear film has been extensively studied.[15,16,43,92,94,120-144] The majority of published studies have reported on the in vivo or in vitro deposition of either "total protein" [138,145,146] or, more specifically, lysozyme.[97,98,131] However, lysozyme only accounts for a proportion of the proteins in the tears, with other major tear film proteins such as lactoferrin, albumin and lipocalin being also present in high quantities.[57,106,110,147-152] To-date, little has been published on the interaction between contact lenses and albumin and the purpose of this review article is to describe the factors that influence the degree to which this protein interacts with various materials used for contact lenses.

Albumin is synthesized in the liver and has an estimated lifetime of 27 days.[153,154] It is the most abundant protein in human serum and is also the most prominent soluble protein in the body of all vertebrates.[153] Hippocrates (circa 460 to 370 BC) was probably the first scientist to mention some distinctive properties of albumin in the human body. Serum albumin keeps the osmotic blood pressure and blood pH value constant and transports various molecules, including hormones, fatty acids and drugs.[155] In a human body weighing 70kg, 41% of the total extravascular albumin is found in the skin (100g) and 40% in the muscles (96g), with small amounts being detected in the liver, gut and subcutaneous region.[156] In the serum (intravascular), an average albumin concentration of 45.1-49.9 ± 2.6 mg/ml has been reported,[155] which approximates to 118g for a typical 70kg bodyweight.[153]

Over the last 60 years information concerning the structure of human serum albumin (HSA) has continually been updated and refined. In 1956 Tanford et al.[154] and Loeb et al.[157] described the hydrated protein as a compact spheroid particle, whereas twelve years later Squire et al.[158] reported a cigar-shaped model of 140 x 40 Å. This was the accepted textbook model until 1990, when Carter and He presented the first low-resolution crystallographic data for HSA.[159] Using this method at a resolution of 4 Å they found a three-dimensional heart-shaped structure for HSA in a crystallized format, which was confirmed ten years later for bovine serum albumin (BSA) in a hydrated state.[160] (Figure 1-2)

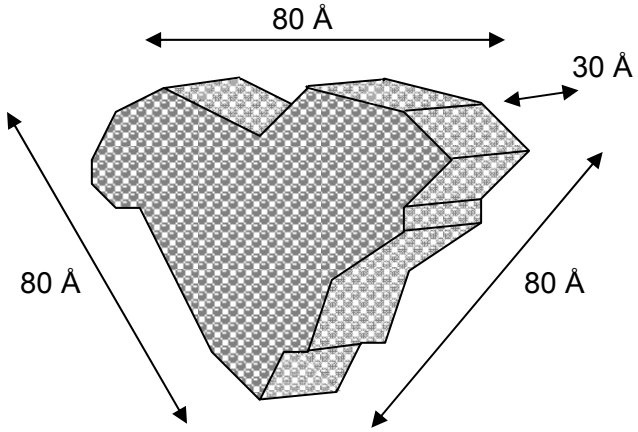

Figure 1-2: Overall dimension of the heart-shaped structure for albumin, as described by Carter and He[159]

The shape and physicochemical properties of albumin from human and bovine serum are very similar (Table 1-3). The secondary structure of albumin consists of three very similar domains (I, II, III) arranged in nine loops with 17 disulfide bridges to stabilize the native form. Each domain has two subdomains (A and B), with subdomain A being composed of six α-helix and subdomain B of four

α-helix. The helices range in size from 5 to 31 amino acids in length.[153,161,162] Due to the similarity of HSA and BSA, and the relative availability and lower cost of BSA, many in vitro studies have used BSA as a surrogate for HSA.[163-165]

Table 1-3: Comparison in structure between HSA and BSA[153]

	Molecular weight (Da)	Isoionic point	Number of fatty acids
Human (HSA)	66,438	5.16	585
Bovine (BSA)	66,411	5.15	583

1.5.3 Albumin in the preocular tear film

Far more than 100 different proteins have been identified in the human tear film.[106,107] Specific tear proteins such as lysozyme, lactoferrin and lipocalin are synthesized by the lacrimal gland; however albumin is a serum protein and becomes mixed with the tear film by leakage from the conjunctival capillaries. The concentration of HSA in the tear film has been investigated by a number of researchers, using a variety of different analytical techniques. In 1993, Bright and Tighe reviewed 9 tear film studies and found a vast range of published concentrations, between 0.0103 mg/ml and 390 mg/ml.[108]

Tears may be collected using "stimulated methods", such as those involving an "eye-flushing" technique or by stimulating a "sneeze", as compared with an "unstimulated method", where tears are collected via a capillary tube which does not touch the ocular surface.[109,111,166,167] Generally, higher HSA concentrations are found during sleep,[57,110] in unstimulated tears [109,111] and in patients with symptoms of

dry eye [168] or when wearing contact lenses.[57,169] Table 1-4 summarizes typical reported albumin levels in the preocular tear film under various conditions.

Table 1-4: Albumin concentrations in the human tear film

	Albumin concentration in the tear film (mg/ml)		
Nonstimulated tears	0.042 ± 0.012 [111]	0.023 ± 0.015 [109]	0.06 ± 0.02 [110]
Stimulated tears	0.012 ± 0.004 [111]	0.008 ± 0.001 [112]	0.02 ± 0.01 [110]
During sleep	0.20 (0.15-0.58) [57]	1.1 ± 0.76 [110]	1.0 ± 0.5 [150]
Dry eyes	Increase 17% [115]	3.7 mg/ml (0.2-22.6) [168]	4.74 ± 0.72 [170]
Wearing contact lenses	0.059 ± 0.054 [169] (healthy eye)	0.079 ± 0.060 [169] (presence of bacteria on CL)	0.54 (0.33-1.24) [57] (wearing Ortho-K CL overnight)

Data from three studies are presented for each condition

Lundh and coworkers fitted 50 eyes with contact lenses and investigated IgG and HSA concentrations in the tear film. The concentration of both serum proteins increased in 20 eyes, indicating a higher permeability of the blood-tear barrier.[171] The impact of etafilcon A lenses worn on an extended wear schedule on protein levels in the tear film was investigated by Carny et al..[172] Lactoferrin, lysozyme and HSA levels in collected tears were measured on 10 neophytes before lens wearing and after a period of six months. There was a trend for increasing HSA concentration in the tear film over the six months of extended wear, but this increase was not statistically significant. In an orthokeratology study, Choy et al. found increasing amounts of HSA, while other tear film proteins (lysozyme, lactoferrin and lipocalin) remained in an unchanged concentration.[57] The ratio

between HSA and lactoferrin has also been reported as an indicator for diagnosing primary Sjogren's Syndrome (SS).[173] Bjerrum measured the protein concentration in patients with connective tissue diseases, SS and controls and concluded that an albumin:lactoferrin ratio above 2:1 is commonly found in patients diagnosed with SS. These findings are of potential significance, since higher protein concentrations in the tear film also appear to lead to increased deposition levels on contact lenses.[132,174-176]

1.5.4 Albumin adhesion to various substrates

The process of protein adsorption from an aqueous solution onto a solid surface is typically described in three steps. Firstly, transportation of the protein from the solution towards the solid surface occurs. This is followed by attachment of the protein to the surface, and finally the protein structure undergoes a conformational change after adsorption.[177] Carter and Ho investigated the physicochemical properties of HSA and described it as a flexible protein that easily changes its molecular structure.[178] Fluorescent X-ray techniques revealed that the BSA molecules flattened when bound on a gold substrate and the heart-shaped protein, with an initial side length of 3 x 80 Å, increased to a side length of 127 Å, with a simultaneous reduction in depth from 30 Å to 11.6 Å, with this short axis being perpendicular to the solid surface.[153,179] The amount of HSA that forms a monomolecular layer on most surfaces is approximately 0.15μg/cm^2.[180]

Ishiguro and colleagues investigated how lysozyme and BSA deposited and underwent conformational changes on poly tris(trimethylsiloxy)silylstyrene (pTTS), a highly hydrophobic polymer.[181] They reported very different adsorption behaviour

for the two proteins. Conformational changes of BSA derived strongly from the amount adsorbed to the surface, regardless of soaking time or BSA concentration in the aqueous solution. This was different to lysozyme, where the adsorption time was the leading factor that influenced changes in lysozyme conformation, regardless of the concentration in the solution or the adsorption amount. During the first 15 minutes, BSA adsorption was nearly complete, with only a minor increase occurring over the following 10 hours, while lysozyme build-up rose significantly over the 10 hour time period. After adsorption on pTTS, both BSA and lysozyme exhibited smaller α-helix contents and larger contents of β-structure, turn and random coil.[181] Similar findings of conformational changes occurring after short periods of time have been noted for contact lens materials. Garret et al. looked at a variety of contact lens materials and reported changes in the HSA structure when adsorbed to vifilcon A, after as little as one hour of exposure.[182]

1.5.5 Albumin adsorption at biomaterial interfaces

It is clear that albumin is found extensively throughout the body and in the tear film. An understanding of the interaction of this protein with biomaterials is of great importance to understanding biocompatibility. Implanted biomaterials are expected to perform a specific task, without being affected by the biological host and without causing side effects such as toxic, carcinogenic, immunogenic or inflammatory responses. Biomaterials are used for contact lenses and a variety of medical applications, including artificial blood vessels, catheters or drug delivery devices.[4,5,183]

Albumin adsorption is the initial event that occurs after the implant comes into contact with blood serum. The protein is then replaced by immunoglobulin-G, which in turn is replaced by fibrinogen and high molecular weight kininogen. This adsorption and desorption process of blood plasma proteins on artificial surfaces is known as the Vroman effect.[184] It has been shown that platelets can adhere to fibrinogen, which significantly increases the risk of thrombogenesis.[185-187] It is desirable to have a minimum amount of adsorbed protein onto the biomaterial and, ideally, this uptake should be reversible, with minimal conformational change occurring to the irreversibly adsorbed protein.[188-190] To improve biocompatibility and minimize the adsorption of fibrinogen and platelets some artificial organs undergo HSA treatment prior to surgery.[191]

Within the eye, the aqueous humour of the interior eye has no cellular components and therefore the response to intraocular lenses (IOL) after cataract surgery is mainly affected by the adsorption of various proteins, such as HSA and various globulins.[192]

On the ocular surface, deposition of albumin may play a significant role in healthy contact lens wear. Taylor and coworkers demonstrated that increased HSA deposition on etafilcon A lenses resulted in increased adherence of bacteria such as Pseudomonas aeruginosa and Staphylococcus epidermidis.[174] However, the opposite was true for polymacon lenses, with higher HSA deposition being associated with lower bacterial adherence. Other studies have confirmed that some tear-coated contact lens materials enhance adhesion of Pseudomonas aeruginosa, but high individual variation is always reported.[141,193]

1.5.6 Albumin adsorption on contact lens materials

Contact lenses represent a very specific type of biomaterial interface, in which the material is exposed to both the tear film and various environmental factors. While the level of protein deposition on contact lenses is strongly influenced by the tear composition, it is also modified by the chemical characteristics of the lens material.[122,182,194,195] It has been shown that material composition [121] and properties like water content [123] and pore size [120,196] roughness of the surface,[128] hydrophobicity [121,122] and charge,[140,176,195] all play a role, in addition to tear film pH and ionic strength.[132,175] Finally, protein characteristics such as size,[120] charge [132] and time of material exposure to the protein [15,119,122-126,129,132,133,137,181,182,194] are all important factors to consider. When patients present with extensively deposited lenses, this deposition will frequently include albumin as a component [43,123,137,139,142,151,152] (Figure 1-3). However, visual inspection by the clinician will be unable to determine the exact composition of the deposition seen, with various laboratory-based assays being required to identify individual components.

In vitro, in vivo and ex vivo studies have all been extensively used to describe protein deposition on contact lens materials. During these studies a number of key variables relating to the material under consideration have all proven to be influential in determining the degree to which albumin deposition occurs.

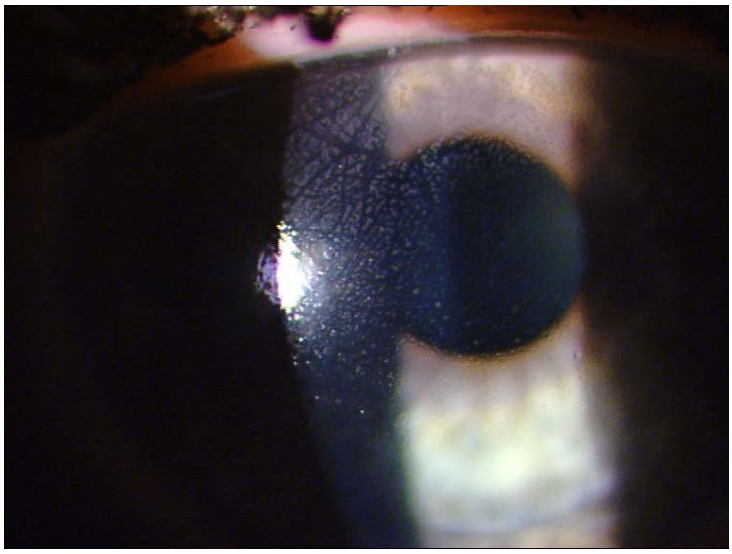

Figure 1-3: Slit lamp appearance of a heavily deposited hydrogel contact lens

1.5.7 Water content

Soft contact lenses based on pHEMA are often combined with other monomers and polymers to enhance surface wettability, strength, flexibility and oxygen permeability.[197] In pHEMA-based hydrogels, increasing water content results in increased oxygen permeability,[197] and it has been shown previously that water content can influence the level of protein deposition.

Garrett and coworkers synthesized a variety of carboxymethylated pHEMA hydrogels with varying degrees of carboxymethylation, with higher levels of carboxymethylation resulting in lenses with a higher ionic charge and water content.[120] Using a radiolabel-tracer technique they found a clear trend, with increasing water content resulting in decreased amounts of albumin deposition.[120] This is in agreement with the results from Keith et al.[123] who found significant differences in albumin deposition between commercially available contact lenses

with low and high water content. All lenses were soaked in an artificial tear solution and two low water content soft lens materials (pHEMA at 38% water content) exhibited albumin deposition, while no detectable levels of albumin were found on four materials with water contents >55%.[123]

Bohnert et al. investigated a variety of commercially available lens materials, in conjunction with a number of pHEMA materials synthesized with N-vinyl pyrrolidone (NVP), acrylamide (AAM) and methacrylic acid (MAA).[122] They found that the deposition of radiolabeled albumin was similar in materials of varying water content, suggesting that water content alone is not the driving force for albumin deposition.[122] This issue of protein deposition and water content is somewhat complicated, as the deposition is driven by both the charge and water content of the material under consideration, in addition to the size and charge of the depositing protein. In general, lower water content materials tend to deposit proteins such as albumin, in comparison with higher water content materials, which tend to deposit proteins such as lysozyme. This trend is exemplified in the study of Bohnert et al., where lysozyme deposition was greatest on an ionic composition of HEMA-MAA with water contents of 35% and 42%, followed by high water content hydrogels, suggesting that both charge and water content are important.[122]

Subbaraman et al. incubated five commercially available pHEMA-based hydrogel materials over 28 days in lysozyme.[97] He found increasing lysozyme uptake with increasing water content, with the exception of etafilcon A (58% water), which adsorbed multiple times more lysozyme than all other materials. He also reported on five silicone hydrogel (SH) lenses. These materials all deposited significantly less lysozyme than the pHEMA-based conventional hydrogels and a

trend for lower water content SH materials to deposit less lysozyme was also apparent.[97]

While some studies indicate that albumin deposition is inversely proportional to water content, others suggest that this is not the case, indicating that water content alone is not the sole driving force for albumin deposition.[121-123,133,176,182]

1.5.8 Hydrophobicity

Hydrogel materials have both hydrophilic and hydrophobic domains, which are influenced by the various monomers used to produce the contact lens material. Factors such as surface wettability and tear film deposition are both markedly affected by the hydrophilicity and hydrophobicity of the lens material. When the surface is covered in a fluid then the surface is orientated such that more hydrophilic components are present at the material interface. In situations where the surface becomes dehydrated (such as that which occurs when the tear film breaks), then chain rotation forces come into play, whereby the hydrophobic polymeric components become reorientated such that they are preferentially expressed on the biomaterial surface. This results in the surface becoming less wettable.

The relatively hydrophobic cross-linking agent ethylene glycol dimethacrylate (EGDMA) is frequently used in the polymerization of pHEMA. Bajpai and Mishra used a spectrophotometric procedure and reported that increasing concentrations of EGDMA increased albumin deposition.[176] Bohnert et al. synthesized lens materials with various concentrations of relatively hydrophobic MMA and hydrophilic HEMA components and reported that increasing levels of HEMA decreased albumin

deposition.[122] In contrast, a study from Pokidysheva et al. investigated four intraocular lenses and they found no significant correlation between hydrophobicity of the material and the level of albumin deposition.[192] However, their results clearly show that hydrophobic PMMA adsorbed the highest level of albumin, and significantly more than pHEMA, which is in agreement with the other studies described above.[198] However, Barbucci and coworkers synthesized hydrogels with different cross-linking agents to increase the hydrophobic component of the material, and investigated adsorption kinetics and potential denaturing of HSA and fibrinogen using infrared spectroscopy coupled with the attenuated total reflection technique (ATR–FTIR).[198] They reported a decreasing HSA uptake with increasing hydrophobicity of the material, but the opposite trend was found for fibrinogen with increasing adsorption at increasing hydrophobicity. Furthermore, the hydrophobic character of the material resulted in significantly stronger conformational changes for HSA compared to fibrionogen. It is worthwhile pointing out that the use of different types of cross-linkers might also affect other chemical properties such as strength and pore size of the polymer and not just the hydrophobic nature of the material.

Studies have shown that with higher concentrations of cross-linking agents the material modulus increases and the pore sizes decrease making it more difficult for larger proteins to penetrate into the matrix.[199,200]

In conclusion, the majority of studies report that albumin deposits in higher concentrations on hydrophobic surfaces,[128,134,182,195,198,201,202] as compared to relatively hydrophilic surfaces.

1.5.9 Charge

Many studies have investigated the pH of the tear film and a range from 5.2 to 8.6 has been reported,[203,204] with a mean pH value of 7.0 to 7.5. Therefore, albumin with an isoionic point (IOP of 5.16) has a negative charge in the tear film, as compared with lysozyme (with an IOP of 11.4) which has a net positive charge. In general, proteins absorb in maximum amounts on solid surfaces if the solution containing the protein has approximately the same isoionic pH as the protein. This is true for albumin interactions with hydrogels, with the highest albumin uptake occurring at a pH around 5.0 [133,175,176] or slightly below.[121]

In addition to the pH of the tear film and the polarity of the protein, the relative charge of the material substrate is also highly relevant for the level of deposition. Contact lens materials are categorized in one of four FDA groups, with FDA groups III and IV being considered ionic or negatively charged.[197] PolyHEMA itself is non-ionic, but the addition of monomers such as methacrylic acid (MAA), which are commonly used to enhance wettability and/or increase the water content, produces a polymer with an overall net negative charge compared with the tear film. Garrett and coworkers investigated the effect of ionic charge on the uptake of radiolabeled HSA and lysozyme.[120] Their results showed that increasing the negative charge of the material increased the deposition of positively charged lysozyme and reduced the deposition of negatively charged HSA.[120] In a later study,[121] Garrett investigated the deposition on materials containing negatively charged MAA and relatively neutral NVP. Once again, increasing MAA resulted in greater deposition of lysozyme and reduced deposition of albumin. Both radiolabeled proteins adsorbed in higher amounts with increasing NVP concentrations; however the amount of

lysozyme detected on the lens was always multiple times higher compared to the albumin uptake.[121] This is in agreement with a study from Moradi et al., where they investigated the same proteins and their interactions with pHEMA and acrylic acid (AA).[132] As before, the negative AA adsorbed less albumin and more lysozyme than the neutral pHEMA, which showed higher albumin uptake.[132]

Contrary to these findings for lysozyme is the study of Lord et al..[195] They investigated HSA uptake on pHEMA, pHEMA-MAA, pHEMA–MAA-NVP and PMMA materials using the quartz crystal microbalance with dissipation (QCM-D) technique. They did not find increased lysozyme uptake on the negatively charged pHEMA-MAA: however, they found the same adsorption pattern for HSA as described in other studies, confirming that HSA adsorbed in highest concentrations to PMMA, followed by pHEMA-MAA-NVP and pHEMA, with the lowest albumin uptake reported for the most negatively charged substrate (pHEMA-MAA).[132] A further study comparing nonionic to anionic (negatively charged) and cationic (positively charged) materials was conducted by Soltys-Robitaille.[140] They used matrix assisted laser desorption ionization mass spectrometry (MALDI-ToF MS) and detected albumin on the cationic lens material but not on the pure pHEMA material. Likewise, lysozyme was detected on the anionic material only.[140]

In conclusion, these studies all reveal that electrostatic attraction has a strong impact on albumin deposition. The negatively charged albumin is more likely to deposit on neutral or positively charged substrates than on materials with a net negative charge.

1.5.10 Pore size and surface roughness

Protein penetration into hydrogel materials depends on the pore size and the density of the polymer chains in the material, as well as the structure and size of the protein under consideration. Albumin is known to be a flexible protein which can easily change its original heart-shaped structure (diameter of approximately 55 Å) when binding to other molecules such as fatty acids or depositing onto a solid surface.[178,205,206] Wood and coworkers determined the pore size of HEMA with different concentrations of the cross-linker EDGMA.[207] They reported pore diameters of 11.82 Å for pure pHEMA, and even at a maximum concentration of EDGMA of $1.59/10^4$ mol cm^{-3} the average pore size only decreased minimally to 11.02 Å. Significantly larger pore dimensions were found by Gatin and coworkers.[208] They used different experimental and simulation techniques to determine the pore size of a pHEMA-based contact lens and reported an average pore diameter of 428 Å. However, most researchers have reported pore sizes < 100 Å for the surface of various contact lens materials.

Gachon et al. reported pore diameters between 56 and 70.6 Å for poly(MMA-VP) lenses, by measuring with a two-dimensional electrophoretic system which protein can penetrate into hydrogels and which ones are blocked due to the proteins being too large.[196] The two hydrogels examined had identical water contents (70%) and monomer composition, but were sourced from different companies. Albumin was detected in both hydrogels, but the larger protein ceruloplasmin (diameter of 66.2 Å) was only found in one of them, indicating the impact of manufacturing on average pore diameter and surface structure. Garrett and coworkers created two different models to calculate the actual average pore

size, based on the water content of the hydrogel material.[120] They added different concentrations of MAA to pHEMA to increase the water content in the material and calculated the changing pore sizes. For a maximum concentration of 5% MAA they calculated an average pore diameter of 34.7 and 29.3 Å for their two models, and therefore predicted that HSA should not penetrate into their material, which they confirmed experimentally.[120]

However, a recent study conducted by Luensmann et al. investigated BSA penetration into a conventional pHEMA-MAA and a plasma-treated SH contact lens using confocal laser scanning microscopy.[209] They labeled BSA with a fluorescent dye and found increasing BSA uptake into the lens matrix for the pHEMA material over time, with the SH lens only detecting the fluorescent signal from the labeled protein on the lens surface. This might suggest that the polymer chains were more dense for the SH lens and the pore size on the surface was < 55 Å, while the surface structure of the pHEMA lens was looser and/or the average pore size was > 55 Å. The impact of different techniques for manufacturing pHEMA contact lenses and albumin adsorption was investigated by Castillo et al..[128,175] After an incubation period of 72 hours they reported a 1.5 times higher HSA uptake on lathe-cut lenses, which provide a rougher surface compared to the spin cast lenses with a smoother surface.

In summary, pore sizes for contact lens materials vary significantly between the polymer composition, manufacturing procedure and the applied measurement technique. It would appear that the average pore size of pHEMA-based contact lenses is between 20 to 70 Å and that albumin uptake can be mediated by this factor, with larger pore sizes exhibiting greater – and faster - penetration.

1.5.11 Temperature and ionic strength

Albumin deposition decreases with increasing temperature of the solution. Demirel et al. measured the albumin uptake onto hydrogels between 5ºC and 40ºC and found more than double the amount of albumin deposited at 5 ºC, as compared to 40 ºC.[175]They suggested that interactions between the hydrogel and the protein were based on hydrogen bonds, which are weakened with increasing temperature.

Ionic strength of the surrounding media also has an impact on the amount of albumin depositing on the biomaterial. Bajpai and Mishra found decreasing BSA adsorption on pHEMA with increasing ionic strength of the solution, measured at pH 7.4.[176] However, no such strong tendency was observed by Moradi et al., who investigated the uptake of lysozyme and chicken egg albumin onto pHEMA and acrylic acid materials by measuring the UV absorbance of the proteins.[132]

1.5.12 Conclusions

Within seconds of insertion, contact lenses are coated with tears, which form a biofilm over the lens surface. This coating, which contains all the components of the tear film, starts to adhere to the lens and progressively increases over time. Increasing levels of HSA in the tear film are found during contact lens wear, especially during overnight wear, and the deposition of HSA is driven by many factors, including the concentration in the tears and the underlying chemical composition of the material being worn. Thus far, most published data have focused on the amount of deposited HSA, and only little is known about its degree of denaturation.[181,182] Future work should examine the potential impact of

denaturation of HSA on immunological responses and clinical consequence of HSA accumulation on contact lenses, as the latest generation of silicone hydrogel materials appears to be deposit only small amounts of protein, but this protein is often denatured.[97,100]

From this review, it can be concluded that many factors impact the adsorption of albumin onto hydrogel and PMMA lens materials. The higher the concentration of albumin in the tear film the greater the degree of deposition that can be expected on the lens material, particularly if the lens is worn overnight, or the patient exhibits dry eye or ocular surface disease. In addition, a larger pore size of the lens polymer will also increase albumin absorption. However, albumin deposition can be minimized if the material exhibits a net negative charge, is relatively hydrophilic and exhibits a high water content. Given these characteristics, deposition on silicone hydrogels, which now comprise a significant proportion of the lens materials fitted worldwide,[29,34] is to be expected and the deposition of albumin and its structural conformation on silicone hydrogels should be a focus of future work .

1.6 Protein evaluation on contact lenses

A number of qualitative and quantitative techniques have been applied to analyze protein deposition on contact lens materials. They can be categorized into three groups: Clinical assessment, assays and imaging techniques. While none of these methods can exactly describe the protein structure, quantity and distribution at the same time, each technique has the advantage of being able to provide very specific information about the deposition.

1.6.1 Clinical assessment

Subjective grading provides a fast, non-destructive method to assess deposition on contact lenses. Rudko and Proby categorized the degree of visible deposition on soft contact lenses using a slit lamp, as described in Table 1-5.[210]

Table 1-5: Rudko classification

Type I	No deposits or films detectable under 7x magnification
Type II	Deposition only visible under 7x magnification
Type III	Deposition visible on dry lens under normal lighting conditions without the aid of magnification; deposition not visible on the wet lens
Type IV	Deposition visible on either dry or wet lens under normal lighting conditions without the aid of magnification

Despite some modifications of this classification, the lack of correlation between Rudko scores and the total amount of protein deposited on lenses remains and differentiation between deposition types are difficult to determine.[138,211] Nevertheless, the assessment of the overall contact lens performance in situ

requires an evaluation of a number of aspects, including ocular health, comfort, surface wettability, lens movement, lens centration and also lens deposition.

1.6.2 Assays

Biochemical assays provide detailed information on the type of deposition. Assays typically require the extraction of the deposit from the contact lens before it can be analyzed and often focus on the identification of the protein content. Chemical reagents that are typically used to undertake the extraction include urea, guanidine hydrochloride, potassium thiocyanate, potassium perchlorate, hydroxylamine, ethylene dithretyl acetamide, sodium dodecyl suphate (SDS), dithiolthreitol, and trifluoroacetic acid/acetonitrile.[39,123] The efficiency of these reagents depends on the type of deposition and lens material and may remove as little as 25% of the deposited substances.[145,212]

General protein assays, amino acid analysis, gel electrophoresis and high performance liquid chromatography (HPLC) have been used to quantify and identify the deposited proteins. Other analytical assays, such as the micrococcyl activity assay, can furthermore determine the conformational state of the protein.[98,100,102] Although most assays have a high specificity, they experience difficulties identifying the few hundred different proteins found in the tears.[106,213] In addition, in many cases the extraction efficiency is unspecified, the location of the deposited protein is unknown, it is uncertain, if denatured proteins can be extracted from the lens material as efficiently as native proteins, and finally it is unstated whether or not the reagent denatures the protein during the extraction process.[43]

1.6.3 Imaging techniques

Microscopic and spectroscopic techniques provide primarily qualitative results, with some techniques providing some level of quantitative information.[214] A number of microscopy techniques have been used to examine gross and fine morphological aspects of the deposition, including light-and dark field microscopy, phase contrast and interference microscopy.[214,215] For higher resolution imaging and elemental analysis, scanning electron (SEM) and transmission electron microscopy (TEM) have successfully been adopted.[151,216,217] Atomic force microscopy (AFM) provides details at the nanometer range and is therefore even more advanced compared to scanning microscopy techniques.[218] In contact lens research, AFM has been used to image surface roughness and tear film deposition.[219-222]

Spectroscopic methods typically measure the energy that is either absorbed or emitted by the deposited species and can, for example, identify proteins, carbohydrates or lipids by analyzing specific absorption bands. Ultraviolet (UV) and fluorescence spectroscopy,[223] attenuated total reflectance (ATR),[129] electron spectroscopy for chemical analysis (ESCA),[224] surface matrix assisted laser desorption/ionisation (MALDI) mass spectrometry [136,213] and radiolabeling [121,225] are just some examples of previously used spectroscopic techniques.

With resolutions of a few nanometers,[215,218] both spectroscopy and AFM microscopy techniques are very powerful for surface analysis. However, all of these techniques can only measure the outermost surface region, with a maximum depth of a few microns.[214]

1.6.3.1 Confocal microscopy

A confocal microscope provides higher transverse (XY) and axial (Z) resolutions as compared to conventional light microscopes, but is inferior when compared to electron or atomic force microscopes.[215,218,226] The resolution of a confocal microscope depends on the sample reflectivity, the numerical aperture of the objective lens, illumination wavelength and intensity. The principle design of a confocal microscope requires two pinholes: The first pinhole focuses the light on the specimen and the second pinhole allows only those light rays to pass through to the detector that are directly returning from the focal plane. Figure 1-4 demonstrates the reflected light path for a simple confocal design.

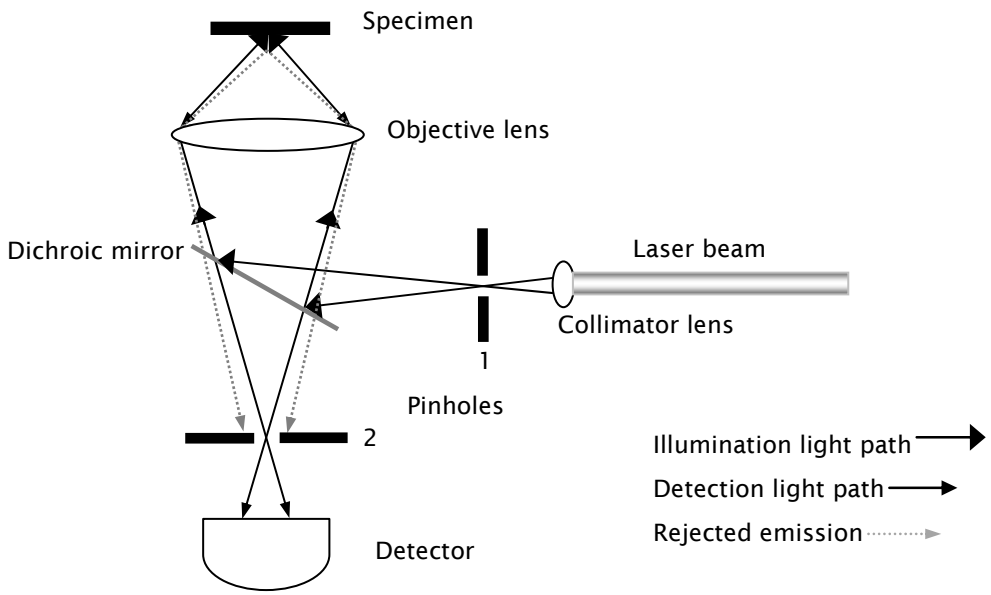

Figure 1-4: Principal design of a confocal microscope

The adjustment of the pinhole provides good observation of the specimen, and allows focusing on different levels of depth. The collection of multiple XY images throughout a transparent sample can finally be used to reconstruct a 3-dimensional image. Marvin Minsky invented the first confocal microscope in 1955 [227] and although modern instruments use more advanced optics and electronics, the key elements are still based on Minsky's design.[228] Most confocal microscopes collect either the reflected light from the specimen or (when using fluorescence) collect the light emitted from the fluorophore applied to the specimen.

1.6.3.1.1 Types of confocal microscopes

The first tandem confocal microscope was developed in 1968 and used rotating Nipkow disks to image living cells and tissue.[229] Two Nipkow disks were built into the system, with each disk being constituted of >100 pinholes, with diameters between 40 and 60 μm. Each pinhole in the illumination path had a conjugated pinhole for the reflected light returning from the sample. However, since the area of holes on the disk covered only 1-2%, only low levels of light reached the sample and made it difficult to image low reflecting tissue.[230] In a similar design, only a single Nipkow disk was used, in which illuminating and reflecting light followed the same optical path. Although it had the advantage of a simpler optical arrangement when compared to a tandem scanning Nipkow disk, the disadvantage of low light transmission remained.[230] Modern clinical tandem confocal microscopes are equipped with discs of 64000 pinholes and bright Xenon or Mercury arc illumination sources, for improved imaging of ocular tissue.[226]

Approximately at the same time that early tandem scanning confocal microscopes became available, slit scanning confocal microscopes were introduced.[231] These microscopes use conjugated slits for illumination and detection, with the distinct advantage of increased light transmittance and reduced scanning time.[226,232] Although true confocal imaging is only possible in the axis perpendicular to the slit height, the image quality is acceptable and slit scanning is successfully implemented in current clinical instruments to image, for example, corneal cell layers.[226,230,233,234] Images can be acquired at a rate of 25 frames/sec, scanning up to 350 images in one session.[228]

Confocal laser scanning microscopy (CLSM) has further been introduced for in vivo and in vitro purposes. The use of a 670nm Helium Neon diode provides better contrast compared to slit scanning microscopes, particularly towards the edges of an image. The beam spot of less than 1 µm in diameter scans over the object and de-scanning of the deflected light gets digitized to form the image. Today, clinical laser scanning confocal microscopes are used for both retinal and corneal imaging.[228]

The main difference between clinical and laboratory-based CLSM is the choice of the illumination source. Clinical instruments are required to use Class 1 lasers, to prevent any ocular damage. The laser intensity in these microscopes is typically limited to <1mW. Laboratory research CLSM devices commonly use 3B lasers, which are limited to a maximum of 500mW. Direct eye exposure to this laser beam is hazardous and may lead to permanent ocular damage.[235]

1.6.3.1.2 Zeiss LSM 510 Meta, Axiovert 200

This CLSM is used in laboratory applications and can perform a number of different microscopy techniques, for transmitted and reflected light imaging. Transmitted light applications include brightfield, differential interference contrast (DIC), phase or Varel contrast. The reflected light application allows fluorescence contrast microscopy (Figure 1-5).

This CLSM is primarily used for fluorescence contrast applications, including single or multi fluorescence imaging, fluorescence resonance energy transfer (FRET), fluorescence recovery after photobleaching (FRAP), fluorescent loss in photobleaching (FLIP), time lapse experiments etc. These techniques have successfully been applied to study cell dynamics, including diffusion and transport of fluorescently conjugated molecules such as proteins, and in materials research.[236-242]

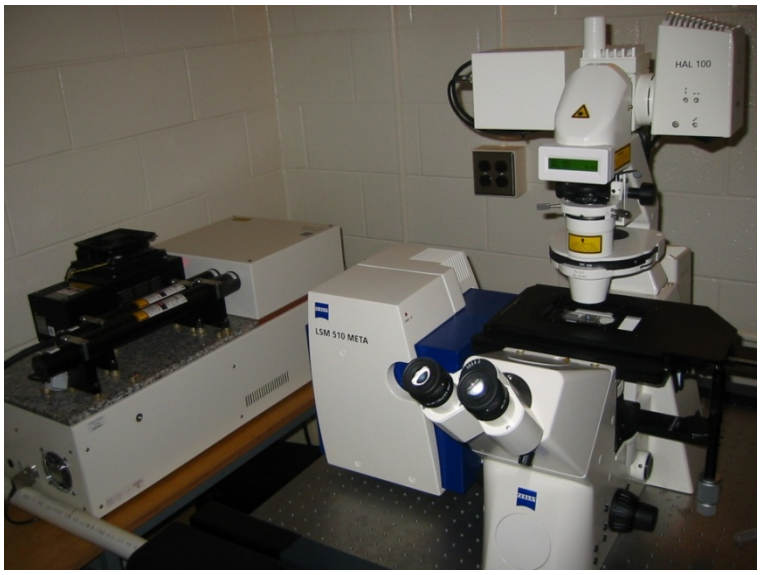

Figure 1-5: Zeiss LSM 510 Meta, Axiovert 200

The Zeiss 510 Meta is equipped with the following lasers: Diode laser – 405nm (25 mW), Argon multi-line gas laser – 458, 477, 488, 514nm (30 mW), Helium Neon gas laser – 543nm (1 mW), Helium Neon gas laser – 633nm (5 mW)

Available objectives provide a magnification range from 10x to 63x for air, water and oil immersion. Predefined main dichroic beam splitters (HFT) have windows for either a single or up to three different excitation wavelengths, depending on the application and the number of fluorophores. An additional secondary dichroic beam splitter (NFT) cut wavelengths below the excitation wavelength for improved image quality. A number of different long pass (LP), band pass (BP), or individual adjustable emission filters can be selected. The object plane is scanned in a point-by-point, line-by-line raster with an XY light deflection system. The detector is a photomultiplier that converts the optical information into electrical signals. Fluorescence imaging can achieve lateral (XY) resolutions of 0.2µm and axial resolutions up to 0.65 µm.[242]

1.6.3.2 Fluorescence

Photoluminescence occurs if a molecule absorbs photons from the UV or visible light spectrum, which raises the molecule into a high-energy electronic state within femtoseconds (10^{-15} sec). If this excited state remains stable for only a few nanoseconds (10^{-9} sec) and is followed by an energy release in form of light, it is called fluorescence. If light emission occurs with a delay between 10^{-4} and 10 sec after excitation has been stopped, it is called phosphorescence.[243] Figure 1-6 shows the different energy levels for fluorescence and phosphorescence.

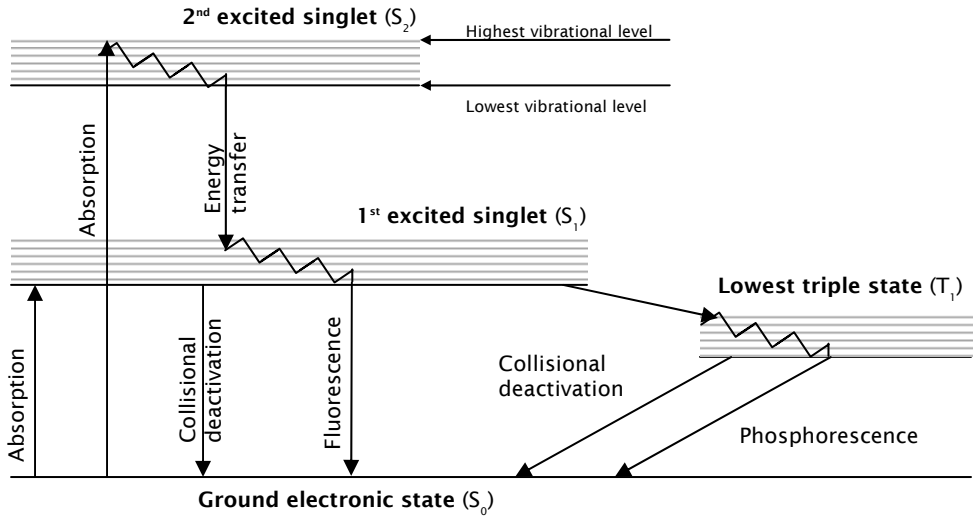

Figure 1-6: Schematic fluorescence and phosphorescence energy states

Light absorption raises the electron from the ground state (S_0) to a singlet excited state (S_1, S_2). The electron within this singlet state loses energy rapidly due to micro-environmental collisions, and drops from a higher vibrational level down, until it reaches the lowest vibrational level within the same singlet state. If the electron was first raised to S_2 it now drops down to the highest vibrational level of S_1. If it was first raised to S_1 it relaxes to S_0 while emitting light in the form of fluorescence, or if the remaining energy dissipated by further collisions the molecule returns to S_0 without light emission. The final relaxation path can also lead from S_1 to the triplet state (T_1). The energy drops down to the lowest vibrational level of T_1 and returns to S_0 either in form of phosphorescence or radiationless, due to collisional deactivation.

The intensity of the emitted light depends on the quantum yield of the fluorophore. The quantum yield describes the ratio between the amount of emitted and absorbed light, with a maximum value of 1 (total amount of absorbed light is emitted = bright light emission) and a minimum of 0 (none of the absorbed light is emitted). The quantum yield is primarily dependent on the molecular absorbance but is further impacted by a number of factors that can either increase or decrease (quench) the emission intensity. Factors that influence the emission signal strength are described in more detail in Chapter 4.

The excitation wavelength is generally different from the emission wavelength for both fluorescence and phosphorescence. In Stokes fluorescence, the emitted light is typically at a longer wavelength, which is explained by the energy loss before emission occurs. However, if thermal energy is added during the excitation process the emitted light may occur at a shorter wavelength, which is known as anti-Stokes fluorescence. The excitation spectrum for a specific molecule is identical to its absorbance spectrum, and depending on the substrate, it is possible to have more than one specific wavelength for excitation. As an example, Lucifer yellow's maximum excitation is at 280nm and 430nm, but maximum emission is always at 525nm.[244,245]

Molecules with no fluorescent or phosphorescent properties absorb light without energy transition of the electrons and the light is reemitted at the same wavelength. This is known as Raleigh scattering and can occur at all wavelengths.

1.6.3.3 Radiolabeling

The use of radioactive iodine isotopes to detect proteins was introduced over 50 years ago.[246] Although 37 iodine isotopes are characterized today, most of them are unsuitable because of their poor availability, stability specific activity, energy spectrum and short half-life of <1 hour.[247] The majority of these isotopes are gamma emitters, except for ^{137}I, ^{138}I and ^{139}I which emit beta rays. Popular isotopes for protein conjugation are ^{125}I and ^{131}I. The attachment of isotopes to proteins necessitates the addition of a reagent, therefore a number of techniques have been applied including iodine monochloride (ICL), peroxidase, electrolytic iodination or oxidizing techniques based on chloro-compounds.[248]

The ICL method was initially used as a halogenating agent in 1840 and became adapted for protein conjugation by McFarlane in 1958.[248,249] A 4-fold molar excess of ICL over protein has been suggested by Helmkamp, providing optimal labeling efficiency and a low impact on protein function.[250] The isotope ^{125}I binds to the aromatic ring of tyrosine, and thus for albumin - which has 21 tyrosine amino acids - approximately half of them may be available for conjugation.[251] The impact of iodine on protein properties has been debated, but the majority of studies seem to agree that radiolabeling causes only minor protein modification.[252-254] Studies investigating the quantity of protein sorption to various materials typically use low contents of radiolabeled protein, which are mixed with native protein to reach the required concentration. Horbett showed that the majority of plasma proteins deposited in similar quantities to pHEMA-based materials regardless of the percentage of radiolabeled protein content in the solution.[253] For the protein albumin, Horbett investigated concentrations of ^{125}I between 0.09 to 0.6%.

2. RATIONALE

Tear film deposition on contact lenses became a major focus of attention for clinicians and researchers almost as soon as the first hydrogel lenses were developed. Tear film components adhere to the lens and can reduce vision and wearer comfort and increase ocular health complications, particularly as the lens ages. The advent of frequent replacement systems resulted in a reduction in interest in tear film contamination of lenses, as lenses were thrown away before the deposits produced a clinical problem. However, although new silicone hydrogel materials are highly oxygen permeable and deposit less protein compared to pHEMA-based lenses, the occurrence rate of some contact lens complications - such as CLAPC that may be associated with deposition - appears higher with these new materials.

Protein adherence to any biomaterial - including contact lenses - is the initial response of the immune system to isolate the “foreign body” from the human system, and occurs within a few minutes after exposure. Although this interaction is a well known phenomenon in biomaterials research, to date no blood contacting material prevents protein adsorption, and the risk of further cell adherence and blood coagulation remains. Albumin is the most abundant protein in blood serum

and is therefore of particular interest when investigating blood-contacting biomaterials.

A number of investigative techniques can either image or quantify the protein accumulation on biomaterials, but it remains unclear whether or not the protein sorbs exclusively on the surface or can also penetrate the material matrix. This might be of interest, as proteins that are tightly bound to a surface are more likely to denature and cause undesirable complications. In contact lens wear, denatured proteins are closely related to the immunological response known as giant papillary conjunctivitis. Therefore the purpose of this research work focuses on the detection of proteins on the surface and throughout contact lenses and intraocular lenses to gain a better understanding of interactions between proteins and hydrogel biomaterials.

In the first study (Chapter 3) confocal laser scanning microscopy (CLSM) technique is introduced to locate proteins throughout contact lens materials. A fluorescein-based dye was conjugated to albumin and sorption profiles to pHEMA-based contact lenses and a surface coated silicone hydrogel (SH) lens were determined.

Chapter 4 evaluated the use of three different organic fluorescent probes on their impact on protein sorption behaviour. Four different contact lens materials were investigated, with some lenses being incubated in conjugated albumin and others incubated in dye solutions containing no protein. Comparisons between sorption patterns caused by the dye only and conjugated proteins are discussed.

Lysozyme is the most abundant protein in human tears and is known to adhere in high amounts to negatively charged surfaces. Chapter 5 applied the confocal technique previously developed to investigate nine different contact lens materials, including SH, neutral and charged pHEMA-lenses. A fluorescein-based dye and lucifer yellow were used for lysozyme conjugation. CLSM detected the fluorescent signal from the conjugated protein and sorption profiles of these two conjugates to the different material types were determined.

Contact lens cleaning solutions are required to disinfect, clean, store and rinse worn contact lenses. Previous studies have shown that their efficiency at removing proteins from a contact lens depends on the care regimen as well as the lens material investigated. However, it remained unclear if manual lens rubbing is more efficient for the removal of surface-deposited proteins, as compared with lens soaking alone. The aim of Chapter 6 was to investigate the efficiency of hydrogen peroxide and a multipurpose cleaning solution to remove lysozyme and albumin from three types of contact lenses. CLSM was used to determine the sorption profile and incubation in radiolabeled protein determined the total amount of protein deposited.

The application of this CLSM method for materials other than contact lenses was demonstrated in Chapter 7. Intraocular lenses (IOL) are frequently implanted into the eye to replace the opaque crystalline lens after cataract surgery. Following the surgery, inflammatory cell responses and cell proliferations are often observed, which is impacted by the surgical technique, the IOL material and design and the surrounding medium. The IOL is typically placed in the remaining capsular bag, which is surrounded by aqueous humour. Because albumin is the primary protein in

the aqueous humour, its interactions between silicone, polymethyl methacrylate and a hydrophilic acrylic materials was investigated. Albumin sorption profiles were qualitatively (CLSM) and quantitatively (radiolabeling) assessed.

In the following chapter of this thesis, the principle of CLSM will be described to detect fluorescently conjugated albumin throughout a pHEMA-based and a silicone hydrogel contact lens material.

3. CONFOCAL MICROSCOPY AND ALBUMIN PENETRATION INTO CONTACT LENSES

This chapter is published as follows:

Doerte Luensmann, Mary-Ann Glasier, Feng Zhang, Vladimir Bantseev,

Trefford Simpson, Lyndon Jones

Centre for Contact Lens Research, School of Optometry, University of Waterloo, 200, University Avenue West, Waterloo, Ontario, N2L 3G1, Canada

Optom Vis Sci 2007;84:839–847 - Reprinted with permission

	Concept / Design	Recruitment	Acquisition of data	Analysis	Write-up / publication
Luensmann	Y	n/a	Y	Y	Y
Glasier	Y	n/a	-	-	-
Zhang	Y	n/a	Y	-	-
Bantseev	Y	n/a	-	-	Y
Simpson	Y	n/a	-	Y	Y
Jones	Y	n/a	-	-	Y

3.1 Overview

Purpose: To develop a novel in vitro method to detect the depth of penetration of the tear film protein albumin into contact lens materials using confocal laser scanning microscopy (CLSM).

Methods: A poly-HEMA-based hydrogel (etafilcon A) and a silicone hydrogel material (lotrafilcon B) were examined. In vitro, bovine serum albumin (BSA) was labeled with 5-(4,6-dichloro-s-triazin-2-ylamino) fluorescein hydrochloride (DTAF). The lenses were incubated in this protein solution (0.5 mg/ml) at 37˚C. After 1 and 7 days incubation, the lenses were examined using CLSM (Zeiss 510, config. META 18) and the location of the fluorescently labeled BSA was identified.

Results: BSA adsorption on the surface and penetration into the lens matrix occurred at a higher concentration for etafilcon compared to lotrafilcon ($p<0.001$). For both materials, BSA was detected on the surface after 1 day of incubation. Significant levels of BSA were detected within the matrix of etafilcon after as little as 1 day ($p<0.001$), but no BSA was detected in the matrix of lotrafilcon at any time ($p>0.05$).

Conclusions: CLSM can be successfully used to examine the depth of penetration of fluorescently labeled proteins into various hydrogel polymers. Our results show that etafilcon lenses both adsorb BSA on the surface and absorb BSA within the matrix, whereas lotrafilcon B adsorbs small amounts of BSA on the surface only.

3.2 Introduction

Deposition of tear film components such as proteins, mucins and lipids on contact lenses can cause discomfort and inflammatory complications such as giant papillary conjunctivitis (GPC) [1-6] and these problems can appear with any type of daily or extended wear lenses.[7] The recently introduced silicone hydrogel (SH) materials have different deposition profiles to that seen with conventional hydrogel lenses (CH) based on pHEMA, with lower levels of protein deposition and higher levels of lipid deposition being measured.[8-12]

Of the tear film proteins that deposit on contact lenses, most of the literature to-date has concentrated on the deposition of the positively charged protein lysozyme, which is the most abundant protein in the tear film, with a concentration of approximately 3 mg/ml,[13-15] and a molecular weight of 14.4 kDa. Another protein of interest is the larger protein serum albumin, with a molecular weight of 66 kDa, which is negatively charged and has a lower concentration in the tear film of approximately 0.04 mg/ml during the daytime. This amount increases to approximately 0.2 mg/ml during sleep and may rise as high as 0.5 mg/ml following wear of orthokeratology lenses.[14,15]

Work to-date on conventional pHEMA-based lens materials has shown that the deposition of lysozyme and albumin depends upon the polymer composition,[16] charge [17-19] and water content,[20] with lysozyme being mainly deposited on negatively charged substrates and albumin being deposited on neutral and/or positively charged materials. Thus far, while the deposition of lysozyme on SH materials has

been determined,[9-12] less information is available describing the deposition of albumin on these new materials.[21]

A variety of methods can be used to examine deposition on contact lenses, including visible clinical grading, surface imaging and analytical methods that require the deposits of interest be removed.[8,22-25] Major disadvantages for clinical grading include substantial inter-subject variability and a lack of biochemical analysis of the deposits. Imaging techniques such as microscopy do not allow for quantification of the species of interest. Methods requiring removal lack certainty both in terms of the removal process and the exact location of the deposited substance on or within the lens material.

The purpose of this study was to develop a novel method to investigate the spatial and temporal penetration profile of serum albumin labelled with a fluorescent marker on and into various hydrogel contact lens materials and to compare the differences between a representative pHEMA-based hydrogel and a siloxane hydrogel.

3.3 Methods

Bovine serum albumin (BSA) with a purity of 99% (agarose gel electrophoresis) and a molecular weight of 66 kDa was purchased from Sigma-Aldrich (St. Louis, MO, USA). BSA was chosen for this study, since it has very similar properties to albumin from human serum (HSA).[26] BSA was labelled with the fluorescent dye DTAF (5-[4,6-Dichloro-s-triazin-2-ylamino] fluorescein hydrochloride) from Sigma-Aldrich (St. Louis, MO, USA). This dye was chosen as it

does not significantly change the molecular weight and size of BSA.[27,28] For the labeling procedure, BSA (180 mg) was dissolved in 0.05M borate buffer (pH = 8.5) containing 0.04M NaCl (18 ml). DTAF (10 mg) was dissolved in dimethylsulfoxide (DMSO; 1 ml; Sigma-Aldrich, St. Louis, MO, USA) and was added drop wise, while stirring the solution. The BSA-DTAF was stirred for two hours at room temperature before separating the conjugate from unreacted labeling agent using PD10 desalting columns (Amersham Biosciences, Piscataway, NJ, USA). Further elimination of unreacted DTAF was done by dialysis against phosphate buffered saline (PBS, pH 7.4) (5x4 litre). The dialysis cassettes were purchased from Pierce, Rockford, IL, USA and the membrane, with pore sizes of 7000 MW, filtered all particles out of the protein solution that were small enough to diffuse through the pores, including free dye and small protein fractions. Subsequent measurements with a fluorescence spectrophotometer (Hitachi F-4500, Tokyo, Japan) verified a continuous decrease of the unbound dye. The calculated labeling ratio was 2 molecules of dye per molecule of BSA, and this solution was diluted with PBS to obtain a final BSA concentration of 0.5 mg/ml. To verify the purity and molecular size of the BSA before and after the labeling process a sodium dodecyl sulfate polyacrylamide gel electrophoresis (SDS-PAGE) was performed. A prestained standard with molecular markers from 10 kDa to 250 kDa was used on a PhastGel Gradient 10-15 (Amersham Bioscience, Uppsala, Sweden)

The lens materials examined were etafilcon A (Acuvue 2; Johnson & Johnson, Jacksonville, FL, USA) and lotrafilcon B (O_2Optix; CIBA Vision, Duluth, GA, USA), details of which can be seen in Table 3-1.

Table 3-1: Hydrogel lens materials

Proprietary name	O_2 Optix	Acuvue 2
United States adopted name	lotrafilcon B	etafilcon A
Manufacturer	CIBA Vision	Johnson & Johnson
Center thickness (@ –3.00 D) mm	0.08	0.084
Water content (%)	33	58
Oxygen permeability ($\times 10^{-11}$)	110	17
Oxygen transmissibility ($\times 10^{-9}$)	138	21
Surface treatment	25nm plasma coating with high refractive index	No surface treatment
FDA group	I	IV
Principal monomers	DMA + TRIS + siloxane macromer	HEMA + MAA

DMA (*N,N*-dimethylacrylamide); HEMA (poly-2-hydroxyethyl methacrylate); MA (methacrylic acid); TRIS (trimethylsiloxy silane)

All lenses examined had powers of -3.00D. They were individually soaked for 30 minutes in 10 ml sterilised PBS, before they were incubated in the protein solution for 1 and 7 days, with four replicates for each condition. The labelled BSA solution was sterilised with syringe filters (Pall Corporation, Ann Arbor MI, USA) and in total 8 lenses of each type were incubated in individual amber vials, which were filled with 1 ml of the protein solutions and kept in an oven at 37 degrees on a gently rotating plate. Negative controls consisted of 8 further lenses for each lens type, incubated for equivalent periods of time in PBS. Thus, 32 lenses in total were examined (2 lens types, 2 doping solutions, 2 incubation times and 4 replicates of each). After the defined incubation time, lenses were rinsed for five seconds with

PBS and a punch press was used to remove a circle of 4 mm diameter from the middle of the lens, which was then placed on a microscope slide (Fisher Scientific, Pittsburgh, PA, USA) using PBS as mounting solution. Samples were covered with cover-slides (VWR, Bridgeport NJ, USA), sealed with nail polish.

Samples were analyzed using a confocal laser scanning microscope (CLSM) Zeiss 510, config. META 18 equipped with an inverted motorized microscope Axiovert 200M, (Zeiss Inc. Toronto, Canada). The Argon laser was set to an output of 50% to obtain a stable laser beam. The beam pathway was assigned to channel 3, and the main (HFT 488nm) and secondary (NFT 490nm) dichroic mirrors were chosen according to the dye specific excitation wavelength. The long pass filter LP 505nm was used to detect the emission wavelength. The water-immersion C-Apochromat objective (numeric aperture 1.2) was chosen to achieve an optimised image quality, and the pinhole size was set to 1 Airy unit to eliminate out of focus rays. Settings for the scan control were: 625 for the detector gain, -0.025 for the amplifier offset and 1 for the amplifier gain. A laser transmission of 5% at 488nm was chosen to minimise photobleaching of the fluorescent dye. For the image settings a frame size of 512x512 pixels, maximum scan speed, a pixel depth of 8 bit and the returning scan direction was used for collection of all images. All described microscope settings remained the same for the duration of the study.

To detect the contact lens surface of the sample under the microscope, a small area on the lens was marked with a pen that was visible using 2% transmitted light. A suitable position on the lens surface was chosen and using the z-stack, which is the module to measure through the sample, the first and last positions on

the sample were determined. With a constant step size of 1 µm, continuous images were captured from the front to the back surface of the sample.

Six scans of each sample were obtained. To investigate the influence of any potential photobleaching effects, two measurements at identical central locations were taken (scan numbers 1 and 6), with a scan size of 190x190 µm. After scan 1 and before scan 6 four other readings (scans 2-5) were obtained in the four corners of the sample (115x65 µm) in a randomised fashion to investigate differences in penetration profiles over the lens. Scans 1 and 6 were measured using 400x resolution and the other locations were measured using 800x resolution. ImageJ (Bethesda, MD, USA) was used to calculate the fluorescence signal of DTAF for each single image along the vertical axis.

The cross-section through the lens material was divided into three regions of interest (Figure 3-1). The “front surface region” was defined as the average of the front fluorescence peak ± 2 µm, the “back surface region” was defined as the average of the rearmost peak ± 2 µm and a “central region” or “bulk” was defined as the average of the 30 central images, using the front and back peaks as borders.

One factor to consider when conducting studies using dye-tagged proteins is whether the data obtained could be due to the absorption of unbound dye and that the results obtained are more indicative of dye-binding rather than protein uptake. To reduce this, the labelled protein solution was extensively dialysed until only very minor amounts of fluorescent signal were detectable in the protein solution. In addition, lenses were incubated in a control PBS-DTAF solution without the addition

of BSA, at a dye concentration approximately 200 times lower than the study solution.

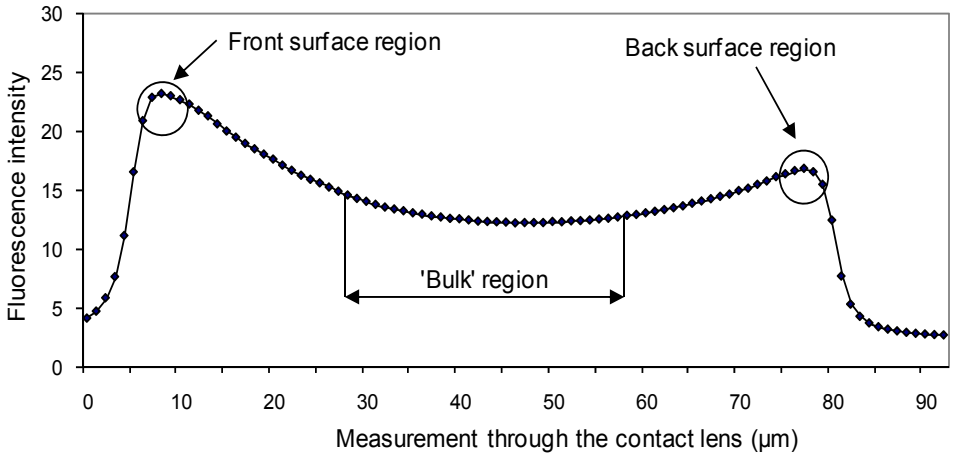

Figure 3-1: Definition of front, back and "bulk" regions for etafilcon A incubated in labeled BSA

The "front surface region" was defined as the average of the front fluorescence peak ±2 µm, the "back surface region" was defined as the average of the rearmost peak ±2 µm and a "central region" or "bulk" was defined as the average of the 30 central images, using the front and back peaks as borders. The x-axis shows the measurement through the thickness of the central lens material (µm) and the y-axis shows the relative fluorescence intensity.

For analysis of the protein uptake on the front, back and "bulk" regions, a repeated measures ANOVA (analysis of equal variance) was applied (significance level $p<0.05$), with the factors being solution (labelled BSA and PBS solution), contact lens type (lotrafilcon B and etafilcon A), incubation time (1 and 7 days) and location (the 4 corner scans). To determine if any photobleaching had occurred during the exposure to the confocal laser beam, the Limits of Agreement (LOA) between scans 1 and 6 were examined, where LOA = d ± 1.96 x sd on the three defined regions (front, back, bulk). The value 'd' is the mean difference between the

two central locations (1 and 6) and 'sd' is the calculated standard deviation. Additionally, the Correlation Coefficient of Concordance (CCC) was calculated to describe the concordance between the repeated scans (1 and 6).[29] CCC describes the deviation between the scans from a perfect 45° line and therefore the repeatability. (CCC=1 = perfect correlation and perfect repeatability; CCC=0 = no correlation and no repeatability).

3.4 Results

SDS-Page was used to verify purity and final molecular weight (approximately 66 kDa) for the unlabelled, labelled and sterilized BSA solutions, as seen in Figure 3-2. The gel also shows that no smaller BSA fractions appear below the standard of 50MW but some proteins aggregated and therefore weaker bands with higher molecular weights were found. These results are of importance, as it may be expected that smaller proteins or protein fractions would penetrate more easily into hydrogels polymers than the original BSA of 66 kDa. This was not the case in this study.

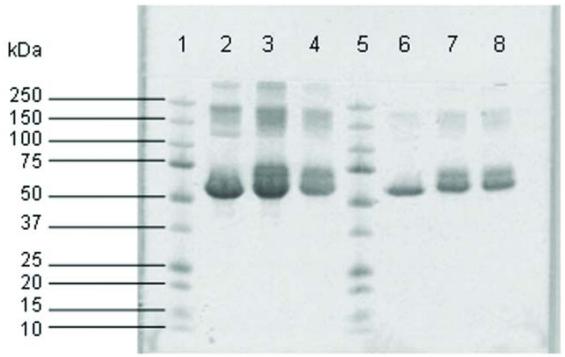

Figure 3-2: SDS-PAGE for different BSA-PBS solutions

SDS-Page was used to verify no proteins are smaller than the expected MW of 66 kDa. Column 1: Molecular marker; Column 2: 1.5 mg/ml BSA; Column 3: 1.5 mg/ml labeled BSA; Column 4: 0.5 mg/ml labeled BSA; Column 5: Molecular marker; Column 6: 0.25 mg/ml BSA; Column 7: 0.25 mg/ml labeled BSA; Column 8: 0.25 mg/ml labeled and sterilized BSA.

The fluorescent signals of the labelled BSA on the lens surfaces and inside the matrix were different for the two contact lens materials ($p<0.001$). Figures 3-3A and 3-3B demonstrate the typical pattern of the fluorescent signal on both surfaces and inside the matrix of etafilcon and lotrafilcon B materials after 7 days incubation with labelled BSA. The image galleries were plotted in a step size of 1 μm through the thickness of the lens materials. The brighter the image, the more fluorescent signal was detected, representing a greater degree of albumin deposition. For the etafilcon material (Figure 3-3A), an almost equally distributed fluorescent intensity was found on the surface regions and inside the matrix, indicating that the surface of the etafilcon lens was not a barrier for penetration of the BSA molecules. This was contrary to the results seen with the plasma-coated lotrafilcon B material (Figure 3-3B), where a weak fluorescence signal was detected on the surfaces and no penetration into the matrix was detected.

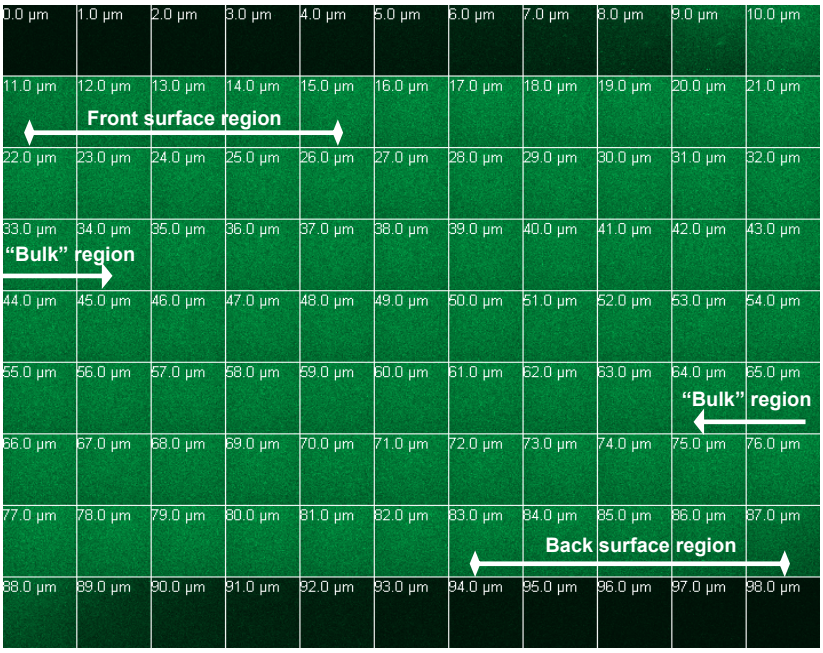

(A)

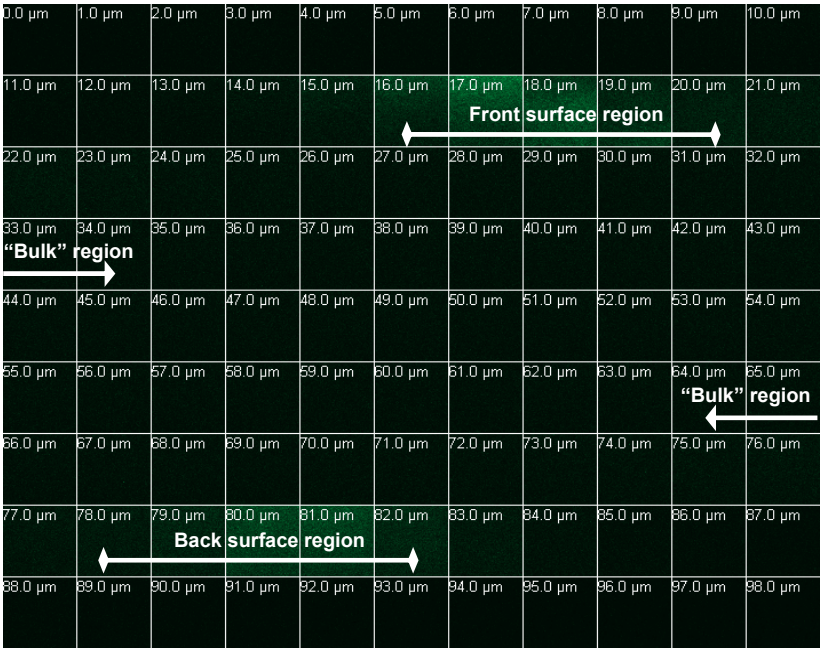

(B)

Figure 3-3: Image galleries of typical x-y-confocal scans for etafilcon A (A) and lotrafilcon B (B)

Images show examples after 7 days of incubation in labeled BSA. Brighter colors indicate an increased fluorescent signal and therefore a higher BSA concentration.

A typical fluorescence intensity profile for each lens material for each incubation time is plotted in figures 3-4A and 3-4B. These scans of individual replicates clearly reveal differences between materials in terms of fluorescence intensity on the lens surface and within the matrix, as well as the impact of time on protein accumulation.

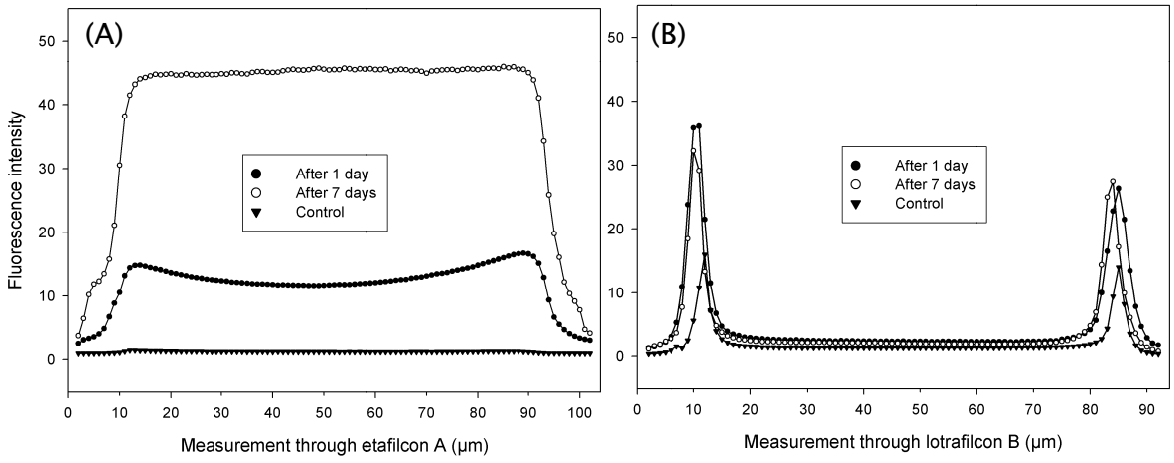

Figure 3-4: Typical pattern for BSA-DTAF penetration into etafilcon A (A) and lotrafilcon B (B)

Single scan were plotted after 1 and 7 days of incubation. The x-axis shows the measurement through the thickness of the central lens material (µm) and the y-axis shows the relative fluorescence intensity.

Figures 3-5(A+B) and 3-6 demonstrate the differences in fluorescence intensity over time for each of the three regions of interest (front-, back surface and 'bulk'), by taking all replicates into consideration.

Figure 3-5A illustrates the average fluorescence intensity for all four replicates for the etafilcon A material, for lenses incubated in both the test and control solutions, for the surface regions only, for both time periods. There was a

significant difference between the control (PBS only) and BSA solution at all times ($p<0.001$), indicating that BSA adsorbed in significant quantities even after one day of incubation. The amount of adsorbed BSA increased significantly between days 1 and 7 ($p<0.001$), with no such change being seen for the PBS control group ($p>0.05$). There was no significant difference in the degree of albumin deposition between the front and back surfaces ($p>0.05$).

Figure 3-5B illustrates the average fluorescence intensity for all four replicates for the lotrafilcon B material, for lenses incubated in both the test and control solutions, for the surface regions only, for both time periods. There was a significant difference between the lenses incubated in the control and labelled BSA solution at all times ($p<0.001$), indicating that BSA adsorbed in significant quantities even after one day of exposure. Examination of figure 3-5B indicates that the amount of adsorbed BSA apparently decreased over time on both the front and back surfaces ($p=0.05$), but at both points in time the fluorescence intensity was greater than that seen in the PBS-doped control lenses ($p<0.001$). A significant difference between the front and back surfaces were found for day 1 ($p<0.001$), but no significant difference was found for day 7 ($p>0.05$).

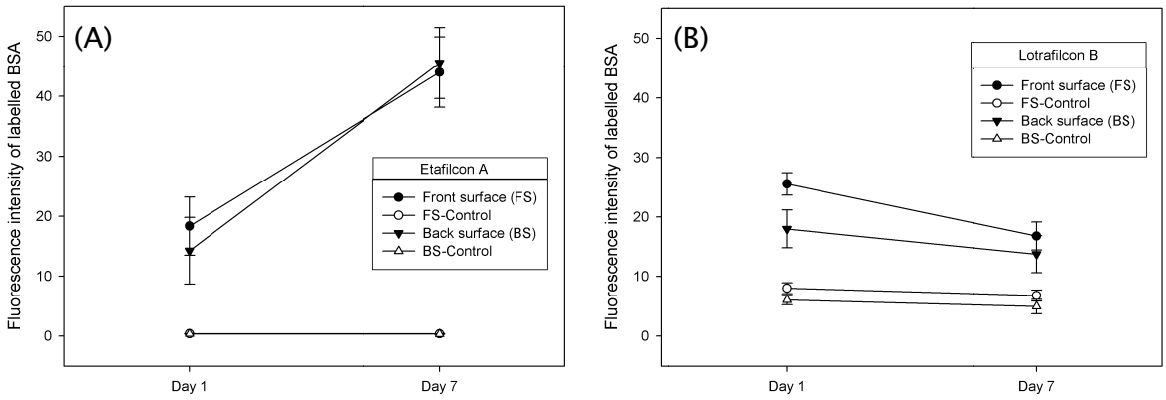

Figure 3-5: Average fluorescence intensity on the surface region for the etafilcon A (A) and lotrafilcon B (B)

Lenses were incubated in both the test and control solutions, for both time periods.

Figure 3-6 illustrates the average fluorescence intensity for all four replicates for both materials, for lenses incubated in both the test and control solutions, for the bulk region only, for both time periods. For etafilcon, the fluorescent intensity for the lenses incubated in the labelled protein solution was significantly higher than the lenses incubated in the PBS-control solution at all times ($p<0.001$), indicating that BSA penetrated into the material in significant quantities even after one day of incubation. In addition, the amount of absorbed BSA significantly increased between days 1 and 7 ($p<0.001$), as compared with the PBS-doped control lenses, which did not alter over time ($p>0.05$). For the lotrafilcon B matrix, there was no significant difference in signal comparing the lenses incubated in labelled BSA to the control solution at any time point ($p>0.05$), indicating that no detectable BSA penetrated into the bulk of the material over the 7 days. Figure 3-6 also shows

that there was a significant difference in absorbed BSA between the materials at both points in time ($p<0.001$).

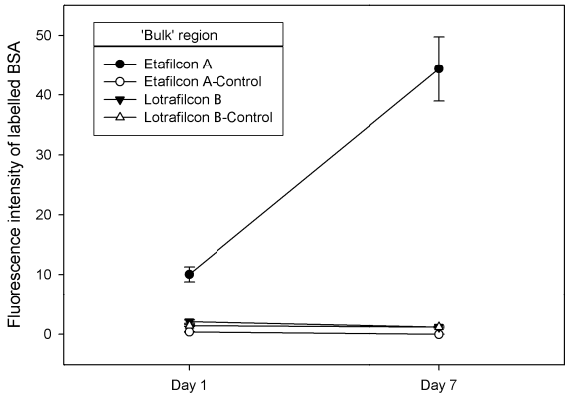

Figure 3-6: Average fluorescence intensity in the bulk region for the etafilcon A and lotrafilcon B

Lenses were incubated in both the test and control solutions for both time periods.

Comparison of Figures 3-5(A+B) and 3-6 indicate that the fluorescence intensity of the labelled protein recorded on day 1 was higher on the surfaces compared to the "bulk" region for both materials, suggesting that after 1 day the amount of protein adsorbed onto the surface of both materials is greater than that absorbed into the bulk. After 7 days of incubation this trend is maintained for lotrafilcon B. However, for etafilcon the amount of absorbed and adsorbed BSA becomes equilibrated after this 7 day incubation period. Looking at the two different contact lens materials incubated in the control PBS solution, a significant fluorescent signal was already detectable on the surface of lotrafilcon B, without the addition of the dye (Figures 3-4B and 3-5B). This finding is of major importance, since the fluorescence intensity from the labelled BSA was only slightly stronger

than the control sample, indicating that only a small amount of BSA adsorbed on the surface of lotrafilcon B. In contrast etafilcon showed no such surface peak (Figure 3-3A), regardless of the incubation solution.

To investigate the potential loss of fluorescence intensity due to light exposure (fluorescence loss in photobleaching - FLIP), two scans of the same location were taken on each lens and the discrepancies between these two measurements (from scans 1 and 6) were calculated and the Limits of Agreement plotted in Figures 3-7(A+B). Exposure to the laser beam was between 60 and 80 seconds for each location. The average intensity loss for the lenses incubated with labelled BSA was 0.8 ± 2.1 units for etafilcon and 0.2 ± 0.8 units for lotrafilcon B. Generally, a slightly lower intensity for the second scan was also found for both control groups (etafilcon 0.01 ± 0.01units; lotrafilcon B 0.39 ± 0.42 units). CCC results were 0.98 for etafilcon and 0.99 for lotrafilcon B both calculated for the incubation in labelled BSA, confirming high concordance for repeated measurements and therefore consistent results for the different lenses. These results confirm that photobleaching effects were negligible.

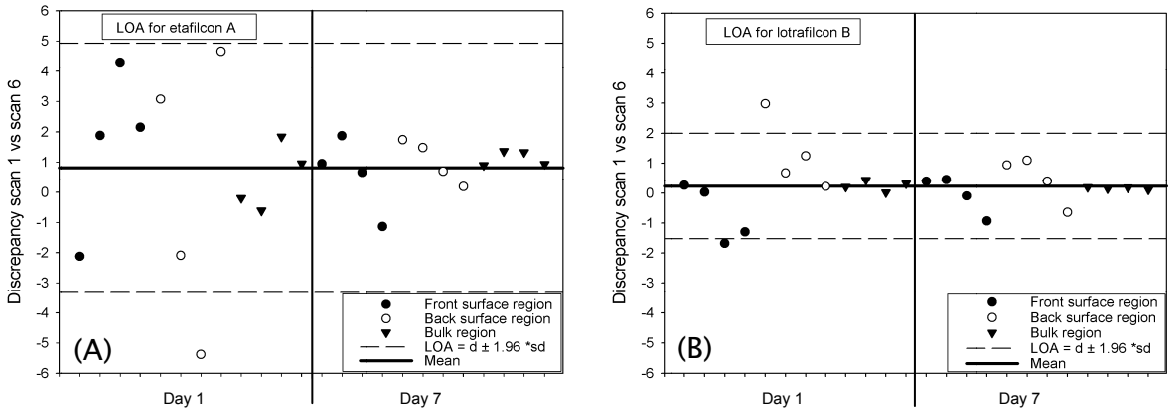

Figure 3-7: Limits of Agreement for etafilcon A (A) and lotrafilcon B (B)

Discrepancies of the fluorescence intensity between the measurements at location 1 and 6 are plotted for all regions (front surface, back surface and "bulk") at day 1 and day 7. Each lens location has 8 points, representing 4 individual scans at 2 time-points that were repeatedly measured. The average intensity loss for all measurements is plotted as the "mean."

The data from the lenses incubated in PBS with a very low concentration of DTAF, but without the addition of BSA, showed a fluorescent signal intensity on and inside both contact lens materials which was in the same range as found in our main study. The only difference to our labelled BSA solution was that we were able to detect significant fluorescent signal in the matrix of etafilcon A and, more importantly, also in lotrafilcon B, confirming that the pure dye does penetrate into both materials. This confirms that the amount of free dye in our solution had no impact on the results reported.

3.5 Discussion

Hydrogels have been shown to be highly biocompatible and as a result they find application in various biomedical and pharmaceutical areas and are frequently used for implanted materials, including artificial blood vessels, catheters or as drug delivery devices.[30,31] Albumin is the most abundant protein in human serum and its adsorption on biomaterials is of major importance, since it is the initial event happening before cell attachments occur. The protein layer works as an interface between the biomaterial and the cellular tissue. However, this biochemical adsorption process can induce a higher risk of thrombogenicity due to conformational changes and irreversible adsorption of the protein on the surface.[32,33]

Contact lens complications due to protein deposition have been reported by many researchers.[1-6] The impact of albumin adhesion alone to contact lenses was studied by Taylor and et al.[34] They demonstrated that increased albumin deposition to etafilcon A lenses resulted in increased adherence of Pseudomonas aeruginosa and Staphylococcus epidermidis, with the opposite result occurring for polymacon lenses.[34] Other studies confirmed that tear-coated contact lens materials are more likely to adsorb Pseudomonas aeruginosa compared to unworn lenses, but high individual variation was always reported.[35,36]

To determine protein adsorption on and/or absorption into hydrogel contact lenses, a variety of different imaging, immunological and microscopic techniques have been successfully used,[8,22-25] but none of these methods adequately describe the locations of proteins within the lens matrix or on the lens surface. A number of

researchers have previously attempted to investigate protein penetration into hydrogel polymers, using both microscopic techniques and, more recently, CLSM. Refojo and Leong [37] used light microscopy and FITC- labelled lysozyme, BSA and dextrans to look at the penetration of these substances into hydrogel polymer films of varying water contents and charge. The authors found that BSA penetrated into high water content gels but not into lower water content pHEMA gels and that lysozyme, with its lower molecular weight, penetrated further than BSA. Subsequently, Bohnert et al. used an "ultraviolet lamp" to investigate protein penetration,[16] but they could not detect any significant penetration of fluorescently-labelled lysozyme or BSA into the bulk of a variety of hydrogel membranes. The most recent microscopy study investigating protein penetration into hydrogels used a staining technique (Coomassie brilliant blue) to investigate lysozyme and BSA penetration into all four FDA groups.[38] It is unclear whether the lenses investigated included silicone hydrogels, but their data showed that BSA was only located on the surfaces of the lens materials, with no visible penetration being observed, as compared to lysozyme, which showed penetration into FDA group IV materials.[38]

One of the most recent advances in microscopy relates to the development of confocal microscopy, which was patented by Minsky in 1961 and became even more popular with the addition of a laser in the late 1980's. Since then various confocal microscopy techniques have been used extensively in ocular research to image cells and tissue, both in vivo and in vitro.[39-44] This form of microscopy has the significant advantage of being able to obtain images through thick samples using small step sizes. It has been previously used in deposition research to provide information about both the contact lens surface and matrix, without the need to

remove the protein of interest. Meadows and Paugh [45] used CLSM to study protein penetration in worn lenses and showed that protein penetrates through both etafilcon and pHEMA lens materials. To-date, they are the only researchers to have used CLSM to study ex vivo lenses, and they were able to show that protein deposition increased in both materials over time. The most recent reports on protein penetration using CLSM are the studies by Garrett et al.[17,18,20] Their study examined both lysozyme and human serum albumin (HSA) penetration, using both commercially available conventional hydrogel materials and fabricated polymeric films of varying water content and charge. The result of this study showed that lysozyme penetrates in significantly greater quantities than HSA and that porosity and surface charge has a significant effect on lysozyme penetration, with ionic materials exhibiting greater penetration than neutral materials. Surface charge had no influence on HSA penetration, with very little penetration being seen after 1 day of exposure.

This study is unique in that we are the first to report on the use of CLSM to study the penetration of BSA with a molecular mass of 66kDa into silicone hydrogel lens materials and one of the first to report that BSA can penetrate into conventional hydrogel materials. We found higher BSA uptake on an FDA group IV pHEMA-based conventional contact lens material (etafilcon A) compared to an FDA group I silicone hydrogel material (lotrafilcon B). Our results confirm previous studies, reporting that silicone hydrogel lenses adsorb very low levels of proteins compared to conventional pHEMA-based materials,[9-12] however, the advantage of this technique is that it does not only indicate differences in the amount of deposited protein, but can also locate the protein in terms of whether it is

predominantly found on the surface or within the bulk providing the spatial and temporal distribution profile.

Figures 3-3A and 3-3B show clearly that the location and degree of BSA deposited differ markedly between lotrafilcon B and etafilcon A. Figures 3-4 to 3-7 demonstrate that a significant amount of BSA penetrated into the matrix of etafilcon A after only one day of exposure, with no detectable labelled BSA being found inside lotrafilcon B and that a greater amount of BSA also accumulated on the surface of etafilcon. Within the matrix of the lens, even after 7 days of incubation no detectable levels of BSA could be seen within lotrafilcon B. Over time, the amount of BSA on and within the matrix of etafilcon A increased and the amount of absorbed BSA became similar to that adsorbed on the surface.

Albumin absorption is influenced by many factors, including pH and ionic strength of the solution, water content and charge of the material, and, importantly, pore size.[46] Garrett et al. estimated two different models to calculate the actual pore size based on the water content of the hydrogel material.[17] They added different concentrations of methacrylic acid (MA) to pHEMA to increase the water content in the material and calculated the changing pore sizes. For a maximum concentration of 5% MA they calculated an average diameter of 34.7 and 29.3 Å for their two models, and therefore predicted that HSA, which has a diameter of approximately 55 Å, should not penetrate into their material, which they confirmed experimentally. However other researchers estimated bigger average pore sizes for various HEMA compositions: Gachon et al. reported pore sizes between 56 and 70.6 Å for poly(MMA-VP) lenses [47] and even bigger pores were found by Gatin et al. who investigated pHEMA-based lenses and measured pore

sizes of 428 Å.[48] Based on these studies it would be possible for BSA to penetrate into HEMA-based materials and our data support the conclusion that BSA with a molecular weight of 66kDa can indeed penetrate into etafilcon A.

One final point to discuss is the surprising finding that the apparent degree of BSA deposition reduced on the lotrafilcon B material between days 1 and 7. This could be due to photobleaching or due to the dye intensity reducing over time. A previous study [49] showed that DTAF has comparably high fluorescence intensity to other dyes, but does tend to bleach faster. In our study we adjusted the argon laser to a very low intensity of 5% to prevent extensive light exposure, which could lead to bleaching effects. Figures 3-7(A+B) demonstrate that for both materials only minor intensity losses were seen in the second scan at the same location, ruling out the possibility of photobleaching being significantly involved. This result confirms that the DTAF had good short time stability for the confocal laser, but it was not stable enough under long incubation conditions at 37 degrees. Fading in the intensity of the dye was confirmed in a separate free-dye study (see Appendix B), confirming that the reason for the relatively small, but statistically significant, reduction in fluorescence intensity after 7 days for the lotrafilcon B material was due to weakening of the DTAF and not BSA desorption. The increased amount of BSA adsorbed onto the etafilcon material prevented this small reduction in intensity being detectable. Further work is underway to locate a dye that remains stable over long periods of incubation.

3.6 Conclusions

CLSM is a useful technique to examine the penetration profile of the protein albumin into different contact lens materials. After incubating etafilcon A in 0.5 mg/ml fluorescently labelled BSA, significant uptake on the surface and within the matrix was seen, which increased over time. The lotrafilcon B material adsorbed very little BSA on the surface and no significant BSA was found in the matrix after 7 days of exposure. This confocal technique is applicable to any study in which biomaterials come into contact with any body fluid containing proteins.

The next chapter will evaluate the use of different fluorescent probes to label albumin. CLSM will monitor the sorption pattern throughout the lens materials, and comparisons will be made between conjugates.

4. IMPACT OF FLUORESCENT PROBES ON PROTEIN SORPTION

This paper is submitted for publication as follows

Doerte Luensmann, Lyndon Jones

Centre for Contact Lens Research, School of Optometry, University of Waterloo, Waterloo, ON, N2L 3G1

Currently under review at *JBMR Part B, Applied Biomaterials*

	Concept / Design	Recruitment	Acquisition of data	Analysis	Write-up / publication
Luensmann	Y	n/a	Y	Y	Y
Jones	Y	n/a	-	-	Y

4.1 Overview

Purpose: To investigate the impact of fluorescent probes on the sorption behaviour of proteins.

Methods: Bovine serum albumin (BSA) was conjugated to three organic fluorescent probes, 5-(4,6-Dichloro-s-triazin-2-ylamino)fluorescein hydrochloride (DTAF), Rhodamine B isothiocyanate (RITC) and Lucifer yellow (LY). The protein sorption profile to one pHEMA-based (etafilcon A) and three silicone hydrogel (SH) contact lens materials (lotrafilcon B, balafilcon A and senofilcon A) was determined using confocal laser scanning microscopy. In addition, all materials were incubated in dye solutions containing the fluorescent probe alone; and finally BSA accumulation was quantified using radiolabeling.

Results: The different conjugates showed similar sorption profiles for the pHEMA-based material, but marked differences for all SH materials. Lotrafilcon B accumulated more protein on the surface as compared to the matrix, independent of the fluorescent probe used for conjugation. Protein sorption varied for senofilcon A, with DTAF-BSA sorbing primarily to the surface region, while the other conjugates penetrated in equal amounts into the matrix. Balafilcon A exhibited smaller differences between conjugates, with LY-BSA allowing the protein to fully penetrate the matrix, while the other conjugates showed minor surface adsorption. Sorption curves of unbound dyes were often similar compared to the conjugated results.

Conclusions: BSA profiles to pHEMA-based and silicone hydrogel materials were highly dependent on the fluorescent probe used and none of the probes accurately reflected quantitative protein levels for the materials investigated.

4.2 Introduction

Fluorescent probes are frequently used as analytical tools in biochemistry and biotechnology [1,2] as well as for clinical and diagnostic applications.[3] The fluorescence quantum yield, which is described as the total energy emitted relative to the energy absorbed, is 1000 times higher compared to most spectrophotometric methods, with detectable quantities of one in a billion.[2,4] However, a number of factors are known to either increase or decrease the emission signal or lead to de-excitation of the fluorescent molecule. Firstly, the fluorophore itself, with molar absorptivity, concentration, luminescence lifetime, phototoxicity, absorption and emission spectra all playing relevant roles. Secondly, the microenvironment, in which the type of solvent, pH, temperature, oxygen level, solvation, ionic strength, viscosity, and molecular collisions- resulting in energy or charge transfer- are known to impact emission intensities. Finally, instrument-specific effects such as the availability of the optimal wavelength for excitation, lack of control over radiation intensity, aging of the light source, and variations in detector sensitivity during measurements are all significant factors.

Fluorescent spectroscopy techniques find a variety of applications in protein characterization,[5] because most proteins exhibit a weak intrinsic fluorescence due to their aromatic amino acids. The molar extinction coefficient of these amino acids is highest for tryptophan > tyrosine > phenylalanine, with maximum absorbance peaks at 279nm, 275nm, 257nm respectively.[6] However, not all analytical techniques allow measurements within the ultraviolet spectrum and frequently require the attachment of an extrinsic fluorescent probe to the protein. Extrinsic fluorescent probes can either non-covalently attach to proteins using electrostatic

and hydrophobic interactions or bind covalently to specific residues with the help of additional reactive derivatives. Examples for covalent conjugations are amine-or thiol-reactive probes. Amine-reactive dyes typically bind to the aliphatic ε-amine of the amino acid lysine and the N-terminal amino acid of the protein under conditions above pH 8.0, while thiol-reactive probes attach to sulfhydryl groups of cysteine and methionine under neutral pH conditions.[4,7,8]

Fluorescent probes have a molecular weight between 300 and 1500 Dalton (Da),[8] and are therefore multiple times smaller compared to most proteins (e.g serum albumin at 66,000 Da). Nevertheless, a number of studies have demonstrated significant changes in charge,[9,10] isoelectric point,[9,11] size,[9,12] binding characteristics,[13-15] and kinetics [16,17] between native and fluorescently conjugated proteins.

Confocal laser scanning microscopy (CLSM) is often used for chromatographic materials research to study their interaction with proteins.[18] However, conjugation effects and material-based factors need to be considered when evaluating fluorescence emission intensities.[19]

The purpose of this work was to determine the sorption profile of albumin to poly-2-hydroxyethyl methacrylate (pHEMA) and silicone hydrogel contact lens materials. In separate experiments, three organic fluorescent probes were covalently conjugated to albumin and using CLSM the protein was located throughout the lenses. Furthermore, all investigated material types were incubated in a dye solution containing no protein and the resulting dye-sorption pattern were compared to the pattern found with conjugated albumin.

4.3 Methods

The protein bovine serum albumin (BSA, 99% agarose gel electrophoresis, Sigma-Aldrich, St. Louis, MO) was selected as a model protein, which is commonly used for research purposes, due to its stability, water solubility, versatile binding capacity and availability.[20] Three organic fluorescent probes, 5-(4,6-Dichloro-s-triazin-2-ylamino)fluorescein hydrochloride (DTAF), rhodamine B isothiocyanate (RITC) and lucifer yellow VS dilithium salt (LY) (all Sigma-Aldrich, St. Louis, MO) were selected due to their differences in molecular composition, spectra for excitation and emission, and protein coupling affinities (Table 4-1).

Table 4-1: Fluorescent probes investigated

	Fluorescent probe	MW (Da)	EXC (nm)	EM (nm)
DTAF	5-(4,6-Dichloro-s-triazin-2-ylamino) fluorescein hydrochloride ($C_{23}H_{12}Cl_2N_4O_5 \cdot HCl$)	532	492	514
RITC	Rhodamine B isothiocyanate ($C_{29}H_{30}ClN_3O_3S$)	536	540	573
LY	Lucifer Yellow VS dilithium salt ($C_{20}H_{12}Li_2N_2O_{10}S_3$)	550	427	525

Da Dalton; EM emission wavelength; EXC excitation wavelength, nm nanometer; MW molecular weight

Four contact lens materials were specifically chosen due to their distinct differences in polymeric composition and surface modification. All lenses had a power of -3.0 D (dioptres), with the material properties listed in Table 4-2. Prior to the experiment, lenses were removed from the blister pack and presoaked in sterile phosphate buffered saline (PBS) (pH 7.4) for 30 minutes. Presoaking of the lenses was performed to minimize the potential impact caused by components of the

packaging solution on subsequent protein sorption behaviour and fluorescence quenching.

Table 4-2: Contact lens materials investigated

Trade Name	USAN	FDA Category	Manufacturer	Centre thickness (μm)	Water Content (%)	Surface Modification	Principal Monomers
ACUVUE®2™	etafilcon A	IV	Johnson & Johnson	80	58	none	HEMA, MAA
AIR OPTIX™ AQUA	lotrafilcon B	I	CIBA Vision	80	33	25nm high refractive index coating	DMA, TRIS, siloxane macromer
PureVision®	balafilcon A	III	Bausch & Lomb	90	36	Plasma oxidation (glassy islands)	NVP, TPVC, NVA, PBVC
ACUVUE® OASYS™	senofilcon A	I	Johnson & Johnson	70	38	PVP is incorporated as a wetting agent	mPDMS, PVP, DMA, HEMA, siloxane macromer, TEGDMA

DMA *N,N*-dimethylacrylamide; HEMA 2-hydroxyethyl methacrylate; MAA methacrylic acid; mPDMS monofunctional polydimethylsiloxane; NVA *N*-vinyl aminobutyric acid; NVP N-vinyl pyrrolidone; PBVC poly[dimethylsiloxyl] di [silylbutanol] bis[vinyl carbamate]; PVP polyvinyl pyrrolidone; TEGDMA tetraethyleneglycol dimethacrylae; TPVC tris-(trimethylsiloxysilyl) propylvinyl carbamate; TRIS trimethyl siloxy silane.

4.3.1 Protein conjugation

For solution 1, the individual fluorescent probes were conjugated to BSA using optimized protocols for each dye, to achieve a degree of labeling (DOL) ≤ 3 to reduce the risk of protein modification seen with overlabeling.[9] The conjugation with DTAF [21] and LY [22] have been described previously. Briefly, 180 mg BSA was dissolved in 0.05M borate buffer (pH = 8.5) containing 0.04M NaCl (18 ml). The hydrophobic fluorescent probes (DTAF - 10 mg; RITC - 2.5 mg) were dissolved in

dimethylsulfoxide (DMSO; 1 ml; Sigma-Aldrich, St. Louis, MO, USA) and the hydrophilic probe (LY – 7 mg) in borate buffer. The dissolved dye was added drop wise to the protein solution, while stirring. Following the reaction time of two hours at room temperature, unconjugated dye was separated using PD10 desalting columns (Amersham Biosciences, Piscataway, NJ, USA) and dialysis against PBS (pH=7.4). The continuous decrease of the unbound dye was monitored using a fluorescence spectrophotometer (Hitachi F-4500, Tokyo, Japan). The labeling efficiency was calculated by determining the BSA concentration in the solution using the DC Protein Assay (Bio-Rad, Hercules, CA, USA) and measuring the absorbance at 492, 543 and 415nm for DTAF, RITC and LY respectively. The resulting degree of labeling was 1.9 for DTAF, 2.3 for RITC and 2.2 for LY (Appendix A). The solutions were further diluted with PBS to obtain final BSA concentrations of 0.5 mg/ml, to mimic the albumin concentration in the tear film.[23,24]

For solution 2, containing free dye only, approximately 1 mg of the fluorescent probe was dissolved in either DMSO or PBS and further diluted with PBS to reach a peak fluorescence intensity which was approximately 4 times lower as compared to the BSA-conjugate. (Dye uptake/intensity in the materials is multiple times higher as compared to the protein conjugate).

4.3.2 Sample incubation

Both the dye and the conjugated BSA were sterilized using 0.2 µm polyethersulfone syringe filtration (VWR, Mississauga, ON, Canada) and 1 ml of the solution was filled in sterile amber glass vials. The contact lenses were individually

incubated for one and seven days at 37ºC under constant rotation of 72 rpm. Three replicates were used for each lens material, solution and time point, resulting in 144 lenses being examined using CLSM.

4.3.3 Localization of the protein

After the incubation, lenses were rinsed in PBS and gently dabbed on lens paper. The central 4 mm section was cut out of the lens using a mechanical punch press and mounted on a microscope slide. The CLSM Zeiss LSM 510 Meta (Zeiss Inc. Toronto, Canada) was utilized to scan each sample, according to the specific excitation wavelength of the individual fluorescent probe: 488nm Argon Laser for DTAF, 543nm Helium Neon Laser for RITC and 405nm Laser diode for LY. Emission filters of >505nm, >560nm and >515nm were chosen for DTAF, RITC and LY respectively. Appropriate settings for detector gain and laser intensity were determined for each solution via a number of preliminary tests. These settings remained constant for all lens types incubated in the same solution throughout the experiment to allow comparisons over time and between materials.

Each sample was scanned on four random locations in a size of 230x230 µm (512x512 pixel) using a step width of 1 µm. A representative scan was selected to show the typical sorption profile for each material for both time points after the incubation in free dye solution and conjugated BSA. Arbitrary fluorescence units were converted into a 1-100 scale.

4.3.4 Protein quantification

Radiolabeled BSA was used to determine the total amount of protein sorbed to each of the four contact lens materials over time. BSA was radiolabeled with ^{125}I

using the iodine monochloride method.[25-27] Three replicates of each material were incubated in a 0.5 mg/ml BSA solution, containing a mixture of 2% labeled and 98% unlabeled BSA. After incubating the lenses for one and seven days, lenses were rinsed with PBS to remove loosely adsorbed protein and the amount of accumulated BSA was determined using a gamma counter (1470 Wallac Wizard PerkinElmer, Woodbridge, ON). For comparisons between the protein accumulation to the different materials over time, repeated measures ANOVA (analysis of equal variance) was applied followed by post-hoc comparisons using Tukey's HSD (honestly significant difference) test.

4.3.5 Confirmation of unbound dye uptake

Unbound LY was further investigated to determine the reduction of fluorescence intensity from the solution after the incubation. After seven days, lenses were removed from the LY dye solution and fluorescence spectrophotometer readings determined the remaining signal strength (Excitation 405nm; Emission 525nm).

4.4 Results

4.4.1 Comparisons between conjugated and unconjugated dyes

Sorption profiles for etafilcon A incubated in free dye and conjugated BSA are plotted in Figures 4-1A-F. This pHEMA-based material has no surface treatment and allows all three dyes (Figures 4-1A, 4-1C and 4-1E) and conjugated BSA (Figures 4-1B, 4-1D and 4-1F) to fully penetrate the matrix.[28] All three unconjugated

fluorescent probes (Figures 4-1A, 4-1C and 4-1E) were almost evenly distributed throughout the material after one day of incubation, with only marginally lower signals detected in the lens center for RITC (Figure 4-1C). Furthermore, no major increase in fluorescence intensity was observed between the two time points, indicating a saturation uptake after 24 hours incubation for all free dye solutions. The conjugated BSA showed higher intensity levels on the lens surface region as compared to the matrix for DTAF-BSA (Figure 4-1B) and RITC-BSA (Figure 4-1D) on Day 1. This was followed by an overall intensity increase on Day 7 with both conjugates, showing an almost even distribution throughout the material. Etafilcon A incubated in LY-BSA (Figure 4-1F) exhibited an even protein distribution on Day 1, with no increase over time. Thus, for etafilcon A, the three fluorescent probes alone and the conjugated BSA showed similar profile curves with different intensity levels after one week of incubation, independent of the fluorophore used.

Conjugated BSA and free dye sorption profiles for lotrafilcon B are seen in Figures 4-2A-F. The surface of this silicone hydrogel material is plasma modified with a 25nm high refractive index coating [28,29] and accumulated higher levels of unbound DTAF and RITC on the surface as compared to the central matrix (Figures 4-2A and 4-2C). A minor increase in dye penetration into the lens matrix was seen for DTAF on Day 7 (Figure 4-2A). No such surface sorption was observed with LY (Figure 4-2E), which allowed the dye to penetrate the full lens on Day 1, with no noticeable increase to Day 7. BSA, when conjugated to any of the fluorescent probes, showed higher uptake levels on the material surfaces as compared to the matrix at both time points (Figures 4-2B, 4-2D and 4-2F). Furthermore, a minor increase within the matrix could be seen for all solutions over time, which was most

apparent for DTAF-BSA (Figure 4-2B). Overall, the three unbound fluorescent probes deposited in different profile pattern to lotrafilcon B. However, conjugated BSA showed increased deposition rates at the surface region compared to the central matrix, regardless of the fluorescent probe used for conjugation.

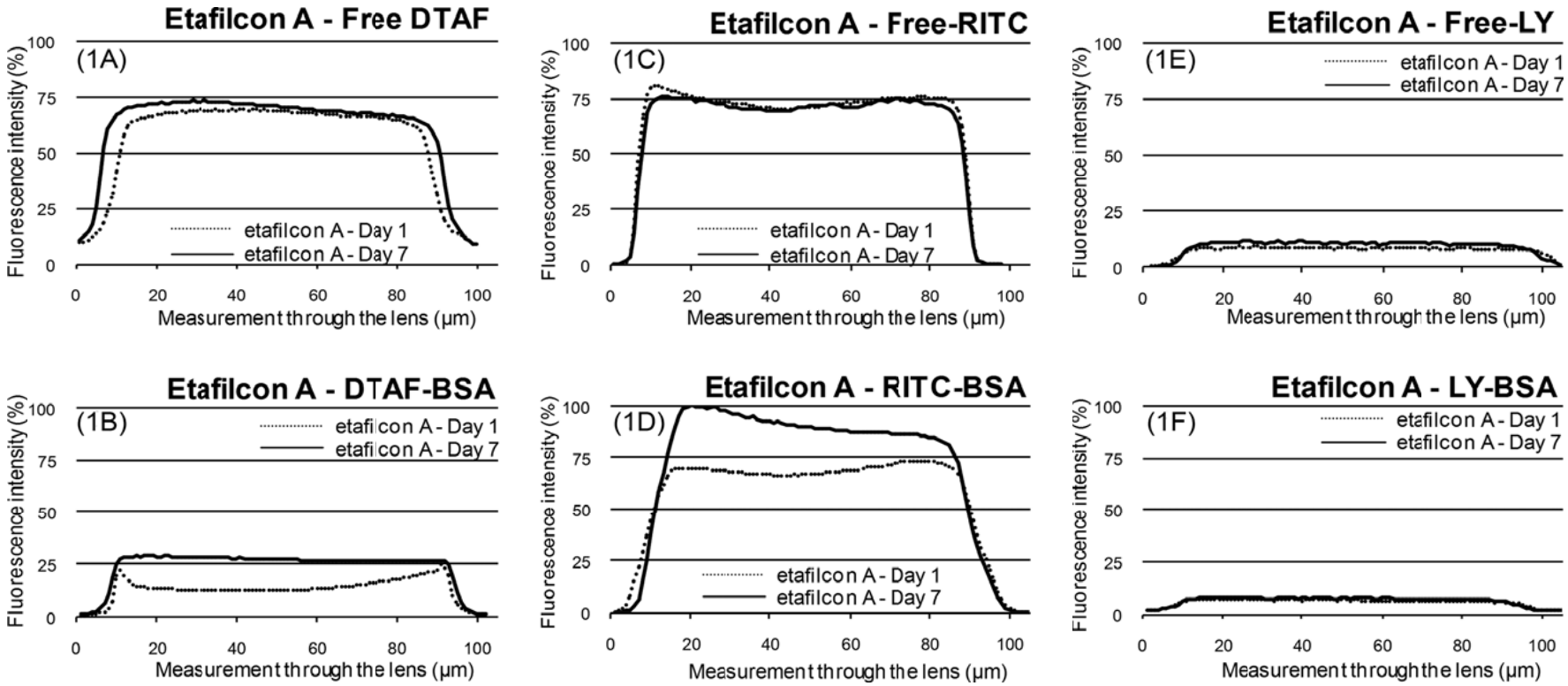

Figure 4-1(A-F): Sorption profiles for etafilcon A incubated in free DTAF (1A), DTAF-BSA (1B), free RITC (1C), RITC-BSA (1D), free LY (1E), LY-BSA (1F) for 1 and 7 days

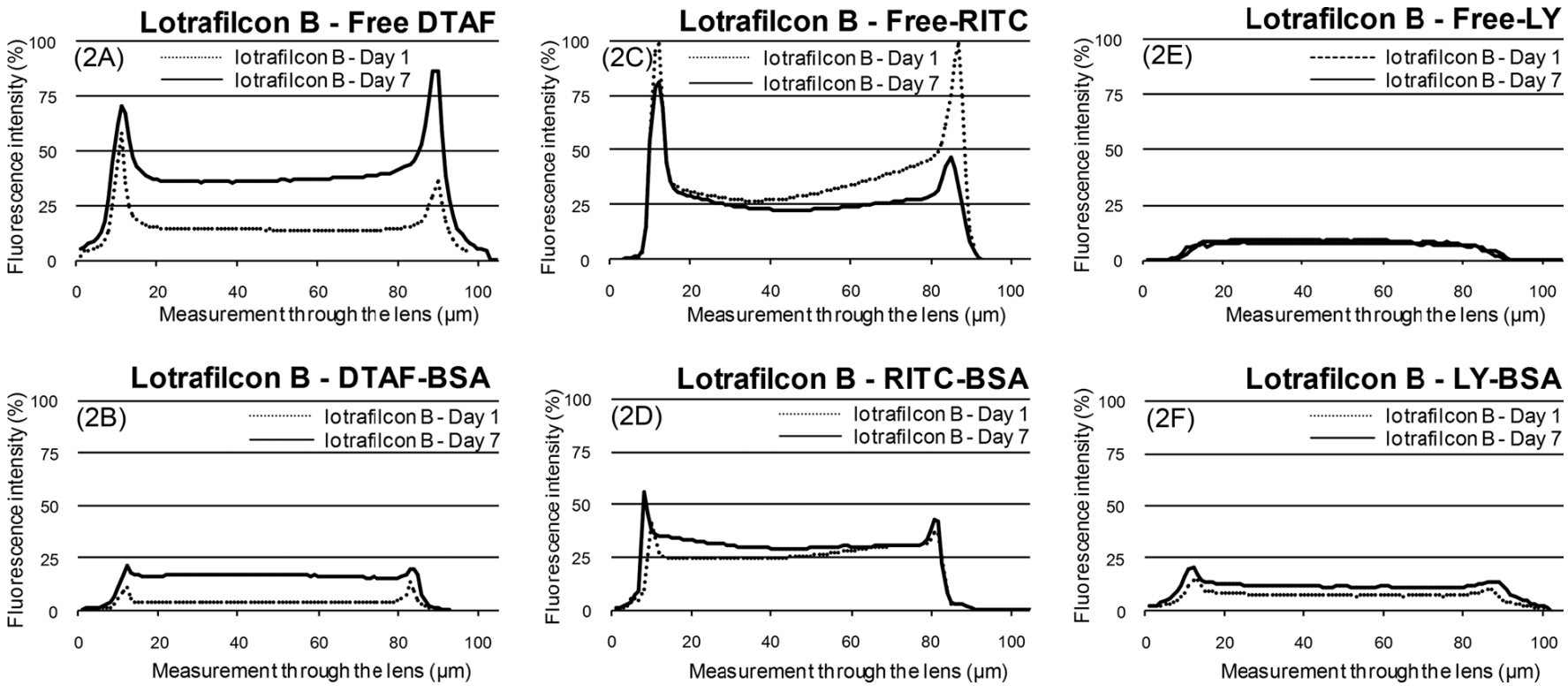

Figure 4-2(A-F): Sorption profiles for lotrafilcon B incubated in free DTAF (2A), DTAF-BSA (2B), free RITC (2C), RITC-BSA (2D), free LY (2E), LY-BSA (2F) for 1 and 7 days

Sorption profiles for balafilcon A incubated in free dye and conjugated BSA are plotted in Figures 4-3A-F. The surface of this silicone hydrogel material is modified using a plasma treatment, which transforms the hydrophobic silicone components into hydrophilic silicate ('glassy-islands'), which is inhomogeneous in appearance.[28,30,31] Unbound DTAF and LY distributed evenly throughout the lens after one day of incubation, with a strong increase in fluorescence intensity seen for LY on Day 7 (Figures 4-3A and 4-3E). RITC was detected primarily at the surface region of the material, with lower intensities being observed within the central matrix (Figure 4-3C). This distribution profile was still apparent after seven days of incubation. After balafilcon A was incubated in DTAF-BSA and RITC-BSA, most protein accumulated on the outer surface region of the lens on Day 1 and allowed only little penetration into the material (Figures 4-3B and 4-3D). After seven days of incubation, the fluorescent intensity within the matrix increased, but remained lower compared to the surface regions for DTAF-BSA. The conjugate LY-BSA penetrated evenly throughout the material on Day 1 and showed an overall intensity increase on Day 7 (Figure 4-3F). Overall, for balafilcon A, free DTAF and LY showed even distributions throughout the materials (Figures 4-3A and 4-3E), while RITC bound stronger to the surface region (Figure 4-3C). The conjugates were likewise not in agreement, with DTAF-BSA showing an increased surface build-up (Figure 4-3B), LY-BSA demonstrating an even sorption profile (Figure 4-3F) and RITC-BSA in-between these two extremes (Figure 4-3D).

Conjugated BSA and free dye sorption profiles for senofilcon A are seen in Figures 4-4A-F. This silicone hydrogel material has no specific surface coating but incorporates polyvinyl pyrrolidone (PVP) as an internal wetting agent.[28,32] The unbound

fluorescent probe DTAF was detected in high amounts at the surface region of the material, with only little penetrating into the central region (Figure 4-4A). This profile did not change markedly over time (Figure 4-4A). RITC and LY distributed evenly throughout the material on Day 1, with a minor increase for LY and a slight decrease for RITC over time (Figures 4-4C and 4-4E). The incubation of senofilcon A in BSA conjugated with DTAF showed protein sorption primarily to the surface of the material on Day 1, which remained surface dominated over time, with only minor penetration into the central matrix of the material (Figure 4-4B). This was in stark contrast to RITC-BSA, which accumulated only slightly less protein in the central matrix as compared to the surface on Day 1 (Figure 4-4D). RITC-BSA amounts increased marginally over time and allowed an even protein distribution on Day 7 (Figure 4-4D). LY-BSA penetrated into the material after one day, with small intensity peaks seen on the lens surface (Figure 4-4F). A minor intensity increase was seen on Day 7, with no change in sorption profile (Figure 4-4F). Thus, for senofilcon A, marked differences in sorption profile were found between unbound fluorescent probes and these differences became more apparent when conjugated to BSA.

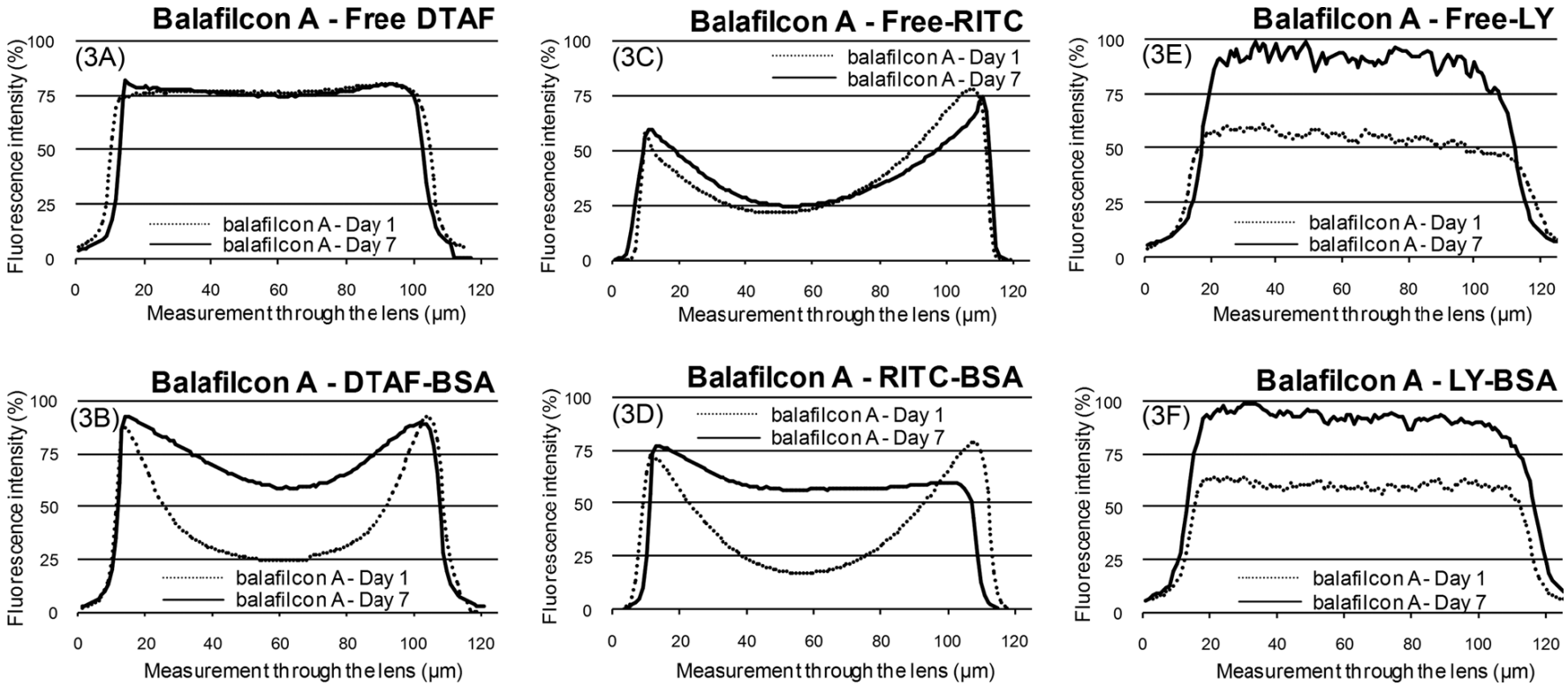

Figure 4-3(A-F): Sorption profiles for balafilcon A incubated in free DTAF (3A), DTAF-BSA (3B), free RITC (3C), RITC-BSA (3D), free LY (3E), LY-BSA (3F) for 1 and 7 days

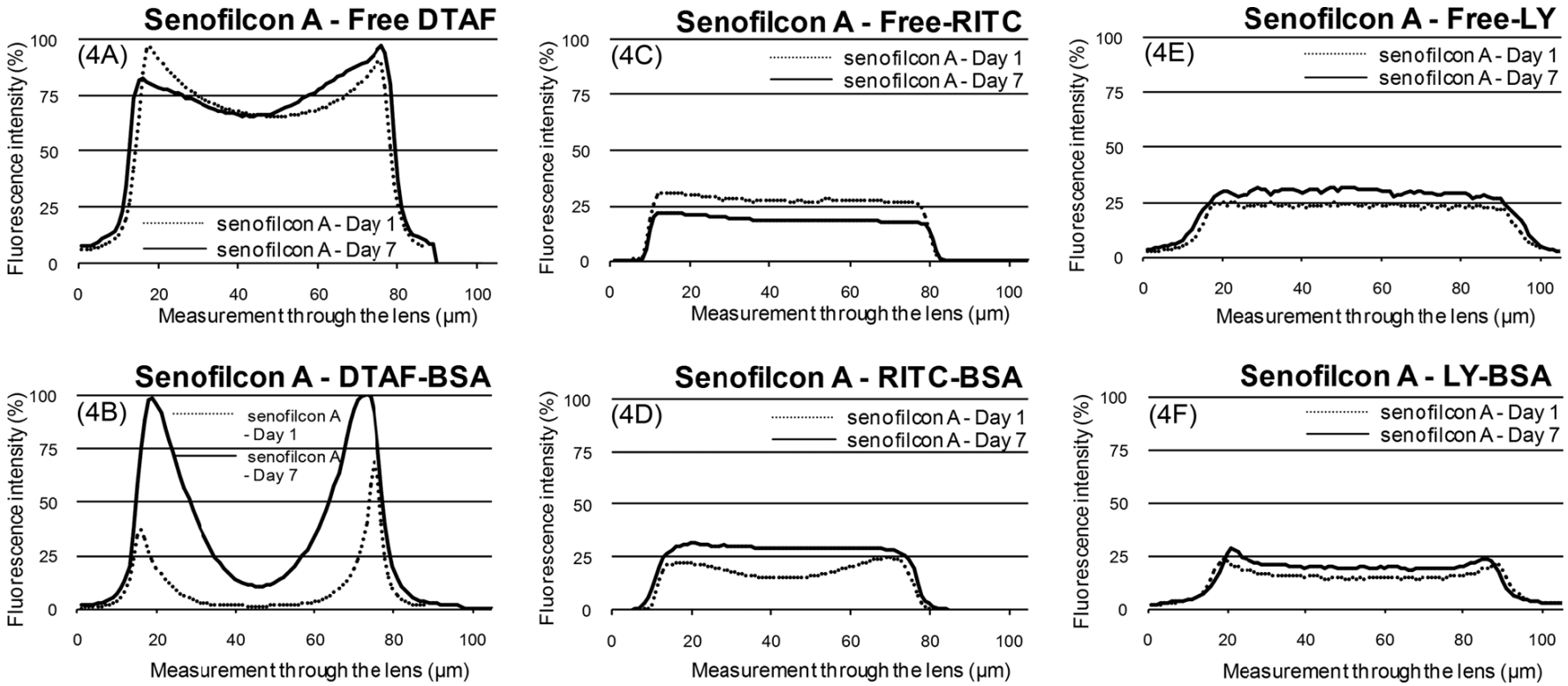

Figure 4-4(A-F): Sorption profiles for senofilcon A incubated in free DTAF (4A), DTAF-BSA (4B), free RITC (4C), RITC-BSA (4D), free LY (4E), LY-BSA (4F) for 1 and 7 days

4.4.2 Comparisons between materials

In general, free DTAF bound to all four materials at a similar intensity (Figures 4-1A, 4-2A, 4-3A and 4-4A). Lotrafilcon B bound DTAF more strongly on the surface and allowed less dye to penetrate the matrix (Figure 4-2A), which was similar to that seen with senofilcon A (Figure 4-4A), but to a lesser extent. DTAF conjugated to BSA showed higher uptake levels for both senofilcon A and balafilcon A (Figures 4-3B and 4-4B), as compared to etafilcon A and lotrafilcon B (Figures 4-1B and 4-2B). An even distribution profile throughout the lens material was seen for both free DTAF (Figure 4-1A) and DTAF-BSA (Figure 4-1B) when sorbed to etafilcon A; likewise a comparable sorption trend for the bound and unbound DTAF was observed for lotrafilcon B (Figures 4-2A and 4-2B) and senofilcon A (Figures 4-4A and 4-4B), which exhibited higher sorption rates on the surface compared to the matrix. For balafilcon A, free DTAF was distributed throughout the lens material (Figure 4-3A), but DTAF-BSA deposited in higher rates to the surface region and allowed less protein to enter the central matrix (Figure 4-3B).

Fluorescence intensities for free RITC were highest on the surface of lotrafilcon B (Figure 4-2C) and within the matrix of etafilcon A (Figure 4-1C), moderate for balafilcon A (Figure 4-3C) and lowest for senofilcon A lenses (Figure 4-4C). As seen with free DTAF, all lens materials exhibited different sorption patterns (intensity and shape). However, the sorption curves were not necessarily identical between these two dyes, with some materials exhibiting markedly different profiles (e.g. Figures 4-3A and 4-3C). The RITC-conjugated BSA accumulated highest on etafilcon A (Figure 4-1D), followed by balafilcon A (Figure 4-3D) and much smaller amounts could be seen for

both senofilcon A (Figure 4-4D) and lotrafilcon B (Figure 4-2D). Comparisons between the shape of free RITC vs RITC-BSA for all four materials (Figures 4-1C, 4-1D, 4-2C, 4-2D, 4-3C, 4-3D, 4-4C and 4-4D) show a strong agreement for the overall intensity levels and sorption curves, suggesting that this fluorescent probe impacts the BSA sorption profile determined with these hydrogel materials.

Free LY was distributed evenly throughout all lens materials at both time points, with no increase in surface sorption (Figures 4-1E, 4-2E, 4-3E and 4-4E), which was different to the other two unbound probes. For unbound LY, the highest intensity levels were observed with balafilcon A (Figure 4-3E), which also increased to the greatest extent over time. Moderate signal strength was seen for senofilcon A (Figure 4-4E) and the weakest intensities were found for both etafilcon A (Figure 4-1E) and lotrafilcon B (Figure 4-2E). Sorption patterns for conjugated LY-BSA also showed the highest intensity for balafilcon A (Figure 4-3F), followed by a similar level for senofilcon A (Figure 4-4F) and lotrafilcon B (Figure 4-2F) and slightly less for etafilcon A (Figure 4-1F). Comparisons between the sorption pattern for free and conjugated LY show similar results, with even distributions of free LY or LY-BSA throughout etafilcon A and balafilcon A materials (Figures 4-1E, 4-1F, 4-3E and 4-3F). In contrast, small surface increases for lotrafilcon B (Figure 4-2F) and senofilcon A (Figure 4-4F) could be detected with the LY-BSA conjugate. These differences between sorption patterns for unbound LY and LY-BSA suggest that the protein sorption pattern observed were more likely determined by the BSA rather than the dye.

4.4.3 BSA quantification

Protein sorption to all four materials was quantified using radiolabeled BSA. Results for both time points are shown in Table 4-3.

Overall, BSA uptake was highest for senofilcon A, followed by similar uptake for lotrafilcon A and balafilcon A (p=0.17), with the lowest amounts being detected on etafilcon A. An increase over the 7 day time period was seen for lotrafilcon B, balafilcon A and senofilcon A, but no statistically significant change was seen for etafilcon A (Table 4-3)

Table 4-3: BSA accumulation to contact lens materials determined by ^{125}I radiolabeling

	etafilcon A	lotrafilcon B	balafilcon A	senofilcon A
Day 1	0.15 ± 0.03 µg	0.84 ± 0.09 µg	0.63 ± 0.07 µg	1.19 ± 0.10 µg
Day 7	0.19 ± 0.04 µg	1.39 ± 0.05 µg	1.28 ± 0.18 µg	1.78 ± 0.18 µg
p value	1.0	0.006	0.002	0.004

Differences between the two time points for each material were determined (p value)

4.4.4 Confirmation of unbound dye uptake

To confirm free dye uptake into the materials, the LY solution was investigated after lenses were removed out of the solution. Fluorescence spectrophotometer measurements determined an intensity of 278 (arbitrary units) at 525nm for free LY prior to lens exposure. Following placement of the lenses into the free dye solution for seven days, a reduction to 236 units for etafilcon A, 244 for lotrafilcon B, 187 for senofilcon A, and 73 for balafilcon A were measured, confirming that dye was taken up into all the lens materials, but to differing extents.

4.5 Discussion

Fluorescent imaging technologies such as CLSM are used for various applications in cell imaging [33] and material research.[18] CLSM provides higher resolution than conventional light microscopes due to the adjustment of the pinhole, which rejects out of focus rays.[34] The focal plane can be moved a few hundred microns deep into the species under investigation, with step sizes of <1 micron, and XY images can be collected without destroying the sample. Images from the XY image gallery finally allow 3D reconstruction of the sample.[34]

In protein research, fluorescent tracers are used successfully in many applications, for example to determine the process of protein refolding and unfolding,[35] protein surface hydrophobicity,[36] aggregation and fibrillation,[37] conformational changes induced by chemical degradation,[38] protein–surfactant interactions [39] and protein kinetics.[1] However, due to the number of factors impacting fluorescence intensity levels, studies primarily report qualitative results.[40-43]

In this study, BSA was conjugated with three different fluorescent probes and the sorption profile of both free and conjugated dye to four contact lens materials, with thicknesses of 70-100 μm, were investigated. The fluorescein-based probe DTAF was chosen over fluorescein isothiocyanate (FITC) for its stability, purity, labeling efficiency at lower pH and minor impact on BSA in respect of molecular weight and size.[9,44,45] In DTAF, the binding derivative cyanuric chloride is constituted of three highly reactive chloro groups, of which the first is replaced by the attachment of the fluorescein molecule, the second reacts with amino groups and the third group either hydrolyzes or remains unbound.[44] The more chloro groups that are substituted, the

less reactive the remaining chloro group becomes, which means that a single DTAF molecule is unlikely to bind to more than a single protein.[44] Under almost neutral conditions (pH 7.0-8.0), DTAF binds primarily to ε-amino groups of lysine and N-terminal amino groups. However, conjugations to sulfhydryl groups, tyrosine or histidine occur at pH >8.0.[44,46]

The chemical reactive group for RITC is isothiocyanate, which is a commonly used derivative for fluorescent probes, due to its high reactivity under basic conditions.[47] Conjugations with RITC provide superior photostability and have been shown to modify BSA to a smaller extent compared to FITC, for dye/protein ratios less than 5.[11,48] The carbon atom of the isothiocyanate is the reactive component, which binds in a similar manner, primarily to lysine and the N-terminal group, as seen with cyanuric chloride.[47,49]

LY is, in contrast to RITC and DTAF, a hydrophilic probe, which can readily be dissolved in water-based solutions.[50] The reactive vinyl sulfone derivative binds primarily to sulfhydryl groups of cysteine, but also to lysine and imino groups of the imidazole ring of histidine.[51-53] Covalent conjugation of LY to human serum albumin does not require a basic environment, but can be performed under neutral pH.[54] LY exhibits a low quantum yield of 0.2,[51,55] compared to 0.92 for DTAF [2,44] and 0.7 for RITC.[2,55] However, LY has a large Stokes shift of approximately 100nm, which allows signal detection over the full emission spectrum, without the concerns that arise from the collection of data from the excitation "tail" that overlaps the emission spectrum.[2,50,55] This also prevents reabsorption of emitted light.

In this current study, the conjugation with all fluorescent probes was performed at pH 8.5, to allow an optimal reactivity of the highly alkali ε-amine of lysine.[56] Although BSA consists of 60 lysines, only a few of them are located on the protein surface and these are only reactive when exposed within a suitable environment. The lysines (Lys) in BSA that are most likely to react are Lys 220, Lys 474 and potentially Lys 350 and Lys 116.[57] The native structure of both human and bovine serum albumin has 35 cysteines, of which 34 are typically paired with disulfide bonds to cystines and the sulphydryl group of the single Cys-34 remains mainly unbound.[57,58] Cys-34 is highly reactive and can possibly be coupled with thiol-reactive probes such as LY.

In this study, we determined both the amount and location of BSA deposition, using two differing techniques. The total amount of BSA accumulation on these four hydrogel contact lens materials was determined using ^{125}I-conjugated BSA. The highest BSA amounts per lens were found for senofilcon A > lotrafilcon B = balafilcon A > etafilcon A ($p< 0.01$ for all comparisons, except for lotrafilcon B and balafilcon A with $p=0.16$). Over time, only lotrafilcon B, balafilcon A and senofilcon A increased in BSA sorption ($p<0.01$). Examination of these quantitative data (Table 4-3) shows that there is an apparent mismatch between some of the quantification data compared with the relative intensities of the fluorescently conjugated BSA. For example, with only 0.19 μg of BSA per lens (Table 4-3), etafilcon A deposited the lowest amount of BSA. However, the RITC-BSA profile for etafilcon A (Figure 4-1D) showed a higher intensity profile throughout this material compared to the other materials incubated in RITC-BSA (Figures 4-2D, 4-3D and 4-4D). Another example is seen for DTAF-conjugations. Table 4-3 shows that senofilcon A deposited the highest amount of BSA, compared

with the other materials. However, this apparently high level of BSA was only reflected by the BSA-DTAF combination (Figure 4-4B), with the other conjugates showing relatively low protein uptakes (Figures 4-4D and 4-4F). To further complicate this issue, the DTAF conjugate showed only minor fluorescent intensities for lotrafilcon B (Figure 4-2B) and high levels for balafilcon A (Figure 4-3B), although similar quantities of BSA were determined on these materials (Table 4-3). In addition, conjugations with LY showed the strongest fluorescent signal for balafilcon A (Figure 4-3F), which was not confirmed by the radioactive uptake (Table 4-3).

These comparisons suggest that none of the fluorescent probes investigated in this study provided "true" levels of fluorescence intensities relative to the total amount of protein sorbed to the material. Due to this fact, it was necessary to clarify whether low fluorescence intensities within samples were observed primarily due to fluorescent quenching within certain materials or due to lower sorption rates of the individual fluorescent probe. To address this query, we determined the remaining fluorescent intensity of the free LY solution after lens removal on Day 7 using fluorescent spectrophotometry. The relative starting intensity of the free dye solution was 278 fluorescent units and the remaining intensities in the solution following exposure of the dye solution to the materials were: 236 for etafilcon A, 244 for lotrafilcon B, 187 for senofilcon A, and 73 for balafilcon A. These numbers can be compared to our intensity values found in the CLSM scans, which confirmed highest fluorescence levels on balafilcon A (Figure 4-3E), moderate intensities for senofilcon A (Figure 4-4E) and lower levels for lotrafilcon B and etafilcon A (Figures 4-2E and 4-1E respectively). These findings confirmed that all materials deposited different amounts of this fluorescent probe, resulting in different fluorescence levels. However,

quenching factors within samples may still partially contribute to the overall emission intensity. Other material-based factors, such as the refractive index, autofluorescence or light absorbance at the specific wavelength may also contribute to the final emission strength. To correct for these light attenuation effects, a number of mathematical models have been proposed.[19]

An important factor to consider relates to which of the conjugate-binding results is most reflective of the location of BSA deposited. This must be considered in light of the binding of unbound dye (which will impact on the apparent protein location) and what is known about the structure of the materials investigated: In this study, only unbound LY showed an even distribution throughout all the materials, with no surface peaks being observed (Figures 4-1E, 4-2E, 4-3E and 4-4E). Senofilcon A and lotrafilcon B appear to adsorb LY-BSA in higher levels on the surface compared to the matrix alone (Figures 4-2F and 4-4F). This result can be accepted with a high level of confidence, as it can only be achieved if the BSA is truly adsorbing on the surface, as the "bigger" protein-dye conjugate is less likely to penetrate as easily as the dye alone into the material matrix, giving rise to the peak at the surface. If this is compared to the results for lotrafilcon B when exposed to unbound RITC (Figure 4-2C) or RITC-BSA (Figure 4-2D), it is possible that the dye will impact the result seen with the conjugated BSA. Thus, it is our opinion that of the three conjugates that it is the LY results that are most likely to be reflective of the protein uptake. (LY sorption profiles to contact lens materials not presented in this chapter can be found in Appendix C.)

Some previous studies have examined the bulk and surface properties of both hydrogel and silicone hydrogel materials,[28,31,59,60] and these data must be considered.

The high water content of etafilcon A (58%) and lack of surface coating results in a porous polymer structure and allows protein penetration into the matrix, as demonstrated with all three conjugates (Figures 4-1B, 4-1D and 4-1F). Scanning electron microscopy confirmed a macroporous structure for balafilcon A but not for lotrafilcon B,[31] which helps to explain our results for balafilcon A, which allowed LY-BSA to fully penetrate the material after only one day of incubation (Figure 4-3F), in comparison to that for lotrafilcon B, which accumulated only small amounts of protein (Figure 4-2F).

The impact of fluorescent dyes on protein-sorption behaviour to ion exchange adsorbents have been investigated by Linden et al.[61] They conjugated human immunoglobulin G and BSA with two fluorescent probes, Cy5 and Oregon Green. Similar protein sorption profiles were found for the conjugates when sorbing to SP Sepharose Fast Flow and Source 30S, regardless of the dye used for conjugation.[61] This provides further support that materials with a homogenous bulk structure and no surface modification allow an equal distribution of the fluorescent probe through the entire sample (as seen for the pHEMA material etafilcon A), while surface modification may exhibit minor differences in charge and hydrophobicity and therefore attract certain dyes to a greater extent.

A final factor to discuss relates to the degree of protein modification due to the attachment of the different dyes, which was not investigated in this study. However, the specific dye-binding location on the protein may impact both the emission intensity of the fluorophore [49] as well as the protein sorption behaviour.[13,14] Although desalting and extensive dialysis were applied to remove unbound dye molecules and small protein fractions from the solutions, it cannot be excluded that weakly bound

dye molecules may release over time and potentially impact the fluorescent pattern of the conjugated BSA uptake.

4.6 Conclusions

When investigating protein sorption to biomaterials using fluorescent probes, preliminary tests must be undertaken to detect specific dye affinities towards the material surface. This will avoid potential misinterpretations of protein sorption patterns when using fluorescently conjugated proteins. From the three probes investigated in this study, only unbound LY distributed evenly throughout the materials, and then subsequently showed varying sorption curves when conjugated with BSA.

However, despite the fact that the location of the sorbed protein could be determined using CLSM, a simultaneous quantitative method remains necessary to provide information on the total amount of protein sorbed to the biomaterial.

4.7 Acknowledgements

The authors would like to acknowledge funding for this study from Natural Science and Engineering Council of Canada (NSERC). The authors would also like to acknowledge the assistance of Professor Heather Sheardown and Lina Liu at McMaster University for providing the radiolabeled BSA.

In the next chapter, lysozyme was conjugated to a hydrophobic fluorescein-based dye (FITC) and a hydrophilic dye (lucifer yellow). Sorption profiles for both conjugates to nine different contact lens materials were imaged using CLSM and quantified using radiolabeled protein. Both results were combined to describe the lysozyme content on the surface and inside the lens matrix.

5. LOCALIZATION OF LYSOZYME SORPTION TO CONVENTIONAL AND SILICONE HYDROGEL CONTACT LENSES USING CONFOCAL MICROSCOPY

This chapter is published as follows:

Doerte Luensmann[1], Feng Zhang[1,2], Lakshman Subbaraman[1], Heather Sheardown[1,2], Lyndon Jones[1,2]

[1]Centre for Contact Lens Research, School of Optometry, University of Waterloo, Waterloo, ON, N2L 3G1

[2]Department of Chemical Engineering, McMaster University, Hamilton, ON, L8S 4L7

Curr Eye Res 2009;34(8):683–697 - Reprinted with permission

	Concept / Design	Recruitment	Acquisition of data	Analysis	Write-up / publication
Luensmann	Y	n/a	Y	Y	Y
Zhang	Y	n/a	Y	Y	-
Subbaraman	-	n/a	Y	-	-
Sheardown	Y	n/a	-	-	-
Jones	Y	n/a	-	-	Y

5.1 Overview

Purpose: To investigate the distribution profile of hen egg lysozyme (HEL) through poly-2-hydroxyethyl methacrylate (pHEMA)-based lens materials and silicone hydrogel (SH) lens materials using confocal laser scanning microscopy (CLSM).

Methods: Five silicone SH materials (balafilcon A, lotrafilcon A, lotrafilcon B, galyfilcon A, senofilcon A) and four pHEMA-based materials (alphafilcon A, etafilcon A; omafilcon A, vifilcon A) were incubated in 1.9 mg/ml protein solution for 24 hours. The protein solution consisted of HEL which was conjugated with either Fluorescein isothiocyanate (FITC) or Lucifer Yellow VS dilithium salt (LY). CLSM (Zeiss LSM 510 META) identified the location of the fluorescently-labeled protein by using 1µm depth scans through the lens. In a second experiment, lenses were incubated with 2% ^{125}I labeled HEL to determine the amount of deposited protein on each lens. Both techniques were combined to describe the individual HEL profiles.

Results: After the incubation in fluorescently-labeled HEL, all pHEMA-based materials and the SH material balafilcon A accumulated protein throughout the entire lens material, while, for the SH lenses lotrafilcon A and lotrafilcon B, HEL was primarily detected on the lens surface alone. Differences in protein uptake pattern due solely to the two conjugated dyes were most apparent for the SH materials galyfilcon A and senofilcon A; HEL was detected throughout these lenses when conjugated with LY but accumulated primarily on the surface when conjugated with FITC.

Conclusions: CLSM in combination with a radiolabel technique can describe both the location and degree of protein deposition on different contact lens materials.

5.2 Introduction

Hydrogel contact lens materials rapidly deposit proteins from the tear film,[1-3] which negatively impact on lens comfort [4,5] and visual performance.[6] Frequent replacement systems, in which the lenses are replaced on a pre-determined basis, limit deposit build-up [4,7-9] and improve both clinical performance and overall success rates.[3,5] Contact lens cleaning and disinfecting systems aim to remove proteins and other tear film contaminants from contact lenses, to reduce the risk of bacterial adhesion [10,11] and other adverse responses such as contact lens associated giant papillary conjunctivitis (CLAPC).[12-14]

Protein deposition profiles on contact lenses have been extensively studied both ex vivo and in vitro.[15-25] In most cases, the focus has been on the identification and quantification of the adsorbed/absorbed components, with minimal interest in the location of the deposited species. In other cases, microscopy techniques have been used to qualitatively describe surface-located deposition.[2,3,26-29] However, none of these methods can adequately describe the distribution of a specific protein throughout the entire contact lens material. The development of confocal laser scanning microscopy (CLSM) [30,31] allows optical slicing through thick samples and provides high resolution images through sections up to a few hundred microns in depth.[31] CLSM has been used in pharmaceutical and cell imaging studies,[32,33] material science [31] and in vivo imaging of the human cornea.[34] Furthermore, this technique has been adapted, using fluorescently-tagged proteins, to describe the depth of penetration and location of protein on both ex- vivo and in- vitro deposited contact lenses.[35-37]

Among tear proteins, lysozyme has been a major focus, since it is the most abundant protein in the tear film [38,39] and can play a dominant role in lens spoliation.[3] Studies have demonstrated that the overall net positive charge, in addition to its relatively small size (14.4 kDa), contributes to its high levels of uptake, particularly in materials with a net negative charge such as those based on combinations of poly-2-hydroxyethyl methacrylate (pHEMA) and methacrylic acid (MAA).[20,40,41]

While pHEMA-based soft lens materials have dominated the market since their introduction in the early 1970's,[42] their relatively poor oxygen transmissibility has resulted in a variety of hypoxic complications.[43-45] The commercialization of siloxane-based, highly oxygen permeable hydrogel materials in 1999 resulted in significant adoption of these so-called "silicone hydrogels" (SH), due to their exceptional oxygen transmissibility [42,46] and lack of hypoxic complications.[47] However, the siloxane component results in materials that are relatively hydrophobic and modification of either the surface or incorporation of wetting agents is necessary to obtain adequate in-eye wettability.[42] Studies investigating tear film deposition with hydrogel lenses indicate, not surprisingly, that pHEMA lenses tend to absorb higher amounts of protein but lower quantities of lipid, when compared to SH lenses.[23,48-50] Despite the reduced protein accumulation, recent observations have shown that SH lenses do not eliminate the risk of CLAPC.[51-53] It would appear that denaturation of proteins on the lens surface and the higher modulus of SH lenses may be involved in the stimulation of palpebral conjunctival responses,[54] independent of the total amount of accumulated protein on the lens.[17,53]

The biocompatibility of contact lenses on the ocular surface is still not fully understood, particularly when lenses are worn on a continuous wear basis for up to

30 nights. While the amount of deposition is fairly well characterized, the location of proteins on the lens surface or within the lens matrix remains unknown. This information may prove useful in understanding the inflammatory processes seen with soft lens materials and could provide valuable information for enhancing current contact lens materials and designs, as well as during the development of more efficient cleaning regimes.

This in vitro study uses CLSM, combined with protein radiolabeling, to locate and quantify protein distribution throughout nine hydrogel lens materials, in an attempt to describe the role of contact lens materials on protein spoilation.

5.3 Methods

The key properties of the soft contact lens materials investigated in this study are summarized in Table 5-1. All lenses examined were unworn lenses with a power of -3.00D.

Table 5-1: Contact lens materials examined

Trade Name	USAN	FDA Category	Manufacturer	Stated centre thickness (μm)	Water content (%)	Principal monomers
Silicone Hydrogel Lens Materials						
ACUVUE® ADVANCE®	Galyfilcon A	I	Johnson & Johnson	70	47	mPDMS, DMA, HEMA, siloxane macromer, EGDMA, PVP
ACUVUE® OASYS™	Senofilcon A	I	Johnson & Johnson	70	38	mPDMS, DMA, HEMA, siloxane macromer, TEGDMA, PVP
NIGHT & DAY®	Lotrafilcon A	I	CIBA Vision	80	24	DMA, TRIS, siloxane macromer
AIR OPTIX™ AQUA	Lotrafilcon B	I	CIBA Vision	80	33	DMA, TRIS, siloxane macromer
PureVision®	Balafilcon A	III	Bausch & Lomb	90	36	NVP, TPVC, NVA, PBVC
Conventional (pHEMA-based) Lens Materials						
ACUVUE®2™	Etafilcon A	IV	Johnson & Johnson	80	58	HEMA, MAA
Focus® Monthly	Vifilcon A	IV	CIBA Vision	100	55	HEMA, PVP, MAA
Proclear® Compatibles	Omafilcon A	II	Cooper Vision	65	62	HEMA, PC
SofLens® 66	Alphafilcon A	II	Bausch & Lomb	90	66	HEMA, NVP

DMA *N,N*-dimethylacrylamide; EGDMA ethyleneglycol dimethacrylate; HEMA 2-hydroxyethyl methacrylate; MAA methacrylic acid; MMA methyl methacrylate; mPDMS monofunctional polydimethylsiloxane; NVA *N*-vinyl aminobutyric acid; NVP N-vinyl pyrrolidone; PBVC poly[dimethylsiloxyl] di [silylbutanol] bis[vinyl carbamate]; PC phosphorylcholine; PVP polyvinyl pyrrolidone; TEGDMA tetraethyleneglycol dimethacrylae; TPVC tris-(trimethylsiloxysilyl) propylvinyl carbamate; TRIS trimethyl siloxy silane.

5.3.1 Fluorescent labeling of lysozyme

Figures 5-1 and 5-2 show the two fluorescent probes that were conjugated with hen egg lysozyme (HEL, Sigma-Aldrich, St. Louis, MO). Fluorescein isothiocyanate (FITC, Molecular Probes, Eugene, OR) and Lucifer Yellow VS dilithium salt (LY, Sigma

Aldrich, St. Louis, MO) were conjugated in two separate experiments, using methods optimized for each dye.

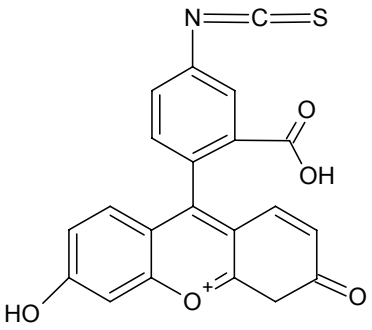

Figure 5-1: Fluorescein isothiocyanate (FITC): $C_{21}H_{11}NO_5S$ MW: 389

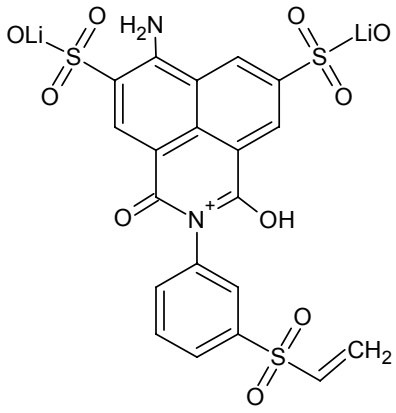

Figure 5-2: Lucifer Yellow VS dilithium salt (LY): $C_{20}H_{12}Li_2N_2O_{10}S_3$, MW: 550

FITC-HEL conjugation: A mass ratio of 20:1: FITC:HEL was used. Briefly, HEL in 0.1 M sodium bicarbonate (10 mg/ml) was prepared. FITC (10 mg) was dissolved in 1mL dimethyl sulfoxide (DMSO, Sigma-Aldrich, St. Louis, MO) and then added to the HEL solution, with gentle stirring for one hour in the dark. As precipitation of the

conjugated protein may occur during the reaction (since FITC-HEL is usually less soluble than native protein), the mixture was centrifuged at 12,000g for 1 minute. Free FITC was removed using a Sephadex G25 column (Amersham Biosciences, Baie d'Urfe, QC, Canada). Elution was performed using PBS, at pH 7.4. A portable UV light was used to monitor the separation process by observing fluorescence in the column. Following this, dialysis against PBS using a 7 kDa molecular weight cutoff dialysis cassette (Pierce, Rockford, IL) was performed, until only a small amount of free FITC was detected with a fluorescence spectrophotometer (Hitachi F-4500, Tokyo, Japan). The efficiency of binding of the fluorescent dye to the protein was determined spectroscopically (Multiscan Spectrum, Thermo Electron, Waltham, MA) by measuring the absorbance at 280nm (to determine the protein concentration) and at 494nm (which is the maximum absorbance for FITC). The resulting degree of labeling (DOL) was 0.94 (0.94 molecules dye per molecule of protein) (Appendix A).

LY-HEL conjugation: Preliminary experiments showed that a mass ratio of 1:1 LY:HEL provided sufficient fluorescence intensity for the conjugated protein to be easily detected. Briefly, HEL in 0.05 M borate buffer (pH = 8.5) and 0.04 M NaCl (10 mg/ml) was prepared. LY is water soluble and 7mg could be dissolved in 1mL of borate buffer (pH 8.5). The LY solution was added to the HEL solution followed by gentle stirring for one hour in the dark. Since no precipitation of the conjugated protein occurred, no subsequent centrifugation step was necessary. Free LY was removed using a Sephadex G25 column. Following this, dialysis against PBS using a 7 kDa molecular weight cutoff dialysis cassette was performed, until only minor free LY was detected with a fluorescence spectrophotometer. The labeling efficiency was calculated by determining the HEL concentration in the solution using the DC Protein

Assay (Bio-Rad, Hercules, CA) and measuring the absorbance at 415nm (which is the maximum absorbance for LY). It was necessary to use the DC Protein assay to quantify the protein in this case as LY has substantial absorption between 250 and 300nm and would therefore interact with the protein absorption measured at 280nm. The resulting DOL was 0.27 (0.27 molecules dye per molecule of protein).

5.3.2 Lysozyme sorption to contact lens materials

The conjugated HEL solutions were sterilized with 0.2 µm syringe filters to prevent microbial contamination of the samples during the incubation phase. Unlabeled HEL was added to the conjugated HEL to give a physiologic tear concentration of 1.9 mg/ml.[55,56] Since lower amounts of labeled protein result in less photobleaching during subsequent confocal analysis, the lowest possible amount of conjugated HEL was used for the experiments. Contact lens materials that were known to accumulate large amounts of lysozyme from previous studies [22,24] were incubated with low levels (2%) labeled and 98% unlabeled HEL, while other materials known to accumulate only small amounts of protein were incubated in 100% labeled HEL.

Prior to protein incubation, all lenses were removed from their blister packs and presoaked for 30 minutes in sterile PBS (phosphate buffered saline) at pH 7.4, to minimize the influence of the lens packaging solution components on protein uptake. Many companies now include a variety of surface-active agents into these packaging solutions, whose influence on protein sorption remains unknown. Following this presoaking phase, lenses were transferred into brown Eppendorf vials using sterile metal forceps and placed in a face up position. 1 ml of the prepared protein solution

was added, and lenses were incubated for 24 hours under constant rotation at 72 RPM at a temperature of 37°C to mimic the approximate human body temperature.

5.3.3 CLSM examination technique

After incubation for 24 hours, the contact lenses were removed from the vials and prepared for confocal microscopy. Following rinsing with PBS, the lens was placed onto the mantel of a mechanical punch press and a round button of 4 mm diameter was cut out of the center of the lens. The punch press was carefully cleaned prior to each use to ensure a clean, dust and protein free surface. Using plastic tweezers, the lens button was gently dabbed dry using lens paper and mounted onto a glass microscope slide. Approximately 40 µL of mounting media containing PBS was placed onto the microscope slide. A glass coverslip was then carefully applied and sealed with nail polish to prevent evaporation and to stabilize the coverslip for use with the immersion objectives of the confocal microscope.

The lens materials were subsequently examined for protein uptake using confocal laser scanning microscopy (CLSM) (Zeiss Inc. Toronto, Canada). The Zeiss 510, configuration Meta 18 was equipped with an inverted motorized microscope Axiovert 200M. Each lens was scanned at a central location using an excitation wavelength of 488nm (Argon Laser) for FITC-HEL and 405nm (Laser Diode) for LY-HEL. The selected emission filters were BP 505-530nm and LP 505nm for FITC and LY respectively. Each section of z stacks was set at 1 µm intervals with image sizes of 512 x 512 µm. Lenses were scanned with a 40x water immersion C-Apochromat objective. Using the software provided with the microscope and ImageJ (Bethesda,

MD),[57] the means of the fluorescence intensity were plotted as a function of the scanning depth.

5.3.4 Protein uptake measured by ^{125}I radiolabeling

For quantification purposes, the intensity values over the 24 hour doping period were converted into microgram amounts per lens based on previous 24 hour data obtained in our laboratory, using a radioactive HEL uptake method.[22] Briefly, HEL was radiolabeled with ^{125}I using the iodine monochloride method, as previously described.[58-60] Lenses were subsequently incubated in a 1.9 mg/ml HEL solution, containing a mixture of 2% labeled and 98% unlabeled HEL. Following incubation for 24 hours, the lenses were rinsed with PBS to remove loosely adsorbed protein and the amount of firmly sorbed HEL was determined using a gamma counter (1470 Wallac Wizard PerkinElmer, Woodbridge, ON).

5.3.5 Determination of lens thickness

As described above, the CLSM measurements were taken at the center of each lens. However, this z-scan does not represent the average thickness across the lens, as contact lenses with a power of -3.0 D (dioptres) increase in thickness from the center towards the lens edge, resulting in an increase in average thickness over any specific chosen diameter.[61] Therefore, an adjustment for thickness over the entire lens was required prior to converting the total amount of protein found with the radiolabeled HEL technique [22] to the CLSM scans.

To measure lens thickness, each contact lens type under examination was slit from the mid-periphery to the edge of the lens using a razor blade, allowing them to be flat mounted on a clear plastic slide with pre-printed concentric rings. Lens

thickness was determined at 20 different points, using an electronic thickness gauge (Rehder Development Company, Castro Valley, CA), which measured to 1 μm steps. Lens thickness was determined in a room with a fixed humidity of 60%, in order to control lens dehydration. Thickness values were obtained centrally and at 1.5, 3.1, 4.8 and 6.9 mm away from the center, which represented on-eye distances of 1.5, 3.0, 4.5, 6.0 mm from the centre of the lens. Measurements were taken at 3, 6, 9 and 12 o'clock locations using two replicates for each lens type (resulting in eight values for each location).

5.3.6 Combining CLSM and radiolabeling results

As described above, our CLSM technique provides an excellent method for determining the location of protein on these hydrogel membranes. However, it cannot be used to accurately quantify the amount of deposited protein. Our previously reported radioactive data [22] is quantitative in nature, but it cannot be used to determine the location of the protein deposition. By combining data from both methods it is possible to accurately quantify the amount and describe the location of the deposited protein of interest associated with the lens or other biomaterial. One problem that arises in trying to reconcile these data is that the previously obtained radiolabeling results used a lens of the commercially available diameter, but our CLSM method only uses a central section of 4 mm diameter. A further confounding factor, as described above, is that the thickness of the hydrogel sample examined is not constant across the entire diameter of the lens, being thicker at the periphery for the -3.00D lenses examined in this study.

In order to address these issues, a method was developed that enabled us to determine the approximate protein accumulation throughout the lens section scanned with the CLSM, independent of the scan thickness. To achieve this, a formula was derived that adjusted the protein amount per CLSM scan for the average thickness of the lens. As an example, if a CLSM scan obtained centrally showed a lens thickness of 80 µm and the average thickness of the lens determined via the Rehder gauge showed an average thickness of 120 µm, then the fluorescence intensity determined via the CLSM needed to be converted into a fluorescence intensity over a lens section that was 40 µm thicker, to compensate for this increase in thickness over the lens diameter. The fluorescence intensity per scan step was converted into the respective HEL amount using the radiolabeled HEL data in Table 5-3. Modifications of the inner matrix of the scan were applied to address for the difference between average lens thickness and scan thickness

$$HELi = \frac{FLi * \sum HEL}{FLm * (aveT - scanT) + \sum FL}$$

where *HELi* is the amount of HEL on an individual scan image (µg), *FLi* is the fluorescence intensity of this individual scan image, *ΣHEL* is the total amount of HEL per lens (µg), *FLm* is the fluorescence intensity of the average inner matrix scan, *aveT* is the average lens thickness (µm), *scanT* is the individual scan thickness (µm) and *ΣFL* is the sum of the fluorescent intensity for the entire scan.

This calculation method was applied solely to approximate the average lens thickness of each lens type investigated in this study.

5.4 Results

5.4.1 Lens thickness

The lens thickness at each of the five points described above and the average thickness over the entire lens, as determined by the Rehder gauge, for all lenses are shown in Table 5-2.

Table 5-2: Contact lens thickness (-3.00D) determined by Rehder gauge

Silicone Hydrogel Lens Materials (Mean ± SD (µm))					
Distance from center	Senofilcon A	Galyfilcon A	Lotrafilcon A	Lotrafilcon B	Balafilcon A
Central	67.0±1.1	70.5±1.5	84.5±2.1	79.6±1.7	81.6±1.8
1.5mm	75.8±1.5	79.8±2.1	91.9±5.3	85.5±10.7	90.3±3.5
3.0mm	101.1±4.1	106.9±3.9	109.1±8.8	110.6±17.8	117.5±4.9
4.5mm	149.8±4.4	166.5±9.4	131.3±14.9	154.9±30.8	172.3±4.2
6.0mm	185.4±3.0	213.3±7.6	132.4±23.6	196.8±40.7	172.4±6.6
Average thickness	**115.8 ± 50.5**	**127.4 ± 60.9**	**109.8 ± 22.0**	**125.5 ± 49.7**	**126.8 ± 43.6**

Conventional (pHEMA-based) Lens Materials (Mean ± SD (µm))				
Distance from center	Etafilcon A	Vifilcon A	Omafilcon A	Alphafilcon A
Central	78.9±1.0	83.5±0.5	79.5±0.5	90.5±3.0
1.5mm	85.9±3.1	91.8±3.2	87.5±1.3	98.1±3.7
3.0mm	111.8±5.1	117.5±4.8	114.6±3.3	122.0±4.9
4.5mm	170.8±11.1	143.6±7.2	154.3±4.2	160.6±4.3
6.0mm	211.8±3.4	169.3±11.8	174.0±5.6	186.8±3.5
Average thickness	**131.8 ± 57.5**	**121.1 ± 35.8**	**122.0 ± 41.2**	**131.6 ± 41.2**

As expected, the lens thickness values for all materials were lowest centrally, ranging from 67 to 91 µm, and increased towards the edge (132.4 to 213 µm). The

majority of the measured centre thickness of the lenses was within 5 µm of the manufacturer stated values. The average thickness of the 5 locations across the lenses was between 110 and 132 µm.

5.4.2 Radiolabeling results

The amount of HEL deposited on the various lens materials after 24 hours of incubation, as determined by the radiolabel method, is reported in Table 5-3.

Table 5-3: Radiolabeled HEL sorption after 24 hours of incubation [22]

Silicone Hydrogel Lens Materials (Mean ± SD (µg))					
	Senofilcon A	Galyfilcon A	Lotrafilcon A	Lotrafilcon B	Balafilcon A
HEL per lens	0.53±0.10	0.75±0.10	0.20±0.08	0.33±0.08	1.40±0.09
Conventional (pHEMA-based) Lens Materials (Mean ± SD (µg))					
	Etafilcon A	Vifilcon A	Omafilcon A	Alphafilcon A	
HEL per lens	620.5±93.0	144.3±36.0	11.0±5.6	16.0±5.8	

5.4.3 CLSM data

Typical CLSM intensity scans for lotrafilcon A and balafilcon A are shown in Figures 5-3A and 5-3B. For the lotrafilcon A lens, fluorescence intensity bands were only detected on the surface of the lens, indicating that the HEL does not penetrate into the lens matrix (Figure 5-3A). This is very different from the balafilcon A material, which shows an even distribution of the labeled HEL throughout the lens, with the surface being no barrier to protein penetration (Figure 5-3B).

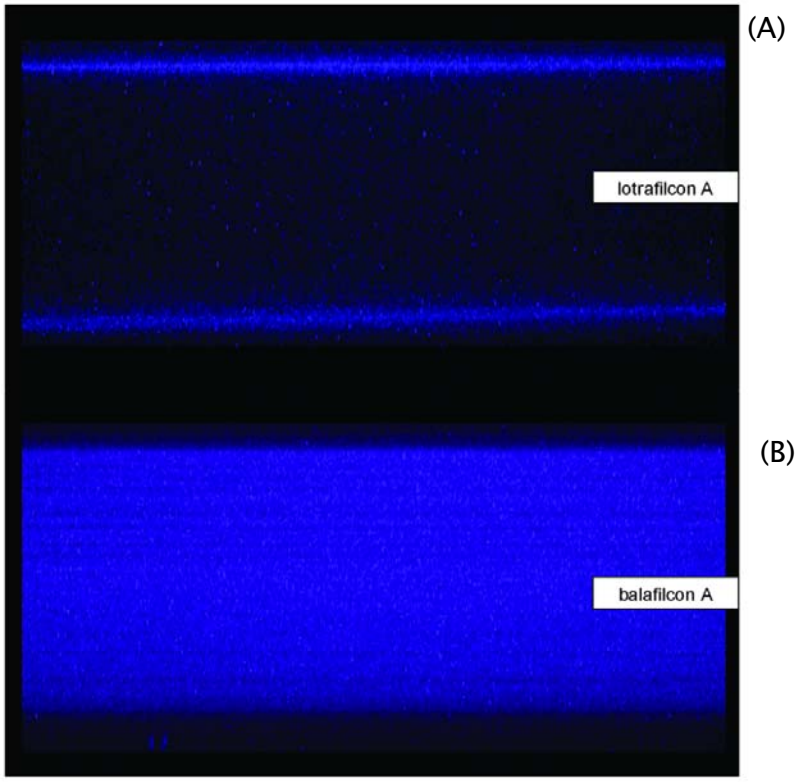

Figure 5-3: Typical CSLM profile scans for LY-HEL sorption to lotrafilcon A (A) and balafilcon A (B) materials after 24 hours of incubation

5.4.4 Combined radiolabel and CLSM data

The HEL sorption for the two FDA group II (high water content, neutral charge) materials, omafilcon A and alphafilcon A, are plotted in Figures 5-4 and 5-5. Both materials absorb similar amounts of HEL (approximately 11 µg/lens for omafilcon A and 16 µg/lens for alphafilcon A), with relatively rapid penetration occurring after 24 hours throughout the entire lens material. Only minor differences can be seen between HEL conjugated with the two dyes for omafilcon A (Figure 5-4). Omafilcon A incubated in FITC-HEL showed small "peaks" at the lens surface, suggesting an accumulation at the lens surface that is slightly larger than that found in the matrix.

This was not confirmed with the HEL-LY conjugation, suggesting that the apparent protein deposition at the lens surface may be due to uptake of the specific fluorescent dye, rather than uptake of protein per se. HEL sorption for the alphafilcon A material (Figure 5-5) was evenly distributed throughout the entire thickness of the lens, regardless of the fluorescent dye used.

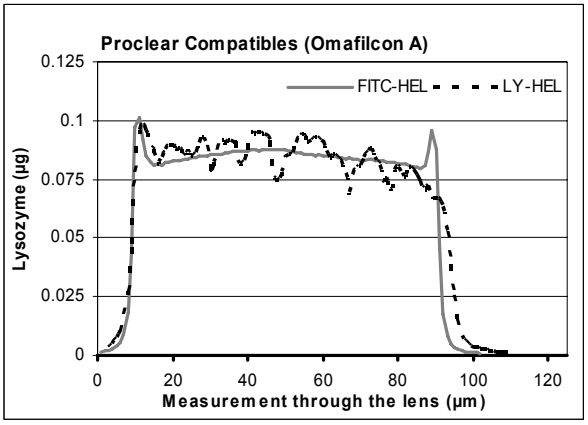

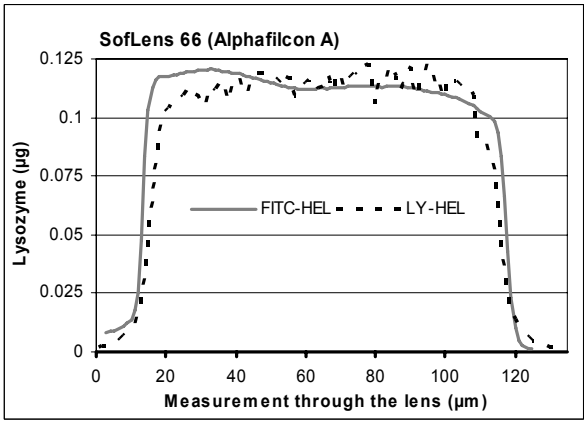

Figure 5-4: FITC-HEL and LY-HEL sorption profiles to omafilcon A

Figure 5-5: FITC-HEL and LY-HEL sorption profiles to alphafilcon A

The x-axis shows the confocal scan through the lens (µm) and the y-axis shows the relative HEL accumulation (µg).

Protein levels associated with both FDA group IV (high water content, ionic charge) materials were significantly greater than all other materials. Figures 5-6 and 5-7 show the deposition curves for etafilcon A and vifilcon A, and these clearly demonstrate that greater HEL deposition occurred with the etafilcon A material. After 24 hours of incubation, etafilcon A accumulated more HEL on the surface compared to the matrix, when conjugated with FITC. However, an even distribution of the protein throughout the material was found when conjugated with LY. Other lenses (see Appendix D) that were incubated for a shorter incubation period of 3 hours

showed that LY-HEL was primary found on the surface, mimicking the pattern shown in Figure 5-6 with the FITC-HEL. However, a longer incubation time of 3 days with FITC-HEL showed an even distribution of HEL between the surface region and the matrix, similar to that shown in Figure 5-6 for LY-HEL. These data suggest that the dyes used for conjugation of the proteins impact the kinetics of HEL uptake for etafilcon A lenses.

Figure 5-7 shows that vifilcon A accumulated slightly more HEL on the lens surface compared to the central region, regardless of the fluorescent dye used. Overall, this lens deposited only approximately half the amount of HEL compared to the etafilcon A lens.

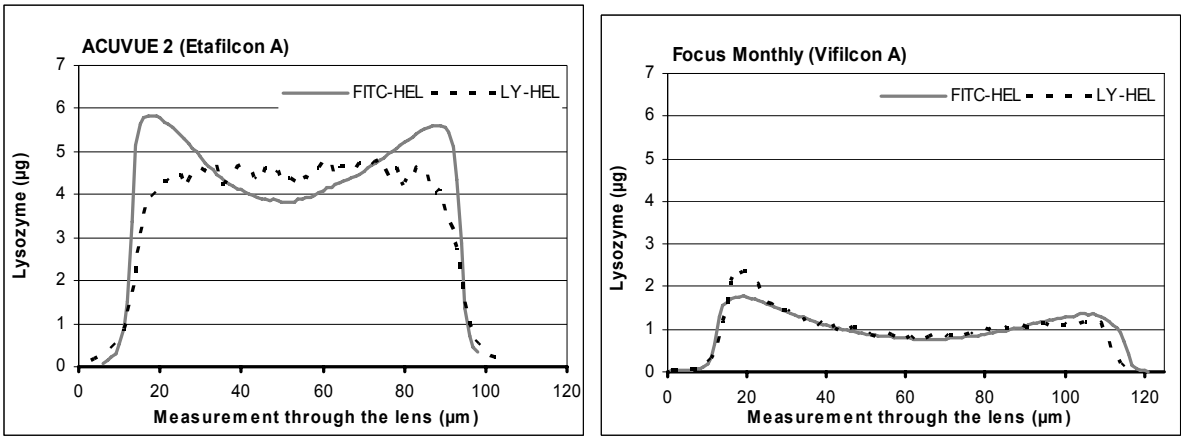

Figure 5-6: FITC-HEL and LY-HEL sorption profiles to etafilcon A

Figure 5-7: FITC-HEL and LY-HEL sorption profiles to vifilcon A

The x-axis shows the confocal scan through the lens (µm) and the y-axis shows the relative HEL accumulation (µg).

The HEL sorption for the two FDA group I (low water content, neutral charge) materials, lotrafilcon A and lotrafilcon B, are plotted in Figures 5-8 and 5-9. These two

silicone hydrogel lenses show HEL sorption almost exclusively on the surface of the lenses, with both materials absorbing the smallest amounts of HEL compared to all other materials investigated, at approximately 0.20 µg/lens for lotrafilcon A and 0.33 µg/lens for lotrafilcon B. Minor penetration of the conjugated HEL into the matrix occurred for lotrafilcon B only, which was more apparent for LY-HEL compared to FITC-HEL.

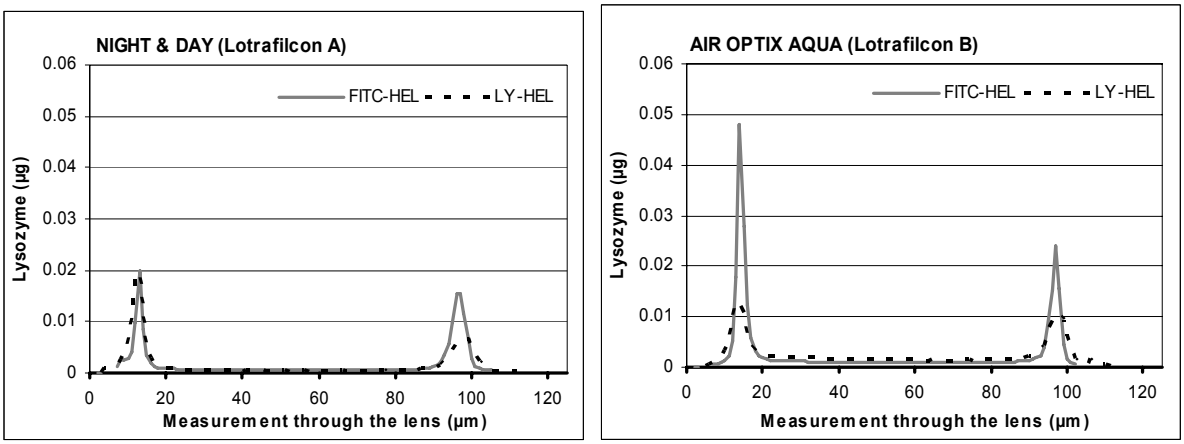

Figure 5-8: FITC-HEL and LY-HEL sorption profiles to lotrafilcon A

Figure 5-9: FITC-HEL and LY-HEL sorption profiles to lotrafilcon B

The x-axis shows the confocal scan through the lens (µm) and the y-axis shows the relative HEL accumulation (µg).

The HEL sorption for the three remaining silicone hydrogel lenses (balafilcon A, galyfilcon A and senofilcon A), are plotted in Figures 5-10 to 5-12. After 24 hours of incubation, HEL could be detected throughout the balafilcon A material in an evenly distributed pattern, which was independent of the fluorescent dye used (Figure 5-10). With approximately 1.4 µg/lens, balafilcon A attracted the highest amount of HEL of the SH materials investigated.

For galyfilcon A, the HEL distribution was strongly dependent on the conjugated dye used (Figure 5-11). When conjugated with FITC, HEL was primarily detected on the surface, with some HEL penetrating a few microns into the matrix. However, no signal could be detected in the central matrix of the material. In contrast, HEL conjugated with LY showed penetration through the entire galyfilcon A material, with only little higher uptake on the surface region.

The discrepancies between the two fluorescent dyes were even more apparent for senofilcon A (Figure 5-12). FITC-HEL was almost exclusively located on the surface of the lens, while the distribution of LY-HEL was throughout the entire lens. The unequal distribution profiles suggest a strong impact of the individual dye used, when investigating galyfilcon A and senofilcon A-type materials. The total amount of HEL uptake on galyfilcon A and senofilcon A was approximately 0.75 and 0.53 µg/lens respectively.

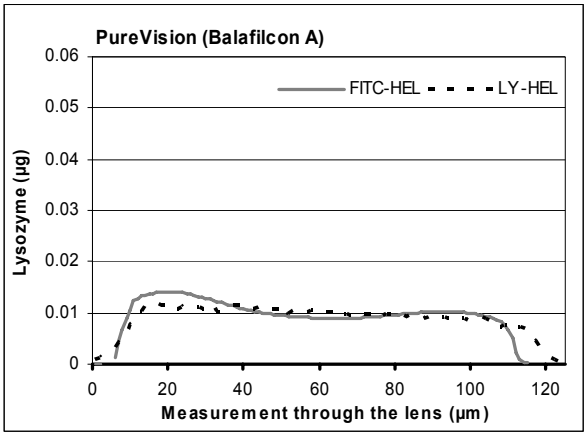

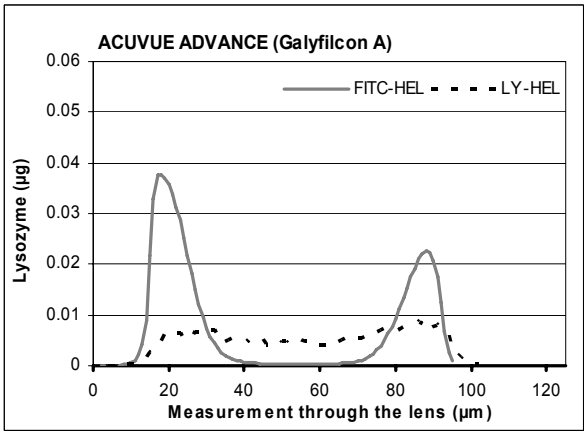

Figure 5-10: FITC-HEL and LY-HEL sorption profiles to balafilcon A
Figure 5-11: FITC-HEL and LY-HEL sorption profiles to galyfilcon A

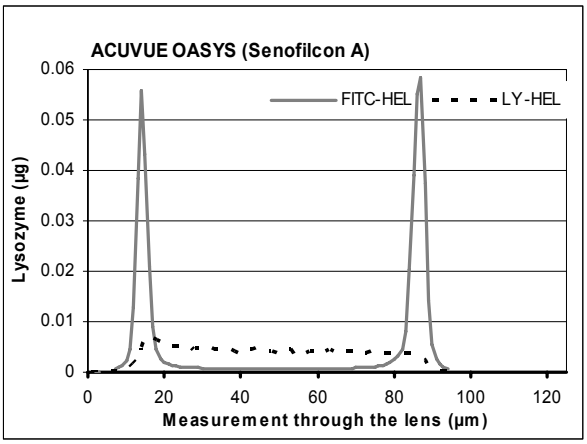

Figure 5-12: FITC-HEL and LY-HEL sorption profiles to senofilcon A

The x-axis shows the confocal scan through the lens (µm) and the y-axis shows the relative HEL accumulation (µg).

5.5 Discussion

5.5.1 Conventional pHEMA materials

The sorption behaviour of tear-film proteins is critical in understanding and investigating mechanisms involved in contact lens spoilation and material biocompatibility. Protein sorption at a liquid-solid interface includes adsorption of the protein at the surface and protein diffusion into the polymer matrix. Previous studies have demonstrated that proteins, particularly lysozyme, rapidly penetrates into commercially available and model pHEMA/MAA copolymers.[35,62] Since commercial contact lens materials are classified by the Food and Drug Administration (FDA) according to their water content and charge, it is of interest to determine how these two properties affect the lysozyme uptake profile. Two previous in vitro studies have used CLSM to determine protein location within hydrogel materials. Garrett and colleagues [20] demonstrated that increased amounts of MAA within hydrogel substrates

resulted in significantly increased lysozyme sorption and penetration, but reduced levels of albumin adsorption. They surmised that this was due to differences in electrostatic attractions between the material and the two proteins studied. Our group [36] used CLSM to locate the deposition profile of albumin on a FDA group IV material (etafilcon A) and a SH material (lotrafilcon B). Different uptake patterns were shown for the overall negatively charged albumin, with the albumin being located only on the surface of lotrafilcon B, but throughout the matrix for etafilcon A.

Our current results show that the location of deposited HEL in this in vitro model is significantly impacted by both bulk and surface material properties. The FDA group II (high water content, neutral charge) material omafilcon A incorporates phosphorylcholine (PC), a synthetic analogue that simulates natural phospholipids, into pHEMA. PC possesses both a positive charge on the nitrogen and a negative charge on the carbonyl groups. It is found in the outer lipid layers of red blood cell membrane and is responsible for cell membrane biocompatibility.[63] Omafilcon A has previously been shown to be deposit resistant to both tear proteins and lipids [64] and exhibited a low dehydration rate compared to other hydrogel contact lens materials.[64,65] Figure 5-4 shows that omafilcon A exhibits a small peak of HEL at the lens surface region, which may be related to the lack of PC present at the lens interface since the presence of PC is widely accepted to reduce protein fouling. The concentration and distribution of PC in omafilcon A is not stated by the manufacturer, but studies investigating the polymer structure of omafilcon A confirmed that PC is found throughout the lens [66] but not in the outermost 100 Å.[67] The other group II material, alphafilcon A, is a pHEMA-based lens that incorporates N-vinyl pyrrolidone (NVP), a non-ionic and water-soluble monomer to increase water content. NVP-

containing contact lenses have been shown to deposit high levels of lipid from the tear film but only small amounts of protein.[7,16] Figure 5-5 shows an equal distribution of HEL throughout the alphafilcon A material, indicating that the high water content of 66% and presumably high porosity allows rapid penetration of the protein into the lens matrix.

In FDA group IV materials (high water content, negative charge), the ionic monomer methacrylic acid (MAA) is incorporated with HEMA to generate a polymer with increased water content. Figures 5-6 and 5-7 show the deposition profiles of etafilcon A (pHEMA/MAA) and vifilcon A (pHEMA/MAA/PVP) after 24 hours incubation in HEL. Etafilcon A incorporates an increased quantity of MAA than vifilcon A, imparting an increased negative charge to the material.[42] Figure 5-6 shows that the HEL in etafilcon A is located relatively uniformly throughout the lens when conjugated with LY, but that the protein is seen in higher concentrations at the surface when conjugated to FITC. Incubation for longer than 24 hours [99] reveals that this difference between the two dyes disappears over time, which suggests that LY-HEL penetrates more quickly into the lens matrix than FITC-HEL, presumably due to size and chemistry differences between the two dyes. Specifically the more hydrophobic character of FITC [68] compared to the hydrophilic LY [69] or a potential change in the overall charge of the conjugated HEL [70,71] may alter the uptake kinetics. Vifilcon A lenses (Figure 5-7) show a similar uptake pattern for both dyes examined. HEL can be detected throughout the material, with slightly higher concentrations within the outermost 20 μm depth. Even with longer incubation times [99] (see Appendix D) HEL remains more abundant on the surface region, with less HEL detected inside the central matrix, regardless of the dye used. As a result of this negative charge,

etafilcon A and vifilcon A attract high levels of positively charged lysozyme, which is in agreement with previous ex- vivo and in- vitro studies.[8,22,23,41,72] While the protein uptake patterns were similar between etafilcon A and vifilcon A, the addition of the PVP to the vifilcon A and possible differences in MAA concentrations for both materials clearly resulted in decreased levels of protein sorption to vifilcon A.

The role of MAA on the bulk absorption of lysozyme to pHEMA/MAA containing materials has been studied extensively by Garrett and coworkers, who reported that lysozyme amounts increased as a function of increasing percentage of MAA in hydrogels.[73] They suggest that this increase in lysozyme penetration with higher MAA content is due to increased water content, porosity and electrostatic force. The results of the current work are in agreement with these conclusions. In contrast, studies investigating the relatively hydrophilic PVP reported reduced lysozyme attraction for PVP-coated surfaces.[74,75]

Our study confirms that the levels of protein associated with both group II lens materials were similar, and significantly lower, compared to those observed in the group IV materials (Figures 5-4,-5-7 and Table 5-3).

5.5.2 Silicone hydrogel materials

Silicone hydrogel lenses have more complex monomer compositions compared to pHEMA-based materials. Commercially available materials contain multiple polymer components such as Tris, PDMS, TPVC, DMA or siloxane macromers (Table 5-1). However, regardless of the polymer makeup, the hydrophobic nature of the silicone component necessitates additional modification or surface treatment. Currently available SH lenses can therefore be divided into two categories, depending upon

their surface characteristics used to overcome their hydrophobic nature.[42] Balafilcon A, lotrafilcon A and lotrafilcon B are modified using a plasma treatment. The balafilcon A material is surface treated using a reactive gas plasma, which transforms the siloxane components on the surface of the lenses into hydrophilic silicate compounds,[46,76,77] whereas lotrafilcon A and lotrafilcon B are permanently modified by gas plasma using a mixture of trimethylsilane oxygen and methane to create a thin (25nm), continuous hydrophilic surface.[42,78,79] Galyfilcon A and senofilcon A utilise a different methodology, in which the wetting agent PVP is incorporated during the polymerization process.[80-82] This non-ionic high molecular chain is very hydrophilic and shields the tear film from the hydrophobic siloxane component in the material, which may enhance comfort during lens wear.[83,84]

Results of this study strongly suggest that within the FDA group I (low water content, neutral charge) SH materials HEL sorption is closely linked to material water content, with higher water content values resulting in higher levels of HEL sorption (Tables 5-1 and 5-3), although there are clearly a number of other factors which can also impact on protein sorption. The highest level of HEL sorption was seen in the FDA group III (low water content, negative charge) SH material (balafilcon A), in which the predominant factor driving deposition was likely to be the negatively charged aminobutyric acid monomer NVA.

The similar material composition and surface coating of lotrafilcon A and lotrafilcon B clearly results in a similar protein uptake pattern (Figures 5-8 and 5-9). Sharp peaks of HEL deposition at or near the lens surface can be detected for both lenses. The plasma coating on lotrafilcon A appears to be a strong barrier to protein entry, as it allows no HEL to penetrate into the inner matrix, however minor but

significant amounts of HEL could be detected throughout the matrix of lotrafilcon B (Figure 5-9). Given that the two lotrafilcon materials undergo identical surface treatment processes, we propose that the higher water content of lotrafilcon B might be responsible for a reduced polymer density, resulting in an increase in pore size within the material, which results in the differences in protein sorption patterns observed.

Examination of Figure 5-9 shows that more HEL was detected inside the matrix of lotrafilcon B when conjugated with LY compared to FITC. It is possible that unbound dye, which is 25-30 times smaller than HEL, could penetrate into the lens material and therefore cause a systematic error. To determine if the binding between the two dyes and HEL were equally stable over time it was necessary to investigate the amount of unbound dye in the solution. This was determined by dialysing the conjugated HEL over 24 hours. This experiment revealed that the LY-HEL conjugation was much stronger than that obtained with FITC-HEL, with the latter showing more dye release over time (data not presented). This enables us to conclude that the result shown in Figure 5-9 is not due to dissociation between the LY-HEL conjugation, but is a true result. This could be due to increased surface attraction for FITC-HEL compared with bulk attraction, as compared with the LY-HEL, which also migrates into the material.

For balafilcon A, the penetration of HEL into the interior of these matrices is likely due to the macroporous nature of this lens, as shown by both scanning electron microscopy and atomic force microscopy.[79,85,86] Under conditions of dehydration and hydration, it was found that the diameter of macropores in the balafilcon A could be as high as 0.5 μm, which is significantly larger than the pore size of conventional

pHEMA-based materials, which have a reported pore size of <0.05 μm.[87-89] Our results (Figure 5-10) confirmed that these macropores are sufficiently large to permit the diffusion of HEL from the bulk solution, without significant pore fouling. After 24 hours of incubation balafilcon A accumulated more FITC-HEL in the surface region compared to the central matrix, while LY-HEL was already distributed evenly throughout the material. Incubation over seven days (see Appendix D) proved that both conjugates are uniformly distributed inside the material. This indicates that FITC-HEL travels slower into the lens matrix, compared to LY-HEL.

Senofilcon A and galyfilcon A (FDA group I, low water content, neutral charge) have similar material compositions, with both materials incorporating the wetting agent PVP, which can act as a protein repellent interfacial layer.[22,74,75] Examination of Figures 5-11 and 5-12 show that there were significant differences between the different conjugates when investigating senofilcon A and galyfilcon A. FITC-HEL was mainly located in the surface region of galyfilcon A and senofilcon A, as compared to LY-HEL which was almost evenly distributed throughout the lens materials. Even with longer incubation times[99] no major changes in the distribution profiles were observed. A comparison between the two materials when incubated in FITC-HEL showed that the protein traveled about 20 μm into galyfilcon A but only 10 μm into senofilcon A. One potential reason for these differences between the two different fluorescent dyes might be an increased electrostatic attraction between FITC-HEL and monomers such as PVP that are located in different concentrations at the surface of the lens. These substantial differences between the two dyes, which drives FITC-HEL to almost exclusively accumulate at the surface of these PVP-containing SH materials, but LY-HEL to be almost evenly distributed between the surface and bulk warrants further

investigation and calls into question the actual distribution of HEL throughout both galyfilcon A and senofilcon A.

5.5.3 Impact of the conjugate on the native protein

Fluorescence analysis of proteins is an extremely useful technique and the majority of proteins exhibit an intrinsic fluorescence in the ultraviolet spectrum due to the aromatic amino acids tryptophan, tyrosine and phenylalanine. However, many analytical techniques do not permit measurements in the UV spectrum or necessitate that proteins are differentiated, which then requires the protein to be tagged with an extrinsic fluorescent dye. Most fluorescent dyes do not bind to a protein unless they are modified with an additional reactive group. This reactive group is covalently attached to the dye and binds under specific conditions with reactive residues of the protein, such as the ε-amino group of lysine.[90] Although fluorescent dyes are multiple times smaller than the protein, many studies report differences in charge, seize and mobility between labeled and unlabeled proteins.[70,91] Bingaman et al.[70] conjugated albumin and α-lactalbumin with five different fluorescent dyes, including FITC. Most apparent physiochemical changes were found for the conjugation with FITC. Molecular size and weight, relative molecular charge, and isoelectric point were different compared to the native protein, which became even more significant with higher DOL. A study by Crandall et al. investigated the properties of albumin, when labeled to I^{125} and FITC.[92] They reported significant changes in chromatographic and electrophoretic behaviour when conjugated with FITC, but only minor changes for radioiodine-labeled albumin.

To investigate the conjugation-bond stability, L-lysine and myoglobin have been conjugated to FITC, dichlorotriazine (DTAF) and succinimidyl ester (CFSE).[93] All three reactive probes achieved similar DOL but the conjugation stability at 37ºC was inferior for FITC compared to DTAF and CFSE.[93]

The high quantum yield for FITC of 0.92 provides higher emission intensities compared to LY, which has a quantum yield of only 0.27.[69,94,95] However, FITC is highly phototoxic compared to other dyes and requires careful consideration for fluorochrome concentration, excitation light intensity and duration of light exposure.[96-98] Furthermore, FITC has a smaller Stokes shift of only 30nm, compared to LY with 110nm, which makes it more difficult for FITC to differentiate between overlapping excitation and emission spectra.

The attachment of a fluorescent dye to a protein inevitably changes the absorption ability of the protein to solid surfaces. A study conducted by Teske et al. compared the competitive adsorption of labeled vs. native lysozyme and observed a displacement of weaker binding labeled lysozyme by stronger binding unlabeled lysozyme.[71,91] Finally, because of its popularity, investigational studies focus more on applications with FITC compared to LY, which makes a direct comparison between the performances of these two dyes impossible and leaves potential downsides of LY unrecognized.

Using fluorescent techniques to quantify protein deposition on a solid surface is very complex, as various factors impact the quantum efficiencies of the dye. These include concentration quenching, pH of the surface and differences between the dipole moments of the surrounding media that affect the energy between ground and

electronically excited states of the dye.[94] As an example, contact lens materials are composed of different principal monomers and with the addition of a surface coating, such as for lotrafilcon A and B, a solid protein layer accumulates on the surface. In contrast, pHEMA-based materials, such as alphafilcon A, have a more sponge-like porous structure, which allows the protein to be carried from the water phase throughout the entire lens and prevents a tightly bound protein layer on the surface. To overcome these challenges, which all impact on the fluorescence intensity determined for each material investigated, we chose to use this technique with one employing radioiodine-labeled HEL to quantify the protein uptake.

5.6 Conclusions

The interaction of tear proteins with hydrogel lens materials is clearly very complex, and is governed by the nature of the materials and the size and charge of the protein in question. In this study, CLSM was used to examine the location of FITC and LY labeled HEL in hydrogel contact lenses. By combining this with a radiolabeling technique, the amount of HEL throughout the lens structure could be quantified. A total of nine different commercially available contact lenses were examined, including conventional pHEMA-based and silicone hydrogel lenses. Different sorption profiles were found, with a variety of factors influencing the HEL uptake, including porosity of the polymer network, charge of the polymer components and choice of the fluorescent probe. Understanding these differences may lead to the development of improved lens materials and will enhance our knowledge of the mechanisms by which protein sorption affects comfort.

5.7 Acknowledgements

The authors would like to acknowledge at this point the work of Feng Zhang (a co-author of the published manuscript), who provided the data in this thesis chapter on the lysozyme conjugated with FITC. This work was published in his Masters thesis through McMaster University.[99]

In the next chapter, the location and quantity of deposited albumin and lysozyme was determined before and after lenses were incubated in contact lens cleaning solutions. Furthermore, the effect of manual lens rubbing on the removal of surface deposited proteins was investigated.

6. THE EFFICIENCY OF CONTACT LENS CARE REGIMENS ON PROTEIN REMOVAL FROM HYDROGEL AND SILICONE HYDROGEL LENSES

This paper is submitted for publication as follows

Doerte Luensmann[1], Miriam Heynen[1], Lina Liu[2], Heather Sheardown[1, 2], Lyndon Jones[1, 2]

[1]Centre for Contact Lens Research, School of Optometry, University of Waterloo, Waterloo, ON, N2L 3G1

[2]Department of Chemical Engineering, McMaster University, Hamilton, ON, L8S 4L7

Currently under review at *Mol Vis*

	Concept / Design	Recruitment	Acquisition of data	Analysis	Write-up / publication
Luensmann	Y	n/a	Y	Y	Y
Heynen	Y	n/a	Y	-	-
Liu	-	n/a	Y	-	-
Sheardown	-	n/a	Y	-	-
Jones	Y	n/a	-	-	Y

6.1 Overview

Purpose: To investigate the efficiency of lysozyme and albumin removal from silicone hydrogel and conventional contact lenses, using a polyhexamethylene biguanide multipurpose solution (MPS) in a soaking or rubbing/soaking application, and a hydrogen peroxide system (H_2O_2).

Methods: Etafilcon A, lotrafilcon B and balafilcon A materials were incubated in protein solutions for up to 14 days. Lenses were either placed in radiolabeled protein to quantify the amount deposited or in fluorescently conjugated protein to identify its location, using confocal laser scanning microscopy (CLSM). Lenses were either rinsed with PBS or soaked overnight in H_2O_2 or MPS with and without lens rubbing.

Results: After 14 days, lysozyme was highest on etafilcon A (2200µg) > balafilcon A (50µg) > lotrafilcon B (9.7µg) and albumin was highest on balafilcon A (1.9µg) = lotrafilcon B (1.8µg) > etafilcon A (0.2µg). Lysozyme removal was greatest for balafilcon A > etafilcon A > lotrafilcon B, with etafilcon A showing the most change in protein distribution. Albumin removal was highest from etafilcon A > balafilcon A > lotrafilcon B. H_2O_2 exhibited greater lysozyme removal from etafilcon A compared to both MPS procedures ($p<0.001$), but performed similarly for lotrafilcon B and balafilcon A lenses ($p>0.62$). Albumin removal was solely material specific, while all care regimens performed to a similar degree ($p>0.69$).

Conclusions: Protein removal efficiency for the regimens evaluated depended on the lens material and protein type. Overall, lens rubbing with MPS prior to soaking did not reduce the protein content on the lenses compared to non-rubbed lenses ($p=0.89$).

6.2 Introduction

The initial response of the immune system to isolate an implanted material from the body prior to fibrous or granulous tissue growths is the development of a coating consisting of a variety of proteins and lipids.[1-3] A similar response is found after a new contact lens is inserted onto the ocular surface, with organic (proteins, mucins and lipids) and inorganic (calcium, potassium and chloride ions) tear film elements, in addition to exogenous components such as cosmetics, forming a coating over the lens within minutes of exposure to the tear film.[4-10] A variety of ocular complications during lens wear can be directly related to such deposition, particularly on soft contact lenses.[11-16] One particularly relevant complication is giant papillary conjunctivitis (GPC), which has been observed with a variety of materials and wearing schedules [14,15,17,18] and has been closely linked with deposition of denatured proteins on the lens surface, potentially through a mechanical lens interaction with the under-surface of the lids.[11]

More than 100 different proteins have been identified in the human tear film [19,20] with a total concentration of 6.5-9.6 mg/ml.[21] This concentration may change over the day,[22] during sleep [23] and under specific conditions, including stimulated tearing,[24,25] increasing age,[26] contact lens wear [27] and in various eye diseases such as Sjögren's syndrome.[28] Lysozyme is of particular interest due to its high abundance and antimicrobial activity in the tear film.[24,25,29] It exhibits an overall positive charge, with an IEP pH =11.1 and is constituted of 129 amino acids, which results in a molecular weight of 14.5 kDa.[30] Lysozyme has a concentration in the tear film of 1.9 mg/ml.[23,25] Albumin is the most abundant protein in blood serum and is involved in the initial response to implanted biomaterials.[2] Albumin has a size of 66kDa

(585amino acids) and the concentration in the tear film ranges from 0.02 to 0.04 mg/ml during the day [22,24] and rises to approximately 0.5 mg/ml after sleep. [23 31 32] Its overall negative charge (IEP pH= 4.7) results in a different sorption behavior compared to lysozyme.[31,33-35]

Multipurpose care solutions (MPS) and hydrogen peroxide-based systems (H_2O_2) are the most commonly used care regimens to clean and disinfect soft contact lenses.[36] Due to their convenience, MPS systems have become increasingly popular over the years and now account for approximately 90% of the market share for care regimens, with H_2O_2 being used by <10% of patients.[36-38] The majority of MPS systems were initially developed for use with conventional pHEMA (poly-2-hydroxyethylene methacrylate)-based materials and were prescribed using a manual rub and rinse-step prior to overnight soaking of the lenses.[39,40] To improve convenience, a number of care systems were developed that were approved as "NO-RUB" products, with a brief rinse and long overnight soak only being required.

Silicone hydrogel (SH) contact lens materials provide high levels of oxygen to the cornea [41,42] and result in fewer hypoxic complications compared with conventional polyHEMA (pHEMA)-based materials.[43,44] The majority of SH materials are worn on a daily wear basis [45] and 90% of the patients wearing these materials on an overnight or continuous wear basis will remove the lenses at some point during the wearing cycle.[46] Once removed, the lenses require cleaning and disinfection prior to reinsertion.

Previous studies have reported that the deposition profile of SH and conventional pHEMA-based materials differ markedly, with SH materials depositing

lower amounts of tear proteins, which are primarily denatured. On hydrogel biomaterials, denatured proteins are more tightly bound than native proteins,[2,47] which raises the question of whether proteins bound to contact lens materials can be removed from the lens by rinsing and/or soaking alone.

6.3 Methods

This in vitro study was conducted to investigate the efficiency of protein removal from pHEMA-based and SH contact lens materials using commonly prescribed care regimens. The location and amount of two tear film proteins (lysozyme and albumin) was determined prior to and after soaking the lenses using either a polyhexamethylene biguanide (PHMB)-based MPS in a RUB or NO-RUB format, or a NO-RUB H_2O_2 system.

Two SH materials (lotrafilcon B, balafilcon A) and one pHEMA-based lens (etafilcon A) were investigated (Table 6-1). All lenses had a power of -3.0 D (dioptres) and were presoaked in sterile phosphate buffered saline (PBS) 24 hours prior to protein incubation, to remove any associated packaging components from the lens material.

Table 6-1: List of contact lenses investigated in this study

Trade Name	USAN	FDA	Manufacturer	Surface modification	Water content (%)	Principal monomers
ACUVUE® 2™	Etafilcon A	IV	Johnson & Johnson	none	58	HEMA, MAA
AIR OPTIX™ AQUA	Lotrafilcon B	I	CIBA Vision	25nm high refractive index coating	33	DMA, TRIS, siloxane macromer
PureVision®	Balafilcon A	III	Bausch & Lomb	Plasma oxidation (glassy islands)	36	NVP, TPVC, NVA, PBVC

DMA *N,N*-dimethylacrylamide; HEMA 2-hydroxyethyl methacrylate; MAA methacrylic acid; NVA *N*-vinyl aminobutyric acid; NVP N-vinyl pyrrolidone; PBVC poly[dimethylsiloxyl] di [silylbutanol] bis[vinyl carbamate]; TPVC tris-(trimethylsiloxysilyl) propylvinyl carbamate; TRIS trimethyl siloxy silane.

Two techniques were used in this study to quantify and locate the protein of interest on the contact lens. In Experiment 1, a radiolabeling technique was used to quantify the overall amount of bound protein per lens and in Experiment 2, confocal laser scanning microscopy (CLSM) identified the location of fluorescently-labeled protein on the surface and inside the lens matrix (for conjugation methods, see below). Hen egg lysozyme (HEL, Sigma-Aldrich, St. Louis, MO) and bovine serum albumin (BSA, Sigma-Aldrich St. Louis, MO) were investigated in separate experiments, applying both the radiolabeling and CLSM method. BSA and HEL were substituted for human albumin and lysozyme primarily due to cost considerations; however, the shape and physicochemical properties between the proteins are very similar and they are expected to behave in an analogous manner.[48-53]

In both experiments lenses were incubated in amber glass vials filled with protein solution, with physiological concentrations of 1.9 mg/ml HEL [23, 25] or

0.5 mg/ml BSA.[31] Etafilcon A is known to accumulate high levels of lysozyme [54,55] and was therefore incubated in 3 ml of HEL solution, to ensure sufficient protein was available over the incubation period of 14 days. All other lens/protein combinations were soaked in 1 ml of solution. Three replicates were used for each condition and the incubation was performed at 37ºC under constant rotation of 72 rpm for time periods of 1 and 14 days. For an overview of the experimental procedures, please refer to Figure 6-1.

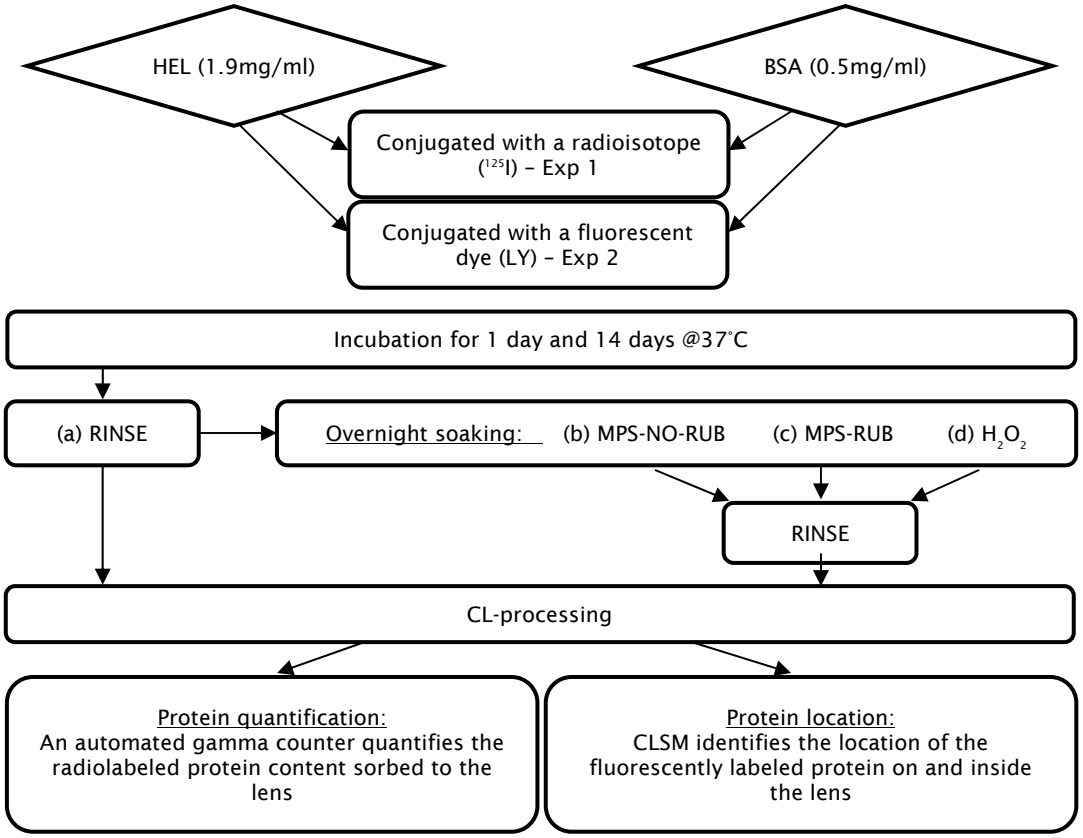

Figure 6-1: Schematic diagram for contact lens incubation in HEL and BSA solution, followed by overnight soaking and the methods to locate and quantify the protein on the lens

After protein incubation, lenses underwent one of four treatments, described below. The contact lens care regimens used in this study are listed in Table 6-2.

- (a) “RINSE” - all lenses were held with plastic-tipped tweezers and gently swirled in 100ml PBS for 3 seconds (repeated twice) and either processed immediately for protein localization or quantification or further prepared for overnight soaking using one of three differing treatments (b), (c), or (d).
- (b) “MPS-NO-RUB” - lenses were individually placed in COMPLETE® Easy Rub contact lens cases (Advanced Medical Optics, Santa Ana, CA), which were filled with 3ml of COMPLETE® Easy Rub (Advanced Medical Optics, Santa Ana, CA) solution.
- (c) “MPS-RUB” - lenses were placed in a nitrile-gloved hand, 200µl of COMPLETE® Easy Rub was added and using the index finger alone, five circular rotations on each side of the lens were performed (10 sec total). The lenses were then briefly immersed in PBS before being placed in 3ml of COMPLETE® Easy Rub solution.
- (d) “H_2O_2” - lenses were individually placed in ClearCare® lens cases (CIBA Vision, Duluth, GA), which were then filled with 9ml of ClearCare® (CIBA Vision, Duluth, GA).

Lenses processed in treatments b, c and d remained in the respective care solution for 12 hours, followed by immersing and swirling for 3 seconds in fresh PBS and further processing for protein localization or quantification (Figure 6-1).

Table 6-2: List of care regimens used in this study

Trade Name	Manufacturer	Disinfectant	Other constituents	Buffer
ClearCare®	CIBA Vision	3% hydrogen peroxide	Pluronic 17R4	Phosphate
COMPLETE® MPS Easy Rub™	Abbot Medical Optics	Polyhexamethylene biguanide (0.0001%)	Poloxamer 237, Edetate disodium, Sodium chloride, potassium chloride	Phosphate

Three replicates for each of the three lens types (etafilcon A, lotrafilcon B, balafilcon A) were incubated in two proteins (HEL, BSA) at two time points (D1, D14) using four cleaning procedures (RINSE, MPS-NO-RUB, MPS-RUB, H_2O_2) and two techniques to either quantify or locate the protein on the lens. This resulted in 288 lenses being examined.

6.3.1 Experiment 1: Protein quantification using ^{125}I

In separate experiments, HEL and BSA were conjugated to ^{125}I using the iodine monochloride method as previously described.[56,57] Lenses were incubated in single protein solutions containing 1.9 mg/ml HEL or 0.5 mg/ml BSA, using a mixture of 2% labeled and 98% unlabeled protein (pH 7.4). Following the four treatments a, b, c or d the remaining protein content on the lens was determined using an automated gamma counter (1470 Wallac Wizard PerkinElmer, Woodbridge, ON). For quantification purposes, the radioactivity on each lens was converted into micrograms of protein.[58,59]

6.3.2 Experiment 2: Protein conjugation for CLSM

In separate labeling procedures, 180 mg HEL and BSA were dissolved in 0.05 M borate buffer (pH 8.5) and 0.04 M NaCl (HEL 5 mg/ml; BSA 10 mg/ml). The water soluble fluorescent dye Lucifer Yellow VS dilithium salt (LY, Sigma Aldrich, St. Louis, MO) was dissolved in 1mL of borate buffer (pH 8.5) (7mg for BSA, 10mg for HEL). The dye was added to the protein solution followed by gentle stirring for one hour in the dark. Free LY was separated from the conjugated proteins using Sephadex G25 PD10 desalting columns (Amersham Biosciences, Piscataway, NJ, USA). Following this, dialysis against PBS using a 7 kDa molecular weight cutoff dialysis cassette was performed, until only negligible amounts of free LY were detected with a fluorescence spectrophotometer. The labeling efficiency was calculated by determining the protein concentration in the solution using the DC Protein Assay (Bio-Rad, Hercules, CA) and measuring the absorbance at 415nm (which is the maximum absorbance for LY). The resulting degree of labeling (DOL) was 0.26 for HEL and 2.94 for BSA (DOL = molecules dye per molecule of protein) (Appendix A).

6.3.3 Contact lens incubation in fluorescently labeled protein

The conjugated protein solutions were sterilized with 0.2 µm syringe filters to prevent microbial contamination of the samples during the incubation phase. Since lower amounts of labeled protein result in less photobleaching during subsequent laser scans and to allow consistent settings on the microscope throughout the experiment, the lowest possible amount of conjugated HEL was used. Contact lens materials that were known to accumulate large amounts of lysozyme from previous studies[58,60] were incubated with 2% labeled and 98% unlabeled HEL, while other

materials known to accumulate only small amounts of protein were incubated in 100% labeled HEL. The final concentration of HEL was 1.9 mg/ml (pH 7.4). Due to the lower BSA sorption rate to contact lens materials,[54] all lens types were incubated in 100% conjugated BSA.

6.3.4 CLSM examination technique

The center 4 mm of the lens was cut out using a mechanical punch-press and the sample was gently dabbed dry on lens paper before it was mounted onto a glass microscope slide. Approximately 40 µL of PBS was used as the mounting media. A glass coverslip was then carefully applied and sealed with nail polish to prevent evaporation and to stabilize the coverslip for use with the immersion objectives of the microscope.

The lens materials were subsequently examined for protein uptake using CLSM (Zeiss Inc. Toronto, Canada). The Zeiss 510, configuration Meta 18 was equipped with an inverted motorized microscope Axiovert 200M. Each lens was scanned at four random locations using an excitation wavelength of 405nm (Laser Diode) and an emission filter LP >505nm. Each section of z stacks was set at 1 µm intervals with image sizes of 512 x 512 µm. Lenses were scanned with a 40x water immersion C-Apochromat objective. Using the software provided with the microscope and ImageJ (Bethesda, MD), the means of the fluorescence intensity were plotted as a function of the scanning depth.

For statistical analysis of the quantitative protein uptake and protein location, repeated measures ANOVA (analysis of equal variance) was applied followed by post-hoc comparisons using Tukey's HSD (honestly significant difference) test. $P<0.05$ was

considered significant. To determine the significance of differences between the amount of protein sorbed to the investigated materials, a comparison between the RINSE data was tested using the factors “Protein” (HEL, BSA), “Material” (etafilcon A, lotrafilcon B, balafilcon A) and “Time” (Day 1, Day 14). The cleaning efficiency was analyzed individually for each lens-protein combination due to the wide range of protein uptake between lens materials. Differences between the amounts of protein were determined separately for each lens material (etafilcon A, lotrafilcon B, balafilcon A) with the two factors “Time” (Day 1, Day 14) and “Treatment” (RINSE, MPS-NO-RUB, MPS-RUB, H_2O_2), including interactions.

To determine differences in protein location, each CLSM lens scan was sectioned into front- and back-surface and ‘bulk’ regions as previously described.[61] Briefly, the fluorescence intensity on the front and back surface was calculated by averaging the five micron scan steps around the front and back ‘surface peak’ and the ‘bulk’ intensity was calculated by averaging the innermost 30 micron of the lens scan.[61] As noted in our previous study,[61] the relative fluorescence signal on the back surface typically showed a minor decrease as compared to the front surface. This is due to increased absorbance of the laser light when measuring deeper into the lens material, and could be seen in the majority of cases. Therefore, comparisons between protein location on and within the lens will focus only on differences in front surface versus the bulk (central) region, with the assumption that both surfaces accumulate similar amounts of protein. The scaling of the CLSM results is based on arbitrary units and solely allows comparisons between a single protein type on one specific material. Using repeated measures ANOVA, significant differences in fluorescence intensity were determined separately for each lens material (etafilcon A, lotrafilcon B, balafilcon

A), with the three main effects "Time" (Day 1, Day 14), "Treatment" (RINSE, MPS-NO-RUB, MPS-RUB, H_2O_2) and "Location" (front surface, back surface, 'bulk'), including interactions. The fluorescence signal does not provide quantitative results and the units cannot be compared directly between materials, therefore radiolabeled protein was used for quantitative comparisons.

6.4 Results

Etafilcon A, lotrafilcon B and balafilcon A incubated in ^{125}I labeled protein showed significantly more HEL on all lens types compared to BSA at all time points ($p<0.001$). An increase in HEL and BSA sorption was found on all three lens materials over time ($p<0.05$), except for BSA in combination with etafilcon A ($p=0.48$).

Following incubation of the three contact lens materials in either 1.9 mg/ml HEL or 0.5 mg/ml BSA, the total amount and location of protein on these materials was determined prior to and after overnight soaking in MPS with and without manual lens rubbing (MPS-RUB, MPS-NO-RUB) or H_2O_2.

Etafilcon A accumulated the highest amounts of HEL (mean 2200 µg/lens) and the lowest amounts of BSA (mean 0.2 µg/lens) compared to the other materials ($p<0.001$) (Table 6-3). After overnight soaking, both care regimens removed significant amounts of both proteins from this lens type ($p<0.001$). After 14 days of incubation, H_2O_2 removed 24.3% of the HEL from etafilcon A, which was significantly more ($p<0.001$) compared to both MPS-RUB (15.8%) and MPS-NO-RUB (16.3%), which were not different to each other ($p=0.88$). The very low amounts of BSA were significantly reduced ($p<0.001$) by 62.4%, 62.2% and 55.5% using H_2O_2, MPS-RUB and

MPS-NO-RUB respectively, with all cleaning procedures performing similarly ($p>0.98$) (Table 6-3).

Table 6-3: Total amount of HEL and BSA sorbed to etafilcon A after 1 and 14 days of incubation, followed by the treatments RINSE, MPS-NO-RUB, MPS-RUB or H_2O_2 (Mean (µg) ± 95% confidence interval)

Etafilcon A	HEL			BSA		
	D1	D14	Difference between treatments*	D1	D14	Difference between treatments*
RINSE (a)	1139.8±7.14	2200.3±15.64	(b), (c), (d)	0.16±0.037	0.20±0.037	(b), (c), (d)
MPS-NO-RUB (b)	909.3±5.52	1852.1±19.16	(a), (c), (d)	0.03±0.006	0.09±0.005	(a)
MPS-RUB (c)	906.6±13.00	1841.5±10.38	(a), (b)	0.02±0.004	0.08±0.013	(a)
H_2O_2 (d)	783.4±11.13	1666.1±15.83	(a), (b)	0.02±0.004	0.08±0.041	(a)

*Overall differences between treatments ($p<0.05$), using the combined time points.

The CLSM results for the different cleaning treatments show the distribution of the fluorescently conjugated protein on the front surface, within the central lens matrix (bulk) and at the back surface of etafilcon A (Figures 6-2A-D). Following the RINSE procedure alone, HEL sorption to etafilcon A showed a slightly higher protein density on the surface compared to the matrix region on Day 1 ($p<0.001$), but this leveled out over time, with no difference being seen on Day 14 ($p=1.0$). For both time-points, soaking in H_2O_2 removed significantly higher amounts of HEL from the surface of etafilcon A compared to all the other procedures ($p<0.001$), and significantly more HEL was measured in the central region than on the surface ($p<0.001$). This

phenomenon was seen to this extent only with this specific lens-protein-care regimen combination. For the MPS on Day 1, both techniques removed significant amounts of protein from both the surface and matrix compared with RINSE alone ($p<0.001$). No differences between the surface and bulk regions were measured for either RUB or NO-RUB methods, but there was a reduction in both regions on Day 1 when the lens was rubbed ($p<0.001$). Both techniques, RUB and NO-RUB, removed more HEL from the surface than from the bulk region on Day 14, but there was no significant difference between the two techniques ($p=0.64$).

The overall BSA sorption to etafilcon A with the RINSE procedure was similar at both time points ($p=1.00$), showing an almost even distribution of the protein at the surface and in the matrix, as seen in Figures 6-2C+D. The use of MPS and H_2O_2 showed a successful removal of BSA from both the surface and the bulk regions ($p<0.001$), with a slightly reduced efficiency on Day 14. There were no significant differences between the three procedures for either time-points ($p>0.95$).

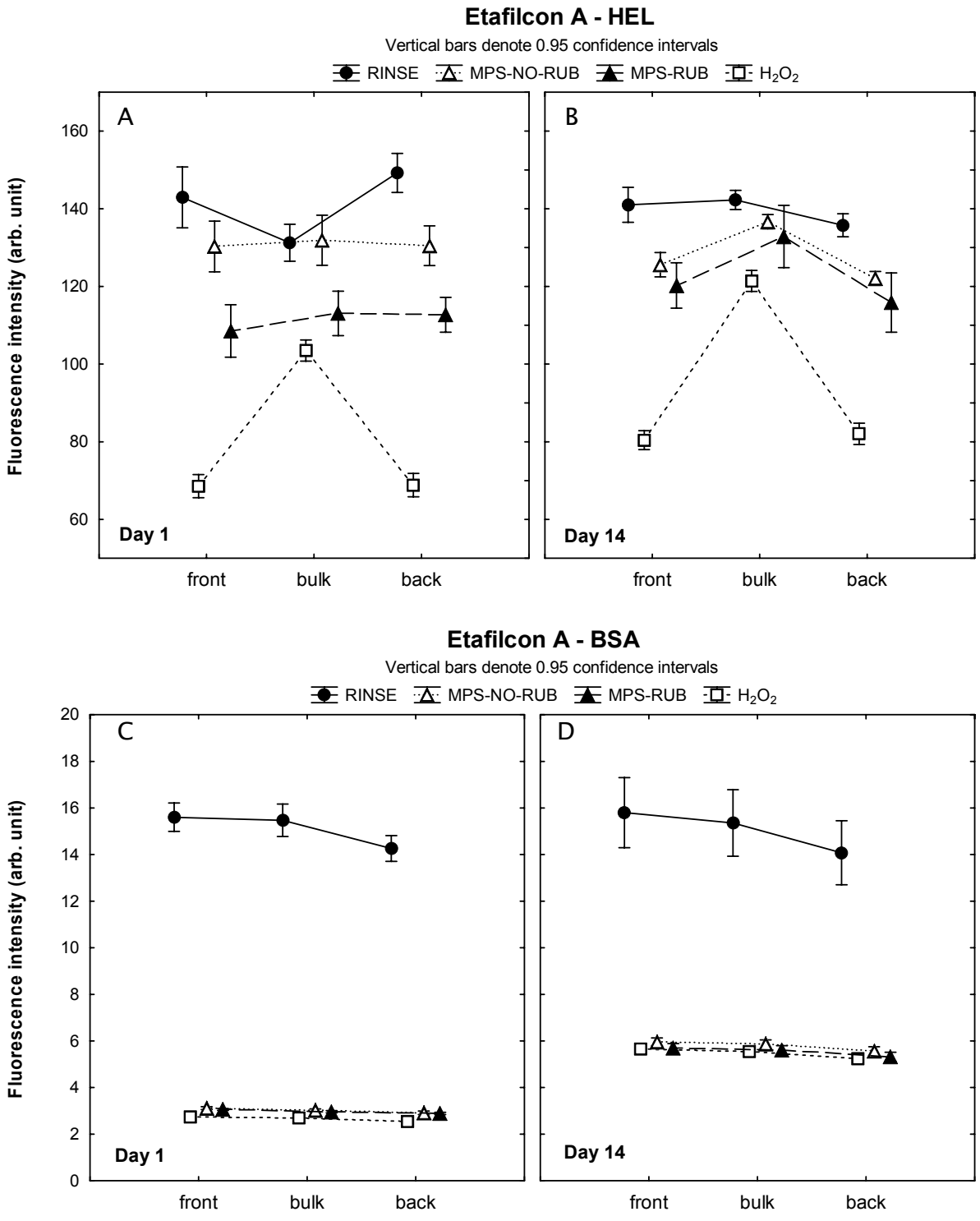

Figure 6-2: CLSM scans were analyzed to locate the fluorescently-conjugated proteins on the front surface, within the bulk region and on the back surface of etafilcon A - HEL (A+B); BSA (C+D)

Lotrafilcon B accumulated higher quantities of HEL (mean 9.65 µg/lens) as compared to BSA (mean 1.82 µg/lens) after 14 days of incubation in radiolabeled HEL solution ($p<0.001$) (Table 6-4). Following overnight soaking, none of the care regimens removed appreciable amounts of HEL from this lens type ($p>0.46$), while a small but statistically significant reduction was seen for BSA when exposed to H_2O_2 ($p<0.049$). After 14 days of incubation, H_2O_2 removed 7.2% HEL from lotrafilcon B, which was similar to both MPS-RUB (3.6%) and MPS-NO-RUB (2.9%) ($p>0.90$). The amount of BSA removed was slightly more, with 14.0%, 11.9% and 11.0% using H_2O_2, MPS-RUB and MPS-NO-RUB respectively, with all cleaning procedures performing similarly ($p>0.89$) (Table 6-4).

Table 6-4: Total amount of HEL and BSA sorbed to lotrafilcon B after 1 and 14 days of incubation, followed by the treatments RINSE, MPS-NO-RUB, MPS-RUB or H_2O_2 (Mean (µg) ± 95% confidence interval)

Lotrafilcon B	HEL			BSA		
	D1	D14	Difference between treatments*	D1	D14	Difference between treatments*
RINSE (a)	5.14±0.64	9.65±1.54	-	0.84±0.10	1.82±0.19	(d)
MPS-NO-RUB (b)	3.28±0.85	9.37±1.72	-	0.54±0.07	1.62±0.08	-
MPS-RUB (c)	3.98±0.43	9.31±2.09	-	0.46±0.19	1.60±0.25	-
H_2O_2 (d)	4.41±0.84	8.96±1.28	-	0.45±0.05	1.57±0.13	(a)

*Overall differences between treatments ($p<0.05$), using the combined time points.

The location of fluorescently conjugated HEL on the surface and within the matrix of lotrafilcon B is shown in Figures 6-3A+B. Significantly higher amounts of HEL were detectable on the surface of lotrafilcon B following the RINSE procedure as compared to the bulk region on Day 1, which became even more distinct on Day 14 ($p<0.001$). Overnight soaking in H_2O_2 or MPS with or without rubbing removed protein solely from the central lens region on Day 1 ($p<0.04$); however the front surface on Day 1 and both locations on Day 14 did not show a significant decrease in protein accumulation using any of the three procedures ($p>0.3$), with the exception of the surface on Day 14 after soaking in H_2O_2 ($p=0.03$).

BSA sorption to lotrafilcon B showed a trend similar to HEL, with more BSA detected on the surface compared to the bulk region after the RINSE procedure, as seen in Figures 3C+D ($p<0.001$). All cleaning techniques removed BSA from the central location at both time points ($p<0.001$). For the surface, only MPS-RUB removed significant amounts of BSA on Day 1 and only MPS-NO-RUB reduced the BSA content on Day 14 ($p<0.001$). On Day 14, both MPS applications removed more protein from the surface compared to the H_2O_2 care solution ($p<0.01$), but no differences could be detected for the bulk region ($p>0.05$). Although MPS-RUB removed more BSA from the surface on Day 1 as compared to the NO-RUB technique, all other locations were not different on either time points for the two MPS procedures ($p>0.35$).

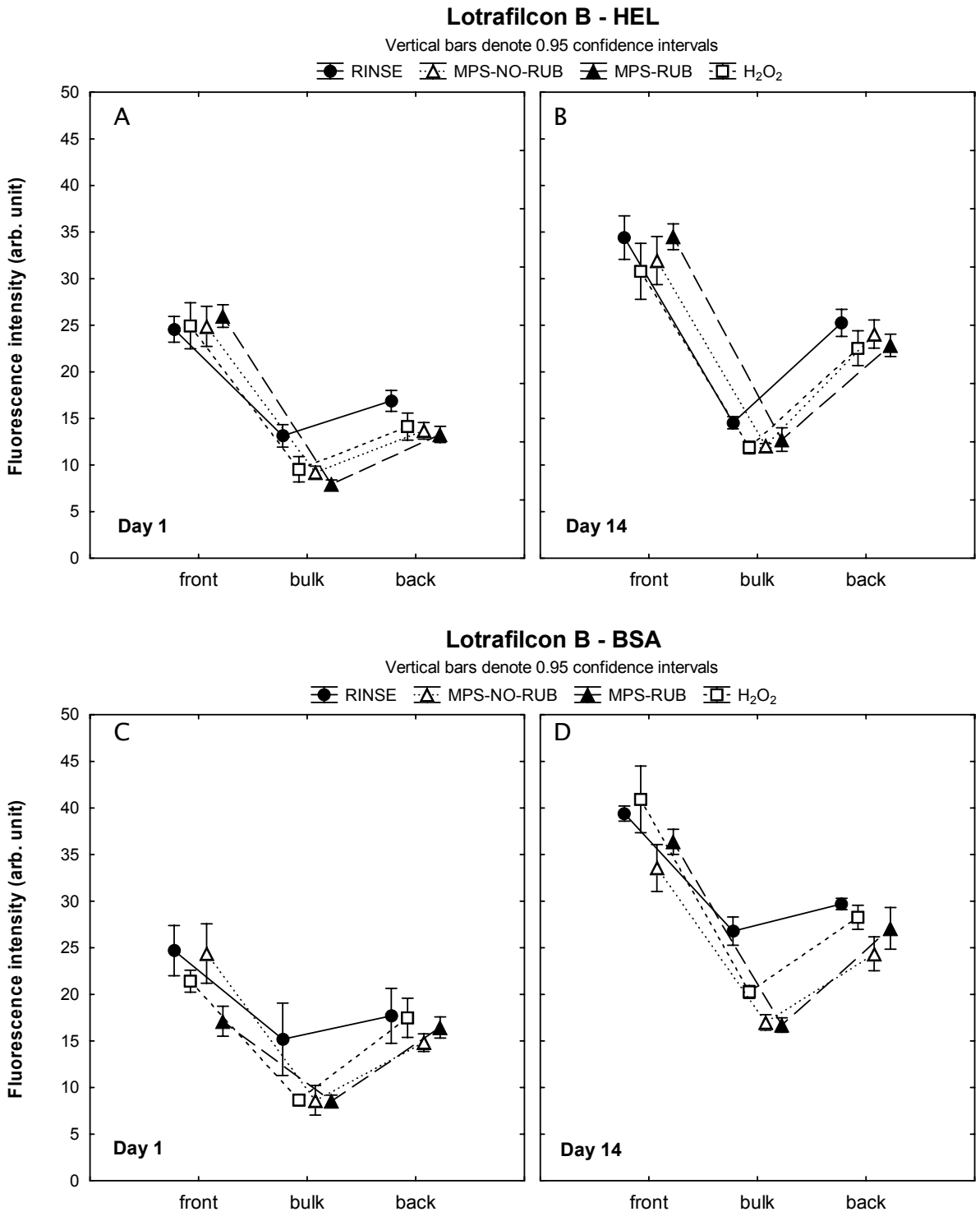

Figure 6-3: CLSM scans were analyzed to locate the fluorescently-conjugated proteins on the front surface, within the bulk region and on the back surface of lotrafilcon B - HEL (A+B); BSA (C+D)

Balafilcon A accumulated much higher amounts of HEL (mean 50.0 µg/lens) compared to BSA (mean 1.90 µg/lens) after 14 days of incubation in ^{125}I conjugated protein ($p<0.001$) (Table 6-5). After overnight soaking, both care regimens removed significant amounts of both proteins from this lens type ($p<0.01$). After 14 days of incubation, HEL was more efficiently removed from balafilcon A as compared to the other two lens materials, with similar proportions of 59.9%, 58.4%, and 61.4% for H_2O_2, MPS-RUB and MPS-NO-RUB respectively ($p<0.001$). For BSA, H_2O_2 removed 31.7%, which was similar compared to MPS-RUB (30.7%) and MPS-NO-RUB (29.2%). The three cleaning procedures showed overall similar protein removal efficiencies for both BSA and HEL ($p>0.69$) (Table 6-5).

Table 6-5: Total amount of HEL and BSA sorbed to balafilcon A after 1 and 14 days of incubation, followed by the treatments RINSE, MPS-NO-RUB, MPS-RUB or H_2O_2 (Mean (µg) ± 95% confidence interval)

Balafilcon A	HEL			BSA		
	D1	D14	Difference between treatments*	D1	D14	Difference between treatments*
RINSE (a)	42.71±1.93	50.00±0.14	(b), (c), (d)	0.63±0.08	1.90±0.37	(b), (c), (d)
MPS-NO-RUB (b)	8.08±0.39	19.31±0.99	(a)	0.24±0.05	1.35±0.31	(a)
MPS-RUB (c)	7.69±0.71	20.80±3.30	(a)	0.20±0.04	1.32±0.30	(a)
H_2O_2 (d)	8.18±0.47	20.08±1.69	(a)	0.21±0.03	1.30±0.31	(a)

*Overall differences between treatments ($p<0.05$), using the combined time points.

Imaging results of the fluorescently conjugated protein indicated a higher HEL density inside the matrix region compared to the surface of balafilcon A following the RINSE procedure at both time points ($p<0.001$) (Figures 6-4A+B). All three cleaning techniques removed significant amounts of HEL from both the surface and bulk region ($p<0.001$). Soaking in H_2O_2 removed more HEL from the surface of balafilcon A on Day 1 compared to the MPS applications ($p<0.02$), however on Day 14 all care regimens performed similarly for both surface and bulk regions ($p>0.09$).

BSA showed an equal distribution throughout the balafilcon A material at both time points following the RINSE procedure ($p=1.0$), as shown in Figures 6-4C+D. All cleaning procedures removed significant amounts of BSA from the surface and the bulk material ($p<0.001$). At both time points, a higher protein reduction was seen when using H_2O_2 as compared to both MPS applications ($p<0.001$), which were not different to each other on Day 1 ($p=1.0$). Small but significant differences could be seen on the lens surface and within the matrix between both MPS procedures on Day 14, with MPS-NO-RUB removing more BSA as compared to MPS-RUB (<0.05).

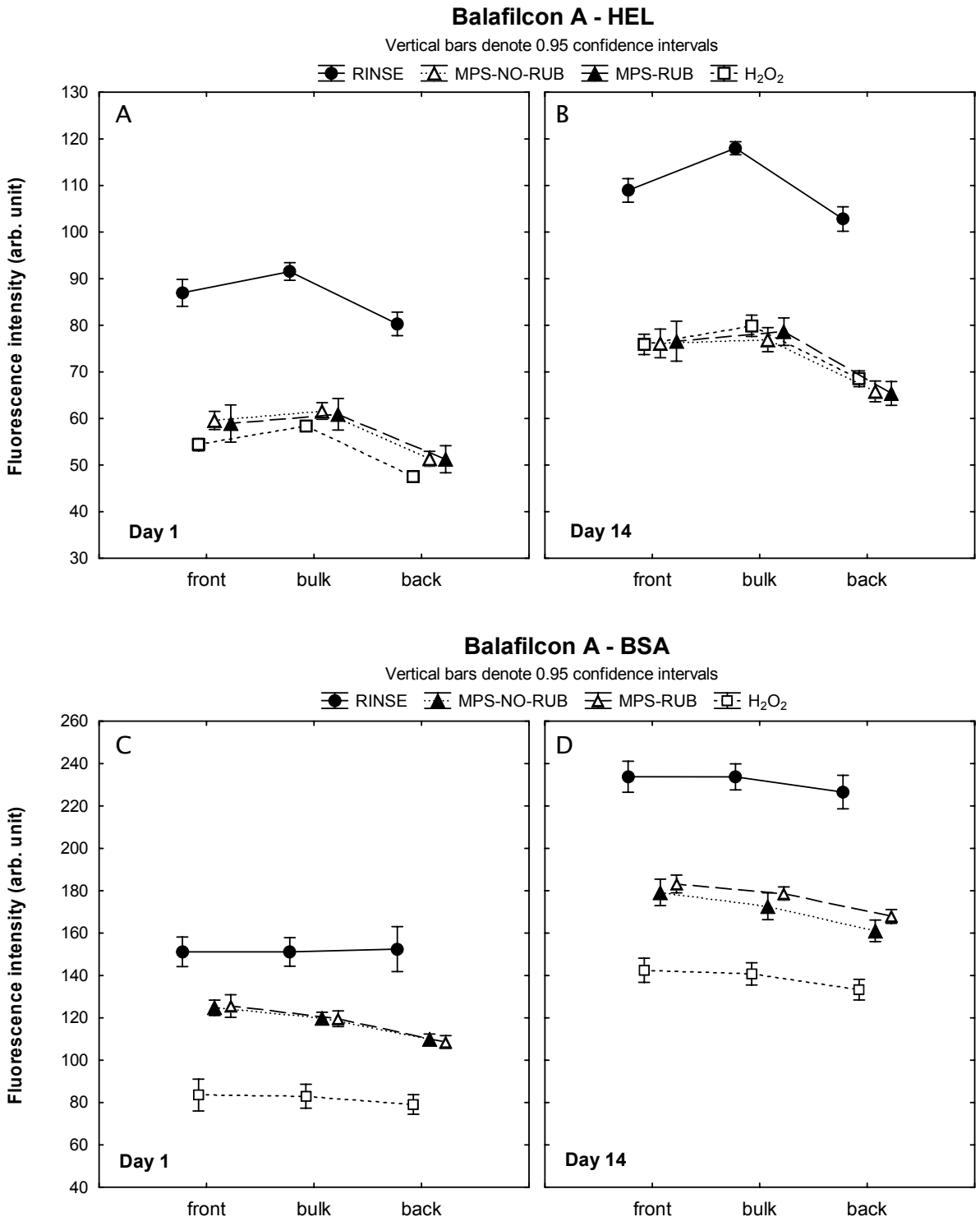

Figure 6-4: CLSM scans were analyzed to locate the fluorescently-conjugated proteins on the front surface, within the bulk region and on the back surface of balafilcon A - HEL (A+B); BSA (C+D)

6.5 Discussion

Current soft contact lens care regimens have been evaluated for their efficiency against both microbial and tear film deposition on various soft lens materials.[40,62-69] Both ex vivo and in vitro studies have demonstrated material specific sorption profiles and confirmed differences between care regimens for removing non-pathogenic (e.g. lipids, proteins) [40,62,66-69] and microbial (e.g. bacteria and fungi) [62-65] components from the lens. Furthermore, manual lens rubbing reduces the appearance of visual deposition by removing general tear film deposition and cosmetics from the lens □□□□□□□□□H□H□□□□, as compared with soaking alone.[70,71] A clinical study conducted by Nichols [70] determined visual deposition on patient-worn SH lenses after using various MPS in a rub and no-rub application. The subjective grading method demonstrated an overall reduction in lens "haze" for manually rubbed lenses that were cleaned using either COMPLETE® MoisturePLUS or Opti-Free Express. Cho et al.[71] reported similar results from an in vitro study investigating ionic high water pHEMA-based lens materials that were artificially deposited with albumin, hand cream and mascara. Lenses that were not rubbed prior to the soaking process showed similar levels of deposition regardless of the rinsing duration. In contrast, all four MPS systems investigated removed significant amounts following extensive lens rubbing.[71]

While both of the above studies clearly describe differences between care regimens and their method of utilization, it still remains unclear if the deposited species were removed primarily from the lens surface or also from the central or "bulk" lens region. Of particular interest to us was the impact of care regimens and rubbing on the removal of tear film proteins, and whether such proteins are removed differentially from the surface or bulk locations. Therefore, the purpose of this study

was to determine the efficiency of various contact lens care regimens on the removal of two typical tear film proteins lysozyme (HEL) and albumin (BSA), which differ markedly in size, charge and concentration.

As shown in previous studies,[59,61] the protein distribution profile for BSA and HEL differs significantly between lens materials. The pHEMA material etafilcon A (FDA group IV) allowed both proteins to penetrate the lens matrix, while the high refractive index coating and/or the properties of the matrix of the lotrafilcon B SH material [72] (FDA group I) minimized protein penetration into the material, with both proteins primarily being deposited on the surface region.[59,61] It may be assumed that protein sorbed onto the lens surface would be easier to remove than protein penetrating the lens matrix. However, results from the current study showed no change in the overall HEL amount (by radiolabeling) and distribution profile (by CLSM imaging) on the lotrafilcon B material after overnight soaking using a RUB or NO-RUB application (Table 6-4 and Figures 6-3A+B). BSA amounts were slightly reduced by 11 to 14% for this material by either lens rubbing or using H_2O_2 systems (Table 6-4) and the CLSM results confirmed that BSA was removed primarily from the bulk and not from the surface region (Figures 6-3C+D).

Etafilcon A allowed both BSA and HEL to fully penetrate the lens matrix over time,[59,61] and this current study demonstrated that using either MPS or H_2O_2 removed significant amounts of 15.8 to 24.3% for lysozyme and 55.5 to 62.4% for BSA from both the lens surface and bulk regions (Table 6-3 and Figures 6-2A-D). When examining the differences between these regimens, it is clear that H_2O_2 removed substantially more HEL from the surface region of etafilcon A than either MPS method (Table 6-3 and Figures 6-2A+B). This phenomenon was not observed with BSA, which

deposited substantially less than HEL (Table 6-3). The high levels of deposition of the positively charged HEL on ionically charged materials such as etafilcon A has been shown previously.[35,58,73]

Our results would suggest that both proteins were less tightly bound when sorbing to the surface of etafilcon A (Figures 6-2A-D) as compared to the lotrafilcon B material (Figures 6-3A-D), which showed no - or minimal - protein removal from the surface following any of the cleaning procedures. These findings were also confirmed in the quantitative results, which showed a higher percentage of protein removal for etafilcon A compared to lotrafilcon B (Tables 6-3, 6-4) This may be due to the conformational state of the proteins which were sorbed to the more hydrophilic surface (etafilcon A), compared to the more hydrophobic surface (lotrafilcon B) typically exhibited by SH materials.[74] Previous studies have already determined changes in secondary structure for HEL and BSA when depositing on contact lenses and show a higher denaturation rate for proteins sorbed to SH materials, as compared to pHEMA materials.[54,55,60,67,75] Furthermore, denatured proteins typically bind more tightly to surfaces as compared to native proteins,[3,47,54] which may explain our difficulties in removing either protein from lotrafilcon B. Thus, our data would suggest that when HEL deposits on lotrafilcon B it is extremely difficult to remove, regardless of the type of protein or care regimen employed. In comparison, BSA sorbs to a lesser extent and is marginally easier to remove.

The balafilcon A material is surface modified using a plasma oxidation method, which results in hydrophilic silicate islands distributed over the lens surface.[76] This study showed that this surface modification procedure was no barrier for either protein, as they both fully penetrated the entire matrix (Figures 6-4A-D). In

comparison to the increased surface build up of both proteins seen on lotrafilcon B, balafilcon A accumulated slightly more HEL in the lens matrix as compared to the surface (Figures 6-4A+B), but showed an almost even distribution for BSA (Figures 6-4C+D). The highly porous and hydrophilic structure of balafilcon A [77-79] allowed easy ingress of both proteins, particularly the smaller HEL, and appeared to allow relatively easy removal of either protein deposited using any of the care regimens investigated, on both the surface and from within the bulk region. The quantitative experiment showed the highest HEL reductions on this material, with 58.4 to 61.4% removal after overnight soaking using any of the three treatments (Table 6-5), which was similarly reflected by the CLSM imaging data showing an equal reduction throughout the balafilcon A material (Figures 6-4A+B). The results for BSA show removal efficiencies of 29.2 to 31.7% and although the results were slightly higher for H_2O_2, significant differences were only seen with the fluorescence imaging technique (Figures 6-3C+D).

The amount of protein removal from the lens materials investigated in this study may be compared to previous findings from both Franklin [39] and Jung,[69] who investigated pHEMA-based materials only. Franklin incubated FDA groups I, II and III in an artificial tear solution containing various proteins and lipids. Lenses were manually rubbed with various single and multipurpose solutions and the protein content was determined using fluorescence spectroscopy. Franklin reported a protein reduction of 27 – 45% for MPS care regimens,[39] which is in close agreement with findings from Jung et al,[69] who reported protein removal efficiencies of 28 – 52% using H_2O_2 and MPS regimens. In Jung's in vitro study, which examined FDA groups I to IV, proteins were extracted and quantified using a protein assay. The results for FDA group IV lenses showed a more efficient protein removal using H_2O_2 as compared to

the PHMB-based MPS system, which is in agreement to the results from our study using etafilcon A as our FDA group IV lens.

The protein removal efficiency in our study, as evidenced by the radiolabeled results, ranged from 2.9 – 62.4%, which suggests that not only do care regimens impact the removal efficiency, but that this removal is also markedly influenced by the specific characteristics of the lens materials investigated.

As described above, two recent studies have shown that rubbing lenses reduces visible deposition, in both in vitro and in vivo studies.[70,71] In this current study, relatively minor differences between deposition of two common tear film proteins were demonstrated, using an MPS system in a RUB or NO-RUB format. Potential reasons why this in vitro study was not able to mimic previous results is that this is the only study to-date to quantify protein removal from SH materials using RUB versus NO-RUB methods. The Nichols' paper [70] examined the removal of visible tear film deposits from a single SH material (galyfilcon A), which was not examined in this study. The study by Cho and colleagues [71] examined visible deposition, including albumin, but used an FDA group IV material (ocufilcon D) that was also not examined in this study. One potential issue to consider relative to patient-use of such systems is that our lab-based experiment used nitrile-gloved hands for the RUB technique. Although the gloves had textured finger tips to improve grip, potential differences to ungloved-hands may occur. Another limitation of this in vitro experiment is that the lenses were incubated in the protein solution alone, which does not provide the intermittent surface-drying that occurs between blinks in in vivo studies, and which may have impacted on the deposition results. In reality, a follow-up ex vivo study in which lenses are harvested and examined for deposited proteins from a clinical study

in which human subjects use an MPS in a RUB and then NO-RUB format is required to unequivocally demonstrate differences between these formats. Although the differences in protein removal between our two techniques using MPS in a RUB and NO-RUB application are minor, it must be considered that this may be entirely different for the removal of lipids, microorganisms [80,81] and other debris.

The use of lysozyme and albumin in single protein solutions describes the interaction between the protein and material of interest, however, this sorption behavior may change with the addition of an artificial tear solution which includes more proteins, lipids, mucins and ions. A competitive process of protein adsorption and desorption is expected, as smaller proteins get replaced by proteins with higher surface affinity.[43]

Biocompatible materials tend to bind proteins relatively loosely, and these proteins are often easy to remove, as they maintain their conformation. This compares with “less biocompatible” surfaces, which are typically more hydrophobic and have a tendency to denature proteins over time, potentially stimulating inflammatory responses in the biological host.[54,82-88] Future work within the contact lens arena should focus on the development of surfaces that maintain protein activity and allow for easier removal of deposited tear film components, possibly by developing contact lens care regimens and SH materials that are optimized to work together.

6.6 Conclusions

The efficiency of protein removal varied greatly between contact lens materials, care regimens and proteins investigated. MPS in a RUB and NO-RUB application and H_2O_2 removed significantly higher amounts of HEL and BSA from etafilcon A and balafilcon A as compared to lotrafilcon B. Comparisons between care regimens showed a slightly better efficiency for the H_2O_2 system as compared to MPS RUB or NO-RUB, which showed negligible differences between these preserved systems.

6.7 Acknowledgements

The authors would also like to acknowledge funding for this study from Natural Science and Engineering Council of Canada (NSERC) and the American Optometric Foundation (AOF) for supporting this study with the 2008 Vistakon Grant.

In the following chapter, CLSM is applied to investigate the sorption profile of albumin to hydrophilic and hydrophobic intraocular lens materials. Protein penetration depth was imaged and quantified over time.

7. Determination of Albumin Sorption to Intraocular Lenses by Radiolabeling and Confocal Laser Scanning Microscopy

7.1 Brief overview

The crystalline lens is surrounded by an elastic capsular bag and is located in the posterior chamber of the eye. With age, the lens progressively lose clarity and cataract develops. This finally results in vision loss. During cataract surgery, this opaque lens is removed and replaced by an intraocular lens (IOL). As long as the capsular bag remains intact, the IOL is placed inside the capsular bag, but in the case of a damaged or unstable bag, various lens designs allow the IOL to be placed in the anterior chamber (AC) of the eye.[1] In general, the success rate and biocompatibility of IOLs is very high, with less than 1% adverse events following cataract surgery.[2]

The first reported extracapsular cataract extraction was performed in 1747, however it took another 200 years until the first IOL was successfully implanted.[1] Early trials to implant glass lenses failed, as they were too heavy and sank down into the

lower portion of the capsule, but with the invention of poly(methyl methacrylate) (PMMA), the first realistic biomaterial for IOLs was found. [1]

The most common type of cataract is “age-related” and affects patients of - typically - 65 years and older. Other types of cataract are “congenital cataract”, which affects newborn babies or children who develop it in the first years of life, “traumatic cataract”, caused by an injury of the eye or “secondary cataract”, which occurs in conjunction with certain systemic diseases such as diabetes or with local ocular conditions such as chronic uveitis.[3] Other less common forms of cataract may be caused by certain drugs, due to metabolic disorders or poor nutrition. In addition to their application in cataract surgery, IOLs are used to correct high levels of refractive myopia or hyperopia. For this phakic surgery an additional IOL is implanted in the anterior or posterior segment of the eye, without restricting accommodation of the crystalline lens. Common keratorefractive surgeries such as LASIK (Laser-assisted in situ keratomileusis) or PRK (Photorefractive keratectomy) reshape the cornea, which limits these techniques to moderate refractive errors only, as the amount of tissue to be removed controls the refractive correction. The implantation of an IOL in the phakic eye maintains the asphericity of the cornea and has a similar predictable refractive outcome as compared to keratorefractive surgeries.[1] Image 7-1 shows the three IOL types investigated in this study.

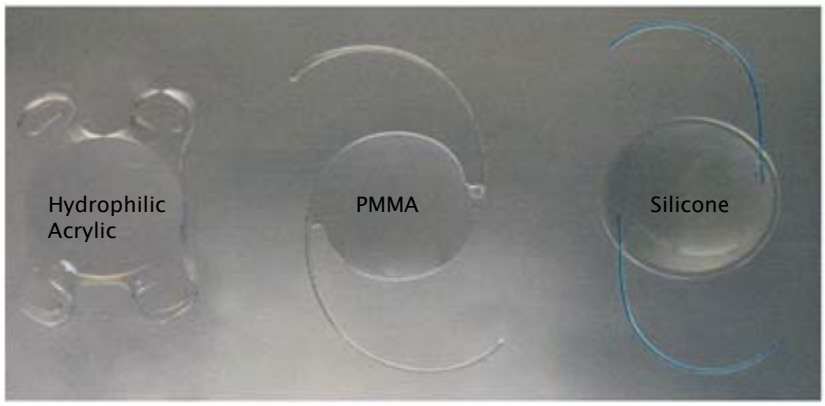

Figure 7-1: Hydrophilic acrylic, PMMA and silicone IOL

This section is published as follows:

Doerte Luensmann[1], Miriam Heynen[1], Lina Liu[2], Heather Sheardown[2], Lyndon Jones[1,2]

[1]Centre for Contact Lens Research, School of Optometry, University of Waterloo, Waterloo, Ontario, N2L 3G1, Canada

[2]Department of Chemical Engineering, McMaster University, Hamilton, ON L8S 4L7, Canada

J Cataract Refract Surg 2009;35(11):2000-2007- Reprinted with permission

	Concept / Design	Recruitment	Acquisition of data	Analysis	Write-up / publication
Luensmann	Y	n/a	Y	Y	Y
Heynen	Y	n/a	Y	-	-
Liu	-	n/a	Y	-	-
Sheardown	-	n/a	Y	-	-
Jones	Y	n/a	-	-	Y

7.2 Overview

Purpose: To determine albumin adsorption profiles and penetration depth of 3 intraocular lens (IOL) materials over time using confocal laser scanning microscopy (CLSM) and radiolabeling.

Methods: Poly(methyl methacrylate) (PMMA), silicone, and foldable hydrophilic acrylic IOLs were incubated in 0.5 mg/ml bovine serum albumin (BSA) for 1, 7, and 14 days. The BSA was conjugated with lucifer yellow VS to allow identification of the protein location by fluorescent imaging with CLSM. Next, the protein uptake was quantified using 2% ^{125}I-labeled BSA.

Results: Confocal laser scanning microscopy showed increasing BSA uptake for silicone and PMMA IOLs after 14 days of incubation ($P<0.05$), with an apparent penetration depth of 8.7 ± 1.9 µm (SD) and 9.2 ± 1.4 µm, respectively. For hydrophilic acrylic IOLs, BSA was detected at a depth of 38 ± 7.4 µm after 1 day, followed by an increase to 192.7 ± 16.2 µm after 14 days. Despite the penetration depth into the hydrophilic acrylic IOLs, quantitative results confirmed that PMMA and hydrophilic acrylic deposited significantly less BSA (mean 278.3 ± 41.7 ng and 296.5 ± 33.1 ng, respectively) than silicone IOLs (mean 392.6 ± 37.6 ng) ($P<0.05$).

Conclusions: Silicone and PMMA IOL materials showed BSA sorption near the lens surface only, while BSA penetrated deep into the hydrophilic acrylic IOL matrix. Combining the qualitative CLSM method and quantitative radiolabeling technique provided detailed information on protein interactions with implantable biomaterials.

7.3 Introduction

In 2006, the rate of cataract surgery in the US was 6500 per 100 000 people, which is expected to increase over time due to the aging population.[4,5] In addition to their use following cataract extraction, intraocular lenses (IOLs) are increasingly used in phakic eyes to correct high levels of refractive error[6-8] and in pediatric aphakia.[9] As the average age of the patients declines, it is possible that the IOL will remain in situ for several decades. Thus, the requirements for biocompatibility and biostability, including chemical, mechanical and optical long-term performance, increase.[10]

The biomaterials used for IOLs can be generally categorized into two broad groups, being acrylic polymers and silicone. The acrylic group may be further sub-divided into rigid polymethyl methacrylate (PMMA), foldable hydrophobic acrylic and foldable hydrophilic acrylic (hydrogel) materials.[11,12] The water content for most IOL materials is <1%, with the exception of hydrophilic hydrogels, which have water contents ranging from 18-38%.[13]

The immunological response of the eye following cataract surgery may be impacted by the incision size, which is directly related to whether the IOL can be folded prior to insertion.[11] Smaller incisions cause less damage to the blood-aqueous barrier (BAB), lower amounts of induced corneal astigmatism and higher resistance to leakage of the aqueous humour (AH). [14] Following insertion, the IOL is directly exposed to the AH, which consists largely of glucose, ascorbate, inorganic ions, various peptides and proteins.[15] The majority of AH components are present in the blood serum and enter the AH by leaking through the blood vessels.[16] The total protein concentration in the AH is approximately 0.7 mg/ml, with albumin being the

most abundant protein, accounting for approximately 50% of the total content.[17] Studies have shown that the AH composition changes with eye disease or following cataract surgery, due to the breakdown of the BAB.[17-20]

This breakdown in the BAB increases cell and protein levels in the AH. As a result, within the first days post surgery, inflammatory cells can be observed on the IOL surface.[21] In cases where significant lens epithelial cell (LEC) growth is observed over the anterior IOL surface, fewer inflammatory cells are found in the anterior chamber, suggesting "superior" biocompatibility.[14,21,22] Different levels of foreign-body response have been reported with different materials, with fewer inflammatory cells in the AH with poly (hydroxyethyl methacrylate) (pHEMA) or hydrophobic acrylic materials compared to PMMA or silicone IOLs.[12,14,21] Protein sorption from the AH to the IOL occurs immediately after the implant is exposed to the AH, and this protein coating influences subsequent cell adhesion.[23-26]

In vitro and ex vivo studies have investigated the interaction between various AH proteins and IOL materials. Johnston and coworkers found differences in albumin and fibronectin sorption onto PMMA and hydrophobic acrylic lenses in vitro,[27] and concluded that incubation time, protein concentration, protein type and material composition influenced the individual uptake. Explanted IOLs have been investigated by Linnola et al.[28] using immunohistochemical staining. They found significantly more fibronectin and vitronectin on acrylic lenses compared to silicone or PMMA. However, the impact of these AH proteins on the biocompatibility of IOL lenses is complex and still not fully understood. In addition, studies to-date have only estimated the total amount of the deposited protein, but cannot describe their location on the lens. This factor may be important, as the response of the eye to the implant may differ

depending upon whether the proteins are sorbed to the surface or absorbed into the bulk of the lens. Additionally, these surface-located proteins may undergo different conformational changes.

In this in vitro study, confocal laser scanning microscopy (CLSM) was used to determine the location of albumin on three distinctly different IOL materials and a radioactive technique quantified the amount of albumin deposition.

7.4 Methods

PMMA, silicone and foldable hydrophilic acrylic IOLs were investigated in this study, whose material properties and dimensions are summarized in Table 7-1.

Table 7-1: Dimensions and properties of the IOLs

	Power	Optic Ø ; Length	Water content	Number of pieces
Hydrophilic Acrylic (B&L Akreos Adapt)	+21.5 D – +26.0 D	6.0 mm ; 10.70 mm	26%	1 piece
PMMA (B&L EZE-55)	+21.00 D	5.5 mm ; 12.75 mm	<1%	1 piece
Silicone (B&L Ll61SE)	+20.50 D	6.0 mm ; 13.00 mm	<1%	3 piece

The bovine serum albumin (BSA) used in this study had a purity of 99% (agarose gel electrophoresis) and a molecular weight of 66 kDa (Sigma-Aldrich St. Louis, MO). The shape and physicochemical properties of albumin from human and bovine serum are very similar and are expected to behave in an analogous manner.[29-31]

The IOLs were incubated in 2 ml of 0.5 mg/ml of BSA, which was either conjugated to a fluorescent dye or a radioactive tracer (for conjugation methods see below). The incubation was undertaken in amber vials, with the lenses hung on plastic threads to prevent them from sinking to the bottom of the glass vial, thus ensuring adequate exposure of the IOLs to the protein solution. The incubation was performed at 37ºC under constant rotation of 72 rpm. After time periods of 1, 7, and 14 days the IOLs were rinsed with PBS prior to further examination.

7.4.1 Determination of albumin location

7.4.1.1 Protein labeling

Prior to the lens incubation, BSA was conjugated with Lucifer Yellow VS (LY - Sigma-Aldrich, St. Louis, MO) to allow identification of the protein location using fluorescent imaging on the CLSM. Briefly, 100mg BSA in 0.05 M borate buffer (pH 8.5) and 0.04 M NaCl (10 mg/ml) was prepared. LY is water soluble and thus 4mg was dissolved in 0.5ml of borate buffer (pH 8.5). The LY solution was added to the BSA solution and was gently stirred for one hour in the dark. Unbound LY was removed using a Sephadex G25 column (Amersham Biosciences, Baie d'Urfe, QC). Following this, dialysis against PBS using a 20 kDa molecular weight cutoff dialysis cassette (Pierce, Rockford, IL) was performed, until only minute amounts of unbound LY were detected with a fluorescence spectrophotometer. The fluorescent labeling efficiency was calculated by determining the BSA concentration in the solution using the DC Protein Assay (Bio-Rad, Hercules, CA) and measuring the absorbance at 415nm (which is the maximum absorbance for LY). The degree of labeling (DOL) was 3.2, indicating that on average, 3.2 dye molecules was bound per molecule of protein (Appendix A).

Prior to incubation, the BSA-LY solution was sterilized using 0.2 µm polyethersulfone syringe filtration (VWR, Mississauga ON).

The IOLs were incubated in BSA-LY with two replicates used for each condition and time point. Additional lenses (used as controls) were incubated in phosphate buffered saline (PBS) for seven days, or in PBS containing the LY dye for one day.

7.4.1.2 CLSM imaging

The CLSM Zeiss LSM 510 Meta (Zeiss Inc. Toronto, Canada) was used to image the fluorescently labeled BSA on the IOLs, using a laser diode with a wavelength of 405nm for excitation and a long pass filter of >505nm for emission. The IOLs were placed in microscopy chamber slides filled with PBS, and CLSM scans were taken in single micron steps, captured with a 40x water Apochromat objective. To obtain comparable results over time, appropriate settings for detector gain and laser intensity were determined via a number of preliminary-tests and these remained constant throughout the experiment.

Each IOL was scanned at four random locations with a scan depth of up to 230 µm. Three dimensional images were constructed from each scan and for each of these a further four random locations were chosen to collect intensity profile scans, that were measured perpendicular to the surface into the lens matrix (Figures 7-2 (A+B)). In total, 32 measurements were used to calculate the sorption depth of the protein for each IOL at each time point.

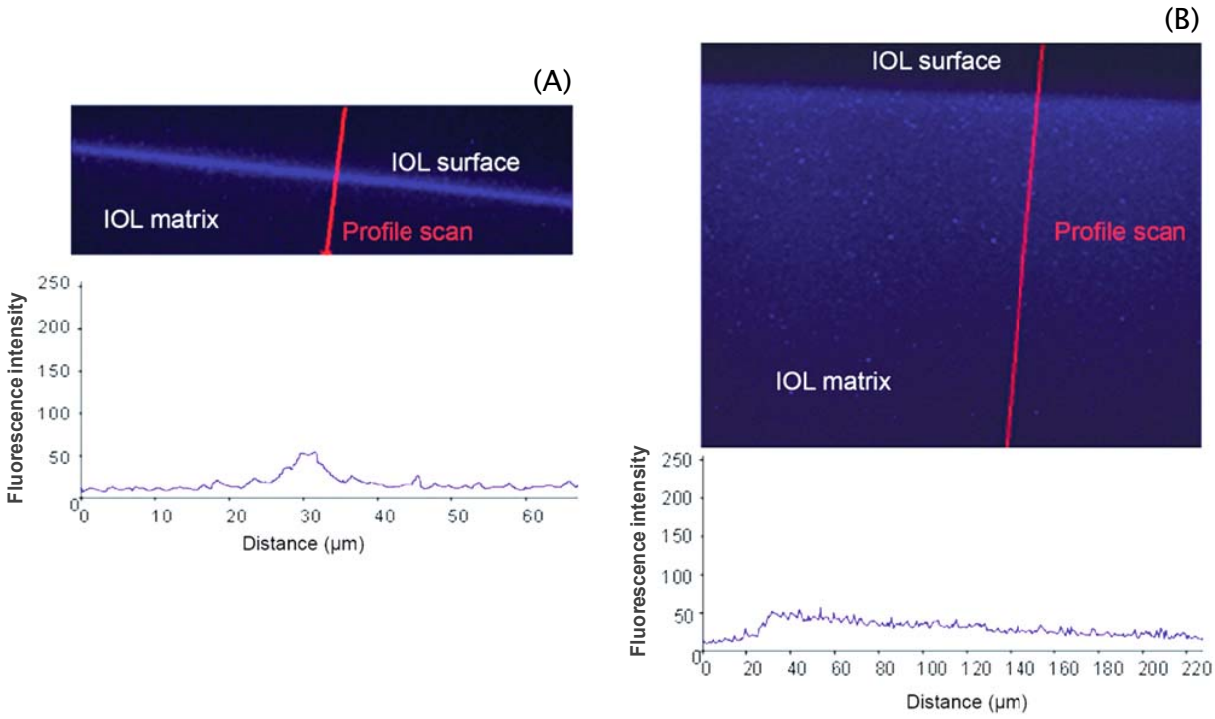

Figure 7-2: BSA-LY detected on the surface of PMMA and silicone IOL materials (A) and throughout hydrophilic-acrylic IOL (B) using CLSM profile scans

7.4.2 Quantification of albumin deposition

In a second experiment, the degree of albumin deposition was quantified by incubating the IOLs in 2ml of 0.5 mg/ml BSA, containing 2% ^{125}I labeled protein. The protein was labeled using the iodine monochloride method.[32,33] IOL incubation conditions were as described above, and two replicates for each time point were determined. The amount of BSA on the IOLs was quantified with the 1480 Wizard Automatic Gamma Counter (PerkinElmer, Woodbridge, ON).

7.4.3 Determination of albumin stability

A major concern when undertaking studies using conjugated proteins is that the properties of the protein could be markedly changed by the labeling process.[34] In this study, native and denatured BSA were evaluated with gel electrophoresis to detect differences between conjugated and unconjugated BSA and to confirm the stability of the BSA-LY during the incubation period. Furthermore, the potential impact of the IOL material itself on the protein solution required investigation.

7.4.3.1 Native polyacrylamide gel electrophoresis (PAGE)

As a protein unfolds different amino acids are exposed, resulting in a different net surface charge. Native PAGE electrophoresis can detect the alterations in surface charge by changes in the relative mobility of the protein along the electrophoresis gel. Samples were prepared in 125 mM Tris-HCl, pH 6.8, 10% glycerol and 0.001% bromphenol blue. In-house native PAGE was performed in 7% polyacrylamide gel (29% acrylamide, 1% N N'-methylenebisacrylamide), 375 mM Tris-HCl, pH 8.8 with 4% stacking gel (125 mM Tris-HCl, pH 6.8). The running buffer was 25 mM Tris, 191 mM glycine, pH 8.6. Samples from the BSA solutions (4 µl) were removed at various times and added to each well of the PAGE. Gels were run at 150 V for two hours, followed by staining in BioSafe Coomassie Stain (Biorad, Hercules, CA). The protein standard used for this gel was Native PAGE Molecular weight Markers™ (Invitrogen, Burlington, ON).

7.4.3.2 Denatured PAGE

To gain more detailed information regarding potential differences in size between the conjugated and unconjugated BSA samples, a high resolution denatured

sodium dodecyl sulfate (SDS) gel was run. Samples were solubilized in 250mM lithium dodecyl sulphate (LDS) (Invitrogen, Burlington, ON) plus 100 mM dithiotheritol (DTT) and heated at 70ºC for 10 minutes. Following this, 0.8 µl of each sample was loaded onto a parafilm-covered template for loading with a 12 X 0.3 µl comb. The protein mass loaded ranged from 0.028 - 0.11 µg. All samples were subjected to SDS-PAGE on 4-15% gradient gels with a 13 mm stacking zone and 32 mm gradient zone on an automated minigel system (Amersham Pharmacia Biotech PhastSystem™, Baie d'Urfe, PQ) using the manufacturer's specified conditions. The gel was run for 20 minutes at 150V / 10mA, followed by staining in BioSafe Coomassie Stain. The protein standards used for this gel were ChemiChrome™ (Sigma-Aldrich St. Louis, MO) and SeeBlue® (Invitrogen, Burlington, ON).

Statistical analysis of the protein uptake on the IOLs was performed using repeated measures ANOVA analysis of equal variance (significance level $p<0.05$). For the CLSM data, the background noise inside the lens matrix was calculated for each material and the width of the fluorescence intensity band was measured, starting at an elevation of 1.5x from the background noise.

7.5 Results

7.5.1 Albumin location

Analysis of the CLSM scans showed an increase in BSA sorption over the incubation period with all three of the IOL types examined ($p<0.05$) (Figures 7-3 (A+B)).

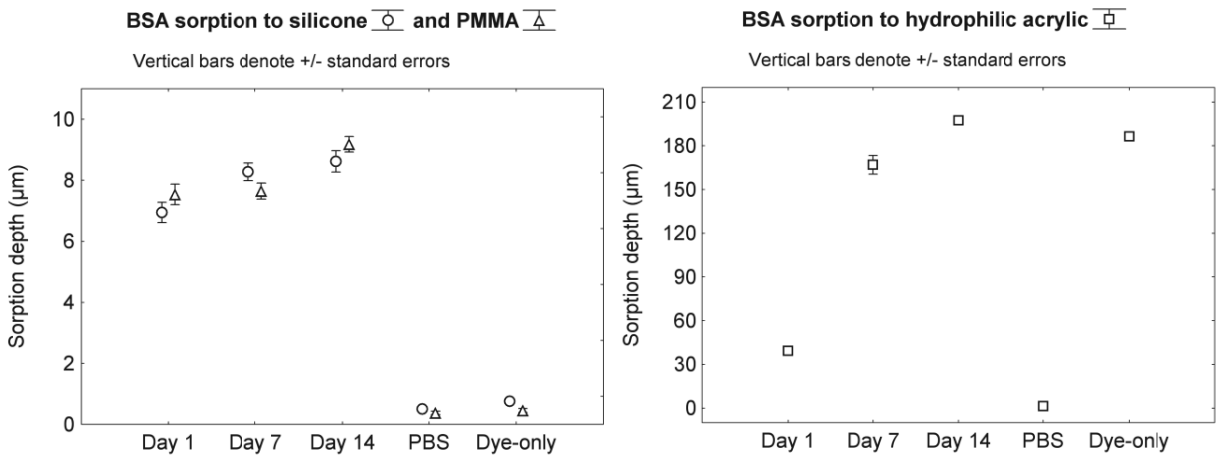

Figure 7-3: BSA-LY sorption to silicone, PMMA (A) and to hydrophilic acrylic (B) over 1, 7 and 14 days of incubation

PBS and Dye-only represent the two control solutions

For the PMMA and silicone IOLs (Figure 7-3A) the fluorescent signal showed an increasing BSA-LY uptake over time, with an apparent penetration depth of 9.2±1.4 and 8.7±1.9 µm respectively on day 14 (see also Figure 7-2A for the result at day 7). The results show a similar BSA-LY sorption profile for both materials ($p>0.05$). The control lenses incubated in PBS or PBS-LY exhibited only a minor fluorescent signal on the surfaces of these IOLs, with no material inherent fluorescence, and the amounts were significantly smaller than that seen for IOLs incubated in conjugated BSA at all time points ($p<0.001$). These results indicate that neither the BSA-LY nor the small dye molecules (550Da) could penetrate to any extent into the matrix of the PMMA or silicone IOL materials.

For the hydrophilic acrylic material (Figure 7-3B), BSA-LY was detected at a depth of 38±7.4 µm after one day, followed by a continuous increase over all time points to a maximum depth of 192.7±16.2 µm after 14 days of incubation (see also Figure 7-2B

for the result at day 7). Following incubation in the control solution containing PBS-LY, the hydrophilic acrylic IOL showed a strong fluorescent signal (Figure 7-3B), with a 184.5±9.7 µm penetration depth after only one day of incubation. For this IOL material, incubated in PBS, only a minor signal could be detected, which was significantly smaller than the conjugated BSA or the dye solution ($p<0.001$), confirming that the IOL alone exhibits no inherent fluorescence at the wavelength chosen for this study.

7.5.2 Albumin quantification

Figure 7-4 describes the BSA sorption as determined using the radiolabel method.

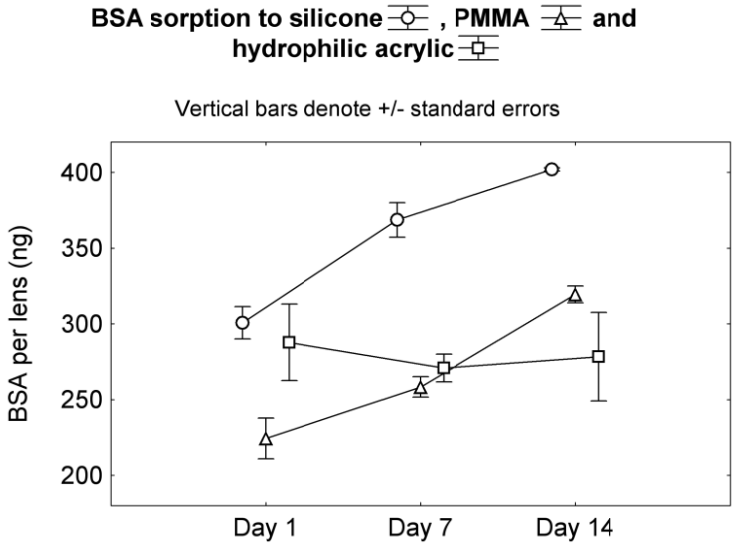

Figure 7-4: Total amount of BSA sorbed on silicone, PMMA and hydrophilic acrylic IOLs over time, obtained using a radiolabeling technique

The silicone and PMMA materials showed increasing BSA levels from day one to day 14 ($p<0.05$). This differs from the hydrophilic acrylic material, which did not

significantly change over the study period ($p>0.05$). After 14 days of incubation in 0.5 mg/ml of BSA, the silicone IOL sorbed 392.6±37.6 ng, PMMA 278.3±41.7 ng and the hydrophilic acrylic 296.5±33.1 ng. The surface adsorption of BSA for the IOLs was calculated to be 660 ng/cm^2 and 556 ng/cm^2 for the PMMA and hydrophobic silicone IOLs respectively. The surface coverage for the hydrophilic acrylic lens could not be determined, as not all the BSA was surface sorbed.

7.5.3 Protein stability: Native PAGE

Samples run on native PAGE showed only minor differences in the relative mobility for conjugated and unconjugated BSA, as seen in Figure 7-5.

The conjugation of the LY dye to the BSA resulted in a slightly more negatively charged protein, as seen by the faster migration in the gel. However, no difference in mobility could be seen in the BSA-LY at 37ºC from day one to day 14, indicating that the protein in the solution was relatively stable over time (Figure 7-5, lanes: 7, 8, 15, 16) Furthermore, keeping the conjugated protein at 37ºC did not induce any changes compared to 4ºC (Figure 7-5, lanes 8, 9, 16). To demonstrate that conformational changes in the protein would result in mobility shifts, BSA samples were heated to 62ºC or 72ºC for 5 minutes. Multiple bands can be seen as a result of the partially unfolded protein and increasing aggregation (Figure 7-5, lanes 11, 12). Investigation of the solutions after the incubation showed the same protein mobility, indicating that the IOL material had no impact on conformation and stability of the protein (Figure 7-5, lanes 1-8, 15, 16).

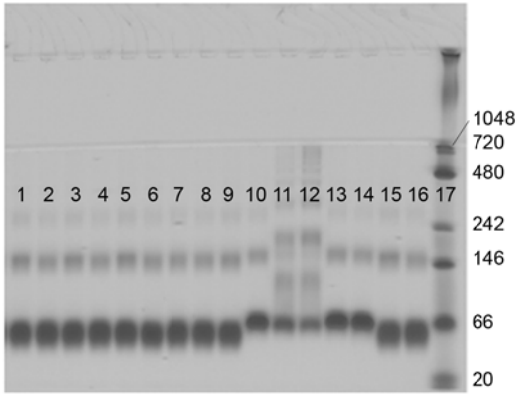

Figure 7-5: Native PAGE loaded with conjugated and unconjugated BSA samples from the solutions used for incubation under various conditions

1. PMMA-sol D1, 2. PMMA-sol D14, 3. Sil-sol D1, 4. Sil-sol D14, 5. Hydr-sol D1, 6. Hydr-sol D14, 7. BSA-LY-D1, 8. BSA-LY D14, 9. BSA-LY +4˚C, 10. BSA-PBS +4˚C, 11. BSA-PBS +62˚C,12. BSA-PBS +72˚C, 13. BSA-PBS D1, 14. BSA-PBS D14, 15. BSA-LY D1, 16. BSA-LY D14, 17. MW (NativePAGE™)

BSA – bovine serum albumin; D – days of incubation (1 or 14) ; Hydr – hydrophilic acrylic; LY – Lucifer Yellow VS; MW – molecular weight marker; PBS – phosphate buffered saline; PMMA – polymethyl methacrylate; Sil - silicone; sol – BSA-LY containing solution.

Each lane represents a sample consisting of a variety of combinations of materials, conjugated and unconjugated BSA, temperatures and duration of incubation. Eg: PMMA-sol D14 describes the lane containing BSA-LY solution after PMMA lens incubation for 14 days at 37˚C; BSA-PBS D1 describes the lane containing BSA dissolved in PBS alone, incubated for 37˚C for 1 day.

7.5.4 Protein stability: Denatured PAGE

To identify smaller differences between conjugated and unconjugated BSA, a Phast™ PAGE containing 4-15% Acrylamide was run (Figure 7-6).

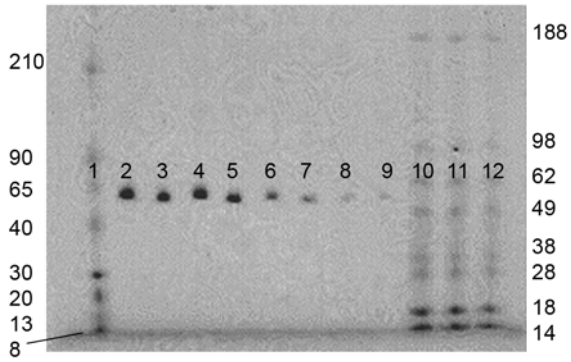

Figure 7-6: SDS-PAGE loaded with different amounts of conjugated and unconjugated BSA

1. MW (ChemiChrome™), 2. BSA - 0.11 µg, 3. BSA-LY - 0.11 µg, 4. BSA - 0.084 µg, 5. BSA-LY - 0.084 µg, 6. BSA - 0.056 µg, 7. BSA-LY - 0.056 µg, 8. BSA - 0.028 µg, 9. BSA-LY 0.028 µg, 10. MW (SeeBlue®), 11. MW (SeeBlue®), 12. MW (SeeBlue®)

BSA – bovine serum albumin; LY – Lucifer Yellow VS; MW – molecular weight marker

The difference in mobility between conjugated and unconjugated protein shown on the gel indicates an apparent molecular weight change of approximately 5%. The conjugated protein appears to be smaller, although it is likely that this is merely a consequence of the fluorescent label increasing the number of charges on the protein.

7.6 Discussion

Most studies to-date investigating the biocompatibility of IOL materials focus on the cell response following surgery, and typically describe capsular [35-37] and uveal [12,21] responses. The impact of proteins on cell adhesion to biomaterials is well known, and the majority of studies report on the extracellular matrix glycoprotein fibronectin

(450 kDa), which is synthesized in the cell and plays a key role in wound healing and cell adhesion.[28,38-41] However, the most abundant protein in the AH is serum albumin,[15,20,42] which enters the AH by leaking through the blood vessels and is part of the biofilm that covers the IOL immediately following insertion.[23-26] A competitive process of protein adsorption and desorption occurs, as smaller proteins get replaced by proteins with higher surface affinity, including glycoproteins such as fibronectin.[43] The protein albumin is believed to increase biocompatibility, is sometimes applied as a coating on blood contacting biomaterials to minimize the adsorption of platelets and is widely thought to have sufficient surface affinity to avoid the Vroman effect.[44,45]

To gain a greater understanding of the interaction between IOLs and proteins, we determined both the location and amount of accumulated BSA on different types of IOLs. To our knowledge, this is the first study of its kind to report on the location of BSA on IOLs, which may be of significance, as the location of the serum albumin could potentially modify subsequent cell adhesion.[45-48] While BSA was used in this study, primary and secondary structures are very similar to human serum albumin [29-31] and therefore it can be assumed that its properties can be approximated by BSA.

Native albumin has a helical structure, but under unfavorable conditions such as heat or when adsorbing to solid surfaces, the protein starts to unfold and beta structures can be detected.[49-51] At a temperature of >45˚C the changes in BSA structure are partially irreversible and by heating the protein to 62˚C a loss of approximately 10% in helical structure has been reported.[49] In this study, we heated the BSA to 62˚C and 72˚C for five minutes and the typical appearance of multiple bands of the denatured protein could be seen in the native gel (Figure 7-5). This indicates that the native gel can detect small changes of ≤10% in protein structure.

It is known that conjugation with a fluorescent tracer has potential to change size and weight, relative molecular charge, and isoelectric point of the protein.[34] However, as demonstrated in the SDS PAGE (Figure 7-6), overall differences between the conjugated and unconjugated BSA were small, with approximately 5% difference being detected

In this study, confocal laser scanning microscopy showed protein sorption solely on the surface of PMMA and silicone IOL materials (Figures 7-2A and 7-3A). However, the hydrophilic acrylic IOL material contains 26% water and therefore clearly has a sufficient pore size for the BSA (which has a diameter of approximately 55Å[52]) to slowly penetrate into the lens matrix over time (Figures 7-2B and 7-3B) The amount of BSA that sorbed onto the silicone IOL was greater than that measured on the PMMA and hydrophilic acrylic IOLs (Figure 7-4). A typical albumin monolayer on solid surfaces is between 150-200 ng/cm^2.[44,53,54] As the CLSM results show, the BSA sorbed onto the PMMA and silicone IOLs could not enter the polymer matrix, and thus the total amount of BSA deposited (as calculated by the radiolabel method) is on the surface alone, at 556 ng/cm^2 and 660 ng/cm^2 respectively, which significantly exceeds a monolayer coverage.[44,53,54]

An in vitro study conducted by Johnston et al.[27] quantified the protein uptake to PMMA and hydrophobic acrylic IOLs. After seven days of incubation they found albumin levels of 205 ng/cm^2 for PMMA and 173 ng/cm^2 for hydrophobic acrylic, which is slightly lower than our data. They further reported that the inflammatory post-surgical response can depend on the dynamic of the protein layer, because irreversible surface-bound proteins are more likely to denature. Although we could confirm that the BSA in the solution did not denature over the time period

investigated, studies have shown that BSA undergoes conformational changes after adsorbing to hydrophobic surfaces such as PMMA.[50,55,56] A study by Pokidysheva et al.[26] found albumin concentrations of 220-460 ng/cm^2 on different IOL materials after less than 30 minutes of exposure to 1 mg/ml of protein. They reported higher protein levels, and more irreversibly adsorbed albumin, for HEMA-based compared to PMMA lenses.

Results from this study suggest that the amount of BSA accumulated on the surface of PMMA and silicone is >100 times larger compared to the BSA found on the hydrophilic acrylic surface. This might be correlated to the rate of posterior capsular opacification and LEC growth over the anterior IOL surface, which is significantly higher for hydrophilic acrylic compared to PMMA, silicone and hydrophobic acrylic materials.[57-59] This may be due to differences in the denatured state of the protein. However, further studies are necessary with cell adhesion proteins to confirm that this is the case.

Significantly higher levels of inflammatory cell deposits on the anterior lens surface have been reported for PMMA,[21] silicone [14] and hydrophobic acrylic [60-62] materials compared to hydrophilic IOLs. These findings suggest that the dense protein layer on the surface could increase cell adherence, which is less pronounced with hydrophilic materials. Furthermore, the porous structure of hydrophilic acrylic lenses could be responsible for the higher rates of calcification, compared with that reported for silicone and PMMA materials.[63]

In this work we have shown that albumin sorption profiles strongly depend on the type of IOL material investigated. In future work, CLSM could provide useful

information by locating the sorption profile of fibronectin and vitronectin, as they are known to significantly impact cell adsorption to the intraocular lens material.

7.7 Conclusions

The biocompatibility of IOLs depends on various factors, such as design, material type, surgery technique, extend of the BAB breakdown, ocular health, etc. Using CLSM we were able to image albumin distribution on PMMA, silicone and hydrophilic acrylic IOLs. Dense surface layers were found for PMMA and silicone materials with 393 and 278 ng per lens respectively. In contrast, the hydrophilic acrylic IOL material allowed the protein to penetrate deep into the lens matrix over time, and deposited no more than 297 ng per lens.

8. GENERAL DISCUSSION AND CONCLUSIONS

The release of soft lenses in the early 1970's resulted in a rapid increase in the use of contact lenses to correct vision, and has grown to approximately 125 million wearers today.[1] Although most soft contact lenses need to be replaced either daily, bi-weekly or monthly, ocular complications due to tear film deposition on lenses are still frequently reported.[2] Silicone hydrogel lenses are highly gas permeable and therefore provide sufficient amounts of oxygen to the cornea to prevent hypoxia related complications. Nevertheless, a higher risk for inflammatory events has been reported if SH lenses are continuously worn for up to 30 days and nights, as compared to pHEMA-lenses worn for up to 7 days and nights.[3]

To provide a better understanding of tear film deposition rates on contact lenses, a number of laboratory-based assays and imaging techniques have been applied in the past to determine the composition and quantity of the deposit.[4] The disadvantage of most imaging techniques is that they can describe deposition on the outer material surface only, but cannot scan deeper than a few micron into the matrix. In this research work, confocal laser scanning microscopy was used, which allows image scanning up to a few hundred microns into the material. To visualize

proteins on the surface and in the material matrix of either contact lenses or intraocular lenses, proteins were conjugated with fluorescent probes.

The conjugation of bovine serum albumin (BSA) with 5-(4,6-Dichloro-s-triazin-2-ylamino)fluorescein hydrochloride (DTAF), contact lens incubation and CLSM imaging techniques were described in detail in Chapter 3. The pHEMA-based material etafilcon A and the surface-coated silicone hydrogel material lotrafilcon B were incubated in the protein solution for one and seven days and the Zeiss LSM 510 Meta was used to detect the conjugate on the surface and inside the lenses. An even protein distribution throughout the material was found for etafilcon A, but protein sorption was mainly detected in the outer surface region for lotrafilcon B. Gel electrophoresis verified that the conjugated BSA solution contained no smaller protein fractions, which may have impacted the results. Furthermore, two scans of the same sample location verified only minor loss in fluorescence (photobleaching). This provided confidence in the protocols for protein conjugation and image acquisition.

In the next study, BSA was conjugated to either DTAF, rhodamine B isothiocyanate (RITC) or lucifer yellow VS dilithium salt (LY) and sorption profiles to different contact lens materials were compared (Chapter 4). In separate experiments, etafilcon A, lotrafilcon B and two other SH materials, balafilcon A and senofilcon A, were either incubated in the conjugated protein solutions or in solution that contained solely the fluorescent probe but no protein. Comparisons between uptake patterns on different contact lens materials suggested a noticeable impact from the probe to the sorption behaviour of the BSA. While for etafilcon A, sorption patterns of the dye solution only and the conjugates were in agreement, the uptake curves for senofilcon A were markedly different. In some cases, conjugated protein showed a

very similar sorption curve to the dye alone, which strongly suggests that the probe had an impact on the protein sorption behaviour. Results from this experiment lead to the conclusion that not every dye is suitable to study protein sorption to biomaterials, particularly if the material surface has different properties compared to the bulk (e.g. due to surface treatment). LY appeared to cause the least amount of impact on the BSA sorption profile and was therefore used in the following experiments.

The major tear film protein lysozyme was investigated in Chapter 5. The protein was either conjugated with fluorescein isothiocyanate (FITC) or LY and the protein accumulation to nine different pHEMA-based and SH contact lens materials was determined. A similar CLSM technique, as described for BSA in Chapter 4, was applied to compare the protein profile after one day of incubation. Quantitative results obtained from the incubation in radiolabeled lysozyme were combined with the confocal scans to describe the amount of protein throughout the lens material. The results showed that lysozyme penetrated into almost every contact lens material within 24 hours. The exceptions were the surface coated materials lotrafilcon A and lotrafilcon B, which showed protein accumulation on the surface, but either no (with lotrafilcon A) or only minor (with lotrafilcon B) penetration into the matrix.

The two fluorescent probes used for conjugation showed only small differences for the lysozyme sorption pattern to most lens types, except for the two silicone hydrogel lenses galyfilcon A and senofilcon A. A strong fluorescent signal was detected on the lens surface when incubated in FITC-lysozyme but an almost even distribution could be seen for LY-lysozyme, particularly for senofilcon A. The internal wetting agent PVP is incorporated in both materials and may have interacted with the

fluorescein-based dye, by either binding this conjugate to the material or by enhancing the fluorescent emission strength.

The efficiency of contact lens care regimens on protein removal was imaged and quantified in Chapter 6. Results from CLSM and radiolabeled data show clearly that protein sorption profiles depended on the protein type (lysozyme or albumin) but also on the contact lens material and the care regimen chosen. In general, hydrogen peroxide removed slightly more lysozyme from the lenses compared to MPS systems. In most cases similar levels of protein were found on the lenses when cleaned with the MPS regimen, independent of whether they were manually rubbed or not before overnight soaking. CLSM confirmed lysozyme removal primarily from the lens matrix for lotrafilcon B, but not the surface. This was different for etafilcon A, which showed reduced amounts of protein at the surface region after cleaning, indicating that lysozyme was more loosely bound to this material. This suggests that the more denatured protein on the SH surface was bound more strongly than the less denatured protein on etafilcon A.[5]

Interactions between intraocular lenses (IOL) and BSA were examined in Chapter 7. Data obtained from the investigation of PMMA, silicone and hydrophilic acrylic IOL materials confirmed protein sorption to the surface of PMMA and silicone, but a steady increase in penetration into a hydrophilic acrylic IOL. Nevertheless, the silicone-based IOL accumulated higher levels of protein compared to the hydrophilic acrylic and the PMMA materials.

The emission data obtained from the CLSM measurements were presented in different ways. In Chapters 3 and 5, the regions for front surface, back surface and

bulk were predefined using the average of either 5 µm for the surfaces or 30 µm for the central matrix region. In Chapters 4 and 5 sorption curves were compared graphically, while Chapter 4 provided additional quantitative information. In Chapter 6, albumin sorption to IOL materials was described by the signal depth, as these samples had thicknesses of >1mm and exceeded the maximum scanning depth of the CLSM. Although the data assessment was partly automated, a subjective component, for example to determine the surface peaks, was necessary.

For future work, a different method could be applied to analyze the CLSM intensity plots using general bilinear models, as suggested by Buchwald.[6] In an example, Statistica 8.0 was used to fit two individual linearized biexponential curves (a) to the front and back surface of the lens scan and a linear regression line (b) to the central lens region (Correlation coefficient R>0.98). Curves were fitted to two material types, etafilcon A and lotrafilcon B following their incubation in BSA conjugated with LY.

Function for the bilinear model:

(a) $y = f(x) = \eta \ln\left[e^{\alpha 1(t-\tau c)/\eta} + e^{\alpha 2(t-\tau c)/\eta}\right] + \chi$

(b) $y = \alpha t + \chi$

The bilinear model requires the following parameters:

y = dependent variable; t = independent variable;
η = transition between the two linear portions; e = Euler's number (2.718);
$\alpha 1$ and $\alpha 2$ = slopes prior to ($\alpha 1$) and after the transition ($\alpha 2$);
τc = shift along the horizontal axis t; χ= shift along the vertical axis y

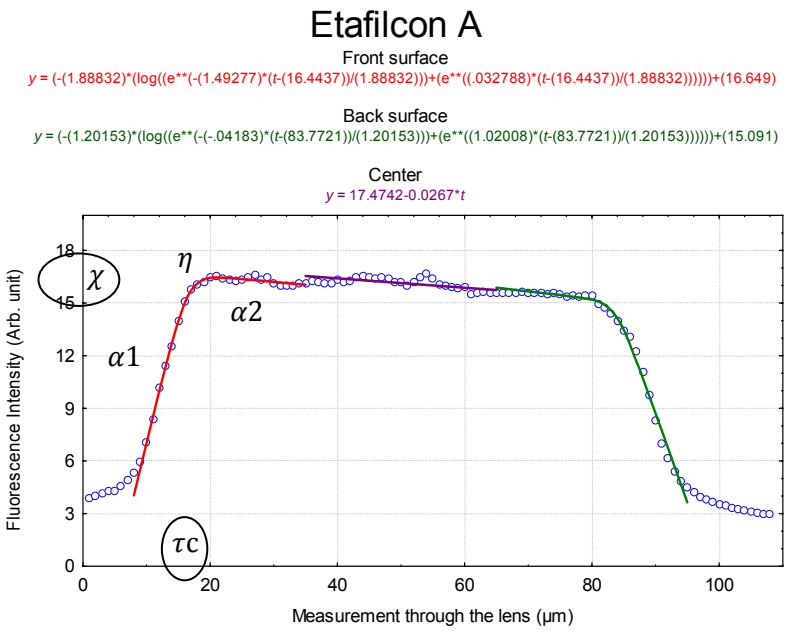

Figure 8-1: Protein sorption to etafilcon A is described by fitting linearized biexponential models to front and back surface regions and a linear regression line to the central matrix

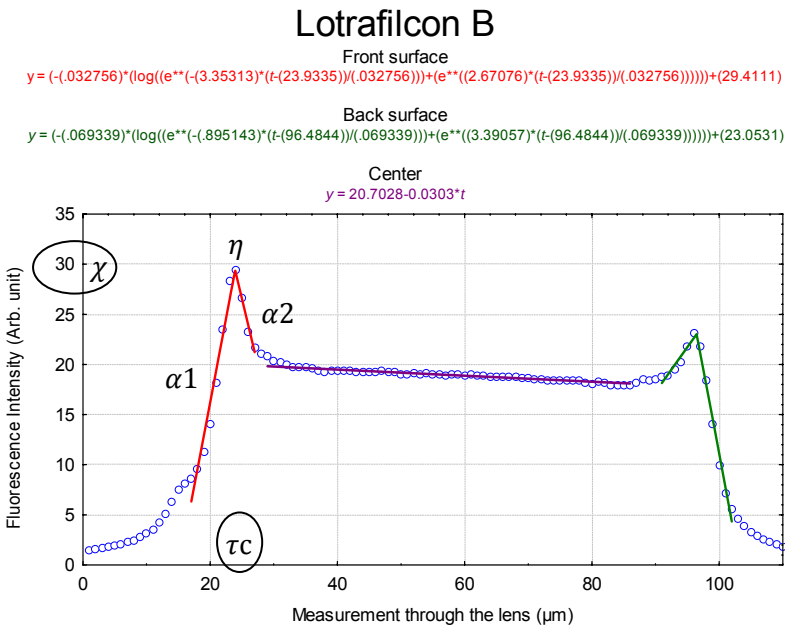

Figure 8-2: Protein sorption to lotrafilcon B is described by fitting linearized biexponential models to front and back surface regions and a linear regression line to the central matrix

After fitting the three functions to the intensity plots, a number of parameters can be chosen to determine differences between sorption curves. The parameters of the biexponential curves describing the smoothness of the transition (η) and the two slopes $(\alpha 1 \text{ and } \alpha 2)$ can be used to perform statistical analysis for comparisons between curve progressions. The slopes $\alpha 2$ of the front surface or $\alpha 1$ of the back surface could differentiate between surface deposited proteins (Figure 8-2) and proteins that penetrate the full matrix (Figure 8-1). Different levels of fluorescence intensity in the surface region can be compared using parameter χ, to identify changes e.g. between time points. Furthermore the material thickness can be estimated by calculating the separation between the parameters τc for the front and back surface. Parameter χ of the linear regression line can further compare intensity changes within the central matrix over time.

This automated curve fitting could reduce the subjective component and may require less time for data processing and analysis.

In addition to the use of mathematical models to examine data obtained from studies such as those conducted in this thesis, there are several other areas that could be considered in future.

The use of fluorescent probes to locate proteins has successfully been applied to various research areas because of their lack of toxicity, high sensitivity, low cost and ease of use. Most fluorescent probes are highly pH sensitive and their emission intensity strongly depends on the microenvironment. When using fluorescent probes in materials research, pH sensitivity, as well as charge components should be

considered, when evaluating sorption curves. This limitation requires a number of preliminary tests investigating dye-uptake into the material and the addition of a quantitative method such as radiolabeling.

In this thesis, single protein solutions were used to determine sorption patterns of albumin and lysozyme to different pHEMA-based and SH materials. Although the results provide useful model data, it remains unclear how protein sorption behaviour changes with the addition of other components from the tear film, or, when investigating IOLs, the addition of components from the aqueous humour. A process of competitive uptake can be expected and it needs to be clarified, whether or not the conjugated fluorescent probe impacts these results.

With the use of multiple fluorescent probes competitive sorption of two or more different proteins to biomaterials could be investigated. However, this requires dyes with differing excitation/emission wavelengths, but similar binding affinities to the materials. None of the dyes should show specific surface affiliation and the uptake pattern for one dye should not significantly change under the presence of a second dye. Finding suitable probes will be difficult, specifically when investigating SH contact lenses with complex material compositions and surface modifications, as demonstrated in Chapter 4. To prove the reliability of the protein data, the fluorescent probes must be conjugated to both proteins and the sorption with each must be compared.

It is generally believed that the protein on the material surface is more denatured than that of the protein located in the material matrix. However, future

studies should investigate whether or not this is true, and methods to determine the conformational state of protein at various locations is worthy of study.

Finally, the advantage of CLSM to detect fluorescent conjugates throughout thick materials may also prove useful when studying biomaterials for drug uptake and release. CLSM could provide useful information on the location of the specific drug into the material and could also monitor the release over time.

REFERENCES

References - Chapter 1

1. Wichterle O, Lim D. Hydrophilic gels in biologic use. Nature 1960;185:117-118.

2. Tighe B. Contact lens materials. In: Phillips A, Speedwell L, editors. Contact Lenses. Edinburgh: Butterworth-Heinemann; 2007. p 59-78.

3. Gonzalez-Meijome JM, Jorge J, Almeida JB, Parafita MA. Contact lens fitting profile in Portugal in 2005: strategies for first fits and refits. Eye Contact Lens 2007;33(2):81-8.

4. Hoffman AS. Hydrogels for biomedical applications. Adv Drug Deliv Rev 2002;54(1):3-12.

5. Peppas NA, Huang Y, Torres-Lugo M, Ward JH, Zhang J. Physicochemical foundations and structural design of hydrogels in medicine and biology. Annu Rev Biomed Eng 2000;2:9-29.

6. Nicolson PC, Vogt J. Soft contact lens polymers: an evolution. Biomaterials 2001;22(24):3273-83.

7. Fonn D, Bruce AS. A review of the Holden-Mertz criteria for critical oxygen transmission. Eye Contact Lens 2005;31(6):247-51.

8. Bonnano JA, Bergmanson JP, Davis LJ, Lebow KA, Josephson JE, Caffery BE, Silbert JA, Jurkus JM, Swarbrick HA, Holden BA and others. Anterior segment complications of contact lens wear. In: Silbert JA, editor. Boston: Butterworth-Heinemann; 2000. p 25-148; 273-328.

9. Holden BA. The Glenn A. Fry Award lecture 1988: the ocular response to contact lens wear. Optom Vis Sci 1989;66(11):717-33.

10. Sweeney DF. The Max Schapero Memorial Award Lecture 2004: contact lenses on and in the cornea, what the eye needs. Optom Vis Sci 2006;83(3):133-42.

11. Snyder C. A primer on contact lens materials. Contact Lens Spectrum 2004;19(2):34-39.

12. Holden BA, Mertz GW. Critical oxygen levels to avoid corneal edema for daily and extended wear contact lenses. Invest Ophthalmol Vis Sci 1984;25(10):1161-7.

13. Harvitt DM, Bonanno JA. Re-evaluation of the oxygen diffusion model for predicting minimum contact lens Dk/t values needed to avoid corneal anoxia. Optom Vis Sci 1999;76(10):712-9.

14. Rogers R. In vitro and ex vivo wettability of hydrogel contact lenses. Waterloo, Ont.: University of Waterloo; 2006. xi, 137 p. p.

15. Jones L, Senchyna M, Glasier MA, Schickler J, Forbes I, Louie D, May C. Lysozyme and lipid deposition on silicone hydrogel contact lens materials. Eye Contact Lens 2003;29(1 Suppl):75-9.

16. Lorentz H, Jones L. Lipid deposition on hydrogel contact lenses: how history can help us today. Optom Vis Sci 2007;84(4):286-95.

17. Nicolson PC, Baron RC, Chabrecek P, Court J, Domschke A, Griesser HJ, et.al.; Extended wear ophthalmic lens. US Patent No. 5760100, 1998.

18. Grobe GL, Kunzler J, Seelye D, Salamone J. Silicone hydrogels for contact lens applications. Polym. Mater. Sci. Eng. 1999;80:108-9.

19. Yasuda H. Biocompatibility of nanofilm-encapsulated silicone and silicone-hydrogel contact lenses. Macromol Biosci 2006;6(2):121-38.

20. Weikart CM, Matsuzawa Y, Winterton L, Yasuda HK. Evaluation of plasma polymer-coated contact lenses by electrochemical impedance spectroscopy. J Biomed Mater Res 2001;54(4):597-607.

21. Lopez-Alemany A, Compan V, Refojo MF. Porous structure of Purevision versus Focus Night&Day and conventional hydrogel contact lenses. J Biomed Mater Res 2002;63(3):319-25.

22. Jones L. Contact lens materials: A new silicone hydrogel comes to market. Contact Lens Spectrum 2007;22(10):23.

23. Steffen R, McCabe K. Finding the comfort zone. Contact Lens Spectrum 2004;13;3(supp 1-4).

24. Steffen R, Schnider C. A next generation silicone hydrogel lens for daily wear. Part 1 - Material properties. Optician 2004;227:23-5.

25. Mccabe KP, Molock FF, Hill GA, Alli A, Steffen RB, Vanderlaan DG, Ford JD; Biomedical devices containing internal wetting agents. US Patent No. 20050154080, 2005.

26. Riley C, Young G, Chalmers R. Prevalence of ocular surface symptoms, signs, and uncomfortable hours of wear in contact lens wearers: the effect of refitting with daily-wear silicone hydrogel lenses (senofilcon a). Eye Contact Lens 2006;32(6):281-6.

27. Brennan NA, Coles ML, Ang JH. An evaluation of silicone-hydrogel lenses worn on a daily wear basis. Clin Exp Optom 2006;89(1):18-25.

28. Tighe B. Trends and Developments in Silicone Hydrogel Materials. http://www.siliconehydrogels.com.; 2006

29. Woods CA, Jones DA, Jones LW, Morgan PB. A seven year survey of the contact lens prescribing habits of Canadian optometrists. Optom Vis Sci 2007;84(6):505-10.

30. Morgan PB, Efron N, Woods CA, Jones D, Pesinova A, Grein H-J, Tranoudis IG, Montani G, Marani E, Motozumi I and others. International contact lens prescribing in 2004. Contact Lens Spectrum 2005;20(1):34-37.

31. Morgan PB, Woods CA, Knajian R, Jones D, Efron N, Tan K-O, Pesinova A, Grein H-J, Marx S, Santodomingo J and others. International contact lens prescribing in 2007. Contact Lens Spectrum 2008;23(1):36-41.

32. Key JE. Development of contact lenses and their worldwide use. Eye Contact Lens 2007;33(6):343-345.

33. Morgan PB, Efron N. The evolution of rigid contact lens prescribing. Cont Lens Anterior Eye 2008;31(4):213-4.

34. Morgan PB, Efron N. A decade of contact lens prescribing trends in the United Kingdom (1996-2005). Cont Lens Anterior Eye 2006;29(2):59-68.

35. Morgan PB, Efron N, Woods CA, Jones D, Tranoudis IG, van der Worp E, Helland M. International contact lens prescribing. Contact Lens Spectrum 2002;17(1):42-45.

36. Nichols JJ. Contact lenses 2008 - Annual Report. Contact Lens Spectrum 2009;24(1):24-32.

37. Morgan PB, Woods CA, Tranoudis IG, Efron N, Knajian R, Grupcheva CN, Jones D, Tan K-O, Pesinova A, Ravn O and others. International contact lens prescribing in 2008. Contact Lens Spectrum 2009;24(28-32).

38. Williams L, Stapleton F. Microbiology, lens care and maintenance. In: Phillips A, Speedwell L, editors. Contact Lenses. Edinburgh: Butterworth-Heinemann; 2004. p 79-109.

39. Wedler FC. Analysis of biomaterials deposited on soft contact lenses. J Biomed Mater Res 1977;11(4):525-35.

40. Tragakis MP, Brown SI, Pearce DB. Bacteriologic studies of contamination associated with soft contact lenses. Am J Ophthalmol 1973;75(3):496-9.

41. Zhao Z, Carnt NA, Aliwarga Y, Wei X, Naduvilath T, Garrett Q, Korth J, Willcox MD. Care regimen and lens material influence on silicone hydrogel contact lens deposition. Optom Vis Sci 2009;86(3):251-9.

42. Hart DE, Plociniak MP, Grimes GW. Defining the physiologically normal coating and pathological deposit: An analysis of sulfur-containing moieties and pellicle thickness on hydrogel contact lenses. CLAO J 1998;24(2):85-101.

43. Brennan NA, Coles ML. Deposits and symptomatology with soft contact lens wear. Int Contact Lens Clin 2000;27(3):75-100.

44. Walker J. New developments in RGP lens care. Optician 1997;213(5583):16-9.

45. Gasson A, Morris J. Care systems. The contact lens manual: A practical guide to fitting. Edinburgh: Butterworth-Heinemann; 2003. p 329-344.

46. Jones L, Christie C. Soft contact lens solutions review: Part 2: Modern-generation care system. Optom Pract 2008;9:43-62.

47. Gasset AR, Ramer RM, Katzin D. Hydrogen peroxide sterilization of hydrophilic contact lenses. Arch Ophthalmol 1975;93(6):412-5.

48. Bergenske PD. Contact lens disinfection. Optom Clin 1994;4(1):47-60.

49. Bilgin LK, Manav G, Tutkun IT, Oner A, Ertoprak Y. Efficacy of a one-step hydrogen peroxide system for disinfection of soft contact lenses. CLAO J 1993;19(1):50-2.

50. Soni PS, Horner DG, Ross J. Ocular response to lens care systems in adolescent soft contact lens wearers. Optom Vis Sci 1996;73(2):70-85.

51. Mondino BJ, Salamon SM, Zaidman GW. Allergic and toxic reactions of soft contact lens wearers. Surv Ophthalmol 1982;26(6):337-44.

52. Jones L, Senchyna M. Soft contact lens solutions review part 1: Components of modern care regimens. Optom Pract 2007;8:45-56.

53. Kline LN, Connors R, DeLuca TJ, Lefland L. Choosing a soft lens care regimen. Contact Lens Forum 1982;7(7-12):85-93.

54. Callender M, Lutzi D. The incidence of adverse ocular reactions among soft contact lens wearers using chemical disinfection procedures. Can J Optom 1979;41(3):138-140.

55. Nilsson SE, Lindh H. Hydrogel contact lens cleaning with or without multi-enzymes. A prospective study. Acta Ophthalmol (Copenh) 1988;66(1):15-8.

56. Kjellsen T, Kiral R, Eriksen SP. Single-enzyme versus multi-enzyme contact lens cleaning system: Speed and efficiency in removing deposits from hydrogel contact lenses. Int Contact Lens Clin 1984;11(11):660-667.

57. Choy CK, Cho P, Benzie IF, Ng V. Effect of one overnight wear of orthokeratology lenses on tear composition. Optom Vis Sci 2004;81(6):414-20.

58. Velasco Cabrera MJ, Garcia Sanchez J, Bermudez Rodriguez FJ. Lactoferrin in tears in contact lens wearers. CLAO J 1997;23(2):127-9.

59. Willcox MD, Lan J. Secretory immunoglobulin A in tears:functions and changes during contact lens wear. Clin Exp Optom 1999;82(1):1-3.

60. Suchecki JK, Donshik P, Ehlers WH. Contact lens complications. Ophthalmol Clin North Am 2003;16(3):471-84.

61. Jones L, Dumbleton K. Soft lens extended wear and complications. In: Hom MM, Bruce A, editors. Manual of contact lens prescribing and fitting. Oxford: Butterworth-Heinemann; 2006. p 393-441.

62. Sweeney DF. Corneal exhaustion syndrome with long-term wear of contact lenses. Optom Vis Sci 1992;69(8):601-8.

63. Dumbleton K. Adverse events with silicone hydrogel continuous wear. Cont Lens Anterior Eye 2002;25(3):137-46.

64. Ang JH, Efron N. Corneal hypoxia and hypercapnia during contact lens wear. Optom Vis Sci 1990;67(7):512-21.

65. Bonanno JA, Polse KA. Corneal acidosis during contact lens wear: effects of hypoxia and CO2. Invest Ophthalmol Vis Sci 1987;28(9):1514-20.

66. Holden BA, Sweeney DF, Vannas A, Nilsson KT, Efron N. Effects of long-term extended contact lens wear on the human cornea. Invest Ophthalmol Vis Sci 1985;26(11):1489-501.

67. Bonanno JA, Polse KA. Measurement of in vivo human corneal stromal pH: open and closed eyes. Invest Ophthalmol Vis Sci 1987;28(3):522-30.

68. Martin DK, Holden BA. Variations in tear fluid osmolality chord diameter and movement during wear of high water content hydrogel contact lenses. Int Contact Lens Clin 1983;10:332-42.

69. Holden BA, Mertz GW, McNally JJ. Corneal swelling response to contact lenses worn under extended wear conditions. Invest Ophthalmol Vis Sci 1983;24(2):218-26.

70. Efron N. Stromal edema. In: Efron N, editor. Contact lens complications. Edinburgh: Butterworth-Heinemann; 2004. p 133-40.

71. Connor CG, Zagrod ME. Contact lens-induced corneal endothelial polymegathism: functional significance and possible mechanisms. Am J Optom Physiol Opt 1986;63(7):539-44.

72. Efron N. Corneal neovascularization. In: Efron N, editor. Contact lens complications. Edinburgh: Butterworth-Heinemann; 2004. p 153-61.

73. Dumbleton KA, Chalmers RL, Richter DB, Fonn D. Changes in myopic refractive error with nine months' extended wear of hydrogel lenses with high and low oxygen permeability. Optom Vis Sci 1999;76(12):845-9.

74. Santodomingo-Rubido J, Wolffsohn JS, Gilmartin B. Adverse events and discontinuations during 18 months of silicone hydrogel contact lens wear. Eye Contact Lens 2007;33(6 Pt 1):288-92.

75. Sankaridurg PS, Holden BA, Jalbert I. Adverse events and infections: shich ones and how many? In: Sweeney D, editor. Silicone hydrogels : continuous-wear contact lenses. Edinburgh: Butterworth Heinemann, British Contact Lens Association; 2004. p 217-74.

76. Holden BA, Reddy MK, Sankaridurg PR, Buddi R, Sharma S, Willcox MD, Sweeney DF, Rao GN. Contact lens-induced peripheral ulcers with extended wear of disposable hydrogel lenses: histopathologic observations on the nature and type of corneal infiltrate. Cornea 1999;18(5):538-43.

77. Willcox M, Sankaridurg PR, Zhu H, Hume E, Cole N, Conibear T, Glasson M, Harmis N, Stapleton F. Inflammation and infection and the effects of the closed eye. In: Sweeney D, editor. Silicone hydrogels: continuous-wear contact lenses. Edinburgh: Butterworth Heinemann, British Contact Lens Association; 2004. p 90-125.

78. Ramachandran L, Sharma S, Sankaridurg PR, Vajdic CM, Chuck JA, Holden BA, Sweeney DF, Rao GN. Examination of the conjunctival microbiota after 8 hours of eye closure. CLAO J 1995;21(3):195-9.

79. Szczotka-Flynn L, Diaz M. Risk of corneal inflammatory events with silicone hydrogel and low dk hydrogel extended contact lens wear: a meta-analysis. Optom Vis Sci 2007;84(4):247-56.

80. Efron N, Morgan PB. Rethinking contact lens associated keratitis. Clin Exp Optom 2006;89(5):280-98.

81. Walline JJ, Holden BA, Bullimore MA, Rah MJ, Asbell PA, Barr JT, Caroline PJ, Cavanagh HD, Despotidis N, Desmond F and others. The current state of corneal reshaping. Eye Contact Lens 2005;31(5):209-14.

82. Phillips CI. Contact lenses and corneal deformation: cause, correlate or co-incidence? Acta Ophthalmol (Copenh) 1990;68(6):661-8.

83. Alba-Bueno F, Beltran-Masgoret A, Sanjuan C, Biarnes M, Marin J. Corneal shape changes induced by first and second generation silicone hydrogel contact lenses in daily wear. Cont Lens Anterior Eye 2009;32(2):88-92.

84. Holden BA, Stephenson A, Stretton S, Sankaridurg PR, O'Hare N, Jalbert I, Sweeney DF. Superior epithelial arcuate lesions with soft contact lens wear. Optom Vis Sci 2001;78(1):9-12.

85. Sweeney D, du Toit R, Keay L, Jalbert I, Sankaridurg PR, Stern J, Skotnitsky C, Stephensen A, Covey M, Holden BA and others. Clinical performance of silicone hydrogel lenses. In: Sweeney D, editor. Silicone hydrogels: continuous-wear contact lenses. Edinburgh: Butterworth Heinemann, British Contact Lens Association; 2004. p 164-216.

86. Forister JF, Forister EF, Yeung KK, Ye P, Chung MY, Tsui A, Weissman BA. Prevalence of contact lens-related complications: UCLA contact lens study. Eye Contact Lens 2009;35(4):176-80.

87. Fonn D, MacDonald KE, Richter D, Pritchard N. The ocular response to extended wear of a high Dk silicone hydrogel contact lens. Clin Exp Optom 2002;85(3):176-82.

88. Donshik PC, Ehlers WH, Ballow M. Giant papillary conjunctivitis. Immunol Allergy Clin North Am 2008;28(1):83-103.

89. Greiner JV. Giant papillary conjunctivitis. In: Abelson MB, editor. Allergic diseases of the eye. Philadelphia: Saunders; 2000. p 141-60.

90. Dumbleton K. Noninflammatory silicone hydrogel contact lens complications. Eye Contact Lens 2003;29(1 Suppl):186-9.

91. Skotnitsky C, Sankaridurg PR, Sweeney DF, Holden BA. General and local contact lens induced papillary conjunctivitis (CLPC). Clin Exp Optom 2002;85(3):193-7.

92. Richard NR, Anderson JA, Tasevska ZG, Binder PS. Evaluation of tear protein deposits on contact lenses from patients with and without giant papillary conjunctivitis. CLAO J 1992;18(3):143-7.

93. Dunn JP, Jr., Weissman BA, Mondino BJ, Arnold AC. Giant papillary conjunctivitis associated with elevated corneal deposits. Cornea 1990;9(4):357-8.

94. Mannucci LL, Moro F, Cosani A, Palumbo M. Conformational state of lacrimal proteins adsorbed on contact lenses. Curr Eye Res 1985;4(6):734-6.

95. Allansmith MR, Korb DR, Greiner JV, Henriquez AS, Simon MA, Finnemore VM. Giant papillary conjunctivitis in contact lens wearers. Am J Ophthalmol 1977;83(5):697-708.

96. Schmid KL, Schmid LM. Ocular allergy: causes and therapeutic options. Clin Exp Optom 2000;83(5):257-270.

97. Subbaraman LN, Glasier MA, Senchyna M, Sheardown H, Jones L. Kinetics of in vitro lysozyme deposition on silicone hydrogel, PMMA, and FDA groups I, II, and IV contact lens materials. Curr Eye Res 2006;31(10):787-96.

98. Senchyna M, Jones L, Louie D, May C, Forbes I, Glasier MA. Quantitative and conformational characterization of lysozyme deposited on balafilcon and etafilcon contact lens materials. Curr Eye Res 2004;28(1):25-36.

99. Chow LM, Subbaraman LN, Sheardown H, Jones L. Kinetics of in vitro lactoferrin deposition on silicone hydrogel and FDA group II and group IV hydrogel contact lens materials. J Biomater Sci Polym Ed 2009;20(1):71-82.

100. Suwala M, Glasier MA, Subbaraman LN, Jones L. Quantity and conformation of lysozyme deposited on conventional and silicone hydrogel contact lens materials using an in vitro model. Eye Contact Lens 2007;33(3):138-43.

101. Baujard-Lamotte L, Noinville S, Goubard F, Marque P, Pauthe E. Kinetics of conformational changes of fibronectin adsorbed onto model surfaces. Colloids Surf B Biointerfaces 2008;63(1):129-37.

102. Glasier MA, Keech A, Sheardown H, Subbaraman LN, Jones L. Conformational and quantitative characterization of lysozyme extracted from galyfilcon and senofilcon silicone hydrogel contact lenses. Curr Eye Res 2008;33(1):1-11.

103. Roach P, Farrar D, Perry CC. Interpretation of protein adsorption: surface-induced conformational changes. J Am Chem Soc 2005;127(22):8168-73.

104. Thevenot P, Hu W, Tang L. Surface chemistry influences implant biocompatibility. Curr Top Med Chem 2008;8(4):270-80.

105. Green-Church KB, Nichols KK, Kleinholz NM, Zhang L, Nichols JJ. Investigation of the human tear film proteome using multiple proteomic approaches. Mol Vis 2008;14:456-70.

106. de Souza GA, Godoy LM, Mann M. Identification of 491 proteins in the tear fluid proteome reveals a large number of proteases and protease inhibitors. Genome Biol 2006;7(8):R72.

107. Fung K, Morris C, Duncan M. Mass spectrometric techniques applied to the analysis of human tears: a focus on the peptide and protein constituents. Adv Exp Med Biol 2002;506(Pt A):601-5.

108. Bright AM, Tighe BJ. The composition and interfacial properties of tears, tear substitutes and tear models. J Br Contact Lens Assoc 1993;16(2):57-66.

109. Ng V, Cho P, Mak S, Lee A. Variability of tear protein levels in normal young adults: between-day variation. Graefes Arch Clin Exp Ophthalmol 2000;238(11):892-9.

110. Sack RA, Tan KO, Tan A. Diurnal tear cycle: evidence for a nocturnal inflammatory constitutive tear fluid. Invest Ophthalmol Vis Sci 1992;33(3):626-40.

111. Fullard RJ, Snyder C. Protein levels in nonstimulated and stimulated tears of normal human subjects. Invest Ophthalmol Vis Sci 1990;31(6):1119-26.

112. Fullard RJ, Tucker DL. Changes in human tear protein levels with progressively increasing stimulus. Invest Ophthalmol Vis Sci 1991;32(8):2290-301.

113. McGill JI, Liakos GM, Goulding N, Seal DV. Normal tear protein profiles and age-related changes. Br J Ophthalmol 1984;68(5):316-20.

114. Farris RL. Tear analysis in contact lens wearers. Trans Am Ophthalmol Soc 1985;83:501-45.

115. Mandel ID, Stuchell RN. The lacrimal-salivary axis in health and disease. In: Holly FJ, Lamberts DW, MacKeen DL, editors. The preocular tear film in health, disease, and contact lens wear. Texas: Lubbock, Dry Eye Institute, Inc.; 1986. p 852-6.

116. Berman ER. Tears. Biochemistry of the eye. New York: Plenum Press; 1991. p 79-80.

117. Imoto T, Johnson LN, North AC, Phillips DC, Rupley JA. Vertebrate lysozymes. In: Boyle PD, editor. The Enzymes. New York: Academic Press; 1972. p 665-868.

118. Jones L, Franklin V, Evans K, Sariri R, Tighe B. Spoilation and clinical performance of monthly vs. three monthly Group II disposable contact lenses. Optom Vis Sci 1996;73(1):16-21.

119. Garrett Q, Garrett RW, Milthorpe BK. Lysozyme sorption in hydrogel contact lenses. Invest Ophthalmol Vis Sci 1999;40(5):897-903.

120. Garrett Q, Chatelier RC, Griesser HJ, Milthorpe BK. Effect of charged groups on the adsorption and penetration of proteins onto and into carboxymethylated poly(HEMA) hydrogels. Biomaterials 1998;19(23):2175-86.

121. Garrett Q, Laycock B, Garrett RW. Hydrogel lens monomer constituents modulate protein sorption. Invest Ophthalmol Vis Sci 2000;41(7):1687-95.

122. Bohnert JL, Horbett TA, Ratner BD, Royce FH. Adsorption of proteins from artificial tear solutions to contact lens materials. Invest Ophthalmol Vis Sci 1988;29(3):362-73.

123. Keith D, Hong B, Christensen M. A novel procedure for the extraction of protein deposits from soft hydrophilic contact lenses for analysis. Curr Eye Res 1997;16(5):503-10.

124. Brennan NA, Coles ML, Comstock TL, Levy B. A 1-year prospective clinical trial of balafilcon a (PureVision) silicone-hydrogel contact lenses used on a 30-day continuous wear schedule. Ophthalmology 2002;109(6):1172-7.

125. Baines MG, Cai F, Backman HA. Adsorption and removal of protein bound to hydrogel contact lenses. Optom Vis Sci 1990;67(11):807-10.

126. Gachon AM, Bilbaut T, Dastugue B. Adsorption of tear proteins on soft contact lenses. Exp Eye Res 1985;40(1):105-16.

127. Tripathi PC, Tripathi RC. Analysis of glycoprotein deposits on disposable soft contact lenses. Invest Ophthalmol Vis Sci 1992;33(1):121-5.

128. Castillo EJ, Koenig JL, Anderson JM, Lo J. Characterization of protein adsorption on soft contact lenses. I. Conformational changes of adsorbed human serum albumin. Biomaterials 1984;5(6):319-25.

129. Castillo EJ, Koenig JL, Anderson JM. Characterization of protein adsorption on soft contact lenses. IV. Comparison of in vivo spoilage with the in vitro adsorption of tear proteins. Biomaterials 1986;7(2):89-96.

130. Michaud L, Giasson C. Comparing the extent of protein build-up on several disposable lenses by two spectrophotometric methods. Cont Lens Anterior Eye 1998;21(4):104-8.

131. Keith DJ, Christensen MT, Barry JR, Stein JM. Determination of the lysozyme deposit curve in soft contact lenses. Eye Contact Lens 2003;29(2):79-82.

132. Moradi O, Modarress H, Noroozi M. Experimental study of albumin and lysozyme adsorption onto acrylic acid (AA) and 2-hydroxyethyl methacrylate (HEMA) surfaces. J Colloid Interface Sci 2004;271(1):16-9.

133. Garrett Q, Milthorpe BK. Human serum albumin adsorption on hydrogel contact lenses in vitro. Invest Ophthalmol Vis Sci 1996;37(13):2594-602.

134. Park JH, Bae YH. Hydrogels based on poly(ethylene oxide) and poly(tetramethylene oxide) or poly(dimethyl siloxane): synthesis, characterization, in vitro protein adsorption and platelet adhesion. Biomaterials 2002;23(8):1797-808.

135. Zhang S, Borazjani RN, Salamone JC, Ahearn DG, Crow SA, Jr., Pierce GE. In vitro deposition of lysozyme on etafilcon A and balafilcon A hydrogel contact lenses: effects on adhesion and survival of Pseudomonas aeruginosa and Staphylococcus aureus. Cont Lens Anterior Eye 2005;28(3):113-9.

136. Kingshott P, St John HA, Chatelier RC, Griesser HJ. Matrix-assisted laser desorption ionization mass spectrometry detection of proteins adsorbed in vivo onto contact lenses. J Biomed Mater Res 2000;49(1):36-42.

137. Lin ST, Mandell RB, Leahy CD, Newell JO. Protein accumulation on disposable extended wear lenses. CLAO J 1991;17(1):44-50.

138. Minno GE, Eckel L, Groemminger S, Minno B, Wrzosek T. Quantitative analysis of protein deposits on hydrophilic soft contact lenses: I. Comparison to visual methods of analysis. II. Deposit variation among FDA lens material groups. Optom Vis Sci 1991;68(11):865-72.

139. Pearce D, Tan ME, Demirci G, Willcox MD. Surface protein profile of extended-wear silicon hydrogel lenses. Adv Exp Med Biol 2002;506(Pt B):957-60.

140. Soltys-Robitaille CE, Ammon DM, Jr., Valint PL, Jr., Grobe GL, 3rd. The relationship between contact lens surface charge and in-vitro protein deposition levels. Biomaterials 2001;22(24):3257-60.

141. Bruinsma GM, Rustema-Abbing M, de Vries J, Stegenga B, van der Mei HC, van der Linden ML, Hooymans JM, Busscher HJ. Influence of wear and overwear on surface properties of etafilcon A contact lenses and adhesion of Pseudomonas aeruginosa. Invest Ophthalmol Vis Sci 2002;43(12):3646-53.

142. Vermeltfoort PB, Rustema-Abbing M, de Vries J, Bruinsma GM, Busscher HJ, van der Linden ML, Hooymans JM, van der Mei HC. Influence of day and night wear on surface properties of silicone hydrogel contact lenses and bacterial adhesion. Cornea 2006;25(5):516-23.

143. Maziarz EP, Stachowski MJ, Liu XM, Mosack L, Davis A, Musante C, Heckathorn D. Lipid deposition on silicone hydrogel lenses, part I: quantification of oleic Acid, oleic Acid methyl ester, and cholesterol. Eye Contact Lens 2006;32(6):300-7.

144. Spurr-Michaud S, Argueso P, Gipson I. Assay of mucins in human tear fluid. Exp Eye Res 2007;84(5):939-50.

145. Yan G, Nyquist G, Caldwell KD, Payor R, McCraw EC. Quantitation of total protein deposits on contact lenses by means of amino acid analysis. Invest Ophthalmol Vis Sci 1993;34(5):1804-13.

146. Santos L, Rodrigues D, Lira M, Oliveira ME, Oliveira R, Vilar EY, Azeredo J. The influence of surface treatment on hydrophobicity, protein adsorption and microbial colonisation of silicone hydrogel contact lenses. Cont Lens Anterior Eye 2007;30(3):183-8.

147. Temel A, Kazokoglu H, Taga Y. Tear lysozyme levels in contact lens wearers. Ann Ophthalmol 1991;23(5):191-4.

148. Zhou L, Beuerman RW, Foo Y, Liu S, Ang LP, Tan DT. Characterisation of human tear proteins using high-resolution mass spectrometry. Ann Acad Med Singapore 2006;35(6):400-7.

149. Sitaramamma T, Shivaji S, Rao GN. HPLC analysis of closed, open, and reflex eye tear proteins. Indian J Ophthalmol 1998;46(4):239-45.

150. Tan KO, Sack RA, Holden BA, Swarbrick HA. Temporal sequence of changes in tear film composition during sleep. Curr Eye Res 1993;12(11):1001-7.

151. Bilbaut T, Gachon AM, Dastugue B. Deposits on soft contact lenses. Electrophoresis and scanning electron microscopic examinations. Exp Eye Res 1986;43(2):153-65.

152. Scott G, Mowrey-McKee M. Dimerization of tear lysozyme on hydrophilic contact lens polymers. Curr Eye Res 1996;15(5):461-6.

153. Peters T. All about albumin : biochemistry, genetics, and medical applications. San Diego, Calif.: Academic Press; 1996.

154. Tanford C, Buzzell JG. The viscosity of aqueous solutions of bovine serum albumin between pH 4.3 and 10.5. J. Phys. Chem 1956;60:225-231.

155. Hostmark AT, Tomten SE, Berg JE. Serum albumin and blood pressure: a population-based, cross-sectional study. J Hypertens 2005;23(4):725-30.

156. Doweiko JP, Nompleggi DJ. Role of albumin in human physiology and pathophysiology. JPEN J Parenter Enteral Nutr 1991;15(2):207-11.

157. Loeb GI, Scheraga HA. Hydrodynamic and thermodynamic properties of bovine serum albumin at low pH. J. Phys. Chem 1956;60:1633-1644.

158. Squire PG, Moser P, O'Konski CT. The hydrodynamic properties of bovine serum albumin monomer and dimer. Biochemistry 1968;7(12):4261-72.

159. Carter DC, He XM. Structure of human serum albumin. Science 1990;249(4966):302-3.

160. Ferrer ML, Duchowicz R, Carrasco B, de la Torre JG, Acuna AU. The conformation of serum albumin in solution: a combined phosphorescence depolarization-hydrodynamic modeling study. Biophys J 2001;80(5):2422-30.

161. Sugio S, Kashima A, Mochizuki S, Noda M, Kobayashi K. Crystal structure of human serum albumin at 2.5 A resolution. Protein Eng 1999;12(6):439-46.

162. He XM, Carter DC. Atomic structure and chemistry of human serum albumin. Nature 1992;358(6383):209-15.

163. Michnik A, Michalik K, Drzazga Z, Kluczewska A. Comparative DSC study of human and bovine serum albumin. J. Therm. Anal. Cal. 2007;84(1):113-117.

164. Kurrat R, Prenosil JE, Ramsden JJ. Kinetics of human and bovine serum albumin adsorption at silica-titania surfaces. J Colloid Interface Sci 1997;185(1):1-8.

165. Miller I, Gemeiner M. Peculiarities in electrophoretic behavior of different serum albumins. Electrophoresis 1993;14(12):1312-7.

166. Ng V, Cho P. The relationship between total tear protein concentrations determined by different methods and standards. Graefes Arch Clin Exp Ophthalmol 2000;238(7):571-6.

167. Bjerrum KB, Prause JU. Collection and concentration of tear proteins studied by SDS gel electrophoresis. Presentation of a new method with special reference to dry eye patients. Graefes Arch Clin Exp Ophthalmol 1994;232(7):402-5.

168. van Bijsterveld OP, Janssen PT. Local antibacterial defense in the sicca syndrome. In: Holly FJ, Lamberts DW, MacKeen DL, editors. The preocular tear film in health, disease, and contact lens wear: Lubbock, Texas, Dry Eye Institute, Inc.; 1986. p 857-864.

169. Baleriola-Lucas C, Fukuda M, Willcox MD, Sweeney DF, Holden BA. Fibronectin concentration in tears of contact lens wearers. Exp Eye Res 1997;64(1):37-43.

170. van Bijsterveld OP, Janssen PT. The effect of calcium dobesilate on albumin leakage of the conjunctival vessels. Curr Eye Res 1981;1(7):425-30.

171. Lundh RL, Liotet S, Pouliquen Y. Study of the human blood-tear barrier and the biochemical changes in the tears of 30 contact lens wearers (50 eyes). Ophthalmologica 1984;188(2):100-5.

172. Carney FP, Morris CA, Willcox MD. Effect of hydrogel lens wear on the major tear proteins during extended wear. Aust N Z J Ophthalmol 1997;25 Suppl 1:S36-8.

173. Bjerrum KB. The ratio of albumin to lactoferrin in tear fluid as a diagnostic tool in primary Sjogren's syndrome. Acta Ophthalmol Scand 1997;75(5):507-11.

174. Taylor RL, Willcox MD, Williams TJ, Verran J. Modulation of bacterial adhesion to hydrogel contact lenses by albumin. Optom Vis Sci 1998;75(1):23-9.

175. Demirel G, Ozcetin G, Turan E, Caykara T. pH/temperature - sensitive imprinted ionic poly(N-tert-butylacrylamide-co-acrylamide/maleic acid) hydrogels for bovine serum albumin. Macromol Biosci 2005;5(10):1032-7.

176. Bajpai AK, Mishra DD. Adsorption of a blood protein on to hydrophilic sponges based on poly(2-hydroxyethyl methacrylate). J Mater Sci Mater Med 2004;15(5):583-92.

177. Dijt JC, Cohen Stuart MA, E. HJ, J. FG. Kinetics of polymer adsorption in stagnation point flow. Colloids and Surfaces 1990;51:141-158.

178. Carter DC, Ho JX. Structure of serum albumin. Adv Protein Chem 1994;45:153-203.

179. Sasaki Y, Suzuki Y, Ishibashi T. Fluorescent X-ray interference from a protein monolayer. Science 1994;263(5143):62-4.

180. Mura-Galelli MJ, Voegel JC, Behr S, Bres EF, Schaaf P. Adsorption/desorption of human serum albumin on hydroxyapatite: a critical analysis of the Langmuir model. Proc Natl Acad Sci U S A 1991;88(13):5557-61.

181. Ishiguro R, Yokoyama Y, Maeda H, Shimamura A, Kameyama K, Hiramatsu K. Modes of conformational changes of proteins adsorbed on a planar hydrophobic polymer surface reflecting their adsorption behaviors. J Colloid Interface Sci 2005;290(1):91-101.

182. Garrett Q, Griesser HJ, Milthorpe BK, Garrett RW. Irreversible adsorption of human serum albumin to hydrogel contact lenses: a study using electron spin resonance spectroscopy. Biomaterials 1999;20(14):1345-56.

183. Peppas NA. Hydrogels in medicine and pharmacy. Boca Raton, Fla.: CRC Press; 1986.

184. Vroman L, Adams AL, Fischer GC, Munoz PC. Interaction of high molecular weight kininogen, factor XII, and fibrinogen in plasma at interfaces. Blood 1980;55(1):156-9.

185. Mandrusov E, Yang JD, Pfeiffer N, Vroman L, Puszkin P, Leonard EF. Kinetics of protein deposition and replacement from a shear flow. AIChE Journal 1998;44(2):233-244.

186. Morrissey BW. The adsorption and conformation of plasma proteins: A physical approach. Annals of the New York Academy of Sciences 1977;283(1):50-64.

187. Missirlis YF, Lemm W. Modern aspects of protein adsorption on biomaterials. Dordrecht: Kluwer Academic Publishers; 1991. x, 262 p.

188. Park H, Park K. Biocompatibility issues of implantable drug delivery systems. Pharm Res 1996;13(12):1770-6.

189. Ratner BD. Biomaterials science: An introduction to materials in medicine. San Diego ; London: Academic Press; 1996. 193-199 p.

190. Pitt WG, Park K, Cooper SL. Sequential protein adsorption and thrombus deposition on polymeric biomaterials. Journal of Colloid and Interface Science 1986 111(2):343-362.

191. Brynda E, Houska M, Jirouskova M, Dyr JE. Albumin and heparin multilayer coatings for blood-contacting medical devices. J Biomed Mater Res 2000;51(2):249-57.

192. Pokidysheva EN, Maklakova IA, Belomestnaya ZM, Perova NV, Bagrov SN, Sevastianov VI. Comparative analysis of human serum albumin adsorption and complement activation for intraocular lenses. Artif Organs 2001;25(6):453-8.

193. Miller MJ, Wilson LA, Ahearn DG. Effects of protein, mucin, and human tears on adherence of Pseudomonas aeruginosa to hydrophilic contact lenses. J Clin Microbiol 1988;26(3):513-7.

194. Willcox M, Pearce D, Tan M, Demirci G, Carney F. Contact lenses and tear film interactions. Adv Exp Med Biol 2002;506(Pt B):879-84.

195. Lord MS, Stenzel MH, Simmons A, Milthorpe BK. The effect of charged groups on protein interactions with poly(HEMA) hydrogels. Biomaterials 2006;27(4):567-75.

196. Gachon AM, Bilbault T, Dastugue B. Protein migration through hydrogels: a tool for measuring porosity-application to hydrogels used as contact lenses. Anal Biochem 1986;157(2):249-55.

197. Tighe B. Contact Lens Materials. In: Phillips A, Speedwell L, editors. Contact Lenses. Edinburgh: Butterworth-Heinemann; 2006. p 59 - 78.

198. Barbucci R, Magnani A, Leone G. The effects of spacer arms in cross-linked hyaluronan hydrogel on Fbg and HSA adsorption and conformation. Polymer 2002;43(12):3541-3548.

199. Novick SJ, Dordick JS. Investigating the effects of polymer chemistry on activity of biocatalytic plastic materials. Biotechnol Bioeng 2000;68(6):665-71.

200. Gomez CG, Alvarez Igarzabal CI, Strumia MC. Effect of the crosslinking agent on porous networks formation of hema-based copolymers. Polymer 2004;45(18):6189-6194.

201. Kita M, Ogura Y, Honda Y, Hyon SH, Cha W, 2nd, Ikada Y. Evaluation of polyvinyl alcohol hydrogel as a soft contact lens material. Graefes Arch Clin Exp Ophthalmol 1990;228(6):533-7.

202. Kim J, Somorjai GA. Molecular packing of lysozyme, fibrinogen, and bovine serum albumin on hydrophilic and hydrophobic surfaces studied by infrared-visible sum frequency generation and fluorescence microscopy. J Am Chem Soc 2003;125(10):3150-8.

203. Abelson MB, Udell IJ, Weston JH. Normal human tear pH by direct measurement. Arch Ophthalmol 1981;99(2):301.

204. Yamada M, Mochizuki H, Kawai M, Yoshino M, Mashima Y. Fluorophotometric measurement of pH of human tears in vivo. Curr Eye Res 1997;16(5):482-6.

205. Curry S, Mandelkow H, Brick P, Franks N. Crystal structure of human serum albumin complexed with fatty acid reveals an asymmetric distribution of binding sites. Nat Struct Biol 1998;5(9):827-35.

206. Rodbard D, Chrambach A. Estimation of molecular radius, free mobility, and valence using polyacylamide gel electrophoresis. Anal Biochem 1971;40(1):95-134.

207. Wood JM, Attwood D, Collett JH. Characterization of poly(2-hydroxyethyl methacrylate) gels. Drug Dev Ind Pharm 1983;9(1-2):93-101.

208. Gatin E, Alexandreanu D, Popescu A, Berlic C, Alexandreanu I. Correlations between permeability properties and the pore - size distribution of the porous media "hydron" useful as contact lenses. Phusica Medica 1999;XVI(1):13-9.

209. Luensmann D, Glasier MA, Zhang F, Bantseev V, Simpson T, Jones L. Confocal microscopy and albumin penetration into contact lenses. Optom Vis Sci 2007;84(9):839-47.

210. Rudko P, Proby JA. A method for classifying and describing protein deposition on hydrophilic lenses. Allergan pharmaceutical report 1974;Series 94.

211. Myers RI, Larsen DW, Tsao M, Castellano C, Becherer LD, Fontana F, Ghormley NR, Meier G. Quantity of protein deposited on hydrogel contact lenses and its relation to visible protein deposits. Optom Vis Sci 1991;68(10):776-82.

212. Subbaraman LN, Glasier MA, Sheardown H, Jones L. Efficacy of an extraction solvent used to quantify albumin deposition on hydrogel contact lens materials. Eye Contact Lens 2009;35(2):76-80.

213. Zhao Z, Wei X, Aliwarga Y, Carnt NA, Garrett Q, Willcox MD. Proteomic analysis of protein deposits on worn daily wear silicone hydrogel contact lenses. Mol Vis 2008;14:2016-24.

214. Ratner BD, Horbett TA, Mateo NB. Contact lens spoilation - part 1: Biochemical aspect of lens spoilation. In: Ruben M, Guillon M, editors. Contact Lens Practice. London: Chapman & Hall; 1994. p 1083-98.

215. Miller B. Observations of deposits on soft contact lenses by different methods of light microscopy, scanning microscopy, and electron microprobe analysis. Int. Contact Lens Clin. 1980;3-4:22-35.

216. Tripathi RC, Tripathi BJ, Ruben M. The pathology of soft contact lens spoilage. Ophthalmology 1980;87(5):365-80.

217. Versura P, Maltarello MC, Roomans GM, Caramazza R, Laschi R. Scanning electron microscopy, X-ray microanalysis and immunohistochemistry on worn soft contact lenses. Scanning Microsc 1988;2(1):397-410.

218. Braga PC, Ricci D. Atomic force microscopy: biomedical methods and applications. Totowa: Humana Press; 2004. 1-394 p.

219. Teichroeb JH, Forrest JA, Ngai V, Martin JW, Jones L, Medley J. Imaging protein deposits on contact lens materials. Optom Vis Sci 2008;85(12):1151-64.

220. Santos L, Rodrigues D, Lira M, Real Oliveira ME, Oliveira R, Vilar EY, Azeredo J. Bacterial adhesion to worn silicone hydrogel contact lenses. Optom Vis Sci 2008;85(7):520-5.

221. Lira M, Santos L, Azeredo J, Yebra-Pimentel E, Oliveira ME. Comparative study of silicone-hydrogel contact lenses surfaces before and after wear using atomic force microscopy. J Biomed Mater Res B Appl Biomater 2008;85(2):361-7.

222. Rebeix V, Sommer F, Marchin B, Baude D, Tran MD. Artificial tear adsorption on soft contact lenses: methods to test surfactant efficacy. Biomaterials 2000;21(12):1197-205.

223. Jones L, Evans K, Sariri R, Franklin V, Tighe B. Lipid and protein deposition of N-vinyl pyrrolidone-containing group II and group IV frequent replacement contact lenses. CLAO J 1997;23(2):122-6.

224. Hart DE, DePaolis M, Ratner BD, Mateo NB. Surface analysis of hydrogel contact lenses by ESCA. CLAO J 1993;19(3):169-73.

225. Holmberg M, Hou X. Competitive protein adsorption - multilayer adsorption and surface induced protein aggregation. Langmuir 2009;25(4):2081-89.

226. Patel DV, McGhee CN. Contemporary in vivo confocal microscopy of the living human cornea using white light and laser scanning techniques: a major review. Clin Experiment Ophthalmol 2007;35(1):71-88.

227. Minsky M. Memoir on inventing the confocal scanning microscope. Scanning 1988;10:128-38.

228. Efron N. Contact lens-induced changes in the anterior eye as observed in vivo with the confocal microscope. Prog Retin Eye Res 2007;26(4):398-436.

229. Petran M, Hadravsky M. Tandem-scanning reflected-light microscope. Optical Society of America 1968;58(5):661-664.

230. Bohnke M, Masters BR. Confocal microscopy of the cornea. Prog Retin Eye Res 1999;18(5):553-628.

231. Svishchev GM. Microscope for the study of transparent light-scattering objects in incident light. OSA 1969;26:171-2.

232. Masters BR, Thaer AA. Real-time scanning slit confocal microscopy of the in vivo human cornea. Appl Opt 1994;33(4):695-701.

233. Masters BR, Bohnke M. Confocal microscopy of the human cornea in vivo. Int Ophthalmol 2001;23(4-6):199-206.

234. Masters BR, Bohnke M. Three-dimensional confocal microscopy of the living human eye. Annu Rev Biomed Eng 2002;4:69-91.

235. Winburn DC. Practical Laser Safety. New York: Marcel Dekker; 1990. 13-46 p.

236. Stricker SA, Whitaker M. Confocal laser scanning microscopy of calcium dynamics in living cells. Microsc Res Tech 1999;46(6):356-69.

237. Foldes-Papp Z, Demel U, Tilz GP. Laser scanning confocal fluorescence microscopy: an overview. Int Immunopharmacol 2003;3(13-14):1715-29.

238. Pygall SR, Whetstone J, Timmins P, Melia CD. Pharmaceutical applications of confocal laser scanning microscopy: the physical characterisation of pharmaceutical systems. Adv Drug Deliv Rev 2007;59(14):1434-52.

239. Linden T, Ljunglof A, Kula MR, Thommes J. Visualizing two-component protein diffusion in porous adsorbents by confocal scanning laser microscopy. Biotechnol Bioeng 1999;65(6):622-30.

240. Hoffmann K, Mix R, Resch-Genger U, Friedrich JF. Monitoring of amino functionalities on plasma-chemically modified polypropylene supports with a chromogenic and fluorogenic pyrylium reporter. Langmuir 2007;23(16):8411-6.

241. Hubbuch J, Kula MR. Confocal laser scanning microscopy as an analytical tool in chromatographic research. Bioprocess Biosyst Eng 2008.

242. Tata B, Raj B. Confocal laser scanning microscopy: Applications in material science and technology. Bulletin of Materials Science 1998;21(4):263-78.

243. Guilbault G. General aspects of luminescence spectroscopy. In: Guilbault G, editor. Practical fluorescence. New York: Dekker, M; 1990. p 1-40.

244. Stewart WW; Aminoaphthalimide dyes for intracellular labelling. 1984.

245. Stewart WW. Lucifer dyes-highly fluorescent dyes for biological tracing. Nature 1981;292(5818):17-21.

246. Fine J, Seligman AM. Traumatic shock. Vii. A study of the problem of the "lost plasma" in hemorrhagic, tourniquet, and burn shock by the use of radioactive iodo-plasma protein. J Clin Invest 1944;23(5):720-30.

247. Regoeczi E. Chemistry and isotopes of iodine. Iodine-labeled plasma proteins. Boca Raton, Fla.: CRC Press; 1984. p 9-33.

248. Regoeczi E. Methods of protein iodination. Iodine-labeled plasma proteins. Boca Raton, Fla.: CRC Press; 1984. p 35-102.

249. McFarlane AS. Efficient trace-labelling of proteins with iodine. Nature 1958;182(4627):53.

250. Helmkamp RW, Goodland RL, Bale WF, Spar IL, Mutschler LE. High specific activity iodination of gamma-globulin with iodine-131 monochloride. Cancer Res 1960;20:1495-1500.

251. Li CH. Iodination of tyrosine groups in serum albumin and pepsin. J Am Chem Soc 1945;67(7):1065-9.

252. Crandall RE, Janatova J, Andrade JD. The effects of radioiodination and fluorescent labelling on albumin. Prep Biochem 1981;11(2):111-38.

253. Horbett TA. Adsorption of proteins from plasma to a series of hydrophilic-hydrophobic copolymers. II. Compositional analysis with the prelabeled protein technique. J Biomed Mater Res 1981;15(5):673-95.

254. Grant WH, Smith LE, Stromberg RR. Radiotracer techniques for protein adsorption measurements. J Biomed Mater Res 1977;11(1):33-8.

References - Chapter 2

1. Dunn JP, Jr., Weissman BA, Mondino BJ, Arnold AC. Giant papillary conjunctivitis associated with elevated corneal deposits. Cornea 1990;9(4):357-8.

2. Skotnitsky C, Sankaridurg PR, Sweeney DF, Holden BA. General and local contact lens induced papillary conjunctivitis (CLPC). Clin Exp Optom 2002;85(3):193-7.

3. Skotnitsky CC, Naduvilath TJ, Sweeney DF, Sankaridurg PR. Two presentations of contact lens-induced papillary conjunctivitis (CLPC) in hydrogel lens wear: local and general. Optom Vis Sci 2006;83(1):27-36.

4. Richard NR, Anderson JA, Tasevska ZG, Binder PS. Evaluation of tear protein deposits on contact lenses from patients with and without giant papillary conjunctivitis. CLAO J 1992;18(3):143-7.

5. Solomon OD, Freeman MI, Boshnick EL, Cannon WM, Dubow BW, Kame RT, Lanier JC, Jr., Lopanik RW, Quinn TG, Rigel LE and others. A 3-year prospective study of the clinical performance of daily disposable contact lenses compared with frequent replacement and conventional daily wear contact lenses. CLAO J 1996;22(4):250-7.

6. Nason RJ, Boshnick EL, Cannon WM, Dubow BW, Freeman MI, Kame RT, Lanier JC, Jr., Lopanik RW, Quinn TG, Jr., Rigel LE and others. Multisite comparison of contact lens modalities. Daily disposable wear vs. conventional daily wear in successful contact lens wearers. J Am Optom Assoc 1994;65(11):774-80.

7. Donshik PC. Contact lens chemistry and giant papillary conjunctivitis. Eye Contact Lens 2003;29(1 Suppl):S37-9; discussion S57-9, S192-4.

8. Minno GE, Eckel L, Groemminger S, Minno B, Wrzosek T. Quantitative analysis of protein deposits on hydrophilic soft contact lenses: I. Comparison to visual methods of analysis. II. Deposit variation among FDA lens material groups. Optom Vis Sci 1991;68(11):865-72.

9. Jones L, Senchyna M, Glasier MA, Schickler J, Forbes I, Louie D, May C. Lysozyme and lipid deposition on silicone hydrogel contact lens materials. Eye Contact Lens 2003;29(1 Suppl):75-9.

10. Senchyna M, Jones L, Louie D, May C, Forbes I, Glasier MA. Quantitative and conformational characterization of lysozyme deposited on balafilcon and etafilcon contact lens materials. Curr Eye Res 2004;28(1):25-36.

11. Subbaraman LN, Bayer S, Gepr S, Glasier MA, Lorentz H, Senchyna M, Jones L. Rewetting drops containing surface active agents improve the clinical performance of silicone hydrogel contact lenses. Optom Vis Sci 2006;83(3):143-51.

12. Subbaraman LN, Glasier MA, Senchyna M, Jones L. Stabilization of lysozyme mass extracted from lotrafilcon silicone hydrogel contact lenses. Optom Vis Sci 2005;82(3):209-14.

13. Bright AM, Tighe BJ. The composition and interfacial properties of tears, tear substitutes and tear models. Journal of the British Contact Lens Association 1993;16(2):57-66.

14. Ng V, Cho P, Mak S, Lee A. Variability of tear protein levels in normal young adults: between-day variation. Graefes Arch Clin Exp Ophthalmol 2000;238(11):892-9.

15. Choy CK, Cho P, Benzie IF, Ng V. Effect of one overnight wear of orthokeratology lenses on tear composition. Optom Vis Sci 2004;81(6):414-20.

16. Bohnert JL, Horbett TA, Ratner BD, Royce FH. Adsorption of proteins from artificial tear solutions to contact lens materials. Invest Ophthalmol Vis Sci 1988;29(3):362-73.

17. Garrett Q, Chatelier RC, Griesser HJ, Milthorpe BK. Effect of charged groups on the adsorption and penetration of proteins onto and into carboxymethylated poly(HEMA) hydrogels. Biomaterials 1998;19(23):2175-86.

18. Garrett Q, Laycock B, Garrett RW. Hydrogel lens monomer constituents modulate protein sorption. Invest Ophthalmol Vis Sci 2000;41(7):1687-95.

19. Soltys-Robitaille CE, Ammon DM, Jr., Valint PL, Jr., Grobe GL, 3rd. The relationship between contact lens surface charge and in-vitro protein deposition levels. Biomaterials 2001;22(24):3257-60.

20. Garrett Q, Garrett RW, Milthorpe BK. Lysozyme sorption in hydrogel contact lenses. Invest Ophthalmol Vis Sci 1999;40(5):897-903.

21. Vermeltfoort PB, Rustema-Abbing M, de Vries J, Bruinsma GM, Busscher HJ, van der Linden ML, Hooymans JM, van der Mei HC. Influence of day and night wear on surface properties of silicone hydrogel contact lenses and bacterial adhesion. Cornea 2006;25(5):516-23.

22. Brennan NA, Coles ML. Deposits and symptomatology with soft contact lens wear. Int Contact Lens Clin 2000;27:75-100.

23. Jones L. A review of techniques for analysing hydrogel lens deposition. J Brit Contact Lens Assoc 1990;13(Trans Ann Clin Conf):36-40.

24. Ratner BD, Horbett TA, Mateo NB. Contact lens spoilation - part 1: Biochemical aspect of lens spoilation. In: Ruben M, Guillon M, editors. Contact Lens Practice. London: Chapman & Hall; 1994. p 1083-98.

25. Tripathi RC, Tripathi BJ, Ruben M. The pathology of soft contact lens spoilage. Ophthalmology 1980;87(5):365-80.

26. Peters T, JR. All about Albumin: biochemistry, genetics, and medical applications: Academic Press, INC; 1996. 432 p.

27. Bingaman S, Huxley VH, Rumbaut RE. Fluorescent dyes modify properties of proteins used in microvascular research. Microcirculation 2003;10(2):221-31.

28. Szewczyk B, Bienkowska-Szewczyk K, LM K. Use of different fluorochromes for monitoring protein elution and transfer. Electrophoresis 1987;8(1):25-28.

29. Lin LI. A concordance correlation coefficient to evaluate reproducibility. Biometrics 1989;45(1):255-68.

30. Peppas NA. Hydrogels in medicine and pharmacy. Boca Raton, Fla.: CRC Press; 1986.

31. Peppas NA, Huang Y, Torres-Lugo M, Ward JH, Zhang J. Physicochemical foundations and structural design of hydrogels in medicine and biology. Annu Rev Biomed Eng 2000;2:9-29.

32. Ratner BD. Biomaterials science: An introduction to materials in medicine. San Diego ; London: Academic Press; 1996. 193-199 p.

33. Pitt WG, Park K, Cooper SL. Sequential protein adsorption and thrombus deposition on polymeric biomaterials. Journal of Colloid and Interface Science 1986 111(2):343-362.

34. Taylor RL, Willcox MD, Williams TJ, Verran J. Modulation of bacterial adhesion to hydrogel contact lenses by albumin. Optom Vis Sci 1998;75(1):23-9.

35. Miller MJ, Wilson LA, Ahearn DG. Effects of protein, mucin, and human tears on adherence of Pseudomonas aeruginosa to hydrophilic contact lenses. J Clin Microbiol 1988;26(3):513-7.

36. Bruinsma GM, Rustema-Abbing M, de Vries J, Stegenga B, van der Mei HC, van der Linden ML, Hooymans JM, Busscher HJ. Influence of wear and overwear on surface properties of etafilcon A contact lenses and adhesion of Pseudomonas aeruginosa. Invest Ophthalmol Vis Sci 2002;43(12):3646-53.

37. Refojo MF, Leong FL. Microscopic determination of the penetration of proteins and polysaccharides into poly(hydroxyethyl methacrylate) and similar hydrogels. Journal of Polymer Science: Polymer Symposium 1979;66:227-237.

38. Okada E, Matsuda T, Yokoyama T, Okuda K. Lysozyme penetration in Group IV soft contact lenses. Eye Contact Lens 2006;32(4):174-7.

39. Bohnke M, Masters BR. Confocal microscopy of the cornea. Prog Retin Eye Res 1999;18(5):553-628.

40. Cavanagh HD, Jester JV, Essepian J, Shields W, Lemp MA. Confocal microscopy of the living eye. CLAO J 1990;16(1):65-73.

41. Jalbert I, Stapleton F, Papas E, Sweeney DF, Coroneo M. In vivo confocal microscopy of the human cornea. Br J Ophthalmol 2003;87(2):225-36.

42. Masters BR, Bohnke M. Confocal microscopy of the human cornea in vivo. Int Ophthalmol 2001;23(4-6):199-206.

43. Petroll WM, Jester JV, Cavanagh HD. In vivo confocal imaging. Int Rev Exp Pathol 1996;36:93-129.

44. Shuman H, Murray JM, DiLullo C. Confocal microscopy: an overview. Biotechniques 1989;7(2):154-63.

45. Meadows DL, Paugh JR. Use of confocal microscopy to determine matrix and surface protein deposition profiles in hydrogel contact lenses. CLAO J 1994;20(4):237-41.

46. Baines MG, Cai F, Backman HA. Adsorption and removal of protein bound to hydrogel contact lenses. Optom Vis Sci 1990;67(11):807-10.

47. Gachon AM, Bilbault T, Dastugue B. Protein migration through hydrogels: a tool for measuring porosity-application to hydrogels used as contact lenses. Anal Biochem 1986;157(2):249-55.

48. Gatin E, Alexandreanu D, Popescu A, Berlic C, Alexandreanu I. Correlations between permeability properties and the pore - size distribution of the porous media "hydron" useful as contact lenses. Phusica Medica 1999;XVI(1):13-9.

49. Benchaib M, Delorme R, Pluvinage M, Bryon PA, Souchier C. Evaluation of five green fluorescence-emitting streptavidin-conjugated fluorochromes for use in immunofluorescence microscopy. Histochem Cell Biol 1996;106(2):253-6.

1. Valeur B. Introduction. In: Valeur B, editor. Molecular fluorescence: principles and applications. Weinheim ; Toronto: Wiley-VCH; 2002. p 3-19.

2. Guilbault G. General aspects of luminescence spectroscopy. In: Guilbault G, editor. Practical fluorescence. New York: Dekker, M; 1990. p 1-40.

3. Pygall SR, Whetstone J, Timmins P, Melia CD. Pharmaceutical applications of confocal laser scanning microscopy: the physical characterisation of pharmaceutical systems. Adv Drug Deliv Rev 2007;59(14):1434-52.

4. Davidson RS, Hilchenbach MM. The use of fluorescent probes in immunochemistry. Photochem Photobiol 1990;52(2):431-8.

5. Hawe A, Sutter M, Jiskoot W. Extrinsic fluorescent dyes as tools for protein characterization. Pharm Res 2008;25(7):1487-99.

6. Demchenko AP. Spectroscopic properties of protein chromophores. In: Demchenko AP, editor. Ultraviolet spectroscopy of proteins. Berlin ; New York: Springer-Verlag; 1986. p 5-26.

7. Brinkley M. A brief survey of methods for preparing protein conjugates with dyes, haptens, and cross-linking reagents. Bioconjug Chem 1992;3(1):2-13.

8. Haugland RP. Invitrogen: A Guide to Fluorescent Probes and Labeling Technologies. Eugene, OR: Molecular Probes; 2005. 1126 p.

9. Bingaman S, Huxley VH, Rumbaut RE. Fluorescent dyes modify properties of proteins used in microvascular research. Microcirculation 2003;10(2):221-31.

10. Crandall RE, Janatova J, Andrade JD. The effects of radioiodination and fluorescent labelling on albumin. Prep Biochem 1981;11(2):111-38.

11. McDonagh PF, Williams SK. The preparation and use of fluorescent-protein conjugates for microvascular research. Microvasc Res 1984;27(1):14-27.

12. Szewczyk B, Bienkowska-Szewczyk K, LM K. Use of different fluorochromes for monitoring protein elution and transfer. Electrophoresis 1987;8(1):25-28.

13. Teske CA, von Lieres E, Schroder M, Ladiwala A, Cramer SM, Hubbuch JJ. Competitive adsorption of labeled and native protein in confocal laser scanning microscopy. Biotechnol Bioeng 2006;95(1):58-66.

14. Teske CA, Simon R, Niebisch A, Hubbuch J. Changes in retention behavior of fluorescently labeled proteins during ion-exchange chromatography caused by different protein surface labeling positions. Biotechnol Bioeng 2007;98(1):193-200.

15. Teske CA, Schroeder M, Simon R, Hubbuch J. Protein-labeling effects in confocal laser scanning microscopy. J Phys Chem B 2005;109(28):13811-7.

16. Rumbaut RE, Harris NR, Sial AJ, Huxley VH, Granger DN. Leakage responses to L-NAME differ with the fluorescent dye used to label albumin. Am J Physiol 1999;276(1 Pt 2):H333-9.

17. Harris NR, Whitt SP, Zilberberg J, Alexander JS, Rumbaut RE. Extravascular transport of fluorescently labeled albumins in the rat mesentery. Microcirculation 2002;9(3):177-87.

18. Tata B, Raj B. Confocal laser scanning microscopy: Applications in material science and technology. Bulletin of Materials Science 1998;21(4):263-78.

19. Hubbuch J, Kula MR. Confocal laser scanning microscopy as an analytical tool in chromatographic research. Bioprocess Biosyst Eng 2008.

20. Peters T, Jr. Serum Albumin. In: Anfinsen CB, Edsall JT, Richards FM, editors. Advances in protein chemistry. Toronto: Academic press, INC.; 1985. p 161-245.

21. Luensmann D, Glasier MA, Zhang F, Bantseev V, Simpson T, Jones L. Confocal microscopy and albumin penetration into contact lenses. Optom Vis Sci 2007;84(9):839-47.

22. Luensmann D, Zhang F, Subbaraman LN, Sheardown H, Jones L. Localization of lysozyme sorption to conventional and silicone hydrogel contact lenses using confocal microscopy. Curr Eye Res 2009;34:683-697.

23. Sack RA, Tan KO, Tan A. Diurnal tear cycle: evidence for a nocturnal inflammatory constitutive tear fluid. Invest Ophthalmol Vis Sci 1992;33(3):626-40.

24. Choy CK, Cho P, Benzie IF, Ng V. Effect of one overnight wear of orthokeratology lenses on tear composition. Optom Vis Sci 2004;81(6):414-20.

25. Horbett TA, Weathersby PK. Adsorption of proteins from plasma to a series of hydrophilic-hydrophobic copolymers. I. Analysis with the in situ radioiodination technique. J Biomed Mater Res 1981;15(3):403-23.

26. Ceska M, Sjodin AV, Grossmuller F. Some quantitative aspects of the labelling of proteins with 125 I by the iodine monochloride method. Biochem J 1971;121(1):139-43.

27. Uniyal S, Brash JL. Patterns of adsorption of proteins from human plasma onto foreign surfaces. Thromb Haemost 1982;47(3):285-90.

28. Teichroeb JH, Forrest JA, Ngai V, Martin JW, Jones L, Medley J. Imaging protein deposits on contact lens materials. Optom Vis Sci 2008;85(12):1151-64.

29. Nicolson PC, Baron RC, Chabrecek P, Court J, Domschke A, Griesser HJ, et.al.; Extended wear ophthalmic lens. US Patent No. 5760100, 1998.

30. Grobe GL, Kunzler J, Seelye D, Salamone J. Silicone hydrogels for contact lens applications. Polym. Mater. Sci. Eng. 1999;80:108-9.

31. Lopez-Alemany A, Compan V, Refojo MF. Porous structure of Purevision versus Focus Night&Day and conventional hydrogel contact lenses. J Biomed Mater Res 2002;63(3):319-25.

32. McCabe KP, Molock FF, Hill GA, Alli A, Steffen RB, Vanderlaan DG, Ford JD; Biomedical devices containing internal wetting agents patent USP 20050154080. 2005.

33. Bohnke M, Masters BR. Confocal microscopy of the cornea. Prog Retin Eye Res 1999;18(5):553-628.

34. Semwogerere D, Weeks ER. Confocal microscopy. In: Bowlin GL, Wnek GE, editors. Encyclopedia of biomaterials and biomedical engineering. Georgia, Atlanta: Informa Healthcare USA; 2005. p 1-10.

35. Righetti PG, Verzola B. Folding/unfolding/refolding of proteins: present methodologies in comparison with capillary zone electrophoresis. Electrophoresis 2001;22(12):2359-74.

36. Cardamone M, Puri NK. Spectrofluorimetric assessment of the surface hydrophobicity of proteins. Biochem J 1992;282 (Pt 2):589-93.

37. Lindgren M, Sorgjerd K, Hammarstrom P. Detection and characterization of aggregates, prefibrillar amyloidogenic oligomers, and protofibrils using fluorescence spectroscopy. Biophys J 2005;88(6):4200-12.

38. Anraku M, Yamasaki K, Maruyama T, Kragh-Hansen U, Otagiri M. Effect of oxidative stress on the structure and function of human serum albumin. Pharm Res 2001;18(5):632-9.

39. De S, Girigoswami A, Das S. Fluorescence probing of albumin-surfactant interaction. J Colloid Interface Sci 2005;285(2):562-73.

40. Hoffmann K, Mix R, Resch-Genger U, Friedrich JF. Fluorescence measurements on functionalized polymer surfaces--problems and troubleshooting. Ann N Y Acad Sci 2008;1130:28-34.

41. Hoffmann K, Mix R, Resch-Genger U, Friedrich JF. Monitoring of amino functionalities on plasma-chemically modified polypropylene supports with a chromogenic and fluorogenic pyrylium reporter. Langmuir 2007;23(16):8411-6.

42. Resch-Genger U, Hoffmann K, Hoffmann A. Standardization of fluorescence measurements: criteria for the choice of suitable standards and approaches to fit-for-purpose calibration tools. Ann N Y Acad Sci 2008;1130:35-43.

43. Wischke C, Borchert HH. Fluorescein isothiocyanate labelled bovine serum albumin (FITC-BSA) as a model protein drug: opportunities and drawbacks. Pharmazie 2006;61(9):770-4.

44. Blakeslee D, Baines MG. Immunofluorescence using dichlorotriazinylaminofluorescein (DTAF). I. Preparation and fractionation of labelled IgG. J Immunol Methods 1976;13(3-4):305-20.

45. Banks PR, Paquette DM. Comparison of three common amine reactive fluorescent probes used for conjugation to biomolecules by capillary zone electrophoresis. Bioconjug Chem 1995;6(4):447-58.

46. Avrameas S, Ternynck T, Guesdon JL. Coupling of enzymes to antibodies and antigens. Scand J Immunol 1978;8(Suppl. 7):7-23.

47. Schnaible V, Przybylski M. Identification of fluorescein-5'-isothiocyanate-modification sites in proteins by electrospray-ionization mass spectrometry. Bioconjug Chem 1999;10(5):861-6.

48. Rumbaut RE, Sial AJ. Differential phototoxicity of fluorescent dye-labeled albumin conjugates. Microcirculation 1999;6(3):205-13.

49. Grunwaldt G, Haebel S, Spitz C, Steup M, Menzel R. Multiple binding sites of fluorescein isothiocyanate moieties on myoglobin: photophysical heterogeneity as revealed by ground- and excited-state spectroscopy. J Photochem Photobiol B 2002;67(3):177-86.

50. Stewart WW. Lucifer dyes-highly fluorescent dyes for biological tracing. Nature 1981;292(5818):17-21.

51. Stewart WW; Aminoaphthalimide dyes for intracellular labelling. 1984.

52. Masri MS, Friedman M. Protein reactions with methyl and ethyl vinyl sulfones. J Protein Chem 1988;7(1):49-54.

53. Lowe KM, McCarty RE. Asymmetry of the alpha subunit of the chloroplast ATP synthase as probed by the binding of Lucifer Yellow vinyl sulfone. Biochemistry 1998;37(8):2507-14.

54. Bailey MP, Rocks BF, Riley C. Use of Lucifer yellow VS as a label in fluorescent immunoassays illustrated by the determination of albumin in serum. Ann Clin Biochem 1983;20 (Pt 4):213-6.

55. Wortberg M, Orban M, Renneberg R, Cammann K. Fluorimetric immunosensors. In: Kress-Rogers E, editor. Handbook of biosensors and electronic noses : medicine, food, and the environment. Boca Raton: CRC Press; 1997. p 369-408.

56. Tung C-H, Weissleder R. Cell-penetrating peptide conjugations and magnetic cell labels. In: Langel Ü, editor. Cell-penetrating peptides: Processes and applications. Boca Raton: CRC PRESS; 2002. p 327-46.

57. Peters T. All about albumin: biochemistry, genetics, and medical applications. San Diego, Calif.: Academic Press; 1996.

58. Oettl K, Stauber RE. Physiological and pathological changes in the redox state of human serum albumin critically influence its binding properties. Br J Pharmacol 2007;151(5):580-90.

59. Gonzalez-Meijome JM, Lopez-Alemany A, Almeida JB, Parafita MA, Refojo MF. Microscopic observations of superficial ultrastructure of unworn siloxane-hydrogel contact lenses by cryo-scanning electron microscopy. J Biomed Mater Res B Appl Biomater 2006;76(2):419-23.

60. Gonzalez-Meijome JM, Lopez-Alemany A, Almeida JB, Parafita MA, Refojo MF. Microscopic observation of unworn siloxane-hydrogel soft contact lenses by atomic force microscopy. J Biomed Mater Res B Appl Biomater 2006;76(2):412-8.

61. Linden T, Ljunglof A, Kula MR, Thommes J. Visualizing two-component protein diffusion in porous adsorbents by confocal scanning laser microscopy. Biotechnol Bioeng 1999;65(6):622-30.

References - Chapter 5

1. Ratner BD, Horbett TA, Mateo NB. Contact lens spoilation - part 1: Biochemical aspect of lens spoilation. In: Ruben M, Guillon M, editors. Contact Lens Practice. London: Chapman & Hall; 1994. p 1083-98.

2. Hart DE, DePaolis M, Ratner BD, Mateo NB. Surface analysis of hydrogel contact lenses by ESCA. CLAO J 1993;19(3):169-73.

3. Brennan NA, Coles ML. Deposits and symptomatology with soft contact lens wear. Int Contact Lens Clin 2000;27(3):75-100.

4. Jones L, Franklin V, Evans K, Sariri R, Tighe B. Spoilation and clinical performance of monthly vs. three monthly Group II disposable contact lenses. Optom Vis Sci 1996;73(1):16-21.

5. Pritchard N, Fonn D, Weed K. Ocular and subjective responses to frequent replacement of daily wear soft contact lenses. CLAO J 1996;22(1):53-9.

6. Gellatly KW, Brennan NA, Efron N. Visual decrement with deposit accumulation of HEMA contact lenses. Am J Optom Physiol Opt 1988;65(12):937-41.

7. Jones L, Mann A, Evans K, Franklin V, Tighe B. An in vivo comparison of the kinetics of protein and lipid deposition on group II and group IV frequent-replacement contact lenses. Optom Vis Sci 2000;77(10):503-10.

8. Keith DJ, Christensen MT, Barry JR, Stein JM. Determination of the lysozyme deposit curve in soft contact lenses. Eye Contact Lens 2003;29(2):79-82.

9. Nason RJ, Vogel H, Tarbell BJ, Yi FP, Mertz GW. A clinical evaluation of frequent replacement contact lenses on patients currently wearing premium reusable daily wear soft contact lenses. J Am Optom Assoc 1993;64(3):188-95.

10. Vermeltfoort PB, Rustema-Abbing M, de Vries J, Bruinsma GM, Busscher HJ, van der Linden ML, Hooymans JM, van der Mei HC. Influence of day and night wear on surface properties of silicone hydrogel contact lenses and bacterial adhesion. Cornea 2006;25(5):516-23.

11. Santos L, Rodrigues D, Lira M, Real Oliveira ME, Oliveira R, Vilar EY, Azeredo J. Bacterial adhesion to worn silicone hydrogel contact lenses. Optom Vis Sci 2008;85(7):520-5.

12. Donshik PC, Ehlers WH, Ballow M. Giant papillary conjunctivitis. Immunol Allergy Clin North Am 2008;28(1):83-103.

13. Jones L, Dumbleton K. Soft lens extended wear and complications. In: Hom MM, Bruce A, editors. Manual of contact lens prescribing and fitting. Oxford: Butterworth-Heinemann; 2006. p 393-441.

14. Donshik PC. Contact lens chemistry and giant papillary conjunctivitis. Eye Contact Lens 2003;29(1 Suppl):37-39.

15. Bohnert JL, Horbett TA, Ratner BD, Royce FH. Adsorption of proteins from artificial tear solutions to contact lens materials. Invest Ophthalmol Vis Sci 1988;29(3):362-73.

16. Jones L, Evans K, Sariri R, Franklin V, Tighe B. Lipid and protein deposition of N-vinyl pyrrolidone-containing group II and group IV frequent replacement contact lenses. CLAO J 1997;23(2):122-6.

17. Tripathi PC, Tripathi RC. Analysis of glycoprotein deposits on disposable soft contact lenses. Invest Ophthalmol Vis Sci 1992;33(1):121-5.

18. Castillo EJ, Koenig JL, Anderson JM. Characterization of protein adsorption on soft contact lenses. IV. Comparison of in vivo spoilage with the in vitro adsorption of tear proteins. Biomaterials 1986;7(2):89-96.

19. Garrett Q, Chatelier RC, Griesser HJ, Milthorpe BK. Effect of charged groups on the adsorption and penetration of proteins onto and into carboxymethylated poly(HEMA) hydrogels. Biomaterials 1998;19(23):2175-86.

20. Garrett Q, Laycock B, Garrett RW. Hydrogel lens monomer constituents modulate protein sorption. Invest Ophthalmol Vis Sci 2000;41(7):1687-95.

21. Zhang S, Borazjani RN, Salamone JC, Ahearn DG, Crow SA, Jr., Pierce GE. In vitro deposition of lysozyme on etafilcon A and balafilcon A hydrogel contact lenses: effects on adhesion and survival of Pseudomonas aeruginosa and Staphylococcus aureus. Cont Lens Anterior Eye 2005;28(3):113-9.

22. Subbaraman LN, Glasier MA, Senchyna M, Sheardown H, Jones L. Kinetics of in vitro lysozyme deposition on silicone hydrogel, PMMA, and FDA groups I, II, and IV contact lens materials. Curr Eye Res 2006;31(10):787-96.

23. Jones L, Senchyna M, Glasier MA, Schickler J, Forbes I, Louie D, May C. Lysozyme and lipid deposition on silicone hydrogel contact lens materials. Eye Contact Lens 2003;29(1 Suppl):75-9.

24. Suwala M, Glasier MA, Subbaraman LN, Jones L. Quantity and conformation of lysozyme deposited on conventional and silicone hydrogel contact lens materials using an in vitro model. Eye Contact Lens 2007;33(3):138-43.

25. Green-Church KB, Nichols JJ. Mass spectrometry-based proteomic analyses of contact lens deposition. Mol Vis 2008;14(8):291-7.

26. Merindano MD, Canals M, Saona C, Potau J, Costa J. Observation of deposits on disposable contact lenses by bio-, light and scanning electron microscopy. Cont Lens Anterior Eye 1998;21(2):55-9.

27. Miller B. Observations of deposits on soft contact lenses by different methods of light microscopy, scanning microscopy, and electron microprobe analysis. Int. Contact Lens Clin. 1980;3-4:22-35.

28. Versura P, Maltarello MC, Roomans GM, Caramazza R, Laschi R. Scanning electron microscopy, X-ray microanalysis and immunohistochemistry on worn soft contact lenses. Scanning Microsc 1988;2(1):397-410.

29. Krcova Z. Image analysis of contact lens visible deposits, haze, and mechanical defects. Int. Contact Lens Clin. 1995;22:23-31.

30. Bohnke M, Masters BR. Confocal microscopy of the cornea. Prog Retin Eye Res 1999;18(5):553-628.

31. Tata B, Raj B. Confocal laser scanning microscopy: Applications in material science and technology. Bulletin of Materials Science 1998;21(4):263-78.

32. Pygall SR, Whetstone J, Timmins P, Melia CD. Pharmaceutical applications of confocal laser scanning microscopy: the physical characterisation of pharmaceutical systems. Adv Drug Deliv Rev 2007;59(14):1434-52.

33. Stricker SA, Whitaker M. Confocal laser scanning microscopy of calcium dynamics in living cells. Microsc Res Tech 1999;46(6):356-69.

34. Masters BR, Bohnke M. Confocal microscopy of the human cornea in vivo. Int Ophthalmol 2001;23(4-6):199-206.

35. Meadows DL, Paugh JR. Use of confocal microscopy to determine matrix and surface protein deposition profiles in hydrogel contact lenses. CLAO J 1994;20(4):237-41.

36. Luensmann D, Glasier MA, Zhang F, Bantseev V, Simpson T, Jones L. Confocal microscopy and albumin penetration into contact lenses. Optom Vis Sci 2007;84(9):839-47.

37. Garrett Q, Garrett RW, Milthorpe BK. Lysozyme sorption in hydrogel contact lenses. Invest Ophthalmol Vis Sci 1999;40(5):897-903.

38. Fullard RJ, Tucker DL. Changes in human tear protein levels with progressively increasing stimulus. Invest Ophthalmol Vis Sci 1991;32(8):2290-301.

39. Zhou L, Beuerman RW, Foo Y, Liu S, Ang LP, Tan DT. Characterisation of human tear proteins using high-resolution mass spectrometry. Ann Acad Med Singapore 2006;35(6):400-7.

40. Soltys-Robitaille CE, Ammon DM, Jr., Valint PL, Jr., Grobe GL, 3rd. The relationship between contact lens surface charge and in-vitro protein deposition levels. Biomaterials 2001;22(24):3257-60.

41. Myers RI, Larsen DW, Tsao M, Castellano C, Becherer LD, Fontana F, Ghormley NR, Meier G. Quantity of protein deposited on hydrogel contact lenses and its relation to visible protein deposits. Optom Vis Sci 1991;68(10):776-82.

42. Tighe B. Contact lens materials. In: Phillips A, Speedwell L, editors. Contact Lenses. Edinburgh: Butterworth-Heinemann; 2007. p 59-78.

43. Holden BA. The Glenn A. Fry Award lecture 1988: the ocular response to contact lens wear. Optom Vis Sci 1989;66(11):717-33.

44. Fonn D, Bruce AS. A review of the Holden-Mertz criteria for critical oxygen transmission. Eye Contact Lens 2005;31(6):247-51.

45. Papas E. On the relationship between soft contact lens oxygen transmissibility and induced limbal hyperaemia. Exp Eye Res 1998;67(2):125-31.

46. Nicolson PC, Vogt J. Soft contact lens polymers: an evolution. Biomaterials 2001;22(24):3273-83.

47. Stapleton F, Stretton S, Papas E, Skotnitsky C, Sweeney DF. Silicone hydrogel contact lenses and the ocular surface. Ocul Surf 2006;4(1):24-43.

48. Lorentz H, Jones L. Lipid deposition on hydrogel contact lenses: how history can help us today. Optom Vis Sci 2007;84(4):286-95.

49. Cheung SW, Cho P, Chan B, Choy C, Ng V. A comparative study of biweekly disposable contact lenses: silicone hydrogel versus hydrogel. Clin Exp Optom 2007;90(2):124-31.

50. Santos L, Rodrigues D, Lira M, Oliveira ME, Oliveira R, Vilar EY, Azeredo J. The influence of surface treatment on hydrophobicity, protein adsorption and microbial colonisation of silicone hydrogel contact lenses. Cont Lens Anterior Eye 2007;30(3):183-8.

51. Dumbleton K. Noninflammatory silicone hydrogel contact lens complications. Eye Contact Lens 2003;29(1 Suppl):186-9.

52. Zhao Z, Fu H, Skotnitsky CC, Sankaridurg PR, Willcox MD. IgE antibody on worn highly oxygen-permeable silicone hydrogel contact lenses from patients with contact lens-induced papillary conjunctivitis (CLPC). Eye Contact Lens 2008;34(2):117-21.

53. Santodomingo-Rubido J, Wolffsohn JS, Gilmartin B. Adverse events and discontinuations during 18 months of silicone hydrogel contact lens wear. Eye Contact Lens 2007;33(6 Pt 1):288-92.

54. Tighe B. Silicone hydrogel materials: How do they work? In: Sweeney DF, editor. Silicone hydrogels: The Rebirth of continuous wear contact lenses. Oxford: Butterworth-Heinemann; 2000. p 1-21.

55. Sack RA, Tan KO, Tan A. Diurnal tear cycle: evidence for a nocturnal inflammatory constitutive tear fluid. Invest Ophthalmol Vis Sci 1992;33(3):626-40.

56. Bright AM, Tighe BJ. The composition and interfacial properties of tears, tear substitutes and tear models. Journal of the British Contact Lens Association 1993;16(2):57-66.

57. Rasband WS. ImageJ. Version 1.38x (07/13/2007). U. S. National Institutes of Health, Bethesda, Maryland, USA; 1997-2008.

58. Horbett TA, Weathersby PK. Adsorption of proteins from plasma to a series of hydrophilic-hydrophobic copolymers. I. Analysis with the in situ radioiodination technique. J Biomed Mater Res 1981;15(3):403-23.

59. Ceska M, Sjodin AV, Grossmuller F. Some quantitative aspects of the labelling of proteins with 125 I by the iodine monochloride method. Biochem J 1971;121(1):139-43.

60. Uniyal S, Brash JL. Patterns of adsorption of proteins from human plasma onto foreign surfaces. Thromb Haemost 1982;47(3):285-90.

61. Fatt I. The definition of thickness for a lens. Am J Optom Physiol Opt 1979;56(5):324-37.

62. Garrett Q, Garrett RW, Milthorpe BK. Lysozyme sorption in hydrogel contact lenses. Invest Ophthalmol Vis Sci 1999;40(5):897-903.

63. Hayward JA, Chapman D. Biomembrane surfaces as models for polymer design: the potential for haemocompatibility. Biomaterials 1984;5(3):135-42.

64. Young G, Bowers R, Hall B, Port M. Six month clinical evaluation of a biomimetic hydrogel contact lens. CLAO J 1997;23(4):226-36.

65. Hall B, Jones S, Young G, Coleman S. The on-eye dehydration of proclear compatibles lenses. CLAO J 1999;25(4):233-7.

66. Taddei P, Balducci F, Simoni R, Monti P. Raman, IR and thermal study of a new highly biocompatible phosphorylcholine-based contact lens. J Mol Struct 2005;744(47):507-14.

67. Braun RM, Ingham SJ, Harmon PS, Hook DJ. Surface and depth profile investigation of a phosphorylcholine-based contact lens using time of flight secondary ion mass spectrometry. J Vac Sci Technol A 2007;25(4):866-71.

68. Haugland RP. Invitrogen: A Guide to Fluorescent Probes and Labeling Technologies. Eugene, OR: Molecular Probes; 2005. 1126 p.

69. Stewart WW. Lucifer dyes-highly fluorescent dyes for biological tracing. Nature 1981;292(5818):17-21.

70. Bingaman S, Huxley VH, Rumbaut RE. Fluorescent dyes modify properties of proteins used in microvascular research. Microcirculation 2003;10(2):221-31.

71. Teske CA, Schroeder M, Simon R, Hubbuch J. Protein-labeling effects in confocal laser scanning microscopy. J Phys Chem B 2005;109(28):13811-7.

72. Senchyna M, Jones L, Louie D, May C, Forbes I, Glasier M. Quantitative and conformational characterization of lysozyme deposited on balafilcon and etafilcon contact lens materials. Curr Eye Res 2004;28(1):25-36.

73. Garrett Q, Laycock B, Garrett RW. Hydrogel lens monomer constituents modulate protein sorption. Invest Ophthalmol Vis Sci 2000;41(7):1687-95.

74. Maissa C, Franklin V, Guillon M, Tighe B. Influence of contact lens material surface characteristics and replacement frequency on protein and lipid deposition. Optom Vis Sci 1998;75(9):697-705.

75. Rovira-Bru M, Giralt F, Cohen Y. Protein adsorption onto zirconia modified with terminally grafted polyvinylpyrrolidone. J Colloid Interface Sci 2001;235(1):70-79.

76. Weikart CM, Matsuzawa Y, Winterton L, Yasuda HK. Evaluation of plasma polymer-coated contact lenses by electrochemical impedance spectroscopy. J Biomed Mater Res 2001;54(4):597-607.

77. Nicolson PC, Baron RC, Chabrecek P, Court J, Domschke A, Griesser HJ, et.al.; Extended wear ophthalmic lens. US Patent No. 5760100, 1998.

78. Grobe GL, Kunzler J, Seelye D, Salamone J. Silicone hydrogels for contact lens applications. Polym. Mater. Sci. Eng. 1999;80:108-9.

79. Lopez-Alemany A, Compan V, Refojo MF. Porous structure of Purevision versus Focus Night&Day and conventional hydrogel contact lenses. J Biomed Mater Res 2002;63(3):319-25.

80. Steffen R, McCabe K. Finding the comfort zone. Contact Lens Spectrum 2004;13;3(supp 1-4).

81. Steffen R, Schnider C. A next generation silicone hydrogel lens for daily wear. Part 1 - Material properties. Optician 2004;227:23-5.

82. Mccabe KP, Molock FF, Hill GA, Alli A, Steffen RB, Vanderlaan DG, Ford JD; Biomedical devices containing internal wetting agents. US Patent No. 20050154080, 2005.

83. Riley C, Young G, Chalmers R. Prevalence of ocular surface symptoms, signs, and uncomfortable hours of wear in contact lens wearers: the effect of refitting with daily-wear silicone hydrogel lenses (senofilcon a). Eye Contact Lens 2006;32(6):281-6.

84. Brennan NA, Coles ML, Ang JH. An evaluation of silicone-hydrogel lenses worn on a daily wear basis. Clin Exp Optom 2006;89(1):18-25.

85. Gonzalez-Meijome JM, Lopez-Alemany A, Almeida JB, Parafita MA, Refojo MF. Microscopic observation of unworn siloxane-hydrogel soft contact lenses by atomic force microscopy. J Biomed Mater Res B Appl Biomater 2006;76(2):412-8.

86. Gonzalez-Meijome JM, Lopez-Alemany A, Almeida JB, Parafita MA, Refojo MF. Microscopic observations of superficial ultrastructure of unworn siloxane-hydrogel contact lenses by cryo-scanning electron microscopy. J Biomed Mater Res B Appl Biomater 2006;76(2):419-23.

87. Gachon AM, Bilbault T, Dastugue B. Protein migration through hydrogels: a tool for measuring porosity-application to hydrogels used as contact lenses. Anal Biochem 1986;157(2):249-55.

88. Wood JM, Attwood D, Collett JH. Characterization of poly(2-hydroxyethyl methacrylate) gels. Drug Dev Ind Pharm 1983;9(1-2):93-101.

89. Gatin E, Alexandreanu D, Popescu A, Berlic C, Alexandreanu I. Correlations between permeability properties and the pore - size distribution of the porous media "hydron" useful as contact lenses. Phusica Medica 1999;XVI(1):13-9.

90. Davidson RS, Hilchenbach MM. The use of fluorescent probes in immunochemistry. Photochem Photobiol 1990;52(2):431-8.

91. Teske CA, von Lieres E, Schroder M, Ladiwala A, Cramer SM, Hubbuch JJ. Competitive adsorption of labeled and native protein in confocal laser scanning microscopy. Biotechnol Bioeng 2006;95(1):58-66.

92. Crandall RE, Janatova J, Andrade JD. The effects of radioiodination and fluorescent labelling on albumin. Prep Biochem 1981;11(2):111-38.

93. Banks PR, Paquette DM. Comparison of three common amine reactive fluorescent probes used for conjugation to biomolecules by capillary zone electrophoresis. Bioconjug Chem 1995;6(4):447-58.

94. Guilbault G. General aspects of luminescence spectroscopy. In: Guilbault G, editor. Practical fluorescence. New York: Dekker, M; 1990. p 1-40.

95. Furstenberg A, Vauthey E. Excited-state dynamics of the fluorescent probe Lucifer Yellow in liquid solutions and in heterogeneous media. Photochem Photobiol Sci 2005;4(3):260-7.

96. Rumbaut RE, Sial AJ. Differential phototoxicity of fluorescent dye-labeled albumin conjugates. Microcirculation 1999;6(3):205-13.

97. Hungerford G, Benesch J, Mano JF, Reis RL. Effect of the labelling ratio on the photophysics of fluorescein isothiocyanate (FITC) conjugated to bovine serum albumin. Photochem Photobiol Sci 2007;6(2):152-8.

98. Benchaib M, Delorme R, Pluvinage M, Bryon PA, Souchier C. Evaluation of five green fluorescence-emitting streptavidin-conjugated fluorochromes for use in immunofluorescence microscopy. Histochem Cell Biol 1996;106(2):253-6.

99. Zhang F. A novel use of confocal microscopy to study lysozyme sorption to silicone hydrogel and conventional hydrogel. Hamilton: McMaster University; 2006. 84 p.

References - Chapter 6

1. Neff AN, Caldwell KD. Property modification. In: Von Recum A, Jacobi JE, editors. Handbook of biomaterials evaluation: Scientific, technical, and clinical testing of implant materials. Philadelphia, PA: Taylor & Francis; 1999. p 201-226.

2. Thevenot P, Hu W, Tang L. Surface chemistry influences implant biocompatibility. Curr Top Med Chem 2008;8(4):270-80.

3. Holmberg M, Hou X. Competitive protein adsorption - multilayer adsorption and surface induced protein aggregation. Langmuir 2009;25(4):2081-89.

4. Brennan NA, Coles ML. Deposits and symptomatology with soft contact lens wear. Int Contact Lens Clin 2000;27:75-100.

5. Jones L, Evans K, Sariri R, Franklin V, Tighe B. Lipid and protein deposition of N-vinyl pyrrolidone-containing group II and group IV frequent replacement contact lenses. CLAO J 1997;23(2):122-6.

6. Hart DE, Plociniak MP, Grimes GW. Defining the physiologically normal coating and pathological deposit: An analysis of sulfur-containing moieties and pellicle thickness on hydrogel contact lenses. CLAO J 1998;24(2):85-101.

7. Lorentz H, Jones L. Lipid deposition on hydrogel contact lenses: how history can help us today. Optom Vis Sci 2007;84(4):286-95.

8. Kidane A, Szabocsik JM, Park K. Accelerated study on lysozyme deposition on poly(HEMA) contact lenses. Biomaterials 1998;19(22):2051-5.

9. Leahy CD, Mandell RB, Lin ST. Initial in vivo tear protein deposition on individual hydrogel contact lenses. Optom Vis Sci 1990;67(7):504-11.

10. Keith DJ, Christensen MT, Barry JR, Stein JM. Determination of the lysozyme deposit curve in soft contact lenses. Eye Contact Lens 2003;29(2):79-82.

11. Donshik PC, Ehlers WH, Ballow M. Giant papillary conjunctivitis. Immunol Allergy Clin North Am 2008;28(1):83-103.

12. Suchecki JK, Donshik P, Ehlers WH. Contact lens complications. Ophthalmol Clin North Am 2003;16(3):471-84.

13. Taylor RL, Willcox MD, Williams TJ, Verran J. Modulation of bacterial adhesion to hydrogel contact lenses by albumin. Optom Vis Sci 1998;75(1):23-9.

14. Skotnitsky C, Sankaridurg PR, Sweeney DF, Holden BA. General and local contact lens induced papillary conjunctivitis (CLPC). Clin Exp Optom 2002;85(3):193-7.

15. Skotnitsky CC, Naduvilath TJ, Sweeney DF, Sankaridurg PR. Two presentations of contact lens-induced papillary conjunctivitis (CLPC) in hydrogel lens wear: local and general. Optom Vis Sci 2006;83(1):27-36.

16. Tan ME, Demirci G, Pearce D, Jalbert I, Sankaridurg P, Willcox MD. Contact lens-induced papillary conjunctivitis is associated with increased albumin deposits on extended wear hydrogel lenses. Adv Exp Med Biol 2002;506(Pt B):951-5.

17. Richard NR, Anderson JA, Tasevska ZG, Binder PS. Evaluation of tear protein deposits on contact lenses from patients with and without giant papillary conjunctivitis. CLAO J 1992;18(3):143-7.

18. Dunn JP, Jr., Weissman BA, Mondino BJ, Arnold AC. Giant papillary conjunctivitis associated with elevated corneal deposits. Cornea 1990;9(4):357-8.

19. de Souza GA, Godoy LM, Mann M. Identification of 491 proteins in the tear fluid proteome reveals a large number of proteases and protease inhibitors. Genome Biol 2006;7(8):R72.

20. Fung K, Morris C, Duncan M. Mass spectrometric techniques applied to the analysis of human tears: a focus on the peptide and protein constituents. Adv Exp Med Biol 2002;506(Pt A):601-5.

21. Bright AM, Tighe BJ. The composition and interfacial properties of tears, tear substitutes and tear models. Journal of the British Contact Lens Association 1993;16(2):57-66.

22. Ng V, Cho P, Mak S, Lee A. Variability of tear protein levels in normal young adults: between-day variation. Graefes Arch Clin Exp Ophthalmol 2000;238(11):892-9.

23. Sack RA, Tan KO, Tan A. Diurnal tear cycle: evidence for a nocturnal inflammatory constitutive tear fluid. Invest Ophthalmol Vis Sci 1992;33(3):626-40.

24. Fullard RJ, Snyder C. Protein levels in nonstimulated and stimulated tears of normal human subjects. Invest Ophthalmol Vis Sci 1990;31(6):1119-26.

25. Fullard RJ, Tucker DL. Changes in human tear protein levels with progressively increasing stimulus. Invest Ophthalmol Vis Sci 1991;32(8):2290-301.

26. McGill JI, Liakos GM, Goulding N, Seal DV. Normal tear protein profiles and age-related changes. Br J Ophthalmol 1984;68(5):316-20.

27. Farris RL. Tear analysis in contact lens wearers. Trans Am Ophthalmol Soc 1985;83:501-45.

28. Mandel ID, Stuchell RN. The lacrimal-salivary axis in health and disease. In: Holly FJ, Lamberts DW, MacKeen DL, editors. The preocular tear film in health, disease, and contact lens wear. Texas: Lubbock, Dry Eye Institute, Inc.; 1986. p 852-6.

29. Berman ER. Tears. Biochemistry of the eye. New York: Plenum Press; 1991. p 79-80.

30. Imoto T, Johnson LN, North AC, Phillips DC, Rupley JA. Vertebrate lysozymes. In: Boyle PD, editor. The Enzymes. New York: Academic Press; 1972. p 665-868.

31. Choy CK, Cho P, Benzie IF, Ng V. Effect of one overnight wear of orthokeratology lenses on tear composition. Optom Vis Sci 2004;81(6):414-20.

32. Tan KO, Sack RA, Holden BA, Swarbrick HA. Temporal sequence of changes in tear film composition during sleep. Curr Eye Res 1993;12(11):1001-7.

33. Garrett Q, Chatelier RC, Griesser HJ, Milthorpe BK. Effect of charged groups on the adsorption and penetration of proteins onto and into carboxymethylated poly(HEMA) hydrogels. Biomaterials 1998;19(23):2175-86.

34. Garrett Q, Laycock B, Garrett RW. Hydrogel lens monomer constituents modulate protein sorption. Invest Ophthalmol Vis Sci 2000;41(7):1687-95.

35. Bohnert JL, Horbett TA, Ratner BD, Royce FH. Adsorption of proteins from artificial tear solutions to contact lens materials. Invest Ophthalmol Vis Sci 1988;29(3):362-73.

36. Efron N, Morgan PB. Soft contact lens care regimens in the UK. Cont Lens Anterior Eye 2008;31(6):283-4.

37. Woods CA, Jones DA, Jones LW, Morgan PB. A seven year survey of the contact lens prescribing habits of Canadian optometrists. Optom Vis Sci 2007;84(6):505-10.

38. Morgan PB, Efron N. A decade of contact lens prescribing trends in the United Kingdom (1996-2005). Cont Lens Anterior Eye 2006;29(2):59-68.

39. Franklin VJ. Cleaning efficacy of single-purpose surfactant cleaners and multi-purpose solutions. Cont Lens Anterior Eye 1997;20(2):63-8.

40. Mok KH, Cheung RW, Wong BK, Yip KK, Lee VW. Effectiveness of no-rub contact lens cleaning on protein removal: a pilot study. Optom Vis Sci 2004;81(6):468-70.

41. Tighe B. Contact lens materials. In: Phillips A, Speedwell L, editors. Contact Lenses. Edinburgh: Butterworth-Heinemann; 2007. p 59-78.

42. Nicolson PC, Vogt J. Soft contact lens polymers: an evolution. Biomaterials 2001;22(24):3273-83.

43. Stapleton F, Stretton S, Papas E, Skotnitsky C, Sweeney DF. Silicone hydrogel contact lenses and the ocular surface. Ocul Surf 2006;4(1):24-43.

44. Fonn D, MacDonald KE, Richter D, Pritchard N. The ocular response to extended wear of a high Dk silicone hydrogel contact lens. Clin Exp Optom 2002;85(3):176-82.

45. Morgan PB, Woods CA, Knajian R, Jones D, Efron N, Tan K-O, Pesinova A, Grein H-J, Marx S, Santodomingo J and others. International contact lens prescribing in 2007. Contact Lens Spectrum 2008;23(1):36-41.

46. Sweeney D, du Toit R, Keay L, Jalbert I, Sankaridurg PR, Stern J, Skotnitsky C, Stephensen A, Covey M, Holden BA and others. Clinical performance of silicone hydrogel lenses. In: Sweeney D, editor. Silicone hydrogels: continuous-wear contact lenses. Edinburgh: Butterworth Heinemann, British Contact Lens Association; 2004. p 164-216.

47. Lenk TJ, Horbett TA, Ratner BD, Chittur KK. Infrared spectroscopy studies of time-dependent changes in fibrinogen adsorbed to polyurethanes. Langmuir 1991;7(8):1755-64.

48. Ikeda K, Hamaguchi K, Miwa S, Nishina T. Circular dichroism of human lysozyme. J Biochem 1972;71(3):371-8.

49. Michnik A, Michalik K, Drzazga Z, Kluczewska A. Comparative DSC study of human and bovine serum albumin. J. Therm. Anal. Cal. 2007;84(1):113-117.

50. Kurrat R, Prenosil JE, Ramsden JJ. Kinetics of human and bovine serum albumin adsorption at silica-titania surfaces. J Colloid Interface Sci 1997;185(1):1-8.

51. Miller I, Gemeiner M. Peculiarities in electrophoretic behavior of different serum albumins. Electrophoresis 1993;14(12):1312-7.

52. Blake CC, Swan ID. X-ray analysis of structure of human lysozyme at 6 A resolution. Nat New Biol 1971;232(27):12-5.

53. Blake CC, Koenig DF, Mair GA, North AC, Phillips DC, Sarma VR. Structure of hen egg-white lysozyme. A three-dimensional Fourier synthesis at 2 Angstrom resolution. Nature 1965;206(986):757-61.

54. Garrett Q, Milthorpe BK. Human serum albumin adsorption on hydrogel contact lenses in vitro. Invest Ophthalmol Vis Sci 1996;37(13):2594-602.

55. Jones L, Senchyna M, Glasier MA, Schickler J, Forbes I, Louie D, May C. Lysozyme and lipid deposition on silicone hydrogel contact lens materials. Eye Contact Lens 2003;29(1 Suppl):75-9.

56. Horbett TA. Adsorption of proteins from plasma to a series of hydrophilic-hydrophobic copolymers. II. Compositional analysis with the prelabeled protein technique. J Biomed Mater Res 1981;15(5):673-95.

57. Ceska M, Sjodin AV, Grossmuller F. Some quantitative aspects of the labelling of proteins with 125 I by the iodine monochloride method. Biochem J 1971;121(1):139-43.

58. Subbaraman LN, Glasier MA, Senchyna M, Sheardown H, Jones L. Kinetics of in vitro lysozyme deposition on silicone hydrogel, PMMA, and FDA groups I, II, and IV contact lens materials. Curr Eye Res 2006;31(10):787-96.

59. Luensmann D, Zhang F, Subbaraman LN, Sheardown H, Jones L. Localization of lysozyme sorption to conventional and silicone hydrogel contact lenses using confocal microscopy. Curr Eye Res 2009;34:683-697.

60. Suwala M, Glasier MA, Subbaraman LN, Jones L. Quantity and conformation of lysozyme deposited on conventional and silicone hydrogel contact lens materials using an in vitro model. Eye Contact Lens 2007;33(3):138-43.

61. Luensmann D, Glasier MA, Zhang F, Bantseev V, Simpson T, Jones L. Confocal microscopy and albumin penetration into contact lenses. Optom Vis Sci 2007;84(9):839-47.

62. Zhao Z, Carnt NA, Aliwarga Y, Wei X, Naduvilath T, Garrett Q, Korth J, Willcox MD. Care regimen and lens material influence on silicone hydrogel contact lens deposition. Optom Vis Sci 2009;86(3):251-9.

63. Santos L, Rodrigues D, Lira M, Real Oliveira ME, Oliveira R, Vilar EY, Azeredo J. Bacterial adhesion to worn silicone hydrogel contact lenses. Optom Vis Sci 2008;85(7):520-5.

64. Kilvington S, Lonnen J. A comparison of regimen methods for the removal and inactivation of bacteria, fungi and Acanthamoeba from two types of silicone hydrogel lenses. Cont Lens Anterior Eye 2009;32(2):73-7.

65. Zhang S, Ahearn DG, Stulting RD, Schwam BL, Simmons RB, Pierce GE, Crow SA, Jr. Differences among strains of the Fusarium oxysporum-F. solani complexes in their penetration of hydrogel contact lenses and subsequent susceptibility to multipurpose contact lens disinfection solutions. Cornea 2007;26(10):1249-54.

66. Emch AJ, Nichols JJ. Proteins identified from care solution extractions of silicone hydrogels. Optom Vis Sci 2009.

67. Subbaraman LN, Woods J, Teichroeb JH, Jones L. Protein deposition on a lathe-cut silicone hydrogel contact lens material. Optom Vis Sci 2009;86(3):244-50.

68. Simmons PA, Ridder III WH, Edrington TB, Ho S, Lau K-C. Passive protein removal by two multipurpose lens solutions: Comparison of effects on in vitro deposited and patient-worn hydrogel contact lenses. ICLC 1999;26:33-8.

69. Jung J, Rapp J. The efficacy of hydrophilic contact lens cleaning systems in removing protein deposits. CLAO J 1993;19(1):47-9.

70. Nichols JJ. Deposition rates and lens care influence on galyfilcon A silicone hydrogel lenses. Optom Vis Sci 2006;83(10):751-7.

71. Cho P, Cheng SY, Chan WY, Yip WK. Soft contact lens cleaning: rub or no-rub? Ophthalmic Physiol Opt 2009;29(1):49-57.

72. Nicolson PC, Baron RC, Chabrecek P, Court J, Domschke A, Griesser HJ, et.al.; Extended wear ophthalmic lens. US Patent No. 5760100, 1998.

73. Garrett Q, Garrett RW, Milthorpe BK. Lysozyme sorption in hydrogel contact lenses. Invest Ophthalmol Vis Sci 1999;40(5):897-903.

74. Santos L, Rodrigues D, Lira M, Oliveira ME, Oliveira R, Vilar EY, Azeredo J. The influence of surface treatment on hydrophobicity, protein adsorption and microbial colonisation of silicone hydrogel contact lenses. Cont Lens Anterior Eye 2007;30(3):183-8.

75. Senchyna M, Jones L, Louie D, May C, Forbes I, Glasier MA. Quantitative and conformational characterization of lysozyme deposited on balafilcon and etafilcon contact lens materials. Curr Eye Res 2004;28(1):25-36.

76. Valint Jr. PL, Grobe GL, Ammon Jr. DM, Moorehead MJ; Plasma surface treatment of silicone hydrogel contact lenses US Patent No. 6193369, 2001.

77. Lopez-Alemany A, Compan V, Refojo MF. Porous structure of Purevision versus Focus Night&Day and conventional hydrogel contact lenses. J Biomed Mater Res 2002;63(3):319-25.

78. Gonzalez-Meijome JM, Lopez-Alemany A, Almeida JB, Parafita MA, Refojo MF. Microscopic observations of superficial ultrastructure of unworn siloxane-hydrogel contact lenses by cryo-scanning electron microscopy. J Biomed Mater Res B Appl Biomater 2006;76(2):419-23.

79. Gonzalez-Meijome JM, Lopez-Alemany A, Almeida JB, Parafita MA, Refojo MF. Microscopic observation of unworn siloxane-hydrogel soft contact lenses by atomic force microscopy. J Biomed Mater Res B Appl Biomater 2006;76(2):412-8.

80. Shih KL, Hu J, Sibley MJ. The microbiological benefit of cleaning and rinsing contact lenses. Intl Contact Lens Clin 1985;12:235-49.

81. Butcko V, McMahon TT, Joslin CE, Jones L. Microbial keratitis and the role of rub and rinsing. Eye Contact Lens 2007;33(6 Pt 2):421-3; discussion 424-5.

82. Ishihara K. The role of water in the surface properties of phosphorlipid polymers. In: Morra M, editor. Water in biomaterials surface science. Chichester ; New York: Wiley; 2001. p 333-51.

83. Lee JH, Li T, Park K. Solvation interactions for protein adsorption to biomaterial surfaces. In: Morra M, editor. Water in biomaterials surface science. Chichester ; New York: Wiley; 2001. p 127-46.

84. Castillo EJ, Koenig JL, Anderson JM, Lo J. Characterization of protein adsorption on soft contact lenses. I. Conformational changes of adsorbed human serum albumin. Biomaterials 1984;5(6):319-25.

85. Baujard-Lamotte L, Noinville S, Goubard F, Marque P, Pauthe E. Kinetics of conformational changes of fibronectin adsorbed onto model surfaces. Colloids Surf B Biointerfaces 2008;63(1):129-37.

86. Park H, Park K. Biocompatibility issues of implantable drug delivery systems. Pharm Res 1996;13(12):1770-6.

87. Ratner BD. Biomaterials science: An introduction to materials in medicine. San Diego ; London: Academic Press; 1996. 193-199 p.

88. Pitt WG, Park K, Cooper SL. Sequential protein adsorption and thrombus deposition on polymeric biomaterials. Journal of Colloid and Interface Science 1986; 111(2):343-362.

1. Paleokastritis GP, Glazer LC, Papadopoulos GP, Azar DT, Adamis AP. Intracoular lenses in cataract and refractive surgery. Philadelphia: W.B. Saunders Company; 2001. 344 p.

2. Bell CM, Hatch WV, Cernat G, Urbach DR. Surgeon volumes and selected patient outcomes in cataract surgery: a population-based analysis. Ophthalmology 2007;114(3):405-10.

3. Brown NP, Bron AJ. Lens disorders: A clinical manual of cataract diagnosis. Oxford; Boston: Butterworth-Heinemann; 1996. p 91-211.

4. Congdon N, O'Colmain B, Klaver CC, Klein R, Munoz B, Friedman DS, Kempen J, Taylor HR, Mitchell P. Causes and prevalence of visual impairment among adults in the United States. Arch Ophthalmol 2004;122(4):477-85.

5. World Health Organisation. 2006. P http://www.who.int/blindness/CSR%202006.pdf.

6. Sandoval HP, de Castro LE, Vroman DT, Solomon KD. Refractive surgery survey 2004. J Cataract Refract Surg 2005;31(1):221-33.

7. Congdon N, Vingerling JR, Klein BE, West S, Friedman DS, Kempen J, O'Colmain B, Wu SY, Taylor HR. Prevalence of cataract and pseudophakia/aphakia among adults in the United States. Arch Ophthalmol 2004;122(4):487-94.

8. Chang DH, Davis EA. Phakic intraocular lenses. Curr Opin Ophthalmol 2006;17(1):99-104.

9. Vasavada AR, Nihalani BR. Pediatric cataract surgery. Curr Opin Ophthalmol 2006;17(1):54-61.

10. Christ FR, Buchen SY, Deacon J, Cunanan CM, Giamporcaro JE, Knight PM, Weinschenk III JI, Yang S. Biomaterials used for intraocular lenses. In: Wise DL, Trantolo DJ, Altobelli DE, Yaszemski MJ, Gresser JD, Schwartz ER, editors. Encyclopedic handbook of biomaterials and bioengineering, Part B: Applications. New York: Marcel Dekker, Inc.; 1995. p 1261-1312.

11. Chehade M, Elder MJ. Intraocular lens materials and styles: a review. Aust N Z J Ophthalmol 1997;25(4):255-63.

12. Werner L. Biocompatibility of intraocular lens materials. Curr Opin Ophthalmol 2008;19(1):41-9.

13. Werner L, Mamalis N. Foldable Intraocular Lenses. In: Kohnen T, Koch DD, editors. Cataract and refractive surgery. Berlin ; New York: Springer; 2005. p 63-100.

14. Hollick EJ, Spalton DJ, Ursell PG. Surface cytologic features on intraocular lenses: can increased biocompatibility have disadvantages? Arch Ophthalmol 1999;117(7):872-8.

15. Zirm M. Proteins in aqueous humor. Adv Ophthalmol 1980;40:100-72.

16. Yu TC, Okamura R. Comparative study of native proteins in aqueous humor and serum--detection of characteristic aqueous humor proteins. Jpn J Ophthalmol 1987;31(2):235-48.

17. Shah SM, Spalton DJ, Taylor JC. Correlations between laser flare measurements and anterior chamber protein concentrations. Invest Ophthalmol Vis Sci 1992;33(10):2878-84.

18. Duan X, Lu Q, Xue P, Zhang H, Dong Z, Yang F, Wang N. Proteomic analysis of aqueous humor from patients with myopia. Mol Vis 2008;14:370-7.

19. Gryzunov Iu A, Deev AI, Kurysheva NI, Komarova MN. [Fluorescent analysis of albumin in aqueous humor and tears]. Biull Eksp Biol Med 1999;128(11):597-600.

20. Kuchle M, Ho TS, Nguyen NX, Hannappel E, Naumann GO. Protein quantification and electrophoresis in aqueous humor of pseudoexfoliation eyes. Invest Ophthalmol Vis Sci 1994;35(2):748-52.

21. Ravalico G, Baccara F, Lovisato A, Tognetto D. Postoperative cellular reaction on various intraocular lens materials. Ophthalmology 1997;104(7):1084-91.

22. Tognetto D, Toto L, Ballone E, Ravalico G. Biocompatibility of hydrophilic intraocular lenses. J Cataract Refract Surg 2002;28(4):644-51.

23. Shigemitsu T. Ultrastructural study of adsorbed protein on extracted intraocular lenses. Jpn J Ophthalmol 1991;35(3):354-8.

24. Poot AA, Beugeling T. Protein adsorption in relation to platelet adhesion and contact activation. In: Missirlis YF, Lemm W, editors. Modern aspects of protein adsorption on biomaterials. Dordrecht: Kluwer Academic Publishers; 1991. p 29-38.

25. Kochounian HH, Kovacs SA, Sy J, Grubbs DE, Maxwell WA. Identification of intraocular lens-adsorbed proteins in mammalian in vitro and in vivo systems. Arch Ophthalmol 1994;112(3):395-401.

26. Pokidysheva EN, Maklakova IA, Belomestnaya ZM, Perova NV, Bagrov SN, Sevastianov VI. Comparative analysis of human serum albumin adsorption and complement activation for intraocular lenses. Artif Organs 2001;25(6):453-8.

27. Johnston RL, Spalton DJ, Hussain A, Marshall J. In vitro protein adsorption to 2 intraocular lens materials. J Cataract Refract Surg 1999;25(8):1109-15.

28. Linnola RJ, Werner L, Pandey SK, Escobar-Gomez M, Znoiko SL, Apple DJ. Adhesion of fibronectin, vitronectin, laminin, and collagen type IV to intraocular lens materials in pseudophakic human autopsy eyes. Part 2: explanted intraocular lenses. J Cataract Refract Surg 2000;26(12):1807-18.

29. Michnik A, Michalik K, Drzazga Z, Kluczewska A. Comparative DSC study of human and bovine serum albumin. J. Therm. Anal. Cal. 2007;84(1):113-117.

30. Kurrat R, Prenosil JE, Ramsden JJ. Kinetics of human and bovine serum albumin adsorption at silica-titania surfaces. J Colloid Interface Sci 1997;185(1):1-8.

31. Miller I, Gemeiner M. Peculiarities in electrophoretic behavior of different serum albumins. Electrophoresis 1993;14(12):1312-7.

32. Horbett TA. Adsorption of proteins from plasma to a series of hydrophilic-hydrophobic copolymers. II. Compositional analysis with the prelabeled protein technique. J Biomed Mater Res 1981;15(5):673-95.

33. Ceska M, Sjodin AV, Grossmuller F. Some quantitative aspects of the labelling of proteins with 125 I by the iodine monochloride method. Biochem J 1971;121(1):139-43.

34. Bingaman S, Huxley VH, Rumbaut RE. Fluorescent dyes modify properties of proteins used in microvascular research. Microcirculation 2003;10(2):221-31.

35. Bertelmann E, Kojetinsky C. Posterior capsule opacification and anterior capsule opacification. Curr Opin Ophthalmol 2001;12(1):35-40.

36. Dewey S. Posterior capsule opacification. Curr Opin Ophthalmol 2006;17(1):45-53.

37. Tognetto D, Toto L, Sanguinetti G, Cecchini P, Vattovani O, Filacorda S, Ravalico G. Lens epithelial cell reaction after implantation of different intraocular lens materials: two-year results of a randomized prospective trial. Ophthalmology 2003;110(10):1935-41.

38. Dufour S, Duband JL, Thiery JP. Role of a major cell-substratum adhesion system in cell behavior and morphogenesis. Biol Cell 1986;58(1):1-13.

39. Cooke CA, McGimpsey S, Mahon G, Best RM. An in vitro study of human lens epithelial cell adhesion to intraocular lenses with and without a fibronectin coating. Invest Ophthalmol Vis Sci 2006;47(7):2985-9.

40. Linnola RJ, Sund M, Ylonen R, Pihlajaniemi T. Adhesion of soluble fibronectin, vitronectin, and collagen type IV to intraocular lens materials. J Cataract Refract Surg 2003;29(1):146-52.

41. Yan Q, Perdue N, Sage EH. Differential responses of human lens epithelial cells to intraocular lenses in vitro: hydrophobic acrylic versus PMMA or silicone discs. Graefes Arch Clin Exp Ophthalmol 2005;243(12):1253-62.

42. Tripathi RC, Millard CB, Tripathi BJ. Protein composition of human aqueous humor: SDS-PAGE analysis of surgical and post-mortem samples. Exp Eye Res 1989;48(1):117-30.

43. Vroman L, Adams AL, Fischer GC, Munoz PC. Interaction of high molecular weight kininogen, factor XII, and fibrinogen in plasma at interfaces. Blood 1980;55(1):156-9.

44. Brynda E, Houska M, Jirouskova M, Dyr JE. Albumin and heparin multilayer coatings for blood-contacting medical devices. J Biomed Mater Res 2000;51(2):249-57.

45. Park K, Mao FW, Park H. Morphological characterization of surface-induced platelet activation. Biomaterials 1990;11(1):24-31.

46. Taylor RL, Willcox MD, Williams TJ, Verran J. Modulation of bacterial adhesion to hydrogel contact lenses by albumin. Optom Vis Sci 1998;75(1):23-9.

47. Scott EA, Nichols MD, Cordova LH, George BJ, Jun YS, Elbert DL. Protein adsorption and cell adhesion on nanoscale bioactive coatings formed from poly(ethylene glycol) and albumin microgels. Biomaterials 2008;29(34):4481-93.

48. Pitt WG, Park K, Cooper SL. Sequential protein adsorption and thrombus deposition on polymeric biomaterials. Journal of Colloid and Interface Science 1986 111(2):343-362.

49. Takeda K, Wada A, Yamamoto K, Moriyama Y, Aoki K. Conformational change of bovine serum albumin by heat treatment. J Protein Chem 1989;8(5):653-9.

50. Ishiguro R, Yokoyama Y, Maeda H, Shimamura A, Kameyama K, Hiramatsu K. Modes of conformational changes of proteins adsorbed on a planar hydrophobic polymer surface reflecting their adsorption behaviors. J Colloid Interface Sci 2005;290(1):91-101.

51. Garrett Q, Griesser HJ, Milthorpe BK, Garrett RW. Irreversible adsorption of human serum albumin to hydrogel contact lenses: a study using electron spin resonance spectroscopy. Biomaterials 1999;20(14):1345-56.

52. Rodbard D, Chrambach A. Estimation of molecular radius, free mobility, and valence using polyacylamide gel electrophoresis. Anal Biochem 1971;40(1):95-134.

53. Sheller NB, Petrash S, Foster MD. Atomic force microscopy and X-ray reflectivity studies of albumin adsorbed onto self-assembled monolayers of hexadecyltrichlorosilane. Langmuir 1998;14(16):4535–4544.

54. Mura-Galelli MJ, Voegel JC, Behr S, Bres EF, Schaaf P. Adsorption/desorption of human serum albumin on hydroxyapatite: a critical analysis of the Langmuir model. Proc Natl Acad Sci U S A 1991;88(13):5557-61.

55. Roach P, Farrar D, Perry CC. Interpretation of protein adsorption: surface-induced conformational changes. J Am Chem Soc 2005;127(22):8168-73.

56. Wu H, Fan Y, Sheng S, Sen-Fang S. Induction of changes in the secondary structure of globular proteins by a hydrophobic surface. Eur. Biophys J 1993;22(3):201-205.

57. Scaramuzza A, Fernando GT, Crayford BB. Posterior capsule opacification and lens epithelial cell layer formation: Hydroview hydrogel versus AcrySof acrylic intraocular lenses. J Cataract Refract Surg 2001;27(7):1047-54.

58. Schauersberger J, Amon M, Kruger A, Abela C, Schild G, Kolodjaschna J. Lens epithelial cell outgrowth on 3 types of intraocular lenses. J Cataract Refract Surg 2001;27(6):850-4.

59. Auffarth GU, Brezin A, Caporossi A, Lafuma A, Mendicute J, Berdeaux G, Smith AF. Comparison of Nd : YAG capsulotomy rates following phacoemulsification with implantation of PMMA, silicone, or acrylic intra-ocular lenses in four European countries. Ophthalmic Epidemiol 2004;11(4):319-29.

60. Richter-Mueksch S, Kahraman G, Amon M, Schild-Burggasser G, Schauersberger J, Abela-Formanek C. Uveal and capsular biocompatibility after implantation of sharp-edged hydrophilic acrylic, hydrophobic acrylic, and silicone intraocular lenses in eyes with pseudoexfoliation syndrome. J Cataract Refract Surg 2007;33(8):1414-8.

61. Roesel M, Heinz C, Heimes B, Koch JM, Heiligenhaus A. Uveal and capsular biocompatibility of two foldable acrylic intraocular lenses in patients with endogenous uveitis--a prospective randomized study. Graefes Arch Clin Exp Ophthalmol 2008;246(11):1609-15.

62. Abela-Formanek C, Amon M, Schild G, Schauersberger J, Heinze G, Kruger A. Uveal and capsular biocompatibility of hydrophilic acrylic, hydrophobic acrylic, and silicone intraocular lenses. J Cataract Refract Surg 2002;28(1):50-61.

63. Nakanome S, Watanabe H, Tanaka K, Tochikubo T. Calcification of Hydroview H60M intraocular lenses: aqueous humor analysis and comparisons with other intraocular lens materials. J Cataract Refract Surg 2008;34(1):80-6.

References - Chapter 8

1. Barr JT. 2004 Annual report. Contact Lens Spectrum 2005;20(1):26-31.

2. Jones L, Dumbleton K. Soft lens extended wear and complications. In: Hom MM, Bruce A, editors. Manual of contact lens prescribing and fitting. Oxford: Butterworth-Heinemann; 2006. p 393-441.

3. Szczotka-Flynn L, Diaz M. Risk of corneal inflammatory events with silicone hydrogel and low dk hydrogel extended contact lens wear: a meta-analysis. Optom Vis Sci 2007;84(4):247-56.

4. Brennan NA, Coles ML. Deposits and symptomatology with soft contact lens wear. Int Contact Lens Clin 2000;27:75-100.

5. Suwala M, Glasier MA, Subbaraman LN, Jones L. Quantity and conformation of lysozyme deposited on conventional and silicone hydrogel contact lens materials using an in vitro model. Eye Contact Lens 2007;33(3):138-43.

6. Buchwald P. A general bilinear model to describe growth or decline time profiles. Math Biosci 2007;205(1):108-36.

APPENDICES

Appendix A

Molar Extinction Coefficient and Degree of Labeling

Determine the molar extinction coefficient ($M^{-1}cm^{-1}$)

Measure the average absorbance at 280nm for a known protein solution (e.g. 100mg/ml).

$$\varepsilon = \frac{\text{Absorption at 280} * \text{MW (Da)}}{\text{Concentration (mg/ml)}}$$

e.g. Absorbance 0.667 for BSA → ε for BSA= 43538

Determine the Degree of Labeling (DOL)

On average, how many dye molecules are attached to one protein molecule?

Mix 100 µl of the conjugate with 900 µl of PBS to get 1ml solution and measure the absorbance of the labeled protein at 280nm and the maximum absorbance peak of the fluorescent probe using a UV Spectrophotometer. (The result should be between 0.1 and 1.0. If it is higher, the solution must be diluted and the dilution factor in the calculation changes.)

Concentration of protein (M) = $\frac{\text{Absorption at 280 – Absorption (fl. dye) * correction Factor}}{\text{Molar extinction coefficient of protein}} * 10$ (*dilution factor)*

Or determine mg/ml using DC Protein Assay (Bio-Rad, Hercules, CA, USA).

e.g. 3.22mg/ml = $3.22/66000 = 4.889 * 10^{-5}$ M

→ The DC assay method has been used to determine the protein concentration in all studies.

Moles dye per mole protein = $\frac{\text{Absorption (fl. dye)}}{\text{Molar extinction coefficient of fluorescent probe} * \text{protein concentration}} *$ 10 (*dilution factor)*

Fluorescent probe	Extinction coefficient ($M^{-1}cm^{-1}$)	→ at (nm) (approximately max absorbance)
DTAF	43538	492
RITC	105789	534
Lucifer Yellow	8754	405

Appendix B

Fluorescent signal decrease for unconjugated DTAF over time (Chapter 3)

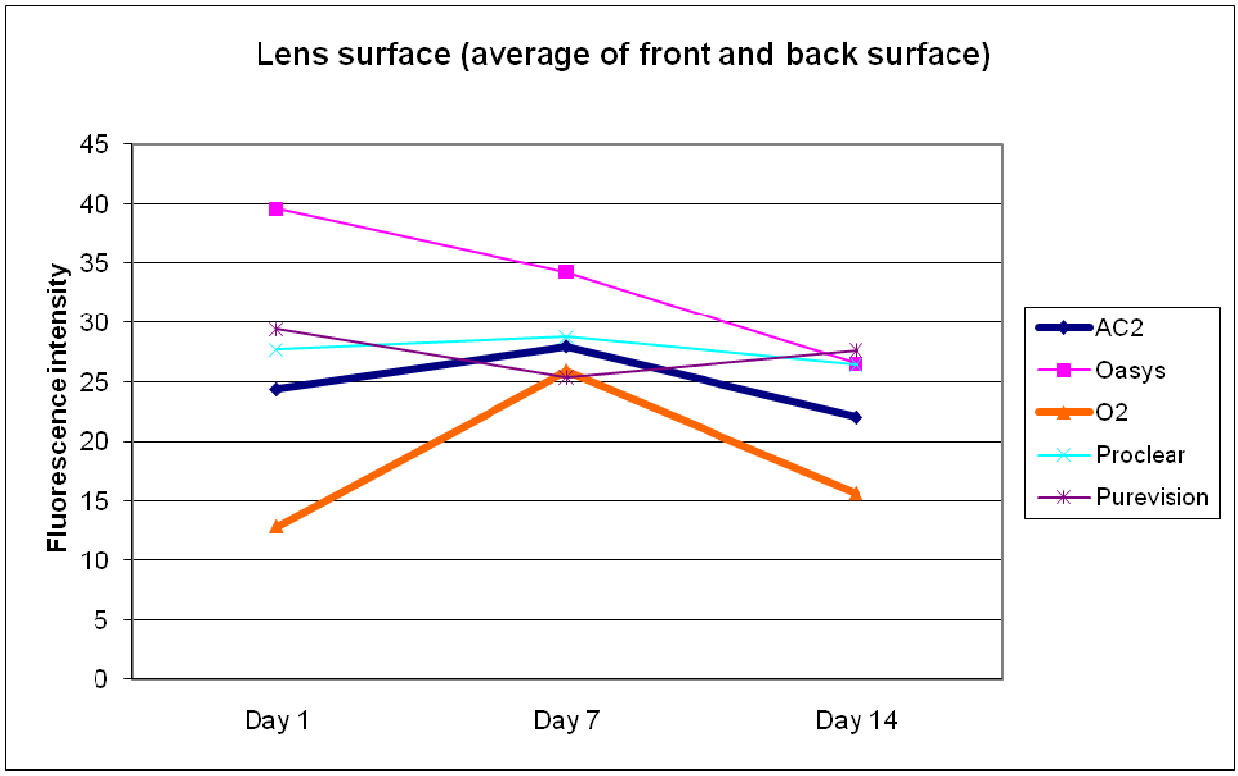

AC2 – etafilcon A; Oasys – senofilcon A; O2 - lotrafilcon B; Proclear - omafilcon A; Purevision – balafilcon A

Appendix C

Sorption profile of unconjugated Lucifer Yellow to different contact lens materials over time (Chapters 4 & 5)

Conventional hydrogel contact lenses (FDA Group IV)

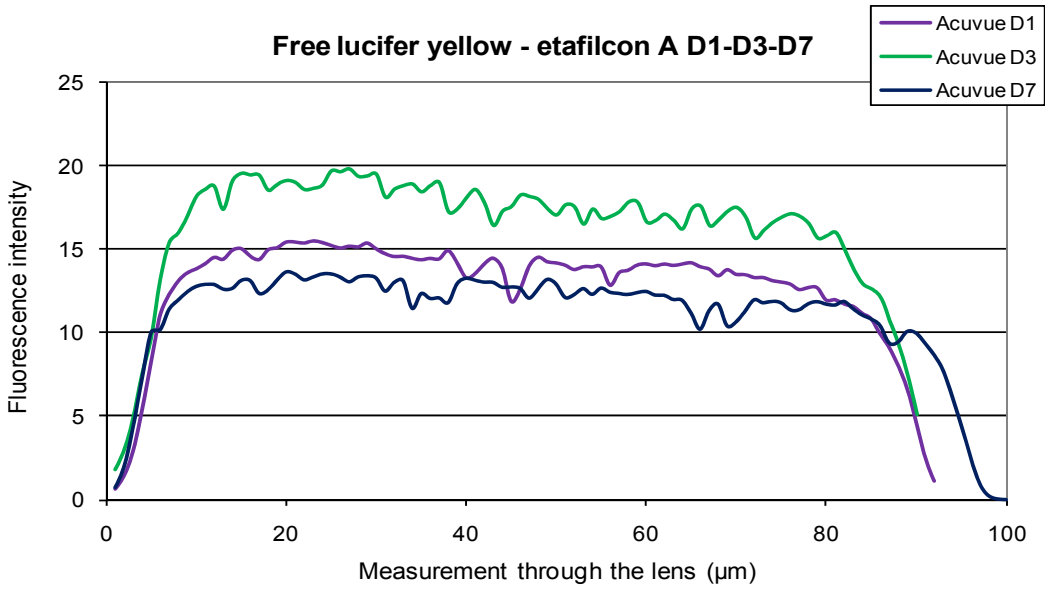

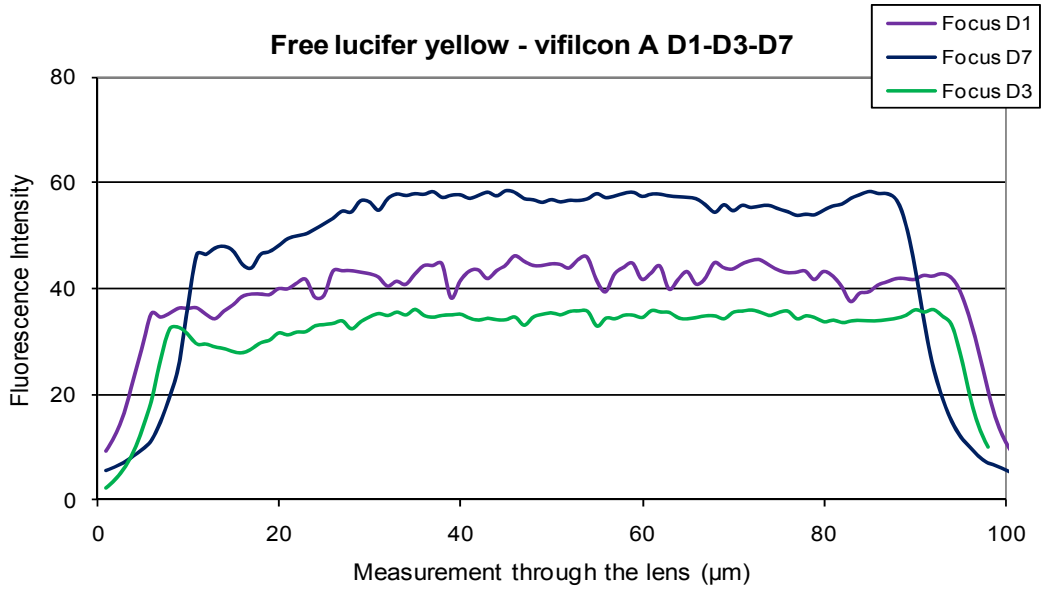

Conventional hydrogel contact lenses (FDA Group II)

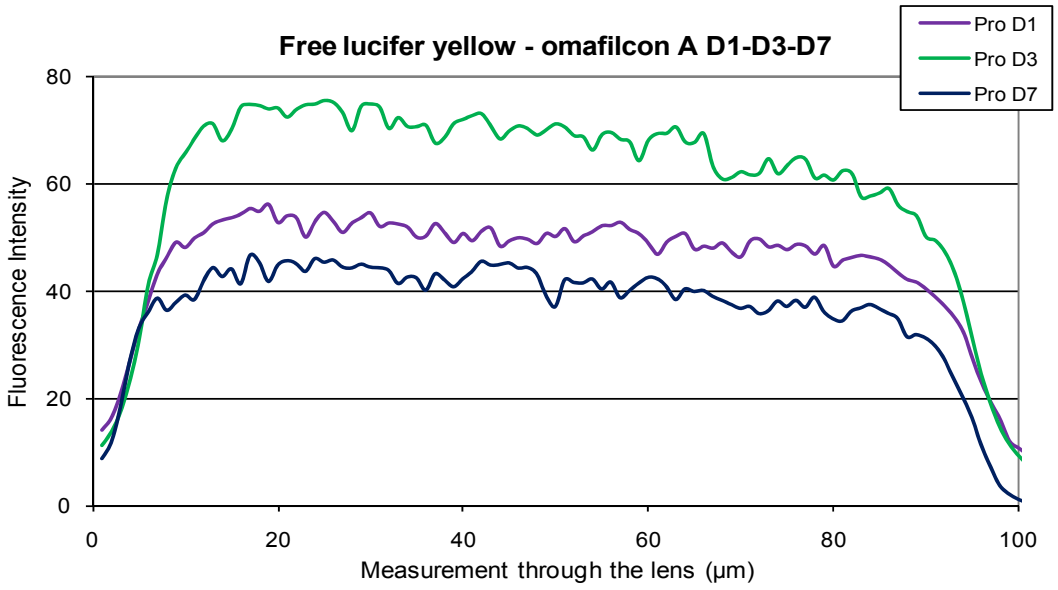

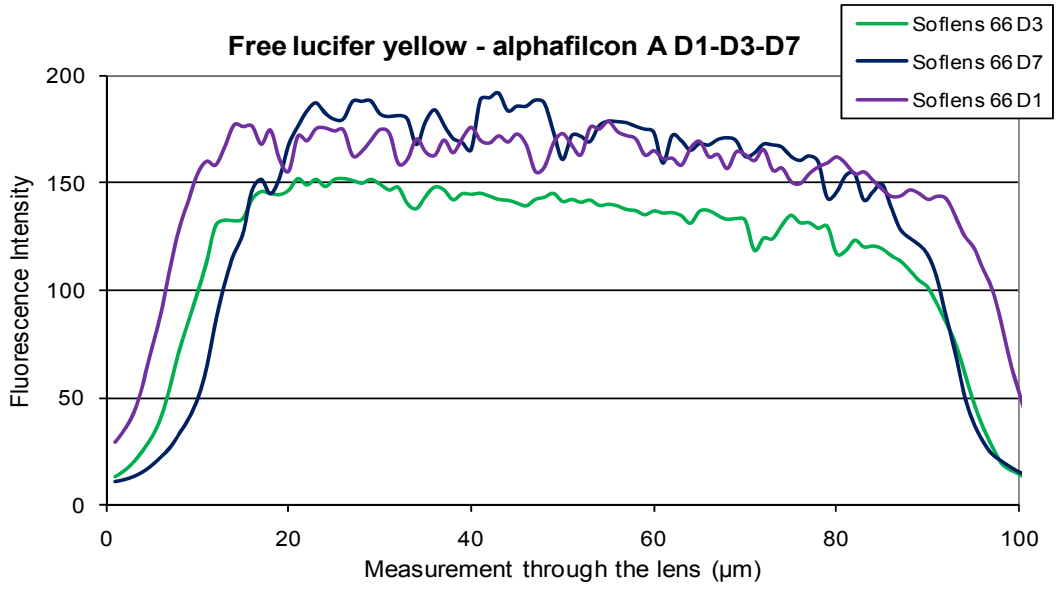

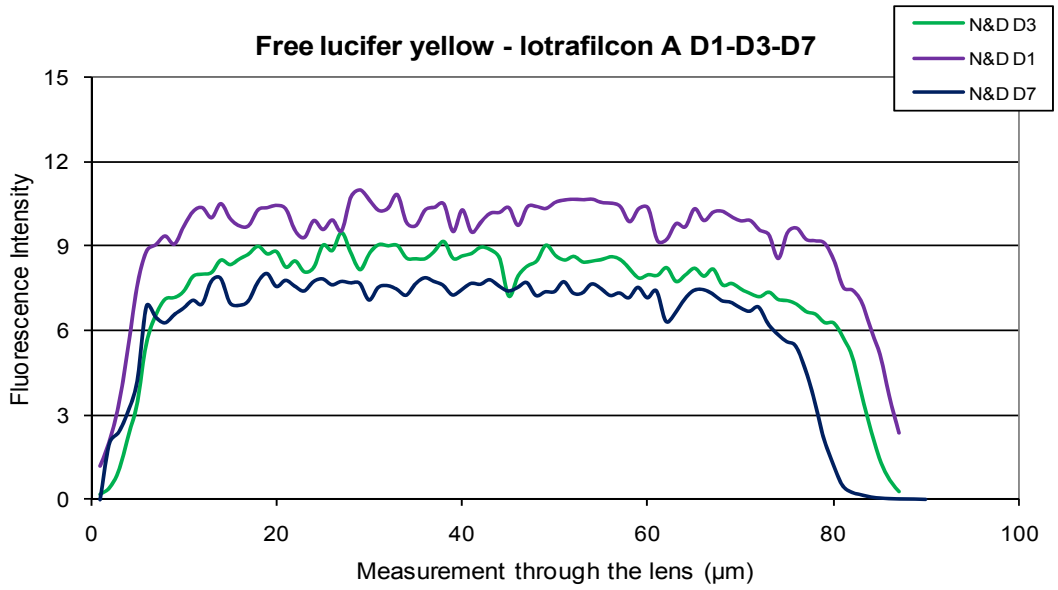
Free lucifer yellow - Iotrafilcon A D1-D3-D7
N&D D3
N&D D1
N&D D7
Fluorescence Intensity
15
12
9
6
3
0
0
20
40
60
80
100
Measurement through the lens (µm)

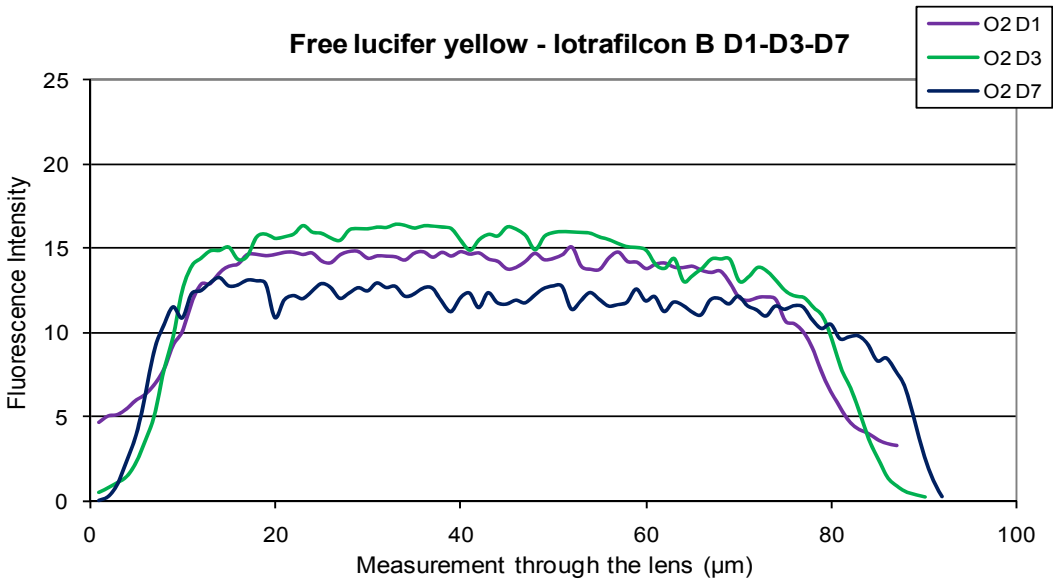
Free lucifer yellow - Iotrafilcon B D1-D3-D7
O2 D1
O2 D3
O2 D7
Fluorescence Intensity
25
20
15
10
5
0
0
20
40
60
80
100
Measurement through the lens (µm)

Silicone hydrogel contact lenses (FDA Group I)

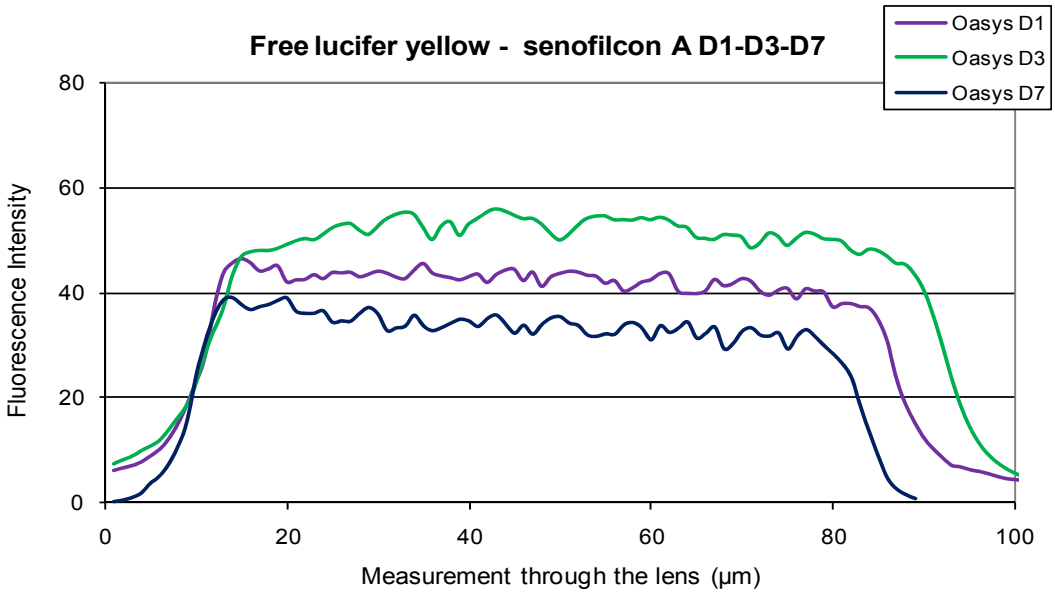

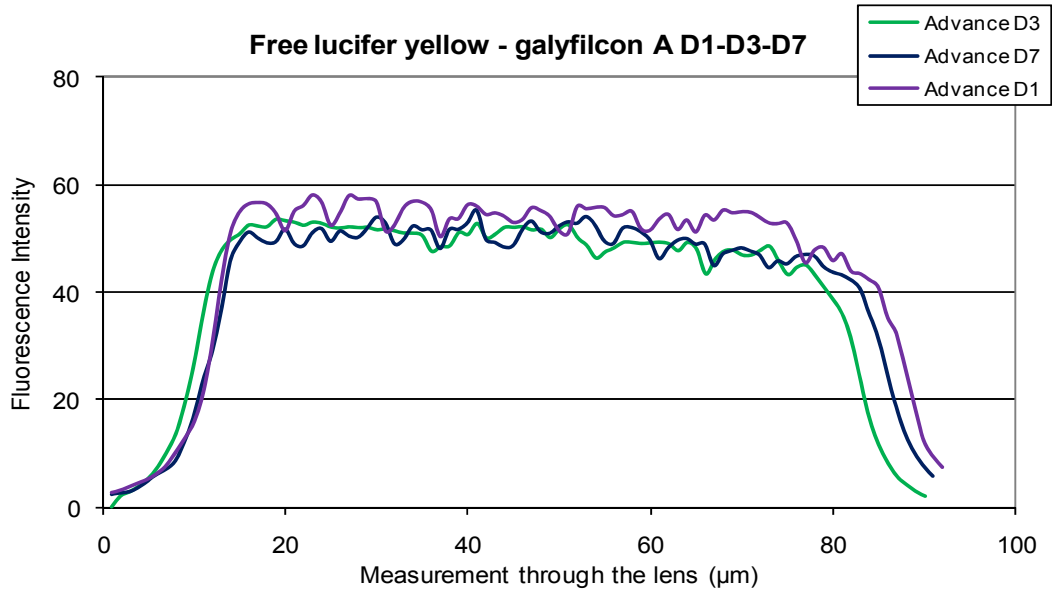

Silicone hydrogel contact lens (FDA Group III)

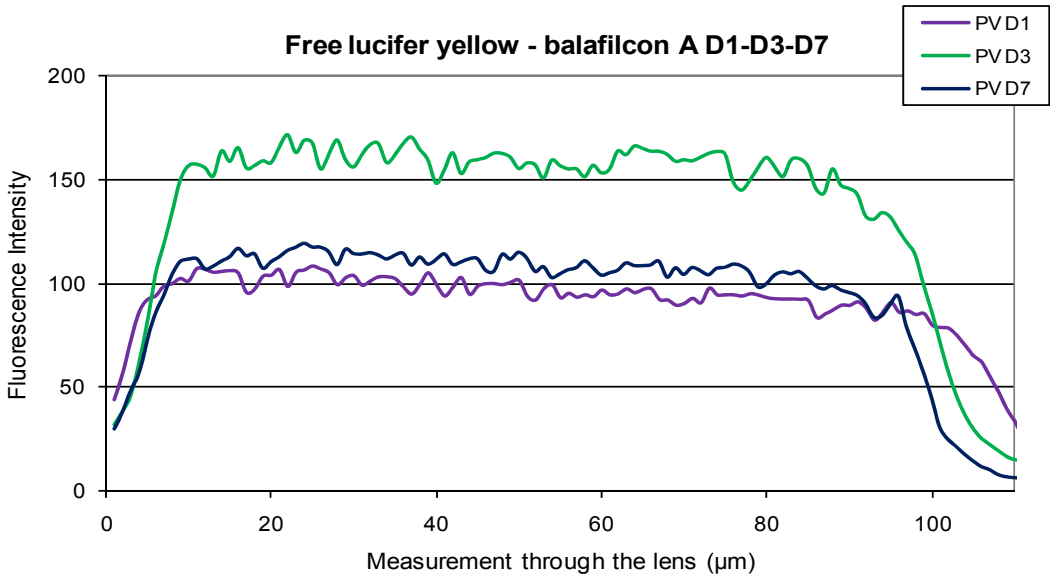

Appendix D

Lysozyme uptake into different contact lens materials over time (Chapter 5)

Hydrogel contact lens materials (FDA Group IV)

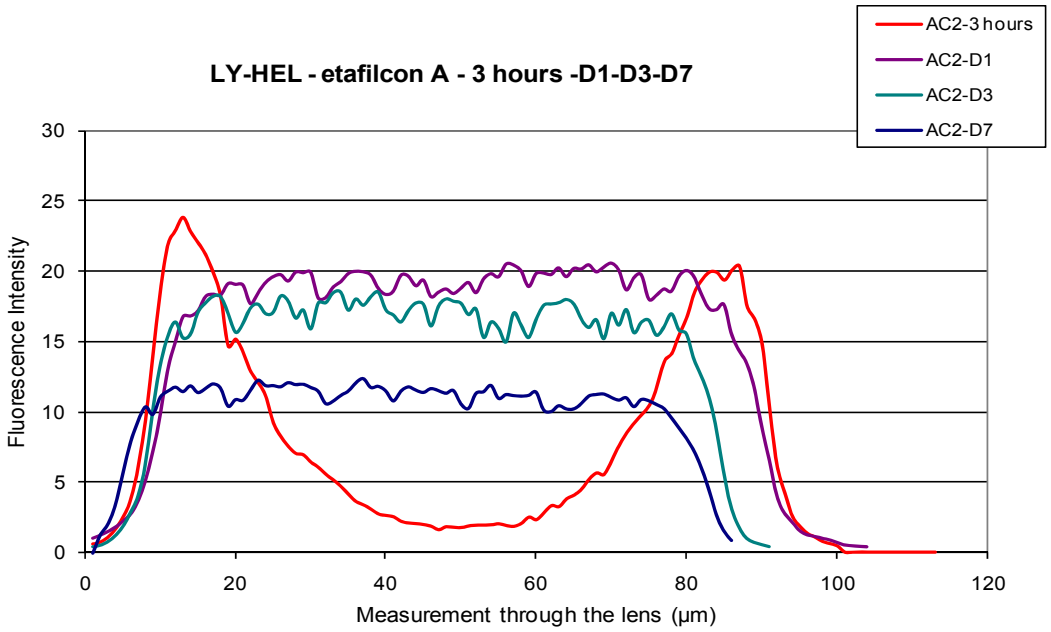

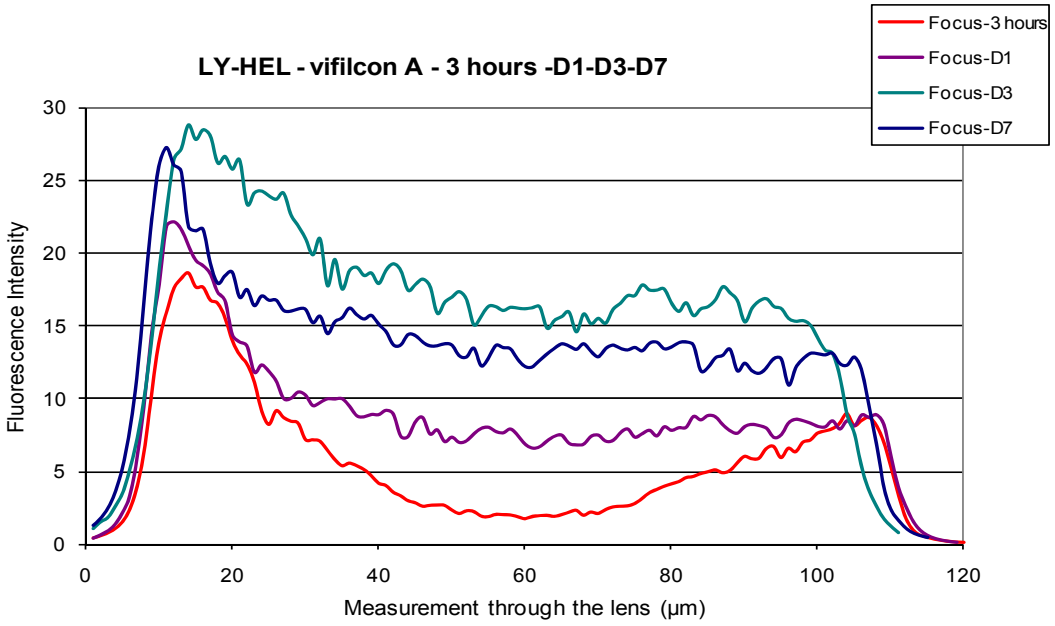

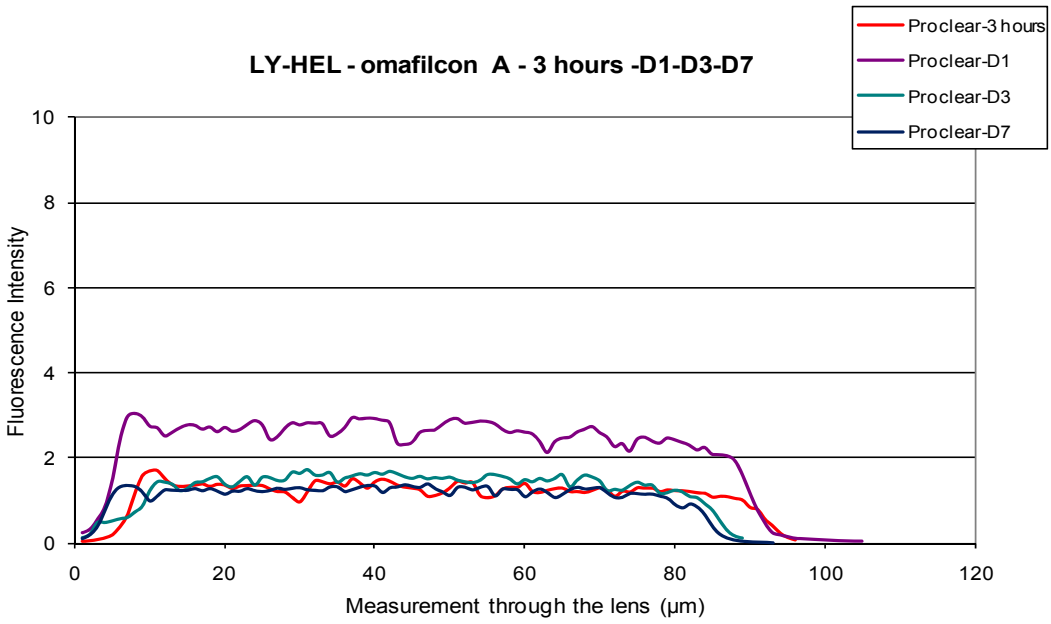
LY-HEL - omafilcon A - 3 hours -D1-D3-D7
Proclear-3 hours
Proclear-D1
Proclear-D3
Proclear-D7
Fluorescence Intensity
0
2
4
6
8
10
0
20
40
60
80
100
120
Measurement through the lens (µm)

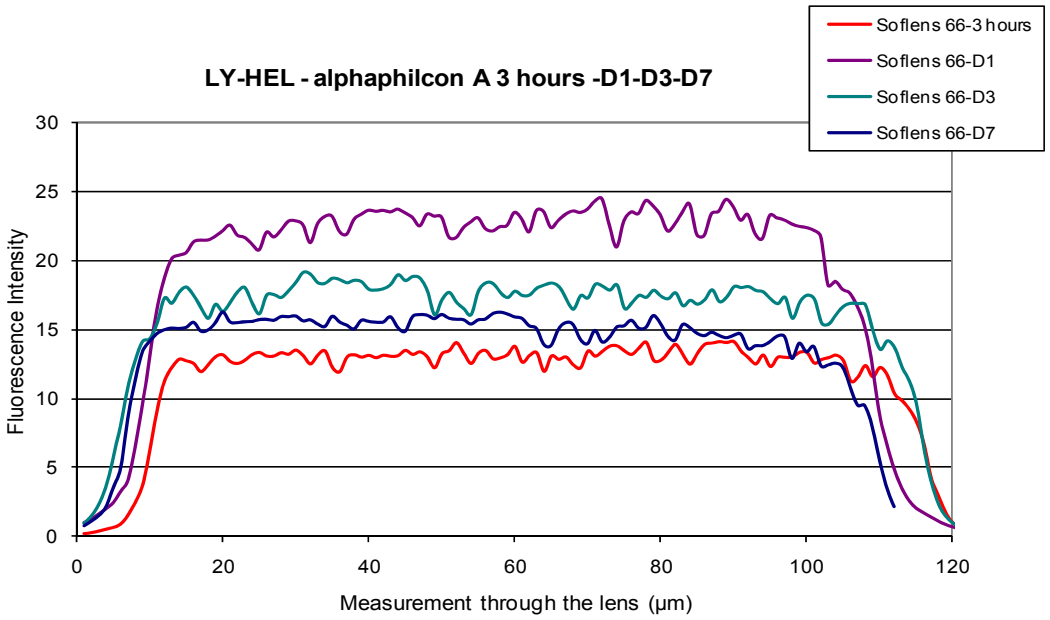
LY-HEL - alphaphilcon A 3 hours -D1-D3-D7
Soflens 66-3 hours
Soflens 66-D1
Soflens 66-D3
Soflens 66-D7
Fluorescence Intensity
0
5
10
15
20
25
30
0
20
40
60
80
100
120
Measurement through the lens (µm)

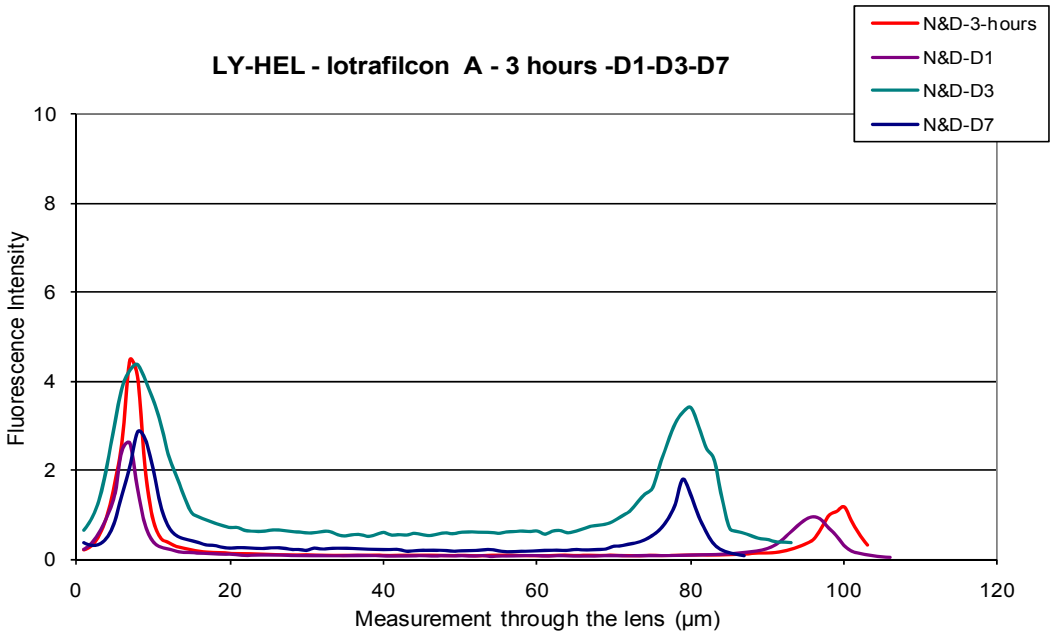
LY-HEL - lotrafilcon A - 3 hours -D1-D3-D7
N&D-3-hours
N&D-D1
N&D-D3
N&D-D7
Fluorescence Intensity
Measurement through the lens (µm)
0
2
4
6
8
10
0
20
40
60
80
100
120

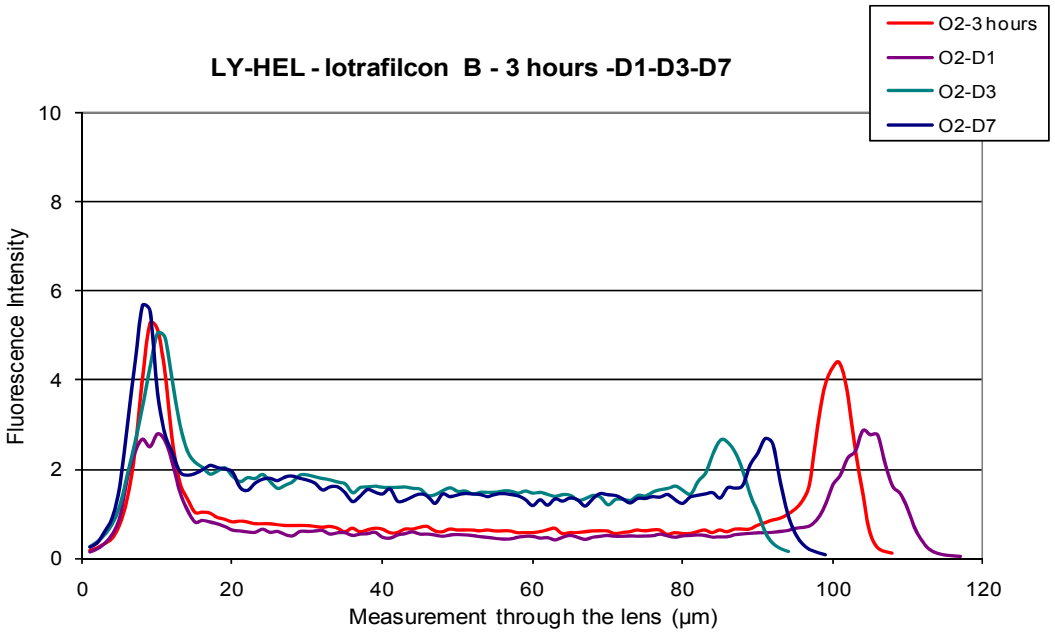
LY-HEL - lotrafilcon B - 3 hours -D1-D3-D7
O2-3 hours
O2-D1
O2-D3
O2-D7
Fluorescence Intensity
Measurement through the lens (µm)
0
2
4
6
8
10
0
20
40
60
80
100
120

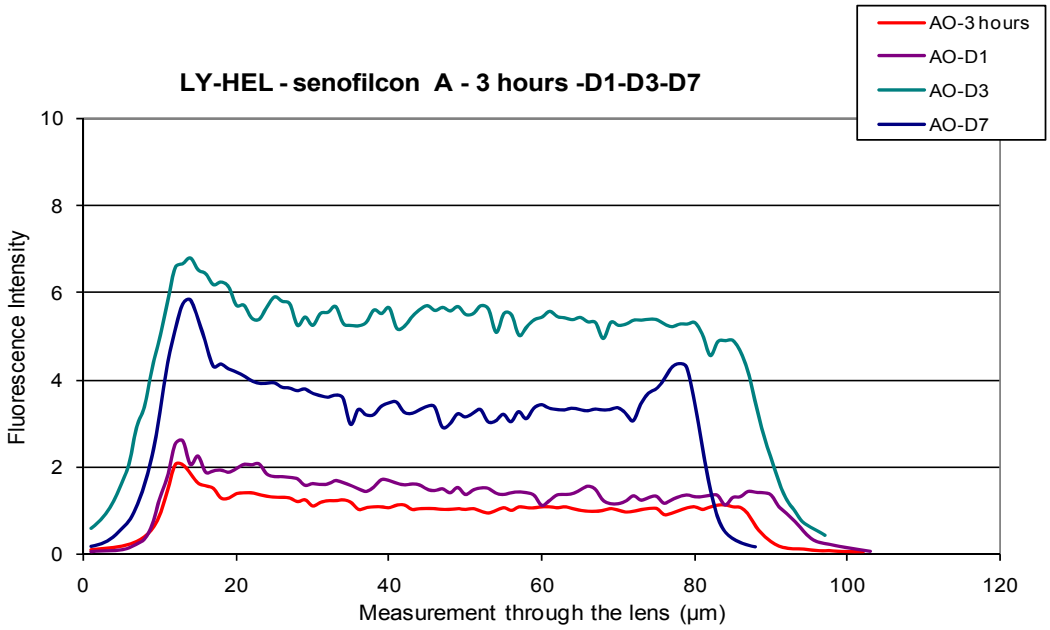
LY-HEL - senofilcon A - 3 hours -D1-D3-D7
AO-3 hours
AO-D1
AO-D3
AO-D7
Fluorescence Intensity
Measurement through the lens (µm)
0
2
4
6
8
10
0
20
40
60
80
100
120

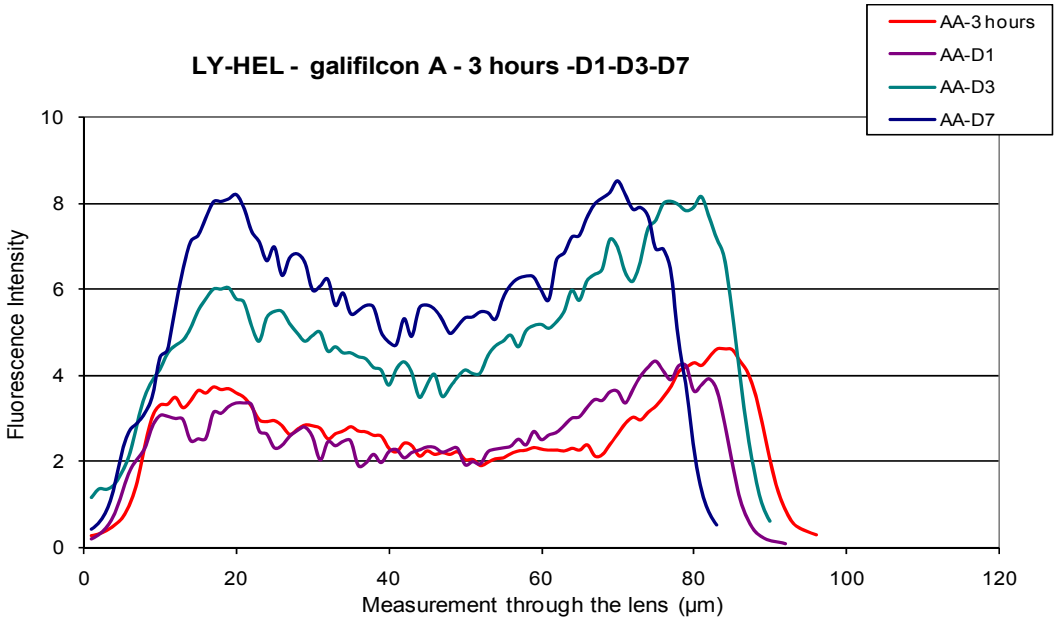
LY-HEL - galifilcon A - 3 hours -D1-D3-D7
AA-3 hours
AA-D1
AA-D3
AA-D7
Fluorescence Intensity
Measurement through the lens (µm)
0
2
4
6
8
10
0
20
40
60
80
100
120

Hydrogel contact lens material (FDA Group III)

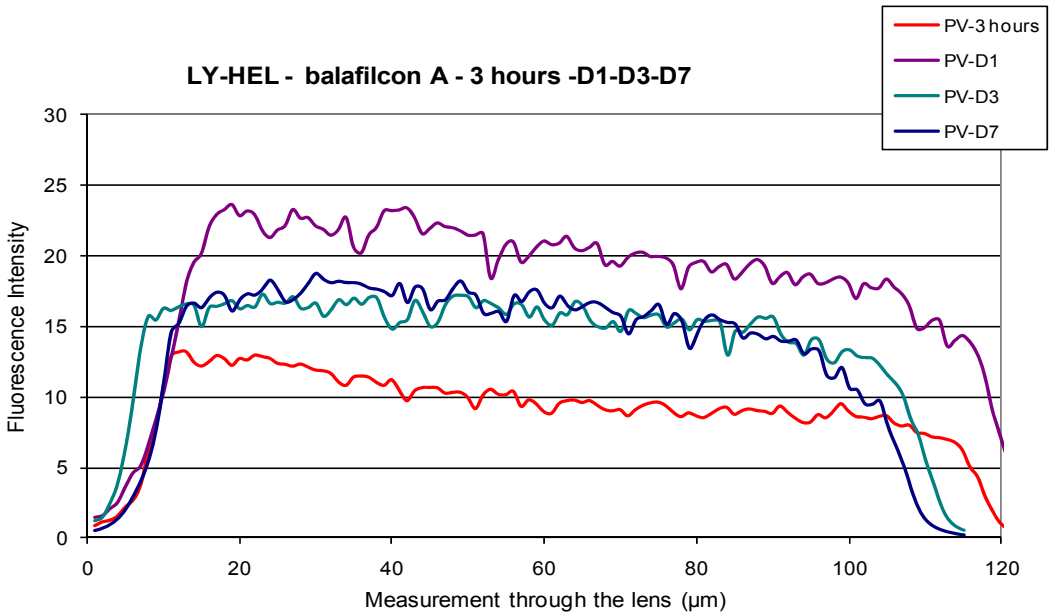

Appendix E

Location for thickness measures (Chapter 5)

Assumption: spherical corneal surface with r=7.8mm

Circumference = 49mm

e.g. sin α = 6.0/7.8mm → α = 50.3

→ 50.3*49/360 = 6.85 mm distance

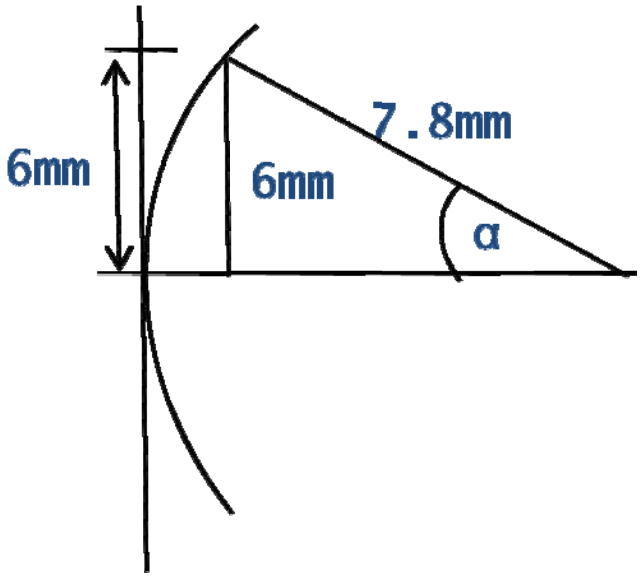

Appendix F

Copyright permissions

Copyright: Contact Lens and Anterior Eye

ELSEVIER LICENSE - TERMS AND CONDITIONS
Aug 10, 2009

This is a License Agreement between Doerte Luensmann ("You") and Elsevier ("Elsevier") provided by Copyright Clearance Center ("CCC"). The license consists of your order details, the terms and conditions provided by Elsevier, and the payment terms and conditions.

All payments must be made in full to CCC. For payment instructions, please see information listed at the bottom of this form.

Supplier	Elsevier Limited The Boulevard,Langford Lane Kidlington,Oxford,OX5 1GB,UK
Registered Company Number	1982084
Customer name	Doerte Luensmann
Customer address	School of Optometry Waterloo, ON N2L 3G1
License Number	2243060457175
License date	Aug 06, 2009
Licensed content publisher	Elsevier
Licensed content publication	Contact Lens and Anterior Eye
Licensed content title	Albumin adsorption to contact lens materials: A review
Licensed content author	Doerte Luensmann and Lyndon Jones
Licensed content date	August 2008
Volume number	31
Issue number	4
Pages	9
Type of Use	Thesis / Dissertation
Portion	Full article
Format	Both print and electronic
You are an author of the Elsevier article	Yes
Are you translating?	No
Order Reference Number	
Expected publication date	

Elsevier VAT number	GB 494 6272 12
Permissions price	0.00 USD
Value added tax 0.0%	0.00 USD
Total	0.00 USD

Terms and Conditions

INTRODUCTION

1. The publisher for this copyrighted material is Elsevier. By clicking "accept" in connection with completing this licensing transaction, you agree that the following terms and conditions apply to this transaction (along with the Billing and Payment terms and conditions established by Copyright Clearance Center, Inc. ("CCC"), at the time that you opened your Rightslink account and that are available at any time at http://myaccount.copyright.com).

GENERAL TERMS

2. Elsevier hereby grants you permission to reproduce the aforementioned material subject to the terms and conditions indicated.

3. Acknowledgement: If any part of the material to be used (for example, figures) has appeared in our publication with credit or acknowledgement to another source, permission must also be sought from that source. If such permission is not obtained then that material may not be included in your publication/copies. Suitable acknowledgement to the source must be made, either as a footnote or in a reference list at the end of your publication, as follows:

"Reprinted from Publication title, Vol /edition number, Author(s), Title of article / title of chapter, Pages No., Copyright (Year), with permission from Elsevier [OR APPLICABLE SOCIETY COPYRIGHT OWNER]." Also Lancet special credit - "Reprinted from The Lancet, Vol. number, Author(s), Title of article, Pages No., Copyright (Year), with permission from Elsevier."

4. Reproduction of this material is confined to the purpose and/or media for which permission is hereby given.

5. Altering/Modifying Material: Not Permitted. However figures and illustrations may be altered/adapted minimally to serve your work. Any other abbreviations, additions, deletions and/or any other alterations shall be made only with prior written authorization of Elsevier Ltd. (Please contact Elsevier at permissions@elsevier.com)

6. If the permission fee for the requested use of our material is waived in this instance, please be advised that your future requests for Elsevier materials may attract a fee.

7. Reservation of Rights: Publisher reserves all rights not specifically granted in the combination of (i) the license details provided by you and accepted in the course of this licensing transaction, (ii) these terms and conditions and (iii) CCC's Billing and Payment terms and conditions.

8. License Contingent Upon Payment: While you may exercise the rights licensed immediately upon

issuance of the license at the end of the licensing process for the transaction, provided that you have disclosed complete and accurate details of your proposed use, no license is finally effective unless and until full payment is received from you (either by publisher or by CCC) as provided in CCC's Billing and Payment terms and conditions. If full payment is not received on a timely basis, then any license preliminarily granted shall be deemed automatically revoked and shall be void as if never granted. Further, in the event that you breach any of these terms and conditions or any of CCC's Billing and Payment terms and conditions, the license is automatically revoked and shall be void as if never granted. Use of materials as described in a revoked license, as well as any use of the materials beyond the scope of an unrevoked license, may constitute copyright infringement and publisher reserves the right to take any and all action to protect its copyright in the materials.

9. Warranties: Publisher makes no representations or warranties with respect to the licensed material.

10. Indemnity: You hereby indemnify and agree to hold harmless publisher and CCC, and their respective officers, directors, employees and agents, from and against any and all claims arising out of your use of the licensed material other than as specifically authorized pursuant to this license.

11. No Transfer of License: This license is personal to you and may not be sublicensed, assigned, or transferred by you to any other person without publisher's written permission.

12. No Amendment Except in Writing: This license may not be amended except in a writing signed by both parties (or, in the case of publisher, by CCC on publisher's behalf).

13. Objection to Contrary Terms: Publisher hereby objects to any terms contained in any purchase order, acknowledgment, check endorsement or other writing prepared by you, which terms are inconsistent with these terms and conditions or CCC's Billing and Payment terms and conditions. These terms and conditions, together with CCC's Billing and Payment terms and conditions (which are incorporated herein), comprise the entire agreement between you and publisher (and CCC) concerning this licensing transaction. In the event of any conflict between your obligations established by these terms and conditions and those established by CCC's Billing and Payment terms and conditions, these terms and conditions shall control.

14. Revocation: Elsevier or Copyright Clearance Center may deny the permissions described in this License at their sole discretion, for any reason or no reason, with a full refund payable to you. Notice of such denial will be made using the contact information provided by you. Failure to receive such notice will not alter or invalidate the denial. In no event will Elsevier or Copyright Clearance Center be responsible or liable for any costs, expenses or damage incurred by you as a result of a denial of your permission request, other than a refund of the amount(s) paid by you to Elsevier and/or Copyright Clearance Center for denied permissions.

LIMITED LICENSE

The following terms and conditions apply only to specific license types:

15. **Translation**: This permission is granted for non-exclusive world **English** rights only unless your license was granted for translation rights. If you licensed translation rights you may only translate this content into the languages you requested. A professional translator must perform all translations

and reproduce the content word for word preserving the integrity of the article. If this license is to re-use 1 or 2 figures then permission is granted for non-exclusive world rights in all languages.

16. **Website**: The following terms and conditions apply to electronic reserve and author websites:
Electronic reserve: If licensed material is to be posted to website, the web site is to be password-protected and made available only to bona fide students registered on a relevant course if:
This license was made in connection with a course,
This permission is granted for 1 year only. You may obtain a license for future website posting,
All content posted to the web site must maintain the copyright information line on the bottom of each image,
A hyper-text must be included to the Homepage of the journal from which you are licensing at http://www.sciencedirect.com/science/journal/xxxxx or the Elsevier homepage for books at http://www.elsevier.com , and
Central Storage: This license does not include permission for a scanned version of the material to be stored in a central repository such as that provided by Heron/XanEdu.

17. **Author website** for journals with the following additional clauses:

All content posted to the web site must maintain the copyright information line on the bottom of each image, and
he permission granted is limited to the personal version of your paper. You are not allowed to download and post the published electronic version of your article (whether PDF or HTML, proof or final version), nor may you scan the printed edition to create an electronic version,
A hyper-text must be included to the Homepage of the journal from which you are licensing at http://www.sciencedirect.com/science/journal/xxxxx , As part of our normal production process, you will receive an e-mail notice when your article appears on Elsevier's online service ScienceDirect (www.sciencedirect.com). That e-mail will include the article's Digital Object Identifier (DOI). This number provides the electronic link to the published article and should be included in the posting of your personal version. We ask that you wait until you receive this e-mail and have the DOI to do any posting.
Central Storage: This license does not include permission for a scanned version of the material to be stored in a central repository such as that provided by Heron/XanEdu.

18. **Author website** for books with the following additional clauses:
Authors are permitted to place a brief summary of their work online only.
A hyper-text must be included to the Elsevier homepage at http://www.elsevier.com

All content posted to the web site must maintain the copyright information line on the bottom of each image
You are not allowed to download and post the published electronic version of your chapter, nor may you scan the printed edition to create an electronic version.
Central Storage: This license does not include permission for a scanned version of the material to be stored in a central repository such as that provided by Heron/XanEdu.

19. **Website** (regular and for author): A hyper-text must be included to the Homepage of the journal from which you are licensing at http://www.sciencedirect.com/science/journal/xxxxx. or for books to the Elsevier homepage at http://www.elsevier.com

20. **Thesis/Dissertation**: If your license is for use in a thesis/dissertation your thesis may be submitted to your institution in either print or electronic form. Should your thesis be published commercially, please reapply for permission. These requirements include permission for the Library and Archives of Canada to supply single copies, on demand, of the complete thesis and include permission for UMI to supply single copies, on demand, of the complete thesis. Should your thesis be published commercially, please reapply for permission.

21. **Other Conditions**None v1.6

Gratis licenses (referencing $0 in the Total field) are free. Please retain this printable license for your reference. No payment is required.

If you would like to pay for this license now, please remit this license along with your payment made payable to "COPYRIGHT CLEARANCE CENTER" otherwise you will be invoiced within 30 days of the license date. Payment should be in the form of a check or money order referencing your account number and this license number 2243060457175.
If you would prefer to pay for this license by credit card, please go to http://www.copyright.com/creditcard to download our credit card payment authorization form.

Make Payment To:
Copyright Clearance Center
Dept 001
P.O. Box 843006
Boston, MA 02284-3006
If you find copyrighted material related to this license will not be used and wish to cancel, please contact us referencing this license number 2243060457175 and noting the reason for cancellation. Questions? customercare@copyright.com or +1-877-622-5543 (toll free in the US) or +1-978-646-2777.

WOLTERS KLUWER HEALTH LICENSE TERMS AND CONDITIONS

Aug 04, 2009

This is a License Agreement between Doerte Luensmann ("You") and Wolters Kluwer Health ("Wolters Kluwer Health") provided by Copyright Clearance Center ("CCC"). The license consists of your order details, the terms and conditions provided by Wolters Kluwer Health, and the payment terms and conditions.

All payments must be made in full to CCC. For payment instructions, please see information listed at the bottom of this form.

License Number 2241990628217
License date Aug 04, 2009
Licensed content publisher Wolters Kluwer Health
Licensed content publication Optometry and Vision Science
Licensed content title Confocal Microscopy and Albumin Penetration into Contact Lenses
Licensed content author DOERTE LUENSMANN, MARY-ANN GLASIER, FENG ZHANG, et al
Licensed content date Jan 1, 2007
Volume Number 84
Issue Number 9
Type of Use Dissertation/Thesis
Requestor type Individual
Title of your thesis /dissertation Albumin adhesion to contact lenses and other biomaterials
Expected completion date Nov 2009
Estimated size(pages) 200
Billing Type Invoice
Billing Address School of Optometry, University of Waterloo, Waterloo, ON N2L 3G1, Canada
Customer reference info
Total 0.00 USD
Terms and Conditions

Terms and Conditions

A credit line will be prominently placed and include: for books - the author(s), title of book, editor, copyright holder, year of publication; For journals - the author(s), title of article, title of journal, volume number, issue number and inclusive pages.

1. The requestor warrants that the material shall not be used in any manner which may be considered derogatory to the title, content, or authors of the material, or to Wolters Kluwer/Lippincott, Williams & Wilkins.
2. Rightslink Printable License https://s100.copyright.com/App/PrintableLicenseFrame.jsp?publisherID=...1 of 2 8/4/2009 11:46 AM

Copyright: Current Eye Research

informa healthcare

Title: Localization of Lysozyme Sorption to Conventional and Silicone Hydrogel Contact Lenses Using Confocal Microscopy

Author: Doerte Luensmann, Feng Zhang, Lakshman Subbaraman et al.

Publication: Current Eye Research

Publisher: Informa Healthcare

Date: Jan 8, 2009

Logged in as:
Doerte Luensmann
Account #:
3000190090

LOGOUT

Thesis/Dissertation Reuse Request

Taylor & Francis is pleased to offer reuses of its content for a thesis or dissertation free of charge contingent on resubmission of permission request if work is published.

BACK CLOSE WINDOW

Copyright: Journal of Cataract and Refractive Surgery

Dear Dr Luensmann,

Thank you for your e-mail which was forwarded to us.

Regarding your query about the permission to use your paper as part of the thesis, this right is permitted without the need to obtain specific permission from Elsevier.

For more of your rights as an author, you may visit the link below:
http://www.elsevier.com/wps/find/authorsview.authors/authorsrights

Should you ask for other permissions, you may find this Elsevier Customer Support solution useful:
http://epsupport.elsevier.com/article.aspx?article=1139&p=3

If responding to this e-mail, please ensure that the reference number remains in the subject line.
Should you have any additional questions or concerns, please visit our self-help site at: http://epsupport.elsevier.com/. Here you will be able to search for solutions on a range of topics, find answers to frequently asked questions and learn more about EES via interactive tutorials. You will also find our 24/7 support contact details should you need further assistance from one of our customer service representatives.

Yours sincerely,
Mae Roxanne Que
Elsevier Customer Support

How are we doing? If you have any feedback on our customer service we would be happy to receive your comments at customerfeedback@elsevier.com

-----Original Message-----
From: dluensma@uwaterloo.ca
Sent: 27/09/2009 14:42:05
To: usinfo@sciencedirect.com
Subject: SD Comment- [Canada] (Academic) inforeq

Details:

To whom this may concern,

I am the first author of the following paper: 'Determination of Albumin Sorption to Intraocular Lenses by Radiolabeling and Confocal Laser Scanning Microscopy', Reference: JCRS 6325
This paper is currently 'in press' and will be releases in the November issue 09. This work is part of my PhD-Thesis which I will complete in November 09 (Thesis title: 'Albumin adhesion to contact lenses and intraocular lenses').I therefore would kindly as you for permission to print this work in my thesis. Best Regards, Doerte Luensmann